Mapping the molecular overlap between CD8+ T cell tolerance and exhaustion

Christian Deo T. Deguit
orcid.org/0000-0003-0759-4035

Submitted in fulfilment of the requirements of the degree of
Doctor of Philosophy

October 2025

Peter MacCallum Cancer Centre
and
Sir Peter MacCallum Department of Oncology
Faculty of Medicine, Dentistry and Health Sciences
The University of Melbourne

TABLE OF CONTENTS

ABSTRACT **6**
DECLARATION **7**
PREFACE **8**
CONTRIBUTIONS **9**
ACKNOWLEDGEMENTS **10**
ABBREVIATIONS **12**
LIST OF FIGURES **14**
LIST OF TABLES **16**
CHAPTER 1 Introduction **17**

1.1. Overview of the Immune System *17*
1.1.1. Innate Immune System and their Role in Antigen Presentation 17
1.1.2. Adaptive Immune System 19
1.1.2.1. Clonal Selection Theory 19
1.1.2.2. T and B cells 20

1.2. CD8+ T cells *21*
1.2.1. Antigen Recognition and Activation 21
1.2.2. Effector and Memory T cell Differentiation 24
1.2.2.1. Effector CD8+ T cell subsets 26
1.2.2.2. Memory CD8+ T cell subsets 26
1.2.2.3. Transcriptional and Epigenetic Control of Differentiation 27
1.2.3. Regulation of CD8+ T cell immunity 28

1.3. Tolerance *29*
1.3.1. Mechanisms of Peripheral Tolerance: Ignorance, Anergy, and Deletion 30
1.3.2. Molecular Control of Tolerance 32

1.4. Exhaustion *34*
1.4.1. Exhausted T cell differentiation 35
1.4.2. Transcriptional and Epigenetic Control of Exhaustion 36

1.5. CD8+ T cell tolerance and exhaustion in Cancer *37*
1.6. Contrasting CD8+ Tolerance and Exhaustion *38*
1.7. TOX control of immune function *41*
1.7.1. TOX function in CD8+ T cells 42
1.7.2. TOX in other immune cells 43

1.8. AP-1 transcription factor biology and function *43*

1.8.1. Jun family 46
1.8.2. AP-1-dependent Transcriptional Regulation in T cells 48
1.9. Research Aims 50
Aim 1: Investigate the role of Tox in CD8+ T cell tolerance 50
Aim 2: Delineate the role of AP-1 transcription factors in CD8+ T cell differentiation 50
CHAPTER 2 Materials and Methods 51
2.1. Reagents, Materials, and Animals 51
2.1.1. Reagents and Materials 51
2.1.2. Media and Buffer Solutions 52
2.1.3. Antibodies 53
2.1.4. Kits 56
2.1.5. Bacterial and Viral Strains 56
2.1.6. Mouse Models 56
2.2. Experimental Methods 57
2.2.1. General Lab Procedures 57
2.2.2. Mouse techniques, procedures, and handling 57
2.2.2.1. Animal Ethics and General Procedures 57
2.2.2.2. Adoptive Transfer 58
2.2.2.3. Infections 59
2.2.2.4. Diabetes Testing and Peptide Injections 59
2.2.3. Cell Isolation 59
2.2.3.1. CD8+ T cell isolation and CTV labelling 59
2.2.3.2. Spleen and lymph node cell isolation and processing 60
2.2.3.3. Peripheral Blood Mononuclear Cell (PBMC) Isolation 60
2.2.4. *In vitro* cultures 61
2.2.4.1. In vitro activation of CD8+ T cells 61
2.2.4.2. IL-7 culture 61
2.2.4.3. Peptide Restimulation 61
2.2.4.4. Cell line culture and maintenance 62
2.2.5. CRISPR Gene Editing 62
2.2.5.1. Design of single guide RNAs (sgRNAs) 62
2.2.5.2. CRISPR/Cas9 ribonucleoprotein (RNP) Electroporation 63
2.2.6. Western Blotting 64
2.2.7. Retroviral Transduction 64

2.2.8. Flow Cytometry 65
2.2.8.1. Flow cytometric staining and analysis 65
2.2.8.2. CaspGLOW staining 65
2.2.8.3. Cell sorting 66
2.2.9. DNA Sequencing of KO genomic regions 66
2.2.9.1. Sample preparation and DNA extraction 66
2.2.9.2. Polymerase Chain Reaction (PCR), DNA sequencing, and CRISPR varian analysis 66
2.2.10. Co-immunoprecipitation / Mass Spectrometry (Co-IP MS) 67
2.2.10.1. Co-IP MS sample preparation 67
2.2.10.2. Co-IP MS bioinformatic analysis 69
2.2.11. Cleavage Under Targets & Release Using Nuclease (CUT&RUN) 69
2.2.11.1. CUT&RUN sample preparation 69
2.2.11.2. Library Preparation and Quality Control 70
2.2.11.3. CUT&RUN bioinformatic analysis 71
2.2.11.3.1. Hybrid genome construction 71
2.2.11.4. CUT&RUN Data pre-processing and analysis 71
2.2.11.5. Peak overlap analysis with NFAT ChIP-Seq data 72
2.2.12. Multiplexed Analysis of Cells Sequencing (MAC-Seq) 72
2.2.12.1. MAC-Seq sample preparation 72
2.2.12.2. MAC-Seq bioinformatic analysis 73
2.2.12.2.1. Alignment, Quality Control, and Integration of MACSeq plates 73
2.2.12.2.2. Differential gene expression 73

2.3. Statistical Analysis 74
2.4. Data Availability 74

CHAPTER 3..... Measuring the influence of TOX on peripheral CD8+ T cell tolerance. 75

3.1. INTRODUCTION 75
3.2. RESULTS 76
3.2.1. TOX is upregulated in tolerance but not as much as in exhaustion 76
3.2.2. TOX deletion via CRISPR functionally mimic established TOX-deficient phenotype in chronic infection 77
3.2.3. TOX is not essential in early commitment of peripheral tolerance 79
3.2.4. TOX is not essential to the maintenance of peripheral tolerance 81

3.3. DISCUSSION 83

CHAPTER 4 Assessing AP-1 Activity during early T cell differentiation 85

4.1. INTRODUCTION 85

4.2. RESULTS 86

4.2.1. AP-1 Jun family members are transiently expressed during *in vivo* effector T cell differentiation 86

4.2.2. Different Jun proteins have distinct protein interactomes 88

4.2.3. Jun proteins exhibit distinct but overlapping genomic binding profiles 94

4.2.4. Jun proteins and NFAT share genomic targets related to T cell signalling 97

4.3. DISCUSSION 100

CHAPTER 5 Evaluating the role of AP-1 in CD8+ T cell effector and memory cell differentiation. 102

5.1. INTRODUCTION 102

5.2. RESULTS 102

5.2.1. Optimisation of AP-1 CRISPR knock-out 102

5.2.2. Loss of AP-1 triggers decreased survival and acquisition of exhausted-like features during effector differentiation 105

5.2.3. JunB deletion is sufficient to phenocopy AP-1 deficiency 110

5.2.4. Different Jun proteins play analogous roles in CD8+ T cell exhaustion 114

5.2.5. Little to no impact on transcriptional induction of the early effector gene program upon AP-1 deletion 116

5.2.6. JunD deficiency selectively disrupts memory cell persistence 118

5.2.7. Deleting cJun may affect memory responses in subsequent immune challenges 121

5.3. DISCUSSION 124

CHAPTER 6 Final Discussion 128

6.1. OVERVIEW 128

6.2. Evidence of differences in how NFAT regulates tolerance and exhaustion 129

6.3. Full AP-1 ablation challenges assumptions about AP-1 function 130

6.4. Distinct roles for different AP-1 complexes in T cell differentiation 132

CHAPTER 7 Appendix 134

REFERENCES 149

ABSTRACT

CD8+ T cells engage immune regulatory checkpoints to maintain homeostasis and prevent inadvertent damage to the host. Critical among these checkpoints are peripheral tolerance and exhaustion, which attenuate effector T cell responses to limit adverse events such as autoimmunity and immunopathology, respectively. Despite arising at fundamentally distinct points of the immune response, both tolerance and exhaustion display superficially overlapping phenotypic features often attributed to a shared NFAT regulatory gene program thought to be engaged due to the absence of AP-1 activation in both states. However, functional evidence to support the idea that tolerance and exhaustion are molecularly similar is limited.

We functionally examined whether tolerance and exhaustion are molecularly distinct using T cell intrinsic gene knockout approaches, comprehensive immunophenotyping, and molecular analysis, in a variety of *in vitro* and *in vivo* models of CD8+ T cell immunity. Chapter 3 evaluates the functional importance of an NFAT-induced factor called TOX, previously shown to be critical for T cell exhaustion but whose function in tolerance is unknown. While TOX is expressed in tolerant cells, it was dispensable for tolerance induction and maintenance, highlighting a fundamental molecular difference between tolerance and exhaustion. Subsequently, in Chapters 4 and 5, the concept that AP-1 insulates cells against exhaustion and tolerance was tested, alongside examining the role of AP-1 in T cell differentiation, by single and compound gene deletion of the Jun proteins *Jun*, *Junb* and *Jund*. All three Jun proteins were strongly but transiently upregulated early during effector differentiation. AP-1 loss by deletion of all 3 Jun proteins resulted in a profound survival defect and cytokine defects at later stages of T cell activation but had surprisingly little impact on T cell proliferation and effector gene induction at early stages of activation. AP-1 deficient cells failed to acquire a tolerant state but did acquire mild features of exhaustion, potentially suggesting differential regulation of tolerance and exhaustion by AP-1. Individual deletion of the Jun genes revealed divergent individual roles in distinct contexts of effector and memory differentiation. JunB emerged as the principal regulator of effector cell differentiation and survival, JunD as a critical regulator of memory persistence, while cJun may play a mild role in supporting memory cell fitness upon serial rechallenge. Overall, these data challenge many assumptions around AP-1 biology in T cells and reveal further differences between tolerance and exhaustion.

Collectively, this thesis provides functional evidence that tolerance and exhaustion are molecularly separable processes. While both tolerant and exhausted cells have superficial similarities, the overall molecular programs that govern each state are fundamentally different. Appreciating these insights will have broad implications in informing the rational design of next-generation immunotherapies.

DECLARATION

This is to certify that:

- This thesis comprises only my original work towards the PhD, except where indicated
- Due acknowledgement has been made in the text to all other material used.
- The thesis is fewer than 100,000 words in length, exclusive of tables, maps, bibliographies, and appendices as approved by the Research Higher Degrees Committee.

Christian Deo T. Deguit
October 2025

PREFACE

The work that is presented within this thesis was conducted at the Peter MacCallum Cancer Centre in the laboratory of Ian Parish.
The project was funded by grants from the National Health and Medical Research Council (NHMRC)

Part of the work described in this thesis is to be published as follows:

Deguit CDT, Sampurno S, Ramsbottom K, Travers A, Trapani J, Parish IA. "**The exhaustion master regulator TOX is dispensable for peripheral CD8+ T cell tolerance"**. *Manuscript in Preparation*

Deguit CDT, Nussing, S, Sampurno S, Ramsbottom K, Saw N, Kulkarni N, Zhang A, Perez-Nunez I, Chan C, Ambani K, Bartonicek N, Martin B, Goel S, Johnstone R, Trapani J, Parish IA. "**Distinct AP-1 complexes control effector and memory CD8+ T cell differentiation"**. *Manuscript in Preparation*

CONTRIBUTIONS

My contribution to experiments in each of the chapters was as follows:

Chapter 3: 95%
Chapter 4: 85%
Chapter 5: 90%

I acknowledge the important contributions of other to experiments and analyses presented here:

Chapter 3: Shienny Sampurno, Kelly Ramsbottom, Avraham Travers
Chapter 4: Ben Martin, Nenad Bartonicek, Krutika Ambani, Ivan Perez-Nunez, Nicole Saw
Chapter 5: Shienny Sampurno, Kelly Ramsbottom, Nihali Kulkarni, Cheok Weng Cherry Chan
Anni Zhang, Nicole Saw

ACKNOWLEDGEMENTS

I've always cringed at the idea of calling myself an "immunologist", let alone a "scientist". But after having gone through the trials and tribulations of doing a PhD, the feeling of *exhaustion has just made me *tolerate this sense of self-doubt. Now, I'm moving forward with a sense of confidence, curiosity, and re-ignited passion, all qualities that I hope will *differentiate me as I enter the next chapter in my career. And this wouldn't have been possible without the support and guidance from the following incredible people.

The first set of thanks really must go to Ian Parish for being an exceptional supervisor and mentor. Despite setbacks with enrolment and lockdowns before I even started, you still took a chance on me and entrusted me to pursue such an exciting fundamental question. Thank you for showing me how to be a well-rounded scientist. You're as knowledgeable in immunology as you are a genuine stand-up guy! And I can honestly say that because of you, I now have an enriched understanding of immunology and a more profound sense of scientific wisdom and values, all of which I will carry with me throughout my scientific career. Thank you for your patience, generosity, and true passion for science! Your leadership and scientific insight will undoubtedly lead to meaningful discoveries in immunology, and I am truly honoured to have been a small part of that as your student.

I want to thank my professional mentors, Joseph Trapani, Kristin Brown, and Rachel Rutishauser, for helping me understand what the PhD journey is about and how to navigate it properly. Joe, your presence in our PhD catchups, along with your support and nuggets of wisdom, has been invaluable. Kristin, I'm truly grateful to you because I can't stress enough that our coffee chats were what helped me build my confidence as a scientist in academia. Rachel, you have been pivotal in sparking my interest in immunology, and I owe much of my decision to pursue a PhD to you. Thank you so much for cheering me on!

I feel so extremely lucky to be a part of such an amazing research team. I want to recognize all the past and current members of the Parish Lab: Sinead, Simone, Shienny, Maria, Avi, Sara, Kelly, Nicole, Brandon, Anni, Nihali, Ivan, Cherry, and Emily. It has been such a pleasure to work with such friendly and professional people like all of you. Thank you also for understanding that early mornings aren't my strong suit for lab meeting and harvests, and for being flexible with the time difference, where 9:00 AM Melbourne time is about 9:30-ish AM Christian time. An extra special thanks to Shienny and Kel for your crucial help with multiple long and complicated mouse experiments, and to Nicole and Ivan for the bioinformatic analyses for this thesis.

Being a PhD student at Peter Mac was nothing short of wonderful. I want to thank the members of my student committee and Committee Chair, Liz Christie, for their guidance and timely evaluation of my research progress. I also want to recognize the invaluable technical

support from the cores and facilities at Peter Mac, including the Animal Facility, Research Flow Core, Molecular Genomics Core, and Victorian Centre for Functional Genomics, without which the crucial data in this thesis wouldn't have been possible. Thanks also to the members of Cluster 10 and the Cancer Immunology Program for maintaining well-organized lab spaces and sharing experiment-saving reagents last minute. Additionally, I would like to acknowledge Krutika, Catherine, and Madusha from the Goel Lab, as well as Ben and Nenad from the Johnstone Lab, for assisting with the experiments and molecular analyses for Chapter 4 of this thesis.

Apart from the actual doctorate itself, I'm equally thankful for the life-long friends I have made at Peter Mac and in Melbourne. A special shout-out to Gurjeet, Nicole, Nihali, and Sinead for all the fun adventures, your invaluable support, and the good-natured roasting that have all kept me sane during my PhD. I can always count on you, gorgeous people, to remind me that life is all about balance (especially when you're already a few cocktails in). I also want to thank Mik, Anni, Brandon, Priyank, Madusha, Zoe, Fatimah, and Cherry for your camaraderie and positive energies. Whenever we hang out and have conversations, you all, in one way or another, have made my PhD journey more meaningful. I also want to acknowledge my Pinoy friends, Erika, Athena, Aaron, Kat, Alex, Ian, Neil, and Carlos, for making me feel at ease in Melbourne with our get-togethers and food trips— salamat sa pakikisama sa akin!

I honestly think I wouldn't have been able to complete this PhD if it weren't for my partner, Renz. Despite the global pandemic, the long distance, and the stress of being a graduate student, you have always made me feel safe and supported. You have and will always be my person through it all. Thank you for easing my mental and emotional burden when I feel lost amid failed experiments and the arduous thesis writing. Our nightly calls have kept me going through the toughest parts of my PhD. I am grateful for your love, patience, and encouragement, all of which have made me resilient and passionate enough to navigate this career in science. I'm excited to share this next chapter with you! Mahal na mahal kita!

Finally, I want to express my gratitude to my family, as this PhD is as much theirs as it is mine. To my siblings Gene, Nikko, and Kara, thank you for holding down the fort back home and giving me the freedom to pursue my dreams. To my parents, Evelyn and Panfilo, your love and support throughout my life have made me reach this significant milestone. You have always encouraged me to be who I am and believed in what I can achieve, and for that, I am beyond grateful. Though we don't say it all the time, but I love you all, and I hope I have made you proud. Daghan kaayo'g salamat sa tanan.

This thesis is dedicated to everyone here and to the many others whose time and effort were essential to the success of this research.

ABBREVIATIONS

ANOVA: Analysis of variance
AP-1: Activator protein 1
APCs: Antigen-presenting cells
Arm: Armstrong strain of LCMV
ASXL1: Additional sex combs like 1
ATF: Activating transcription factor
BACH2: BTB domain and CNC homology 2
BAF: BRG1/BRM-associated factor
BATF: Basic leucine zipper ATF-like transcription factor
BCR: B cell receptor
Bcl2: B-cell lymphoma 2
Bcl6: B-cell lymphoma 6
Bim: Bcl-2-like protein 11
Blimp-1: B-lymphocyte-induced maturation protein 1
bZIP: Basic leucine zipper
CA-NFAT1-RIT: Constitutively active NFAT1-R468, I469, and T535
CAR-T: Chimeric antigen receptor T cell
CCA: Canonical correlation analysis
CCR7: C-C chemokine receptor type 7
CD: Cluster of differentiation
CD127: Interleukin-7 receptor alpha chain
CFU: Colony forming units
Cl.13: Clone 13 strain of LCMV
Co-IP MS: Co-immunoprecipitation Mass Spectrometry
CRE: cAMP-responsive element
CRISPR: Clustered regularly interspaced short palindromic repeats
CTV: CellTrace Violet
CUT&RUN: Cleavage Under Targets & Release Using Nuclease
CX3CR1: C-X3-C chemokine receptor 1
CXCR3: C-X-C chemokine receptor 3
CXCR5: C-X-C chemokine receptor 5
cRPMI: Roswell Park Memorial Institute Medium
CTLA-4: Cytotoxic T-lymphocyte-associated protein 4
DAG: Diacylglycerol
DGKζ: Diacylglycerol kinase zeta
DMEM: Dulbecco's Modified Eagle Medium
DNMT3A: DNA methyltransferase 3A
DC: Dendritic cells
EECs: Early effector cells
EED: Embryonic ectoderm development
EGR2: Early growth response protein 2
EGR3: Early growth response protein 3
Eomes: Eomesodermin
ERK: Extracellular signal-regulated kinase
FACS: Fluorescence-activated cell sorting
FOXO1: Forkhead box O1
GSEA: Gene set enrichment analysis
GO: Gene Ontology
HMG: High-mobility group
ICB: Immune checkpoint blockade
IFN: Interferon
IKZF2: IKAROS family zinc finger protein 2
IL: Interleukin
ILC: Innate lymphoid cell
IP3: Inositol trisphosphate
IRF4: Interferon regulatory factor 4
ITAMs: Immunoreceptor tyrosine-based activation motifs
JAK-STAT: Janus kinase-signal transducer and activator of transcription pathway
JNK: cJun N-terminal kinase
KLRG1: Killer cell lectin-like receptor subfamily G member 1
LAG3: Lymphocyte-activation gene 3
LCMV: *Lymphocytic choriomeningitis virus*
LM-33: *Listeria monocytogenes*- gp33
LM-OVA: *Listeria monocytogenes*-Ovalbumin
MAC-Seq: Multiplexed analysis of cells sequencing
MACS: Magnetic-activated cell sorting
MAPK: Mitogen-activated protein kinase
MFI: Mean/median fluorescence intensity
MHC: Major histocompatibility complex
MNN: Mutual nearest neighbour
mTECs: Medullary thymic epithelial cells
NF-κB: Nuclear factor kappa-light-chain-enhancer of activated B cells
NFAT: Nuclear factor of activated T cells
NGS: Next-generation sequencing
NK cells: Natural killer cells
NR4A1: Nuclear receptor subfamily 4 group A member 1
OVA: Ovalbumin
PAMPs: Pathogen-associated molecular patterns
PCR: Polymerase chain reaction
PD-1: Programmed cell death protein 1
PFU: Plaque-forming units
pMHC: Peptide-major histocompatibility complex
P.I.: Post-infection
PI3K: Phosphatidylinositol 3-kinase
RIP-OVA: Rat insulin promoter–ovalbumin
ROIV: Retro-orbital intravenous injection
RUNX: Runt-related transcription factor

SLECs: Short-lived effector cells
sgRNA: Single guide RNA
SLAMF6: Signaling lymphocytic activation molecule family member 6
SWI/SNF: Switch/sucrose non-fermentable complex
TCF1: T cell factor 1
TCR: T cell receptor
TCSM: Stem cell–like memory T cells
T_{CM}: Central memory T cells
TCPTP: T cell protein tyrosine phosphatase
TEM: Effector memory T cells
T_{EX}: Exhausted CD8+ T cells
Tfh: T follicular helper cells
TGF: Transforming growth factor
TIGIT: T cell immunoreceptor with Ig and ITIM domains
TIM-3: T cell immunoglobulin and mucin-domain containing-3
TITCs: Tumour-infiltrating T cells
TME: Tumour microenvironment
TPA: 12-O-Tetradecanoylphorbol-13-acetate
T_{PEX}: Progenitor exhausted T cells
TPMs: Transitional/precursor memory T cells
TOX: Thymocyte selection-associated high mobility group box protein
T_{RM}: Tissue-resident memory T cells
TRE: TPA-responsive element
Tregs: Regulatory T cells
UMAP: Uniform Manifold Approximation and Projection
V(D)J: Variable, diversity, and joining gene segments
WEHI: Walter and Eliza Hall Institute
ZAP70: Zeta-chain-associated protein kinase 70
ZEB2: Zinc finger E-box-binding homeobox 2

LIST OF FIGURES

Chapter 1

Figure 1.1 Tolerance and Exhaustion within CD8+ T cell Differentiation

Chapter 3

Figure 3.1 TOX expression of distinct differentiation states

Figure 3.2 Optimisation and functional validation of TOX gene deletion via CRISPR

Figure 3.3 TOX loss neither impairs tolerance induction nor promotes effector differentiation

Figure 3.4 Maintenance of tolerance is not disrupted upon TOX deletion, even under supplemented differentiation signals

Chapter 4

Figure 4.1 Transient expression kinetics of Jun family members during *in-vivo* CD8+ T cell differentiation

Figure 4.2 *In vitro* activation protocol for Co-IP MS analysis

Figure 4.3 Shared protein interaction partners of all Jun family members

Figure 4.4 Protein interaction partners unique to JunB

Figure 4.5 Protein interaction partners unique to cJun

Figure 4.6 Protein interaction partners unique to JunD

Figure 4.7 Genomic binding profiles of Jun family members

Figure 4.8 Genomic occupancy of Jun proteins at known NFAT binding sites

Chapter 5

Figure 5.1 Optimisation of CRISPR-mediated gene deletion of AP-1

Figure 5.2 Reduced NFAT/AP1 transcriptional activity following CRISPR-mediated deletion of AP-1

Figure 5.3 AP-1 deletion impairs effector CD8+ T cell survival and function

Figure 5.4 Re-expression of Jun proteins ex vivo at days 3, 5, and 8 p.i.

Figure 5.5 Expression of canonical markers associated with tolerance or exhaustion by residual AP-1 sgRNA cells

Figure 5.6 Phenotypic effects of individual and combined gene deletion of AP-1 family members during effector differentiation

Figure 5.7 Genome editing outcomes of CRISPR-edited cells pre- and post-adoptive transfer and infection

Figure 5.8 Influence of AP-1 deletion on exhausted cell differentiation

Figure 5.9 Transcriptomic profiling of AP-1 deficient cells during early activation by MAC-seq

Figure 5.10 Memory formation and maintenance following cJun and/or JunD deletion

Figure 5.11 Effects of cJun deletion on memory recall

Figure 5.12 cJun deficient memory cell fitness after repeated immune challenge

Chapter 6

Figure 6.1 Interrogating the function of TOX and AP-1 in tolerance and exhaustion

Appendix

Figure S1 Gating strategies to identify TCR transgenic CD45.1+ CD8+ T cells within different *in vivo* models

Figure S2 Gating strategy to identify CD8+ T cells transduced with NFAT/AP1-driven GFP reporter

Figure S3 Gating strategy for sort

LIST OF TABLES

Chapter 1

Table 1. General definitions of terms related to CD8+ T cell regulation

Table 2. Summary of TOX function in different immune cell types

Table 3. Summary of features and reported human protein interactors of AP-1 family members

Chapter 2

Table 4. Summary of Reagents and Materials

Table 5. List of antibodies used and their relevant information

Table 6. Summary of experimental kits

Table 7. Mouse pathogens used for infection studies

Table 8. Mouse strains utilised and their relevant information

Table 9. Summary of adoptive transfer experiments

Table 10. Summary of *in vitro* stimulation conditions according to each experiment

Table 11. Summary of sgRNAs used in this thesis

Table 12. Primers used for PCR for DNA sequencing of KO regions

Table 13. Touchdown PCR Parameters for DNA sequencing of KO regions

Table 14. PCR Parameters for CUT&RUN Library Preparation

Chapter 4

Table 15. Top enriched Reactome pathways of genes associated with CUT&RUN peaks shared among all Jun family members

Table 16. Top enriched GO Biological processes of genes associated with CUT&RUN peaks shared among all Jun family members

Table 17. Top enriched Reactome pathways of genes associated with peaks shared with all Jun family members (CUT&RUN) and NFAT (ChIP-Seq).

Table 18. Top enriched GO Biological processes of genes associated with peaks shared with all Jun family members (CUT&RUN) and NFAT (ChIP-Seq).

Chapter 6

Table 19. Comparison of phenotypic and molecular features between T cell tolerance and exhaustion

Appendix

Table S1. Significant protein interaction partners of JunB (LogFC>0, p. value<0.05, n=136) in CD8+ T cells activated *in vitro* for 24hrs

Table S2. Significant protein interaction partners of cJun (LogFC>0, p. value<0.05, n=127) in CD8+ T cells activated *in vitro* for 24hrs

Table S3. Significant protein interaction partners of JunD (LogFC>0, p. value<0.05, n=70) in CD8+ T cells activated *in vitro* for 24hrs

Table S4. Top enriched transcription factor binding motifs among bound genomic regions shared by all Jun family members

Table S5. Top enriched Reactome pathways and GO Biological processes of genes associated with the unique CUT&RUN peaks of JunB

Table S6. Top enriched Reactome pathways and GO Biological processes of genes associated with the unique CUT&RUN peaks of cJun

Table S7. Top enriched Reactome pathways and GO Biological processes of genes associated with the unique CUT&RUN peaks of JunD

CHAPTER 1 Introduction

1.1. Overview of the Immune System

An essential requirement of living organisms is their ability to detect and eliminate harmful entities from within themselves and their surrounding environment. Many organisms' survival is constantly challenged by external threats of toxic substances, opportunistic foreign invaders, and the internal risk of host cells and/or homeostatic processes going askew. This makes it evolutionarily advantageous for organisms to develop properties that will fend off all these potential threats to survival[1]. As life became more complex, an intricate network of molecules, cells, and tissues safeguarded the survival of various species against an assortment of biological threats across multiple generations. This impressive biological network is collectively referred to as the "Immune System", and our capacity to resist these threats is referred to as "immunity"[2].

The fundamental concept of "immunity" can range from physical barriers, such as the cell wall of a unicellular organism[3] that protects it from harsh environments, all the way down to the vast repertoire of receptors in vertebrates that recognise dangerous non-self-entities[2]. Vertebrates, such as humans, possess one of the more sophisticated iterations of the immune system. The vertebrate immune system is canonically comprised of two distinct but synergistic arms: the innate immune system and the adaptive immune system[4,5]. The interplay between these arms empowers the body to tackle diseases of varying aetiologies and severity, ranging from the common cold to a metastatic tumour. Conceptually, innate immunity is responsible for an immediate but less specific response against a disease-causing entity, while adaptive immunity is a delayed but amplified coordinated response that is exceptionally precise at eliminating a specific target[4,6].

1.1.1. Innate Immune System and their Role in Antigen Presentation

The innate immune system represents the first line of defence against harmful substances and pathogens. It includes physical and chemical anatomical barriers to prevent the entry of anything harmful into the body. As these initial barriers sometimes get breached, a diverse array of haematopoietic cell types (mostly white blood cells i.e. leukocytes), are recruited to eliminate and control the pathogen or malignancy[6]. These innate immune cells, such as dendritic cells (DCs), macrophages, neutrophils, eosinophils, and basophils, achieve this through potent phagocytic capacity and the ability to release toxic materials by degranulation[7]. However, to ensure that these potent cells recognise and attack only the harmful agents and not the host cells, elaborate molecular recognition mechanisms are employed. These include pattern recognition receptors (PRR), which include Toll-like receptors (TLRs) expressed by innate immune cells, that specifically bind to the pathogen-associated molecular patterns (PAMPs) of various pathogens, such as evolutionarily

conserved bacterial/fungal cell wall components and viral nucleic acids[7,8]. Innate immune cells also secrete various soluble factors, such as inflammatory cytokines, to aid in the recruitment of additional immune cells (both innate and adaptive) to the response site[7].

While innate and adaptive immunity are often presented as distinct arms of the immune response, coordinated crosstalk between these two components of the immune system is critically important for immune function. Notably, a crucial feature of innate immune cells is their role in "antigen-presentation", which is their ability to constantly survey their molecular environment and process it into a form called "antigens" that can be recognised by a specific type of adaptive immune cell, called "T cells" (discussed further in Section 1.2)[6,9]. Importantly, the context of antigen-presentation allows the innate immune system to dictate the magnitude of the immune response to limit the potentially adverse effects of adaptive immunity such as immunopathology and attack of self-tissues (autoimmunity). Thus, antigen presentation is not a passive process, with the cells that present antigen instead playing an active role in guiding the downstream adaptive immune response. Antigen presentation is primarily performed by professional antigen-presenting cells (APCs), which primarily comprise of dendritic cells and macrophages, but also another adaptive immune cell called "B cells"[10-12]. APCs can recognise and phagocytose exogenous antigens (i.e. outside the cell), such as molecules from extracellular pathogens such as bacteria and fungi, as well as endogenous antigens (i.e. originating from within the cell), which include viral particles in infected cells or potential oncogenic proteins[7]. Within the APC, these antigens are internalised into endosomes and broken down into smaller peptide fragments that can then bind to Major Histocompatibility Complex (MHC) molecules to form stable peptide-MHC (pMHC) complexes [13]. These pMHC complexes can then be transported to the cell surface of the APC to facilitate presentation of the peptide antigen to T cells, a critical process in engaging and regulating T cell immunity (see Section 1.2)[14-16].

Depending on the origin and size of the peptide, two distinct classes of MHC molecules, namely MHC Class I and MHC Class II, exist to "present" the antigen. MHC Class I molecules present endogenous antigen-derived peptides comprising of 8-10 amino acids and are utilised by most nucleated cells[17-19], especially in cases of infection or tumorigenesis, where the antigen is derived from within the cell. On the other hand, MHC Class II molecules typically present longer peptides (13-18 amino acids) that come from extracellular antigens and are almost exclusively found on APCs[19,20]. The only exception to the rule that extracellular and intracellular antigens are segregated between MHC Class II and MHC Class I, respectively, is a process called "cross-presentation". Cross-presentation is a process where certain types of dendritic cells can present exogenous phagocytosed antigens on MHC Class I[21,22]. This allows APCs to activate T cell immunity against MHC Class I antigens even when the target intracellular antigens are not endogenously produced by the APC (such as antigens

derived from tumour mutations or viral infection, where APCs are typically not virally infected/transformed but will phagocytose material from dying infected/transformed cells). More importantly, the two MHC molecules also differ in the type of adaptive immune cell that they engage; MHC Class I primarily activates CD8+ T cells[15], which is a type of adaptive immune cell and will be discussed in more detail in Section 1.3. Conversely, MHC Class II activates CD4+ T cells, which are a different type of adaptive immune cell that are crucial in regulating the activity of CD8+ T cells and other adaptive immune cells[23]. Thus, the innate immune system is not only important as a distinct arm of the immune system but additionally as a critical regulator of the adaptive immune response.

1.1.2. Adaptive Immune System

The adaptive immune system is defined by two vital tenets, namely high specificity and memory. Adaptive immunity is uniquely equipped to mount an acute response tailored against a specific antigenic threat and then develop "immunological memory", referring to the generation of a quicker and more robust immune response upon re-exposure to the same antigen[6]. This branch of the immune system is primarily composed of a subset of leukocytes called lymphocytes. Lymphocytes originate from lymphoid progenitor cells and can be further subdivided into B or T lymphocytes, which were both designated in the 1950s and 60s according to the tissue site where they were first discovered to mature in: B lymphocytes or B cells in the Bursa of Fabricius of birds (or in the bone marrow within other animals), while T lymphocytes or T cells in the thymus of mice[24,25].

1.1.2.1. Clonal Selection Theory

Lymphocytes uniquely operate under Burnet's clonal selection theory which provides the conceptual foundation of adaptive immunity[26,27]. This theory describes how B and T lymphocytes facilitate the adaptive immune response at the cellular level through 4 key principles.

First, the clonal selection theory postulates that each lymphocyte expresses a unique genetically encoded receptor that can recognise a specific antigen. The relevant antigen receptors that fulfill this criteria were subsequently identified as the B cell receptor (BCR) in B cells, and similarly, the T cell receptor (TCR) in T cells[6]. The required diversity of lymphocyte antigen receptors is stochastically generated through V(D)J recombination, or the random rearrangement of the many variable (V), diversity (D), and joining (J) gene segments encoded within the DNA of lymphocyte progenitor cells as they mature into either T or B cells[28,29]. Generation of a functional antigen receptor requires the productive assembly of a single V, D and J gene segment. Given that there are many gene segments to randomly select (e.g. ~50 V segments, 27 D segments and 6 J segments for just the heavy chain of the human BCR[30]),

coupled with error prone repair mechanisms that add in additional nucleotides during recombination, there is an enormous number of potential lymphocyte receptors. For example, it's been estimated that there are 100 trillion possible human TCRs[31]. This random recombination process occurs independently in each developing T or B cell, meaning every newly generated lymphocyte bears a unique antigen receptor. Furthermore, given that the immune system of a healthy adult is comprised of about 600-920 billion lymphocytes it can be posited that the adaptive immune system possesses a vast magnitude of antigen-specificities[32,33]. This incredible diversity means that the adaptive immune system can respond to a wide range of endogenous and exogenous threats.

However, this random recombination process can result to antigen receptors that can recognise almost any potential molecule, which will include "self" molecules derived from the body's own tissues, and benign environmental molecules[34]. Thus, the second principle of clonal selection theory is that immature lymphocytes bearing receptors specific for ubiquitous "self" molecules will be deleted during maturation, thereby preventing rampant autoimmunity via the exclusion of self-reactive lymphocytes from the adaptive immune pool.

The third principle of clonal selection posits that "antigen recognition", or the interaction between the antigen and its specific lymphocyte receptor (e.g. BCR or TCR), results in the activation and proliferation of the lymphocyte specific for that antigen[35]. Finally, the clonal selection theory also correctly hypothesises that following antigen recognition, the activated lymphocyte will proliferate and produce "clones", i.e. progeny with the same antigen-receptor specificity[36]. Given that the antigen receptor is genetically encoded within the DNA of the responding lymphocyte and will thus be replicated and passed on to daughter cells during cell division, it is easy to understand how the proliferative expansion of a clone occurs. This "clonal expansion" process will immediately create a pool of "effector cells" responsible for carrying out the appropriate immune response against the target antigen. T cells can undergo this process of clonal expansion up to 50,000 times in an acute infection[37-39]. Furthermore, this process also ensures that the immune response remains highly specific against antigens that "selected" the lymphocytes bearing the corresponding unique receptor. This, in turn, leads to the generation of a diverse clonal effector immune pool, of which a small fraction persists long-term, forming the cellular basis for immunological memory[40,41] . Thus, the clonal selection theory explains both the capacity of the adaptive immune system to specifically recognise almost any foreign antigen while sparing self, and additionally how the adaptive immune system retains a memory of past infections.

1.1.2.2. T and B cells

Although both T and B cells undergo clonal selection, they differ in terms of their canonical immune functions[6]. B cells generate humoral immunity, which involves the

production of protective antibodies, which are secreted versions of the B cell receptor capable of directly binding and neutralising, or flagging for downstream immune attack, both pathogens and toxins. In addition, B cells also can present antigens compared by their B cell receptor on MHC. In contrast, T cells do not have antigen-presentation capacities and do not produce soluble antigen receptors. Instead, T cells are crucial in cell-mediated immunity, which is responsible for detecting and directly eliminating infected or tumorigenic cells, as well as phagocytosed extracellular pathogens, in a regulated manner[42].

T cells are conventionally further subdivided into two very distinct subsets on the simple basis of expression of two types of "cluster of differentiation" (CD) markers: CD4 and CD8, which both are cell surface glycoproteins that act as coreceptors for the TCR during antigen recognition. Discovered during the advent of flow cytometry in the late 1970s, this convenient delineation between CD4+ and CD8+ T cells signifies the two widely accepted classical roles of T cells in facilitating the immune response[43-45]. As mentioned above, CD4+ T cells, traditionally referred to as helper T cells, are important regulators of the immune response. Their widely recognised function is to produce cytokines and provide the necessary costimulatory signals to help other immune cells to mount an effective and appropriately regulated immune response capable of clearing a pathogen[46,47].Relevant to this thesis, various types of CD4+ T cells also regulate the activity of the CD8+ T cells[48]. In this dissertation, the focal point will be the functionality of CD8+ T cells in various *in vivo* and *in vitro* models and their implications for human health, particularly in cancer. Hence, all subsequent sections of this introduction will focus on the knowledge, paradigms and unanswered questions within the CD8+ T cell field.

1.2. CD8+ T cells

CD8+ T cells, often referred to as "killer T cells" or "cytotoxic T cells", are pivotal mediators of adaptive immunity, responsible for the detection and direct killing of infected cells and abnormal host cells, such as in cancer[42,49]. Many of the immune-related therapies that have had a broad societal impact, such as vaccines, immune checkpoint blockade, and chimeric antigen receptor (CAR)-T cell technology, are at least in part if not largely dependent on the functionality of CD8+ T cells. This highlights the potential of CD8+ T cells to influence human health.

1.2.1. Antigen Recognition and Activation

Like their CD4+ counterparts, conventional CD8+ T cells express an αβ T cell receptor (i.e. a TCR encoded by the TCRα and TCRβ gene loci) that principally recognises a diverse array of peptide antigens[18]. However, unlike CD4+ T cells, CD8+ T cells are MHC-I antigen restricted and uniquely express the CD8 co-receptor, which interacts almost exclusively with

MHC-I molecules thereby contributing to the MHC-I restriction of CD8+ T cell antigen recognition[50]. In particular, the CD8 co-receptor, a member of the immunoglobulin superfamily (IgSF) of coreceptors, can increase the antigen sensitivity of CD8+ T cells, fortify the immunological synapse formed upon TCR:pMHC engagement, and boost the signalling pathways engaged following antigen recognition[51,52]. As MHC-I can be expressed by almost all nucleated cells, CD8+ T cells can recognise antigens derived from both pathogens within infected cells, and somatic mutation-associated neoantigens from transformed host cells.

CD8+ T cell immunity is initiated from a pool of “naïve” CD8+ T cells that constantly recirculate between the blood and secondary lymphoid organs, such as the spleen and lymph nodes. Naïve CD8+ T cells are mature T cells that have not yet encountered their specific antigen and exist in a metabolically and functionally quiescent state[53]. This inherent latency conserves metabolic resources, enabling long-term persistence while maintaining a state poised for activation upon antigen recognition. As mentioned before, these naïve CD8+ T cells also have a broad range of TCR specificities, with the overall TCR repertoire recently predicted to be approximately 100 million clonotypes[54]. In addition to TCR diversity, there is also evidence of transcriptional and epigenetic heterogeneity within the naïve T cell pool that influences the magnitude and quality of their differentiation (see Section 1.2.2) into more specialised subsets that elicit the CD8+ T cell-specific immune response[55,56].

For naïve CD8+ T cells to differentiate into functional effector cells, they must first find their antigen and then receive the appropriate signals for productive T cell activation. Naïve CD8+ T cells constitutively transit through lymphoid organs, constantly surveying lymphoid resident APCs (typically dendritic cells (DCs)) for antigens presented on their surface[57,58]. As the lymph nodes and spleen collectively capture antigen from all the body’s tissues, this provides a rapid and efficient way for naïve T cells to constantly monitor antigens across the body within a relatively short period of time (every ~24h). Upon encounter of their specific, or “cognate”, antigen, naïve cells undergo productive T cell activation which requires at least three distinct classes of extracellular signals. The first signal (i.e. Signal 1) is delivered downstream of antigen recognition when the TCR engages with pMHC complexes on the APC surface. In addition to the TCR-pMHC signal, productive activation of T cells typically also requires a second signal provided by co-stimulatory molecules (Signal 2)[59,60]. This signal is classically considered to be delivered through the interaction of the immunoglobulin superfamily coreceptor, CD28, on the T cell surface with its ligands, CD80 (or B7.1) or CD86 (or B7.2), expressed on the surface of the APCs[61,62], although a range of other co-stimulatory receptor-ligand pairs have been identified[63,64]. The importance of the first two signals in efficient T cell activation is emphasised with the success of CD28 immunomodulators in preventing T cell transplant rejection, and T cell autoimmunity in arthritis[65]. Finally, productive activation often also requires signals from cytokines secreted by APCs and/or other immune

cells, such as IL-12, IL-21 and type I interferons (IFN-α/β), which is often referred to as Signal 3[62,66]. Recent papers have also proposed for additional signal classes (e.g. metabolic signals as "Signal 4")[67-69], although ultimately separating these signals into discrete classes is probably an over-simplification. For example, some cytokines are presented in a membrane-bound manner (e.g. IL-15) like Signal 2, and many costimulatory molecules use cytokine related signalling domains (e.g. TNF receptor related signalling domains)[70,71] .

Productive T cell activation triggers formation of "the T cell immunological synapse". This coordinated interface between the TCR and the APC incorporates the pMHC-bound TCRs, costimulatory molecules, adhesion molecules and structural components important for the specialised functions of T cells[72]. It is through the immunological synapse that various signalling pathways are activated to ensure robust clonal expansion and survival of the responding T cells upon activation. Each of the 3 activation signals contributes to the downstream signalling events required for T cell activation. Signal 1 initiates the phosphorylation of a surface glycoprotein within the TCR complex called CD3, which contains immunoreceptor tyrosine-based activation motifs (ITAMs). Recruitment of the CD8 coreceptor to the pMHC-bound TCR complex by CD8 binding to MHC-I allows the intracellular Src-family tyrosine kinase, Lck, to phosphorylate the ITAMs of the CD3 complex[73,74]. This initiates an intricate signalling cascade, starting with the recruitment of another tyrosine kinase, ZAP-70 that facilitates the assembly of multiple protein signalling complexes called "signalosomes"[75]. Downstream signalling pathways induced by these signalosomes cause release of calcium from intracellular stores, activation of protein kinase C, as well as the production of the secondary messengers, diacylglycerol (DAG) and inositol trisphosphate (IP3), which subsequently activate the MAPK/ERK pathways[76-79]. Together, these signalling processes converge to activate transcription factor such as NF-κB, NR4A1, NFAT and AP-1[80-82]. These pathways are reinforced by Signal 2, particularly through activation of phosphatidylinositol 3-kinases (PI3Ks) that are required for many processes, including metabolic reprogramming of T cells. In contrast to Signals 1 and 2, Signal 3 typically activates cytokine signalling pathways by, for example, JAK-STAT signalling. This activates transcription factors such as STAT4, which are critically required for effector differentiation[83,84] . The transcription factors collectively activated by Signals 1, 2 and 3 induce the expression of a broad range of genes that enable the diverse cellular processes required for T cell activation, such as cytoskeleton reorganization, cytokine production, cell cycle initiation, metabolic adaptation, and epigenetic reprogramming[79,85-90]. For example, recently our lab demonstrated that the synergistic actions of Signals 1, 2 and 3 are required in early activated CD8+ T cells for induction of the transcription factor MYC that in turn enables the sustained protein translation capacity needed for robust proliferation and productive effector differentiation[91].

The evolutionary reason for multiple signals being required for productive initial T cell activation is to provide points of regulation to limit the detrimental aspects of a dysregulated T cell response (see Section 1.3). Once activated CD8+ T cells overcome these initial regulatory checkpoints, they then classically undergo effector and memory T cell differentiation.

1.2.2. Effector and Memory T cell Differentiation

A dynamic and adaptable differentiation process downstream of initial CD8+ T cell activation is crucial to appropriately tailor the T cell response to the specific immune challenge. As clonal expansion proceeds post-activation, incremental transcriptional, metabolic, and epigenetic changes occur within each progeny cell, ultimately resulting in a diverse cell population with a spectrum of CD8+ T cell differentiation states that have differential capacity to seed the immediate "effector" T cell response to eliminate the threat versus the long-term "memory" T cell response required to protect against reinfection (see Sections 1.2.2.1 and 1.2.2.2, respectively)[92-95]. Over the past 2 decades, various models have been proposed to explain T cell commitment to the effector versus memory lineages, and it remains a topic of contention within the immunology field [93,95-106]. Our constantly evolving understanding of this developmental process is based on studies utilizing various mouse acute infection models to dissect the differentiation trajectory of CD8+ T cells. These include mouse infection with acute lymphocytic choriomeningitis virus (LCMV)[107], *Listeria monocytogenes*, Vesicular stomatitis virus (VSV) and Herpes simplex virus 1 (HSV-1) among others[108,109]. By tracking the downstream anti-pathogen T cell response via a variety of methods (e.g. tetramer staining for virus-specific CD8+ T cells, tracking of adoptively transferred virus-specific TCR transgenic T cells) in the presence or absence of genetic or environmental perturbations, these controlled systems have allowed researchers to track and dissect the molecular and functional dynamics of effector and memory T cell formation in response to acute infection. Interestingly, single-cell and fate-mapping analyses suggest that these early divergence events are partially probabilistic in nature, influenced by transcriptional and epigenetic features that stochastically vary between CD8+ T cells, as well as the strength and duration of external cues such as antigen stimulation, nutrients, and cytokines[110-113]. Despite ongoing debate around models of effector and memory T cell commitment, there are key concepts that are widely accepted in the field, which are summarised in this section.

After initial priming, the CD8+ T cell response to an acute challenge comprises 3 distinct phases, namely the effector, contraction, and memory phases[97]. During effector differentiation, cells first enter a phase of rapid proliferation and early fate determination. Responding naïve CD8+ T cells initially transition into less committed states that can include stem-like memory T cells (T_{SCM}) [114] or early effector cells (see Section 1.2.2), before eventually adopting a spectrum of more differentiated states by 5 to 8 days post-activation. At the extreme

ends of this differentiation spectrum are the more differentiated short-lived effector cells (SLECs) and the less differentiated memory precursor effector cells (MPECs) [115-118].

SLECs are marked by KLRG1 expression and represent the most expanded and terminally differentiated cell population that likely performs the bulk of target cell killing and cytokine production attributed to CD8+ T cells. Additionally, as their name suggests, SLECs also have diminished proliferative and survival capacity. Conversely, MPECs express the receptor for the homeostatic IL-7 cytokine, CD127, which contributes to long-term MPEC persistence. Although most MPECs acquire effector functions, a small proportion of these cells remain less differentiated, and these cells in particular (alongside MPECs more broadly) are likely the primary source of long-lived memory CD8+ T cells[117,119-121]. Thus, MPECs are regarded as the cellular foundation of immunological memory[104,115,122,123]. In contrast, once antigen (i.e. infected cells) is eliminated, the majority of SLECs rapidly die within the next ~7 days, with the remainder of SLECs slowly dying within the ensuing months. This process is mediated downstream of BIM-dependent apoptosis[124] and is referred to as the contraction phase of the response. The persisting cells that survive contraction seed the memory T cell pool. Long-lived, circulating antigen-specific memory CD8+ T cells adopt quiescent features akin to those of naïve CD8+ T cells and can in some cases persist for the lifetime of the host. However, unlike naïve T cells, long-lived memory CD8+ T cells are transcriptionally and epigenetically poised to reacquire potent effector characteristics (i.e. cytokine production, cytotoxicity) should the same antigen re-challenge the host. Memory T cells also possess strong proliferative capacity to enable clonal expansion upon antigen re-encounter. Remarkably, memory CD8+ T cells can sustain their proliferative and functional capacities even through multiple rounds of antigen challenge, exceeding the lifespan of the host organism [125]. Nevertheless, repeated antigen encounter can reduce the memory functionality, especially if the gap between antigen encounters is relatively short[126,127]. It is worth noting that the effective clearance of antigens is crucial for the transition to memory [128,129]. Failure to effectively clear the antigen can lead to a negative regulatory state, termed “exhaustion” (see Section 1.4), as is observed in chronic infections and multiple cancers where inflammation and antigen stimulation are still prevalent.

There is a significant heterogeneity within the memory CD8+ T cell pool, including specialised subsets such as effector memory T cells (T_{EM}), central memory T cells (T_{CM}), and tissue resident memory T cells (T_{RM}) [130]. Though each of these subsets has characteristic features of memory, they vary in their localisation and function (see Section 1.2.2.2). This diversity ensures that a secondary immune response is more effective and rapid upon rechallenge. Given the critical role of effector and memory cell differentiation in T cell immunity, understanding how these subsets are generated, alongside how they function and

how they're maintained, is vital to enable development of CD8+ T cell-based therapies for a multitude of diseases.

1.2.2.1. Effector CD8+ T cell subsets

The effector CD8+ T cell population can kill target cells by caspase-dependent apoptosis, either through the release of lytic molecules (e.g. perforin and granzyme), engagement of death receptors (e.g. via Fas) or by cytokine-induced cell death (e.g. via TNFα) [131-137] . As described above, effector cells can be subdivided into population with either more or less memory potential, such as SLECs and MPECs. In addition to differences in memory potential, these populations have different migratory properties. SLECs upregulate the chemokine receptor CXCR31 and fractalkine receptor CX3CR1, which both facilitate migration away from the lymph node and into inflamed peripheral tissues where the infected or transformed target cells typically reside[138]. In contrast, MPECs, are largely retained in the T cell zone of lymph nodes in part due to expression of the lymph node homing receptor, CCR7[139,140]. Cytokine production and killing capacity is largely comparable between bulk MPECs and SLECs outside of slightly enhanced IL-2 production by MPECs[117] meaning that the intrinsic capacity to eliminate target cells is largely comparable between the subsets. However, the enhanced capacity of SLECs to infiltrate inflamed tissues means that they likely are greater contributors to immediate target cell elimination.

Differentiation of early effector cells into either SLECs or MPECs depends on their stochastic exposure to a range of signals, including magnitude of antigen stimulation, pro-effector (IL-12, IL-2) [141,142] and pro-memory (IL-7, IL-15) cytokines, and exposure to niches that favour or restrain differentiation[139]. Other processes, such as asymmetric cell division, may contribute to the diversity within the effector T cell pool[99,143], although ultimately the cumulative exposure of early effector cells to these signals and processes likely determines the extent of differentiation. Cells that receive weaker differentiation signals are more likely to seed the MPEC pool, while in contrast increased differentiation erodes memory potential and drives SLEC formation. Exposure to these signals engages transcriptional programs that either drive terminal differentiation or restrain differentiation to maintain stemness, as will be discussed in more detail in Section 1.2.2.3.

1.2.2.2. Memory CD8+ T cell subsets

Consistent with the concept that memory potential is eroded with increasing differentiation, the earliest and least differentiated memory CD8+ T cell subset becomes evident from as early as day 3 of the immune response[121]. This population is sometimes termed "stem cell memory" or T_{SCM}, and is identified by ID3, TCF1, CD62L and Sca-1 expression alongside low expression of effector markers such as GzmB. Factors such as IL-

1 family cytokines [144] and inhibitory receptors[120] promote persistence of this subset likely by restraining differentiation. While they resemble naïve cells (i.e. display longevity and quiescence), these antigen-experienced cells can self-renew independent of antigen and inflammation, possess greater differentiation potential [106,145], and open chromatin around memory-relevant genes[146]. This population persists as a sub-population of the MPECs present at the peak of expansion and is important in seeding the long-lived circulating memory pool[121].

Once the infection or immune challenge is cleared, a diversity of subsets arises within the resulting memory cell pool. T_{EM} (CD62L-CCR7-CX3CR1+) rapidly surveys peripheral tissues and provide immediate cytotoxicity upon rechallenge, while T_{CM} (CD62L+CCR7+CX3CR1-) recirculate primarily through lymphoid organs, produce more IL-2, and exhibit superior persistence and antigen-independent self-renewal downstream of IL-7 and IL-15 signalling[147-150]. While T_{CM} do not have immediate cytotoxic capacity, they retain the capacity to rapidly re-express effector genes upon antigen re-exposure due to retention of an open chromatin structure at these loci [103,110,151-154] . T_{CM} are thus an important reservoir of effector T cells upon proliferative expansion after antigen re-encounter. T_{CM} predominantly derive from the early stem-like T cell subset described above and from the broader MPEC pool, while T_{EM} arise from a combination of more differentiated MPECs and persisting SLEC populations. While T_{CM} and T_{EM} are often considered independent subsets, there is evidence of limited interconversion between these subsets[101]. Moreover, intermediate populations between these subsets exist, such peripheral memory CD8+ T cells (T_{PM})[138,155], suggesting that memory cells likely exist on a continuum rather than purely being restricted to two distinct subsets.

While these circulating memory populations are critical for systemic immune surveillance, a specialised memory subset, tissue-resident memory T cells (T_{RM}), is situated mostly in the barrier tissues (e.g. skin, gut, and lungs), where they serve as frontline defenders against threats re-encountered at the tissue site of initial immune response[156-158]. T_{RM} constitutively express surface molecules that promote tissue retention, such as CD69 [159] and CD103[160], and the T_{RM} fate is driven by distinct transcriptional programs from circulating memory populations[161-163]. Recent data also show that T_{RM} display considerable heterogeneity in terms of function and transcriptional state across tissue sites[164]. Collectively, both T_{RM} and the diversity of circulating memory populations provide a multi-layered immune defence against rechallenge by pathogens or tumours.

1.2.2.3. Transcriptional and Epigenetic Control of Differentiation

T cell differentiation into effector cells requires large scale alterations in the T cell transcriptome. As noted in the sections on T cell activation, early TCR and costimulatory signals activate multiple transcription factors that mediate these transcriptional changes. Gene

expression changes are achieved via two main mechanisms: direct transcriptional induction or repression of genes that are already epigenetically "poised" for activation or repression, and opening of chromatin regions around differentiation-associated gene loci to enable changes in gene expression[165-169]. A range of transcription factors, often called "pioneer" factors that include AP-1 factors (see Section 1.8)[165,170-172] (e.g. BATF) and RUNX3[173-176], mediate these epigenetic changes by recruiting chromatin remodelling machinery (and other epigenetic regulatory factors) to relevant gene loci. The changes in gene expression mediated by transcription factors activated during initial T cell activation enable and support the cell cycle and metabolic changes required to enable T cell growth, proliferative expansion, and transcription and translation of the proteins required for effector T cell function.

As differentiation proceeds, competing gene programs are engaged depending on the signals that each cell is exposed to that either restrain differentiation to promote memory potential or accelerate expansion and terminal differentiation (see Section 1.2.2). This is often reflected by the differential expression and/or engagement of various antagonistic pairs of transcription factors that either reinforce the effector or memory gene program and often also antagonise each other's expression and/or activity. Notable examples include the homologous T-box transcription factors, T-bet and Eomes [177-179], where high T-bet levels promote terminal differentiation[180,181], while elevated Eomes supports memory differentiation[182]. As T-bet is induced by inflammatory cytokines that drive terminal differentiation, such as IL-12 via STAT4, environmental signals can shift the Tbet:Eomes balance to favour effector or memory differentiation[183]. Other examples of antagonistic pairs include Blimp1 and Bcl6[116,184-187], and Id2 and Id3 [188-190]. Similar to T-bet, Blimp-1 (induced by IL-2 via STAT5)[191,192] and Id2 (via IL-2/STAT5 and IL-12/STAT4) [190] are induced by inflammatory factors linked to terminal differentiation. Conversely, many of the memory-associated transcription factors, such as Bcl6[193] [193,194] and Eomes[194,195] are induced by STAT3 cytokines such as IL-10 and IL-21 that have been linked to memory formation[194]. Thus, environmental signals that T cells are cumulatively exposed to during clonal expansion and differentiation ultimately engage self-reinforcing transcriptional programs that either promote or restrain differentiation, with downstream implications for memory potential.

1.2.3. Regulation of CD8+ T cell immunity

While effector and memory CD8+ T cells are demonstrably beneficial to host health due to their capacity to clear pathogens and prevent re-infection, the same features that make these cells potent immune effector cells also pose a threat to the host if left un-regulated. CD8+ T cells pose two main classes of threat to host health. First, CD8+ T cells can be "on-target" (i.e. directed against something useful, such as a pathogen) but the effector response may be excessive and thus risk causing excessive collateral tissue damage

("immunopathology")[196,197]. This type of immune response is useful, so should ideally be retained but dampened to restrain tissue damage[198]. Second, CD8+ T cells can be off target, such as directed against self-antigens, in which case the response could cause an inappropriate attack on self-tissues ("autoimmunity")[199,200]. This type of response is typically not useful to the host, so ideally should be blocked from being initiated[201]. Due to the different regulatory requirements for these two classes of threat, two different types of regulatory checkpoints namely "tolerance" and "exhaustion", have evolved to respectively restrain autoimmunity and immunopathology during CD8+ T cell differentiation (Fig. 2.1). These regulatory processes are considered in detail in the next two sections. Understanding these regulatory processes is not only important because it provides insights into the causes of immunopathology and autoimmunity, but also because these regulatory processes are exploited by chronic infections and tumours to evade immunity and are thus a focus of immunotherapy approaches.

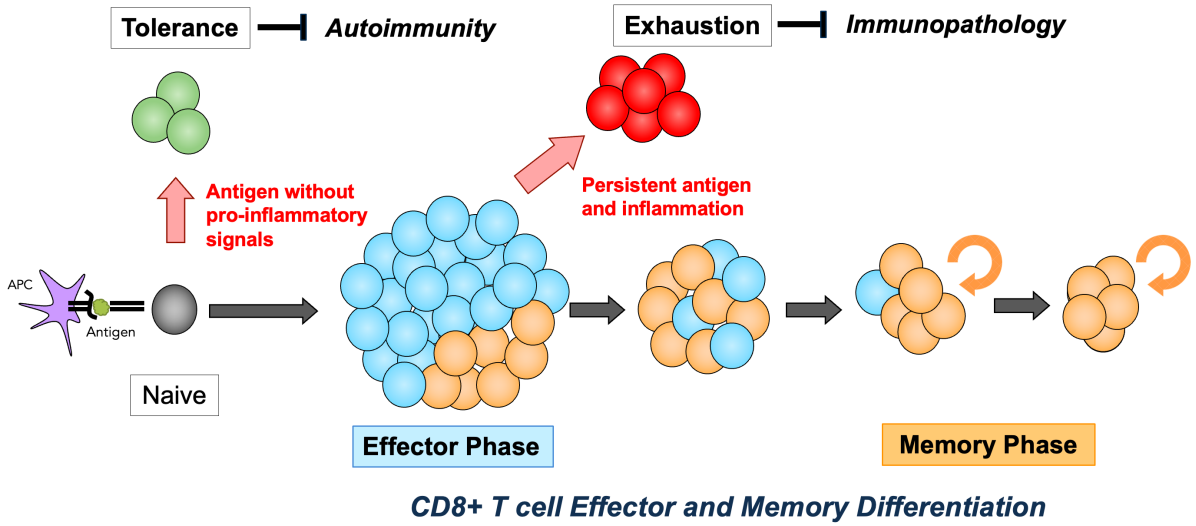


Figure 1.1. Tolerance and Exhaustion within CD8+ T cell Differentiation
CD8+ T cells adopt context-dependent regulatory cell states, tolerance and exhaustion, to prevent autoimmunity and immunopathology, respectively. Tolerance blocks initial activation and differentiation of cells exposed to chronic antigen without the necessary inflammatory signals (Section 1.3). Exhaustion dampens effector cell function and memory cell potential in response to chronic antigen coupled with immunosuppressive and pro-inflammatory cytokines (Section 1.4).

1.3. Tolerance

The clonal selection theory postulates that the adaptive immune system will delete lymphocytes bearing receptors specific for "self" molecules during development[202]. This process is called "central tolerance", and in the case of T cells, this process occurs during thymic development. Thymic development involves two main steps: "positive selection" (i.e. enrichment) of developing thymocytes bearing TCRs capable of binding MHC, followed by "negative selection" (i.e. elimination) of T cells bearing TCRs specific for self-antigens [203]. Thymic negative selection is thus the major "central tolerance" mechanism for T cells.

Negative selection occurs when developing thymocytes strongly bind self-antigens presented by both medullary thymic epithelial cells (mTECs) and thymic DCs [204,205]. These self-reactive thymocytes are then eliminated via BIM-dependent apoptosis [206,207]. However, this selection process is not perfect, and self-reactive lymphocytes still escape into the periphery. For example, T cells with low-avidity self-reactive TCRs often escape negative selection[208,209], with an estimated 25–40% of self-antigen-specific T cells bypassing thymic deletion due to lower avidity TCRs[210]. Additionally, not all self-antigens are efficiently expressed and/or presented in the thymus [211-213]. Moreover, T cells specific for harmless environmental antigens, such as food and commensal antigens, will unintentionally be generated and have the potential to initiate an aberrant inflammatory immune response[214-216]. For these reasons, a second layer of regulatory mechanisms, collectively referred to as "peripheral tolerance" mechanisms[201,217], have evolved to restrain the activity of these potentially dangerous peripheral T cells.

1.3.1. Mechanisms of Peripheral Tolerance: Ignorance, Anergy, and Deletion

While the term "peripheral tolerance" is sometimes used to describe the collection of processes that prevent overt autoimmune disease (which can involve a range of processes, including T cell exhaustion), in this thesis "peripheral tolerance" will be used to describe the mechanisms that block initial effector T cell activation and differentiation. Peripheral tolerance by this definition is widely recognized to occur when antigen recognition occurs in the absence of the innate immune cell-derived signals required for productive T cell activation (see Section 1.2.1)[218,219]. Depending on the dose or level of antigen encountered, there are 3 main peripheral tolerance outcomes for T cells: ignorance, anergy, and deletion[201,220].

Ignorance occurs when T cells fail to encounter sufficient antigen to become activated and thus remain in a naïve state[221]. This can occur for a variety of reasons, including antigen sequestration in tissues[221,222], low levels of antigen expression[220], or sufficiently low-avidity TCRs within the responding T cell population[208,221,223]. Unlike during anergy and deletion, ignorant T cells are not functionally inactivated and thus retain their competency to productively differentiate. This can occur if they encounter their antigen in an immunogenic environment, such as when their target antigen is released from peripheral tissues by inflammatory tissue damage in sufficient quantities to initiate antigen presentation[224] or if the T cells encounter a cross-reactive pathogen-derived antigen capable of engaging their TCR [208,225,226]. If sufficient self-reactive effector T cells are generated by activation of the ignorant T cell population, this can result in autoimmunity[208,222,225]. Recruitment of ignorant self-reactive T cells into the immune response likely explains the concept of "molecular mimicry", where a pathogen-derived antigen that mimics a self-antigen can trigger autoimmunity[221,227,228].

In contrast to ignorance, anergy and deletion result from productive antigen recognition in "steady-state" conditions (i.e. in the absence of infection, inflammation and/or innate

immune activation). In both anergy and deletion, the initial response to antigen is similar. Cells in both contexts proliferate after antigen encounter, however they typically fail to acquire effector functions (cytokine production and killing capacity), usually do not gain the capacity to infiltrate peripheral tissues, and instead exit cell cycle alongside upregulating a regulatory gene program that attenuates TCR signalling[91,201,229,230]. The primary difference between anergy and deletion is the outcome of the responding T cells. Anergic T cells persist long-term in a hypofunctional state characterised by ongoing TCR signalling deficiencies [231] while cells in deletion models progressively die by BIM-dependent apoptosis[232,233]. A proposed hypothesis is that these mechanisms are antigen load-dependent, where tolerance models with high antigen loads lead to anergy, potentially because strong TCR signalling is able to keep tolerant cells alive, while deletion occurs in models with lower antigen loads[234,235]. Of note, these assumptions are based on findings from reductionist peptide models, and more work is needed to fully elucidate these mechanisms *in vivo*. Nevertheless, the net immunological outcome for both anergy and deletion is that the responding T cells are effectively blocked from participating in a future immune response. Crucially, these tolerance mechanisms are actively enforced and maintained by sustained antigen exposure [236,237], which means that in some contexts, e.g. cancer, tolerant cells may constitutively "leak out" of this state (see Section 1.5).

Multiple cell types contribute to the tolerant state. Dendritic cells (DCs) are arguably one of the most important regulators of tolerance induction[48,62,238]. In the absence of infection or inflammation, the "default state" of DCs is to induce tolerance within responding T cells[62,201]. This ensures that self-reactive T cells are constitutively tolerised, as self-reactive T cells will respond to antigen in the absence of infection. The exact signals provided by DCs to promote tolerance versus effector differentiation are unclear. Based on early *in vitro* studies, it was classically assumed that tolerance occurs when co-stimulation is limiting, and that steady-state DCs would thus induce tolerance downstream of low co-stimulatory molecule expression. However, migratory DCs with high surface co-stimulatory molecule expression can still induce tolerance, suggesting that more complex combinations of signals dictate the outcome of T cell-DC interactions[62,238]. The most likely explanation is that the outcome of initial priming is not controlled solely by any one signal but is instead dictated by the overall sum of positive and negative signals encountered by the responding T cell in line with previous models of T cell differentiation[239].

Foxp3+ regulatory T cells (Tregs), a dedicated subset of immune suppressive $CD4^+$ T cells, are also important contributors to peripheral tolerance induction[48]. While loss of Tregs is known to lead to multifocal autoimmunity in mice and humans[240,241], and Tregs have been shown to inhibit immune responses at many different levels and in many ways[240,242]. It is still unclear to what extent Tregs prevent autoimmunity by directly enforcing tolerance versus

restraining later stages of the immune response (e.g. inhibiting autoreactive effector T cells). Nevertheless, there is strong evidence that Tregs directly enforce tolerance by competing for IL-2 access with tolerant CD8+ T cells via their expression of the high affinity IL-2 receptor, CD25. Treg depletion disrupts CD8+ T cell peripheral tolerance in experimental models in an IL-2 dependent manner[243] and there is evidence that Tregs constitutively quench IL-2 during steady-state T cell tolerance induction[244,245]. Given that IL-2 signalling is sufficient to breach CD8+ T cell tolerance[246], this axis is likely important in the peripheral tolerance process. Although Tregs have many other functions that may contribute to tolerance induction (e.g. they constitutively strip costimulatory molecules from DCs[247], more research is needed to definitively prove that these pathways directly contribute to tolerance induction. Other cell types likely contribute to the tolerance process but are out of scope for this thesis and have been reviewed elsewhere[201,248-250]. The extrinsic signals that CD8+ T cells encounter during tolerance induction collectively engage multiple downstream regulatory pathways within the T cell that will be considered in the next section.

1.3.2. Molecular Control of Tolerance

Tolerant CD8+ T cells transcriptionally diverge from differentiating functional effector cells *in vivo* within 12 hrs of initial activation[91]. While a portion of genes are similarly up- or down-regulated in differentiating tolerant and effector cells (e.g. cell cycle associated genes and activation markers such as *Cd44* and *Pdcd1*), tolerant cells selectively up-regulate regulatory genes (e.g. factors that inhibit TCR signalling such as *Dgkz*, *Cblb* and *Btla*) while failing to up-regulate key effector genes (e.g. *Gzmb*, *Tbx21*, *Il2ra*, *Ifng*). A large body of literature suggests that this altered transcriptional program is due to altered NFAT activity in the absence of AP-1 activation. Current models suggest that in the setting of productive effector T cell activation, both NFAT and AP-1 (classically in the form of a cJun and c-Fos heterodimer) are activated simultaneously and enter the nucleus together, which leads to the formation of high-affinity NFAT:AP-1 complexes that target and induce expression of genes that promote effector differentiation (see Section 1.2.2.3). During tolerance induction, however, AP-1 activation is muted, as evidenced by reduced chromatin accessibility at AP-1 binding motifs, resulting in an accumulation of partnerless NFAT in the nucleus[91,251-253]. While the cause of this imbalance is not fully understood, one hypothesis is that it relates to the duration of T cell-DC interactions during tolerance induction. In contrast to the long duration, stable interactions that occur between T cells and DCs during effector differentiation, T cell-DC interactions during *in vivo* tolerance induction are often transient[254-257]. Moreover, selective disruption of long-duration T cell-DC interactions during effector differentiation induces features of tolerance in the responding T cells[297]. As AP-1 is exported more quickly from the

nucleus than NFAT, sporadic contact between T cells and DCs causes NFAT accumulation in the nucleus in the absence of AP-1[258]. This enables the formation of low-affinity NFAT homodimers with an altered set of gene targets compared to the higher-affinity NFAT:AP-1 complex. In particular, NFAT homodimers induce a suppressive transcriptional program enriched for genes associated with anergy[252,259]. This includes induction of the transcription factors EGR2 and EGR3, regarded as transcriptional "master regulators" of tolerance[260,261]. EGR2 and EGR3 in turn induce factors that inhibit TCR signalling, including the E3 ubiquitin ligases, CBL-B and ITCH, which degrade proximal TCR signalling proteins[262,263], and the kinases DGKζ and DGKα, which inactivate the MAPK pathway[264,265]. In addition to EGR2 and EGR3, other NFAT-induced transcription factors may contribute to the tolerance gene program. For example, NFAT-induced NR4A1 expression[266] can augment tolerance through competitive binding with AP-1[267]. Collectively, this gene program causes the hypofunctional TCR signalling that is the hallmark of anergy, although this gene program is also induced prior to cell death during peripheral deletion consistent with diminished TCR signalling in cells undergoing deletion[91,229]. Of note, the pro-apoptotic protein BIM is transcriptionally induced during peripheral deletion, which may explain BIM-dependent death during deletion[229,232], although the transcriptional pathways responsible for *Bim* induction are still unknown.

Inhibitory receptors, such as PD-1, CTLA4 and LAG-3, are also induced in tolerant cells[91,229] and play functional roles in enforcing tolerance in some tolerance models[268-272]. These factors likely promote tolerance by disrupting TCR and/or CD28 signalling[273-275], and disrupting stable T cell-DC interactions[273,276-278]. However, despite evidence that these inhibitory receptors are NFAT homodimer targets[141] these receptors are typically induced to lower levels in tolerance relative to effector cells and other regulatory states, such as exhaustion[91]. Thus, these inhibitory receptors are not tolerance-specific genes and are instead likely activation-induced regulatory factors common to most activated T cell states.

Tolerant cells also adopt a distinct epigenetic state within 60hrs after antigen encounter that is characterised by a failure to open effector-associated chromatin regions, alongside retained naïve-specific regions, linked to diminished AP-1 motif accessibility (likely because of diminished AP-1 expression and/or activity)[91]. These changes align with previous observations in CD4+ T cells, indicating a failure to open effector-specific loci during tolerance induction[279]. Previous work has suggested that tolerant cells retain a "memory" of their prior tolerant state, suggesting that this unique epigenetic state may be heritable[280,281]. However, our lab has preliminary data suggesting that at least in the first week of tolerance induction, tolerant cells can be reprogrammed into effector cells by rechallenge with infection (S. Nüssing and I.A. Parish, unpublished observations). More work is needed to define the epigenetic stability of tolerance.

While the tolerant transcriptional state is important in tolerance maintenance, additional post-transcriptional mechanisms enforce tolerance. Innate immune activation by bystander infection (i.e. inflammation) is sufficient to both silence the anergy-specific gene program and rescue effector gene expression (i.e. override the tolerant transcriptional state), however it is not sufficient to breach tolerance because of a failure to up-regulate the translational machinery required to translate the effector gene program into protein[91,272]. Instead, additional antigen (i.e. stronger TCR signalling) in combination with inflammation is required to up-regulate protein translation capacity and breach tolerance[91]. This phenomenon was because only the synergistic actions of antigen and inflammation could trigger MYC-dependent induction of protein translation, consistent with prior work demonstrating that optimal MYC induction requires both TCR stimulation and inflammatory cytokines [282]. As most self-reactive T cells that escape thymic selection will be either low avidity or specific for a low abundance self-antigen, the extra requirement for strong TCR signalling to breach tolerance likely acts as an additional regulatory checkpoint to prevent bystander recruitment of ignorant self-reactive T cells into the immune response during infection (see Section 1.3.1).

1.4. Exhaustion

As noted in Section 1.2.3, an excessive effector CD8+ T cell response against a widely disseminated pathogen risks causing collateral tissue damage to the host ("immunopathology"). As chronic antigen encounter by effector T cells is an indication of widespread pathogen dissemination (i.e. a high risk of immunopathology), chronically stimulated early effector cells progressively lose effector functions and partially relinquish memory differentiation potential in a process called "exhaustion"[283-286]. Exhausted CD8+ T cells (T_{EX}) have been documented in human bacterial and parasitic infections, chronic viral infections such as Human Immunodeficiency Virus (HIV) and Hepatitis C Virus (HCV), and in cancer (see Section 1.5)[287,288]. T cell exhaustion has also been observed in autoimmune diseases, such as Type 1 diabetes and systemic lupus erythematosus (SLE)[289,290], which likely occurs downstream of chronic antigen engagement within self-reactive effector cells that have bypassed the tolerance checkpoint.

Exhausted CD8+ T cells exhibit sustained upregulation of various inhibitory receptors, altered metabolism, and a transcriptional and epigenetic profile distinct from conventional effector and memory T cell differentiation[288,291,292]. While sustained antigen exposure is the primary signal that drives exhaustion, other factors including immunosuppressive (e.g. IL-10, TGF-β, and IL-35) and pro-inflammatory cytokines (e.g. Type I IFNs) contribute to commitment to an exhausted fate[283,293,294]. As cell progressively commit to an exhausted state, they eventually enter an irreversible state of terminal exhaustion[283]. While sustained high expression of inhibitory receptors is a hallmark of exhaustion, inhibitory receptor expression

alone is not sufficient to identify exhausted T cells as many inhibitory receptors are also early activation markers (see Section 1.3.2), albeit often at lower levels than those observed during exhaustion. PD-1 is the best studied inhibitory receptor in exhausted T cells[91,277,295,296], however exhausted cells express many other inhibitory receptors, including CD160, CTLA4, LAG3, TIGIT, TIM3 and 2B4[297-305] . Inhibitory receptors are sometimes erroneously described as factors that "enforce" or "program" exhaustion, but they instead restrain exhausted T cell differentiation and expansion to enable long-term persistence in the face of chronic stimulation[306-308]. Nevertheless, PD-1 is important is restraining excessive expansion of exhausted T cells that can otherwise result in immunopathology [295]. In the case of PD-1 (and likely other inhibitory receptors), proliferation and differentiation is inhibited through disruption of both TCR and CD28 signalling[273-275].

The functional impairment associated with exhaustion does not equate to a complete loss of T cell function. Exhausted T cells still produce cytokines, kill targets and proliferatively differentiate, though often not to the same level as conventional effector cells. Nevertheless, their retained effector functions are important in pathogen control, such as during macaque infection with simian immunodeficiency virus (SIV)[309,310]. Moreover, exhausted cells gain features that conventional effector cells lack, such as the capacity to persist in the face of chronic stimulation[311], making these cells better suited to containment of a persistent infection. Thus, exhaustion is an adaptive response to a host-pathogen "stalemate", where the immune system, upon recognising its inability to fully clear the infection, establishes a long-term equilibrium to contain the pathogen while protecting the host from immunopathology [286].

1.4.1. Exhausted T cell differentiation

Exhaustion is a progressive differentiation process that generates cells along an exhaustion differentiation continuum[312-316]. CD8+ T cells first commit to an exhausted state in mouse infection models by ~day 5 post-infection, when a stem-like effector CD8+ T cell precursor population found in both acute and chronic infection is chronically stimulated[106,144,145,317]. These cells then enter a "progenitor exhausted T cell", or T_{PEX}, state[317-320], a stem-like exhausted cell state that represents the least differentiated exhausted cell population. T_{PEX} sustain the exhausted immune response by constitutive proliferative differentiation into downstream exhausted cell populations[318,319,321]. As cells progress from T_{PEX} into more differentiated downstream subsets, they progressively lose cytokine production capacity and increase inhibitory receptor expression. However, T_{PEX} lack cytotoxic capacity and reside in regions away from peak pathogen or tumour burden, meaning that the downstream exhausted subsets that both gain cytotoxic capacity, and infiltrate tumours and infected tissues, are more important than T_{PEX} in direct target cell killing. Instead, T_{PEX} serve as a resource population that sustains these downstream cytotoxic populations.

Multiple subsets of differentiated (i.e. non-T_{PEX}) exhausted populations have been identified, including a less committed intermediate exhausted population that can bifurcate to give rise to two terminally differentiated populations: a more functional and terminally differentiated “effector exhausted” population, or a less functional “terminally exhausted” population[292,318,322-328]. Effector exhausted cells are important in immune control of pathogens [325,327,329]. In contrast, the role of terminally exhausted cells, the least functional exhausted cell subset[325,326,330], remains unclear. Terminally exhausted cells have immunosuppressive properties[331], but given their residual cytotoxic and cytokine production capabilities, they may still play a net positive role in the immune response.

Upon antigen withdrawal, while differentiated exhausted populations disappear, T_{PEX} can persist and acquire features of T_{CM}[332]. However, these surviving cells retain a transcriptional and epigenetic “memory” of exhaustion that blunts expansion and leads to rapid re-expression of exhaustion-associated genes upon antigen re-encounter[333-338]. This adaptation may pre-emptively limit immunopathology upon re-encounter with a pathogen likely to rapidly disseminate.

1.4.2. Transcriptional and Epigenetic Control of Exhaustion

Chronic TCR stimulation during exhaustion has been hypothesised to trigger formation of low affinity NFAT homodimers in the nucleus likely due to low nuclear levels of AP-1 (see Section 1.8)[141]. Similar to tolerance, these NFAT homodimers are viewed as critical transcriptional regulators of commitment to exhaustion[141,339]. Nevertheless, evidence exists that NFAT may additionally form a complex with two non-canonical AP-1 family members/interaction partners, IRF4 and BATF, to promote exhausted cell differentiation, suggesting more complex transcriptional dynamics[340]. NFAT is then thought to induce downstream gene targets, including NR4A family transcription factors[266], EGR2[341] and TOX (see Section 1.7.1) that reinforce transcriptional and epigenetic commitment to an exhausted state, as well as enabling exhausted cell persistence. After commitment to exhaustion, transcriptional networks with parallels to those employed during effector and memory differentiation control the balance of exhausted subsets. T_{CM} associated transcription factors, including TCF1, ID3, FOXO1, MYB and BCL6[144,319-321,342-344], support T_{PEX} maintenance while SLEC-linked factors, such as TBET, BATF, ZEB2 and STAT5[312,316,345-347], promote formation of effector exhausted cells. Terminally exhausted cells in contrast are induced by a unique combination of transcription factors, including IRF7, IRF2, EGR2 and TOX[306,311,316,341,348-350]. Interestingly, in addition to promoting terminal exhaustion, TOX also promotes T_{PEX} maintenance (see Section 1.7.1). Alongside these transcription factors, epigenetic regulators such as DNMT3A, TET2, and ASXL1 facilitate downstream differentiation of T_{PEX}[351]. Thus,

collectively, the exhausted cell transcriptional program co-opts portions of the conventional effector and memory gene programs, alongside transcriptional regulators also linked to the tolerance program paired with novel regulators (e.g. TOX, IRF7, IRF2).

1.5. CD8+ T cell tolerance and exhaustion in Cancer

In recent years it has become increasingly clear that CD8+ T cells actively recognise and respond to cancer[69,352,353].This process, often called “cancer immune surveillance”, likely constantly prevents malignant cell outgrowth in healthy individuals, as evidenced by the increased cancer incidence seen in patients treated with immunosuppressive drugs[354-356]. For this reason, evasion of CD8+ T cell immunity is an essential requirement for tumour development[357]. A key means by which tumours evade immunity is by hijacking the tolerance and exhaustion processes. As tumours derive from self-tissues, tumours with low mutational burdens may not possess sufficient genetic changes to be easily genetically distinguishable from self. These tumours will often fail to elicit an immune response due to normal self-tolerance mechanisms. Consistent with this idea, low mutational burden tumours often do not induce a T cell response, leading to tumours not infiltrated by T cells (i.e. “cold” tumours)[358]. However, even when initial tumour mutations generate immunogenic antigens (often called “neoantigens”), the (often) uninflamed tumour will typically not activate (or potentially even actively suppress) the innate immune system. This can lead to antigen presentation within the tumour draining lymph node (TLDN) by steady-state tolerogenic DCs. Consistent with this idea, many experimental tumour models trigger tolerance-like processes during CD8+ T cell priming within the TDLN[91,359-362]. While this concept is still being investigated, it is thus possible that tolerance-like processes may be responsible for at least a subset of “cold” tumours.

Despite the barriers to the priming of an effector T cell response against cancer, many tumours are infiltrated with activated tumour-reactive T cells (“hot” tumours)[358] indicating that in at least a subset of tumours, T cells can bypass tolerance checkpoints to induce an immune response. However, unless the T cells eradicate the tumour (as occurs during cancer immune surveillance), the growing tumour may begin to outpace the T cell response. The resulting chronic antigen stimulation coupled with other tumour-derived signals, such as hypoxia[331,363,364] and/or relevant cytokines (see Section 1.4.1), can then induce CD8+ T cell exhaustion within those tumour-reactive T cells that have infiltrated the tumour[353]. While this enables tumour progression, such “hot” tumours still have better clinical outcomes than “cold” tumours[358,365] likely because of this pre-existing, albeit muted, immune response. Notably, “hot” tumours infiltrated by an exhausted tumour-reactive T cell population have emerged as the tumour type most likely to respond to cancer immunotherapies, such as PD-1 blockade. PD-1 blockade is thought to operate by mobilising tumour-reactive T_{PEX} to proliferatively expand and differentiate into downstream subsets, in particular effector exhausted cells[353]. The increased number of exhausted effector cells is then thought to enable tumour control.

Interestingly, the exhausted CD8+ T cell pool within the tumour is constitutively sustained by a population of stem-like CD8+ T cells within the TDLN[366-372]. This population has classically been considered a less differentiated subset of T_{PEX}, however the priming processes that give rise to these cells closely resemble tolerance induction[361,362] and these stem-like populations are transcriptionally and epigenetically almost identical to tolerant cells from classical self-antigen tolerance models[91]. Inversely, bona-fide tolerant cells up-regulate expression of genes previously associated with T_{PEX}, which include *Cxcr5*, *Slamf6*, *Bcl6*, *Eomes* and *Tcf7*[91]. It is thus more likely that the T_{PEX} population, represents cells arrested in a tolerance-like state that inefficiently but constitutively leak out of this state to seed the exhausted response within the tumour. This has clinical implications; as PD-1 blockade acts predominantly by mobilising this stem-like population in the TDLN rather than via the classical T_{PEX} in the tumour[319,366,372-377]. Hence, it is possible that PD-1 blockade operates by disrupting tolerance more than exhaustion.

1.6. Contrasting CD8+ Tolerance and Exhaustion

Tolerance and exhaustion emerge at different stages of the immune response, have different functional outcomes (i.e. tolerance prevents immunity, while exhaustion sustains a muted immune response), and likely evolved to combat different detrimental aspects of CD8+ T cell immunity. However, the fact that both are regulatory processes that have phenotypical similarities and overlapping molecular pathways has sometimes led to the misconception that these processes are effectively the same. Terms such as hyporesponsive, dysfunctional, anergic, exhausted, tolerant and quiescent have been used interchangeably to describe diverse negatively regulated states, including *bona fide* tolerant and exhausted T cells[284,378-380]. These terms are broadly defined in Table 1. This misconception continues to this day despite compelling evidence that tolerance and exhaustion are transcriptionally and epigenetically distinct[91,229,381]. Part of this confusion stems from a lack of consensus on the definition of the terms “tolerance” and “exhaustion”. For example, as noted in Section 1.3.1, “tolerance” is often defined as the processes that prevent overt autoimmunity, and multiple processes beyond classical tolerant states can prevent/limit autoimmune pathology (e.g. exhaustion[141,198,283,284,286,288]). However, beyond problems with definitions, this confusion exists in large part because features that are common to both states are often used to identify regulatory states. For example, cells are often labelled “exhausted” or “anergic” based on cytokine production and/or cytotoxicity deficiencies. This is problematic, as both tolerant and exhausted cells exhibit similar effector deficiencies, meaning that defects in effector function alone are not sufficient to label a cell “exhausted” or “tolerant”.

Table 1. General definitions of terms related to CD8+ T cell regulation

Terms	Definition
Tolerance[201]	Regulatory processes that prevent autoimmunity and maintain immune homeostasis. Canonically categorised into the following: • Central Tolerance: developmental checkpoints that prevent maturation of autoreactive thymocytes in primary lymphoid organs • Peripheral Tolerance: mechanisms that prevent or restrain T cell priming in secondary lymphoid organs, either through non-exposure to antigen (ignorance) or through responses following antigen recognition in the absence of innate immune signals which causes blunted TCR signalling and impaired effector function leading into either apoptosis (deletion) or long-term persistence (anergy). Throughout this thesis, the term "tolerance" will largely refer to processes associated with anergy and deletion.
Anergy	Tolerant cell fate characterised by long-term persistence, defective TCR signalling capacity, and failed acquisition of effector functions.
Deletion	Tolerant cell fate characterised by progressive BIM-dependent apoptosis
Ignorance	A scenario where functional self-reactive T cells have not encountered their cognate antigen
Exhaustion	Distinct T cell fate in response to chronic antigen and inflammation, characterised by restrained effector function, increased inhibitory receptor expression, and reduced memory potential to contain the pathogen while reducing immunopathology risk[283-286]
Quiescent	Cell state characterised by being in the G0 stage of the cell cycle, along with metabolic, transcriptional, and transcriptional dormancy, while retaining the potential to be activated[53]
Dysfunctional	Broad term proposed to describe T cell states arising from alterations in the activation and differentiation process[378]
Hyporesponsive	Broad term proposed to unify all known negative feedback processes that attenuate T cell activity during elevated and prolonged immune responses to limit immunopathology[382]

The overlapping molecular features associated with the induction, commitment, and maintenance of both tolerance and exhaustion fosters their conflation by the field. Deficiencies in TCR signalling capacity[201,344] are observed in both tolerance and exhaustion, but it's unclear whether these are caused by similar pathways. Regardless, these deficiencies, along with other upstream signals, trigger NFAT homodimer formation in the absence of AP-1, which is thought to underpin both states via a common/shared gene program (see Section 1.3.2 and 1.4.2). Key downstream transcriptional regulators of the NFAT homodimer regulatory gene program are then induced to variable degrees to facilitate transcriptional and/or epigenetic commitment to the tolerant and exhausted fates. These include TOX, NR4A transcription factors and EGR2[91,141,229,267,311,341,349,383]. Of these, EGR2 is a validated [285]critical transcriptional regulator of differentiation during both exhaustion[341] and tolerance[260,261]. Whether the shared induction of TOX and/or NR4A meaningfully result to the same differentiation program between tolerance and exhaustion is still unclear. Another shared feature are the signals utilised by both tolerant and exhausted cells to ensure survival and persistence. For example, the maintenance of both tolerance and exhaustion is driven by continuous antigen engagement. Furthermore, upregulation of PD-1 and other inhibitory receptors, such as

CTLA4 and LAG3, (see Sections 1.3.2 and 1.4.2) serves as a shared mechanism that characteristically dampens hyperactivation and differentiation, thus promoting long-term survival of tolerant and exhausted cells.

While notable, the overlapping features described above are minor compared to increasing evidence from detailed molecular profiling studies showing that tolerance and exhaustion are molecularly distinct processess[229,350,381,384]. Tolerant and exhausted T cells from both chronic infections and tumours do not share any common cell populations or differentiation intermediates based on comprehensive single cell transcriptomic profiling studies[91]. Tolerant cells are also epigenetically different from exhausted cells, including lacking the signature exhaustion-specific peaks within the *Pdcd1* and *Tox* loci[91]. Moreover, EGR2 targets completely different genes in the context of exhaustion versus anergy[341]. While the comparison in this later study was limited as it involved comparing EGR2 targets in exhausted CD8+ T cells versus anergic CD4+ T cells (meaning that some these differences may be due to CD4+ versus CD8+ T cell differences), these data collectively support the idea that tolerance and exhaustion are epigenetically and transcriptionally distinct. This aligns with the functional differences between exhaustion and tolerance. Tolerant cells almost completely lack effector functions (and in most cases likely never gain effector functions), do not typically infiltrate peripheral tissues and slowly die in the context of low antigen levels. Exhausted cells are derived from early stem-like cells that have already acquired effector functions, they retain some degree of effector functions and contribute to the immune response and can migrate into tissues (see Section 1.4). As mentioned at the beginning of this section, these functional differences likely exist because of differing evolutionary roles: blocking an immune response to prevent self-reactivity (tolerance) versus dampening but otherwise retaining a useful immune response to limit immunopathology (exhaustion). The fact that these states are molecularly different is clinically important given that immunotherapies may be variably targeting a combination of tolerant and exhausted states (see Section 1.5). If the way that these distinct regulatory states respond to therapy is different, then this could influence how we design the next generation of cancer immunotherapies.

Nevertheless, despite their molecular differences, data functionally demonstrating that different transcriptional pathways underlie both states are lacking. While the EGR2 study from our laboratory mentioned above is suggestive of different transcriptional programs between tolerance and exhaustion, this study still relied on the assumption that tolerance-associated EGR2 targets are conserved between CD4+ and CD8+ T cells[341]. In this thesis, I attempt to address this knowledge gap. First, I ask whether the transcriptional regulator, TOX, which is required for exhaustion but is also induced in tolerance (see Sections 1.3.2 and 1.4.2), is needed for tolerance induction. Second, given that NFAT activation in the absence of AP-1 has been proposed to induce both the exhaustion and tolerance gene programs, I investigate

the fate of AP-1 deficient cells in acute infection: do they become tolerant, exhausted or a combination of both states? Given their importance to this thesis, TOX and AP-1 are considered in more detail in the following sections.

1.7. TOX control of immune function

Thymocyte selection-associated high-mobility group box proteins or TOX proteins represent a subfamily of the high-mobility group (HMG) box superfamily of proteins with critical functions within the immune system (Table 1). A characteristic of TOX family proteins is the presence of a highly conserved and centrally located HMG box motif with an adjacent bipartite nuclear localisation signal sequence. Flanking these regions is an acidic N-terminal domain, mostly conserved among family members, which facilitates protein interactions, and a divergent C-terminal domain. Whether or not TOX has a specific DNA binding motif is still debated[385]. Unlike most other DNA-binding transcription factors, TOX proteins form part of the "structure-specific" sub-family of HMG-box factors that is thought to bind to DNA structures rather than sequences[386]. Members of this subfamily include TOX1, TOX2, TOX3 and TOX4[383,387,388] with TOX1, encoded by the *Tox* gene, usually referred to as "TOX"[389]. TOX was originally discovered as a highly expressed transcription factor in CD4+ CD8+ double-positive thymocytes whose transgenic over-expression altered CD8 versus CD4 lineage commitment during thymic development[390]. TOX is primarily expressed by various immune cells in lymphoid tissues[391]. TOX is also oncogenic in T cells, with transgenic over-expression facilitating T-acute lymphoblastic leukemia development by exacerbating genomic instability and promoting tumour cell proliferation[392]. However, in recent years, most work on TOX has focused on its role in T cell differentiation, particularly in CD8+ T cell exhaustion.

Table 2 Summary of TOX function in different immune cell types

Cell Type	Specific Role
Various Immune cells	Alters DNA shape via the HMG-box domain, allowing binding of other transcription factors [386,393]
Thymocytes (CD4+CD8+)	Regulates thymocyte differentiation during positive selection by activating lineage-determining transcription factors, i.e. RUNX3 and ThPOK[383,394]
CD4+ T cells	Promotes chromatin accessibility of genes that drive differentiation of T follicular helper cells (Tfh), Th2 cells and Tregs[395-398]
CD8+ T cells	Master regulator of exhaustion; facilitates early epigenetic reprogramming of CD8+ T cells towards the exhausted cell fate (see Section 1.7.1)
Innate Lymphoid Cells	Controls transcriptional regulation of early innate lymphoid cell progenitors[399]
NK cells	Facilitates IL-15-mediated NK cell differentiation and maturation[400]
T lymphoblasts	Drives oncogenesis by promoting genomic instability through inhibition of nonhomologous end joining (NHEJ) repair[392]

1.7.1. TOX function in CD8+ T cells

TOX is often regarded as the transcriptional "master regulator" of CD8+ T cell exhaustion[401]. Its role in exhaustion was first investigated due to its selectively high expression within exhausted CD8+ T cells in mouse and human chronic viral infection, and mouse and human tumours[306,311,349,350,402,403]. This strong induction during exhaustion is likely downstream of the regulatory NFAT homodimer gene program triggered by chronic antigen engagement, although NR4A factors and soluble factors, such as VEGF-A, may reinforce NFAT-induced TOX expression[141,349,350]. Subsequent functional data using *Tox* knock-out cells revealed three main impacts of TOX on exhausted cell differentiation: induction of the exhausted epigenetic and transcriptional state, suppression of the effector gene program, and long-term maintenance of exhausted T cell survival likely through T_{PEX} maintenance. Specifically, TOX deficient cells exhibited widespread loss of exhaustion-specific open chromatin regions, and parallel deficiencies in expression of key exhaustion-associated genes, including multiple inhibitory receptors (e.g. PD-1, CD160, TIGIT, TIM3, LAG3)[306,311,349,350,402,403]. In the case of PD-1, TOX deficient cells fail to open exhaustion-specific peaks in the *Pdcd1* locus, which may explain diminished PD-1 expression[306,350]. In parallel, TOX loss leads to the aberrant opening of chromatin regions linked to effector CD8+ T cell-associated genes (e.g. *Klrg1*), and causes a partial recovery of exhausted T cell cytokine function[311,349,350]. Thus, TOX transcriptionally and epigenetically promotes exhaustion-specific genes while repressing effector genes. Finally, TOX loss leads to severely impaired long-term exhausted T cell persistence likely downstream of T_{PEX} loss[306,311,349,350,402,403]. This may be due to direct epigenetic and transcriptional induction of T_{PEX} gene expression by TOX[306,311,349,350,402,403], but could also be downstream of diminished PD-1 expression given the known role of PD-1 in T_{PEX} maintenance (see Section 1.4). In addition to T_{PEX} loss, downstream exhausted cell differentiation is also disrupted. TOX loss causes diminished Eomes expression and elevated T-bet, leading to the expansion of effector exhausted T cell populations and loss of terminally exhausted cells[312]. In fact, partial TOX downregulation is likely normally required for the formation of effector exhausted cells, and this TOX down-regulation during differentiation may be driven by STAT5-dependent cytokines[312,347]. Thus, TOX loss enriches for effector-like populations at the expense of exhausted cell subsets (T_{PEX} and terminally exhausted cells), which in turn enhances function at the expense of persistence. Nevertheless, deletion of *Tox* improved the anti-tumour efficacy of T cells in adoptive cell therapy models[349,350], suggesting that this short-term boost in function can be therapeutically leveraged in certain contexts.

One consideration with the above TOX studies is that most of the transcriptional and epigenetic analyses were conducted on bulk knock-out cell populations. Given the loss of T_{PEX} and terminally exhausted cells in the absence of TOX, it's possible that many of the described effects of TOX (i.e. loss of exhaustion and gain of effector genes/chromatin regions) are due

to the loss of these subsets. An alternative interpretation of the TOX findings is thus that TOX is a maintenance factor that predominantly acts by sustaining T_{PEX} and terminally exhausted cell survival/maintenance, and the observed transcriptional and epigenetic changes are secondary to the loss of these populations. Nevertheless, the TOX-dependent transcriptional and phenotypic changes seen at day 8 post-infection prior to gross changes in subset proportions argue that TOX still directly contributes to the exhaustion transcriptional program.

While TOX is widely considered as the master regulator of exhaustion, it is also expressed to varying degrees in conventional effector and memory cells, in addition to during tolerance induction (see Section 1.5)[91,229,311,349]. While TOX expression during tolerance is likely downstream of the same NFAT-dependent pathways that induce TOX during exhaustion (see Section 1.5), TOX expression within effector and memory cells may be induced by cytokines such as IL-12, IL-15, and IL-18, which can induce TOX independent of TCR-signalling[404]. TOX is also expressed in CD8+ tissue resident intestinal intraepithelial T lymphocytes, suggesting that other tissue-derived factors may contribute to TCR-independent TOX expression [405]. These TCR-independent signals likely explain the elevated TOX expression seen in circulating human memory cells (i.e. T_{CM} and T_{EM}) compared to naïve T cells[406]. Interestingly, elevated TOX expression in both human and mouse memory T cells is not linked to diminished effector functions[403,406]. The role of TOX in these contexts (if any) is unclear, but these findings argue that TOX expression alone is not always sufficient to induce exhaustion, with other TCR-induced factors likely needed.

1.7.2. TOX in other immune cells

In addition to its role in CD8+ T cells, TOX also regulates the development of several other immune cell types. TOX is required for the development of innate lymphocytes, such as innate lymphoid cells (ILC) and NK cells [399,407]. As mentioned above, TOX is highly expressed by developing thymocytes during β-selection and positive selection, where it plays important roles in thymic T cell development. Specifically, germline *Tox* deletion in mice disrupted thymic development of all CD4+ lineage T cells (i.e. all conventional CD4+ T-helper subsets and Foxp3+ Tregs) due to TOX-dependent control of CD4+ lineage-enforcing transcription factors, such as ThPOK and ID2[386]. Outside of thymic development, TOX also promotes the differentiation of various CD4+ T cell subsets, such as T follicular helper cells (Tfh)[397,398] Th2 cells and Tregs[395,396]. Collectively, these data highlight that the effects of TOX on gene expression and differentiation are highly context dependent.

1.8. AP-1 transcription factor biology and function

Activator protein 1 (AP-1) is a broadly expressed family of dimeric transcription factors categorised into different gene sub-families, namely Jun (*Jun* (also cJun), *Junb*, *Jund*), Fos

(*Fos* (also c-Fos), *Fosb*, *Fosl1* (also FRA-1) and *Fosl2* (also FRA-2)), ATF (activating transcription factor; *Atf2*, *Atf3*, *Batf*, *Batf2*, *Batf3* (also JDP1), and *Jdp2*), and Maf (*Maf* (also c-Maf), *Mafb*, *Mafa*, *Mafg*, *Maff*, *Mafk*, and *Nrl*) families[408,409]. These AP-1 factors regulate various critical cellular processes in almost all cell types, including apoptosis, metabolism, differentiation, and proliferation[409-412]. The AP-1 family is often considered to control the cellular response to diverse extracellular signals, from environmental stressors like UV radiation to highly specific signals, such as TCR stimulation in T cells[409]. AP-1 has also been linked to various diseases, playing either a protective or harmful role depending on the cell type and disease context. DNA motifs targeted by AP-1 (discussed below) are differentially accessible in diverse contexts of cell differentiation, which can in turn influence the transcriptional output of AP-1. Specific AP-1 complexes are also oncogenic when combined with other pathways (e.g. YAP/TAZ and Ets), where they promote cancer progression through aiding cell transformation[413,414]. Conversely, in other contexts, therapy-induced AP-1 activity can have anti-tumour effects[415,416]. Overall, this underscores AP-1's complex and nuanced role in various cell processes, where the specific AP-1 complex involved and broader physiological context can both shape its impact on cellular processes.

AP-1 proteins all possess a basic leucine zipper (bZIP) domain composed of two functional regions: a hydrophobic leucine-rich heptad repeat that enables dimerisation with another AP-1 family member, and an adjacent basic region that binds specific DNA sequences. The makeup of the AP-1 dimeric complex dictates the specificity of DNA binding, and downstream impact on gene regulation (i.e. transcription initiation/inhibition, epigenetic remodelling, etc.)[408,417,418]. AP-1 complexes containing Jun and Fos proteins (predominantly, Jun/Jun homodimers and Jun/Fos heterodimers) preferentially bind to ~7 bp long DNA motifs with a 5'-TGA(C/G)TCA-3' consensus sequence referred to as TPA responsive-elements ("TRE", or alternatively called "AP-1 motif"). Jun/Fos heterodimers are considered more stable and display stronger DNA-binding activity than their Jun homodimer counterparts[418,419]. Jun/Jun and Jun/Fos dimers can also bind, with lower affinity, to cAMP-responsive elements (CRE) that have sequence homology to TRE motifs (5'-TCACGTCA-3'). However, CREs are more often selectively bound by ATF family members, often in partnership with another member of the Jun family[420]. Additionally, sequences that flank TRE and CRE motifs can facilitate the binding of Maf family members, which recognise extended versions (i.e. 14 bp) of TRE and CRE, known as Maf recognition elements (MAREs)[421]. AP-1 factors, either as monomers or dimers chiefly from the Jun and Fos sub-families, can also form complexes with other non-bZIP containing transcription factors, these include nuclear factor-κB (NF-κB), IRF4 and NFAT, among others (Table 2)[422].Collectively, this leads to a wide diversity of potential AP-

1 complexes, with potential for some degree of functional redundancy due to the similarities between the various DNA binding motifs.

Table 3 Summary of features and reported human protein interactors of AP-1 family members[423]

AP-1 Subfamily	Binding Motif	Members	Description	Number of reported interactors	Notable interactors
JUN	TRE, CRE	JUN (also cJUN)	jun proto-oncogene	445	FOS, NFATC2, JUN, JUNB, JUND, NFKB1, MAPK1, SP1, RUNX1
		JUNB	jun B proto-oncogene	139	FOS, BATF, JUN, JUND, BCL6, BRCA1, IRF4, SMARCA4, EP300
		JUND	jun D proto-oncogene	92	FOS, JUN, JUNB, MAPK8, SMAD3, CEBPA, MEN1, BRCA1
FOS	TRE, CRE	FOS (also cFOS)	FBJ osteosarcoma viral oncogene homolog	272	JUN, JUNB, JUND, NFATC2, MAF, CREB5, RUNX1, EGFR, UBE2I
		FOSB	FBJ osteosarcoma viral oncogene homolog B	44	JUN, JUNB, JUND, ATF2, NFE2L2, DNMT3L, FOS, FOXP3
		FOSL1 (also FRA-1)	FOS-like antigen 1	73	JUN, JUNB, JUND, USF1, CREB5, LDOC1, TAB2, DNMT3L
		FOSL2 (also FRA-2)	FOS-like antigen 2	90	JUN, JUNB, JUND, CREB5, ATF2, BACH2, RFWD2, ATF2
ATF	CRE	ATF2	activating transcription factor 2	249	JUN, JUNB, JUND, FOS, MAPK14, ATF2, BACH1, CREB5, SMAD3
		ATF3	activating transcription factor 3	101	JUN, JUNB, JUND, DDIT3, TP53, HDAC6, CEBPB, SMAD3
		ATF4	activating transcription factor 4	104	JUN, JUNB, FOS, EP300, BTRC, FBXW11, LDOC1, MDM2
		ATF5	activating transcription factor 5	23	CCND3, EP300, CDC34, CEBPA, KEAP1, EIF2B1
		ATF6	activating transcription factor 6	153	ATF6, ATF6B, ERLEC1, YY1, CLEC3A, HLA-E, RFWD2
		ATF6B	activating transcription factor 6 beta	84	ATF6, ATF6B, AK4, ERLEC1, HLA-E, BTNL2, LYRM7
		ATF7	activating transcription factor 7	91	JUN, JUNB, JUND, FOS, ARIH1, CREB5, ATF2, BACH2, CEBPB
		BATF	basic leucine zipper transcription factor, ATF-like	22	JUNB, JUN, DDIT3, ATF2, BATF, BATF3, CEBPA, IRF4, MEN1
		BATF2	basic leucine zipper transcription factor, ATF-like 2	30	JUNB, JUN, ATF4, DAZAP2, HLA-C, MAFF, BACH1, ATXN1
		BATF3 (also JDP1)	basic leucine zipper transcription factor, ATF-like 3	57	JUN, JUNB, JUND, BACH2, ATF2, CREB5, DDIT3, LDOC1L, ZBTB10
		JDP2	Jun dimerization protein 2	26	JUN, JUND, JDP2, HDAC6, ATF2, IRF2BP1, CEBPA, HDAC4, TP53
MAF	MARE	MAF (also cMAF)	v-maf avian musculoaponeurotic	57	MAF, FOS, ATF4, MYB, UBE20, USP5, SOX9, CEBPA

			fibrosarcoma oncogene homolog		
		MAFA	v-maf avian musculoaponeurotic fibrosarcoma oncogene homolog A	14	HERC4, NEUROD1, PDX1, TOMM20, MAPK14, STAT3
		MAFB	v-maf avian musculoaponeurotic fibrosarcoma oncogene homolog B	271	MAFB, MAF, BACH1, DDB1, USP7, ACAD11, RPL17
		MAFF	v-maf avian musculoaponeurotic fibrosarcoma oncogene homolog F	52	BACH1, BACH2, NFE2L2, MAFF, BATF3, MYC, LDOC1L
		MAFG	v-maf avian musculoaponeurotic fibrosarcoma oncogene homolog G	43	BACH1, BACH2, NFE2L2, MAFF, MAFG, ATF, BATF3, CUL3, PARP1
		MAFK	v-maf avian musculoaponeurotic fibrosarcoma oncogene homolog K	36	BACH1 BACH2, NFE2L2, CEBPA, CUL3, MAFF, MYC, NFATC2
		NRL	neural retina leucine zipper	11	FIZ1, OPTN, CRX, MAPK1, NR2E3

Since its discovery in the late 1980s, AP-1's activity has been ascribed to countless cellular processes. It was first observed to interact with the metallothionein gene promoter region in the genome of HeLa cells, along with other TREs, in a wide array of cell types[424]. Despite decades of work identifying numerous genomic targets of AP-1, our understanding of the specific gene programs it regulates and the molecular mechanisms it engages to control transcription is incomplete. Many of the seminal studies that elucidated AP-1 activity utilised artificial *in vitro* activation conditions in transformed cell lines (i.e. Jurkat T cells activated with PMA/ionomycin), and *in vitro* methods to assess promoter binding (e.g., gel mobility shift assays) in only a handful gene targets, e.g. metallothionein and IL-2 promoter [424-426]. As current paradigms were guided by these reductionist seminal studies, this may have led to an over-simplified or biased view of AP-1 biology. Some of these concepts have been challenged by more recent whole-genome profiling of AP-1 activity. For example, the assumption that AP-1 largely acts through binding to promoter and enhancer regions of genes [427] has been revised upon the discovery that AP-1 also influences gene expression through binding to distal regulatory elements[170,428,429]. In addition to direct gene regulation via co-activator and/or co-repressor recruitment to regulatory elements[430,431]. AP-1 can also epigenetically influence gene expression by remodelling chromatin[170,432-434] or potentially even altering 3D chromatin architecture[434], although further work is needed in this area. Hence, AP-1 employs a variety of mechanisms to influence gene expression and that there are still significant knowledge gaps in its mechanisms of action.

1.8.1. Jun family

In the context of T cell activation, most studies of AP-1 function have focused on Jun containing complexes, with early studies prioritising cJun complexes, particularly c-Fos/cJun heterodimers[435,436], and more recent studies focusing on ATF/Jun complexes[173,176,437-439]. Jun proteins are a major focus in thesis and thus are considered in more detail in this section.

Jun proteins were first discovered as novel retroviral oncogenes in Avian sarcoma virus 17. This led to the isolation and sequencing of the viral *Jun* oncogene, (v-Jun), named as an abbreviation of the Japanese word for 17*,* "ju-nana"[440]. The cellular homologue of v-Jun, cellular Jun (cJun), was subsequently identified and found to share a target sequence with the independently discovered AP-1[441,442], with later work revealing that cJun containing dimers were in fact, AP-1[443-445]. Most paradigms on Jun and AP-1 functionality were derived from early studies of cJun and c-Fos heterodimers[446]. Subsequently, two additional genes, *Junb and Jund,* encoding proteins with high sequence homology to cJun were discovered in mouse fibroblast cell lines[447-449]. Aptly named JunB and JunD, these additional Jun proteins also contain the bZIP domain characteristic to cJun/AP-1 and recognise the same TRE motifs that cJun recognises. JunB and JunD proteins also contained a bZIP domain and could bind TRE motifs, with binding affinity increasing upon interaction with c-Fos[450,451]. JunD is unique as it can exist in two isoforms due to the presence of two translation start sites in its transcript: a full-length variant and a truncated isoform lacking 48 amino acids in the N-terminal region. These two isoforms differ slightly in their function, with the full-length variant exhibiting stronger transcriptional activity[452].

Structurally, in most cases, unlike the Fos and ATF families, Jun proteins have the dual ability to form homo- and hetero-dimeric complexes in T cells[453]. While their DNA-binding and dimerisation domains are almost identical, Jun proteins do differ in their phosphorylation domains, which are phosphorylated by cJun N-terminal kinases (JNK), a class of mitogen-activated protein kinases. JNKs act downstream of various extracellular stimuli to alter gene expression through induction of AP-1 dimerisation and nuclear translocation. cJun is the most efficiently JNK phosphorylated Jun protein, with phosphorylation sites at serine residues 63 and 73. JunB lacks these serine residues and instead is phosphorylated at threonine residues 102 and 104. JunD is unique in that it requires heterodimerisation with cJun or another JNK-interacting protein to be phosphorylated[454,455]. In addition to phosphorylation differences, cJun, JunB, and JunD also exhibit distinct affinities to TRE- or CRE-binding sites[456]. Jun proteins also differ in their biological function and expression patterns during development. *Jun* deficient mice only survive until mid-to-late gestation due to defects in foetal liver development and erythropoiesis[457]. Although embryonic fatality was similarly found in *Junb*-deficient mice, this was likely due to the failure of the foeto-maternal circulatory system and placentation[458]. Targeted disruption of *Jund* did not result in embryonic lethality, but instead reduced postnatal growth and caused defects in various male reproductive processes (i.e. hormone imbalance

and impaired spermatogenesis)[459]. Thus, despite their homology, different Jun proteins have non-overlapping biological functions. These differences may in part relate to expression patterns, as Jun gene replacement studies, where mice were engineered so that one Jun gene was replaced by another, could partially rescue these phenotypes[460]. However, the failure to fully rescue these phenotypes indicates that intrinsic biological differences in Jun protein activity also underlies these disparate knock-out phenotypes.

1.8.2. AP-1-dependent Transcriptional Regulation in T cells

The involvement of AP-1 in regulating T cell processes has been documented extensively, including studies that focused on Jun family members (see Sections 1.2.2.3, 1.3.2, and 1.4.3). Though they are not actively expressed in naïve CD4+ and CD8+ T cells, the signalling pathways downstream of TCR activation and co-stimulation (namely the PLCγ, PI3K/PKC, and MAPK/JNK pathways) all converge to induce the synthesis, phosphorylation, and activation of the Jun proteins. Among the Jun family members, cJun has been the most well studied, in part due to the field's focus on the "canonical" c-Fos/cJun AP-1 complex[409,443-445,461]. The importance of AP-1 in T cell activation was largely inferred from early gene promoter studies, often using luciferase reporter assays in T cell lines or *in vitro* DNA/transcription factor binding assays. These studies implicated a critical role for AP-1 in induction of key T cell activation genes, such as *Il2*[427,462,463]. Subsequent work implicated AP-1 in the induction of lineage-related transcription factors required for differentiation of various effector CD4+ T cell subsets[464]. In most of these early studies, NFAT:AP-1 complexes were identified as the predominant complex involved in AP-1 dependent gene activation[427]. Although other Jun:Jun (e.g. JunD-JunB) and Jun:Fos (e.g. cJun-Fra1) dimers interact with NFAT, the cJun-cFos AP-1 dimer typically exhibits the strongest capacity to induce transcription in reporter assays when in complex with NFAT[451]. Subsequent genome profiling studies in primary T cells have demonstrated that the NFAT:AP-1 complex can increase chromatin accessibility in gene regulatory regions, thereby indirectly promoting transcription by allowing other factors to access the DNA[170,279]. On top of epigenetically priming gene regulatory regions in activated T cells, Jun proteins also play a central role in directly facilitating transcription at NFAT:AP-1 composite sites. For example, cJun must undergo phosphorylation by JNKs for the NFAT:AP-1 complex to also recruit transcriptional machinery such as the CREB-binding protein and RNA Pol II to promoter regions[465].

In the case of CD8+ T cells, much of the evidence for a role for AP-1 in activation is indirect. While AP-1 transcription factor motifs are demethylated and become accessible in CD8+ T cells undergoing *in vivo* effector differentiation[154,466], tolerant cells have deficiencies in AP-1 expression and in remodelling at AP-1 binding sites[91], and, as noted in Section 1.3.2, over-expression of a mutant form of NFAT unable to interact with AP-1 induces transcriptional

and functional features of both tolerant and exhausted T cells[141]. Beyond initial activation, elevated AP-1 expression and increased AP-1 motif accessibility has also been linked to CD8+ T_{RM} formation[467].

Nevertheless, there is accumulating data demonstrating functional roles for various Jun-containing AP-1 complexes in T cell activation and differentiation. Although JunD is the least studied Jun in T cells, it has been implicated in regulating proliferation and cytokine production by Th2 cells and CD8+ T cells *in vitro*[468,469]. In contrast, JunB containing AP-1 complexes have been more widely studied. JunB is involved in Th17, Tfh13, and Treg differentiation through the interaction with NFAT, IRF4 and other AP-1 factors, such as the ATF factor BATF[389,451,470-473]. BATF, in complex with IRF4, is also critically important in effector CD8+ T cell differentiation, where it is transiently expressed and controls expression and chromatin remodelling of early effector genes[176,437,474]. Given that BATF preferentially complexes with JunB[176,472,475], this implicates JunB in early effector CD8+ T cell differentiation. Indeed, JunB co-localises with almost 94% of BATF-bound regions during early CD8+ T cell activation[176], and JunB deletion in CD8+ T cells resulted in defects during *in vivo* effector differentiation analogous to the BATF knock-out phenotype, with accompanying dysregulation of BATF target genes[438]. Loss of BATF leads cells to acquire augmented memory/stem-like features and, intriguingly, in the absence of BATF, JunB instead co-localises with JunD[176]. This implicates a potential competition between JunB-JunD and JunB-BATF complexes in regulating memory versus effector differentiation, respectively[176]. While this suggests a role for JunD in T cell memory, other work has linked BACH2-dependent inhibition of JunD DNA binding with enhanced memory differentiation[476]. Furthermore, the transcription factor, FOXO1, which is required for memory T cell differentiation, directly represses *Junb* and *Jund* expression[477]. These conflicting findings mean that more comprehensive studies of AP-1 function during *in vivo* CD8+ T cell differentiation are needed.

Despite the significant knowledge gaps surrounding AP-1 function in CD8+ T cells, AP-1 factors are currently being used to engineer CD8+ T cells for adoptive cell therapy approaches against cancer, such as in Chimeric Antigen Receptor (CAR) T cells[416,478-486]. Ectopic expression of cJun in CAR or TCR T cells augmented exhaustion resistance, increased persistence, and improved anti-tumour efficacy[416,478]. This was speculated to be due to disruption of other detrimental AP-1 complexes (including BATF-JunB complexes). In line with this concept, BATF and JunB have been demonstrated to impair CAR T cell efficacy in other studies[480,481]. However, in direct contradiction to this idea, overexpression of BATF can augment CAR T cell anti-tumour efficacy in a manner that significantly outperforms cJun over-expression[479]. These data further highlight the considerable knowledge gaps in the AP-1 field and demonstrate that it will be difficult to leverage AP-1 biology for therapeutic applications unless the function of AP-1 factors in T cells is better understood.

1.9. Research Aims

This dissertation broadly aims to functionally define the transcriptional differences between tolerance and exhaustion via the following specific aims:

Aim 1: Investigate the role of Tox in CD8+ T cell tolerance

While the role of TOX in exhaustion is well defined, its function in T cell tolerance is less clear. In Chapter 3, I investigate whether TOX deletion impacts tolerance induction in a mouse model. Ultimately, defining the function (if any) of TOX in tolerance induction will help to functionally delineate the molecular overlap between tolerance and exhaustion.

Aim 2: Delineate the role of AP-1 transcription factors in CD8+ T cell differentiation

AP-1 factors have been proposed to insulate effector CD8+ T cells against both tolerance and exhaustion by complexing with NFAT. However, tolerance and exhaustion are molecularly distinct processes that arise at different points in the immune response. It is unclear if AP-1 ablation would preferentially skew effector CD8+ T cells towards a tolerant state, an exhausted state or another state entirely. The reason for this knowledge gap is that CD8+ T cells fully devoid of AP-1 factors have never been generated or studied, in part due to the many AP-1 family members that would need to be knocked out to achieve this. In Chapter 4, I profile the biology of AP-1 factors during *in vivo* effector T cell differentiation. In Chapter 5, I identify triple deletion of the 3 Jun proteins as the simplest path to generate fully AP-1 deficient CD8+ T cells, optimise an acute CRISPR deletion approach to achieve this, and then study the impact of AP-1 deficiency on effector and memory T cell differentiation. This allows me to functionally test the importance of AP-1 in suppressing tolerance and exhaustion, and more broadly examine AP-1 function in CD8+ T cell differentiation.

CHAPTER 2 Materials and Methods

2.1. Reagents, Materials, and Animals

2.1.1. Reagents and Materials

Table 4. Summary of Reagents and Materials

Material	Manufacturer	Reference Number
2-Mercaptoethanol (2ME)	Gibco	21985-023
6-well cell culture plate	Sigma-Aldrich	CLS3516
24-well cell culture plate	Sigma-Aldrich	CLS3527
7AAD Viability Staining Solution	Invitrogen	00699350
16-well Nucleocuvette Strip	LONZA	PDH-2104
96 well cell culture plate, Flat-bottomed with lid	Sigma-Aldrich	CLS3599
96 well cell culture plate, Round-bottomed with lid	Sigma-Aldrich	CLS3799
Alt-R® S.p. Cas9 Nuclease V3 (Cas9) (10 µg/µL)	Integrated DNA Technologies (IDT)	1081059
Brilliant Stain Buffer Plus	BD Biosciences	566385
Cell culture flask, 175cm²	Greiner	660160
Counting chambers	HIRSCHMANN	8100203
Diastix Urinalysis Reagent Strips	Bayer	2804
EasyStrainer 70µM	Greiner	542070
eBioscience™ Fixation/ Perm Diluent	Invitrogen	00-5223-56
eBioscience™ Fixation/ Permeabilization Concentrate	Invitrogen	00-5123-43
Ethylenediamine tetra Acetic Acid Disodium salt Dihydrate (EDTA)	Westlab	EA023-500G
GlutaMAX™ Supplement (100X)	Gibco	35050-061
Brefeldin A (BFA)	BD Biosciences	555029
High Sensitivity D1000 ScreenTape	Agilent Technologies	5067-5584
Histopaque-1077	Sigma-Aldrich	10771
HyClone Characterised Foetal Bovine Serum (FBS)	Cytiva	SH30084.03
Ionomycin Ca2+ Salt	abcam	ab120116
LCMV-glycoprotein (GP) 33-41 (KAVYNFATM) peptide	Biomolecular Resource Facility, Australian National University (ANU)	
Minimum Essential Medium, α	Gibco	12571063
Normal Goat Serum (NGS)	Vector Laboratories	VES1000
Ovalbumin 257-264 (SIINFEKL) Peptide	Biomolecular Resource Facility, Australian National University (ANU)	
Penicillin- Streptomycin (10,000U/mL)	Gibco	15140122
Phorbol 12-myristate 13-acetate (PMA)	abcam	ab120297
Phosphate Buffered Saline (PBS) 1X	Manufactured in-house by Peter Mac Research Laboratory Support Services	
Q5 High-Fidelity DNA Polymerase	New England Biolabs	M0491S
Recombinant Human Interleukin-15	Miltenyi Biotec	130-095-765
Recombinant Human Interleukin-2	Frederick National Laboratory for Cancer Research	Ro 23-6019

Recombinant Mouse Interleukin-7	STEM CELL Technologies	78054.1
Sodium Azide Solution, 10%	Australian chemical reagents (ACR)	3902
Sodium citrate dihydrate, ≥99%	Sigma-Aldrich	W302600-1KG-K
RetroNectin Recombinant Human Fibronectin Fragment	TaKaRa	T100B
Trypan Blue Solution, 0.4%	Gibco	15250061
TrypLE Express Enzyme (1X)	Thermo Fisher Scientific	12604021
Ultrafiltered Water (H_2O)	Manufactured in-house by Peter Mac Research Laboratory Support Services	
UltraPure Distilled Water	Invitrogen	10977-015

2.1.2. Media and Buffer Solutions

Fluoresence Activated Cell Sorting (FACS) Buffer
1x PBS containing 2.5% FBS and 0.1% Sodium Azide

Magnetic Activated Cell Sorting (MACS) Buffer
1x PBS containing 0.5% FBS and 2mM EDTA

Trypan Blue Counting Solution
1x PBS containing 0.08% Trypan Blue Solution

1% complete Roswell Park Memorial Institute Medium (cRPMI):
RPMI containing 1% FBS, 100U/mL penicillin/streptomycin (Pen/Strep), 2mM Glutamax, 55μM 2-ME

10% cRPMI:
RPMI containing 10% FBS, 100U/mL penicillin/streptomycin (Pen/Strep), 2mM Glutamax, 55μM 2-ME

10% complete Dulbecco's Modified Eagle Medium (cDMEM):
DMEM containing 10% FCS, 100U/mL penicillin/streptomycin (Pen/Strep), 2mM Glutamax, 55μM 2-ME

Red Blood Cell (RBC) Lysis Buffer:
Ultrafiltered H_2O containing 0.83% NH_4CL

Sodium Citrate Solution for Bleeds:
1x PBS containing 40% sodium citrate dihydrate

Radioimmunoprecipitation assay (RIPA) Lysis Buffer:
50 mM Tris pH 8.0, 150 mM NaCl, 1% NP-40, 0.1% SDS and 0.5% sodium deoxycholate containing protease inhibitor cocktail

Sodium Citrate Solution for Bleeds:
1x PBS containing 40% sodium citrate dihydrate

2.1.3. Antibodies

Table 5. List of antibodies used and their relevant information

Target	Clone	Fluorophore /Conjugate	Laser | Filter	Isotype	Manufacturer	Reference Number	Dilution Factor
Extracellular Antibodies							
B220	RA3-6B2	Biotin	N/A	Rat	Biolegend	103204	1/100
CD101	Moushi101	PE-Cy7	561 | 780/60	Rat	eBioscience	25101182	1/200
CD11b	M1/70	Biotin	N/A	Rat	Biolegend	101204	1/800
CD11b	M1/70	AF700	637 | 730/45	Rat	BD Biosciences	557960	1/800
CD122	TB-b1	PE	561 | 586/15	Rat	eBioscience	12122282	1/100
CD127	A7R34	PE-Cy7	561 | 780/60	Rat	Biolegend	135014	1/400
CD19	1D3	AF700	637 | 730/45	Rat	BD Biosciences	557958	1/100
CD200	OX90	BV786	405 | 780/60	Rat	BD Biosciences	744653	1/100
CD25	PC61	APC-Cy7	637 | 780/60	Rat	Biolegend	102026	1/200
CD27	LG3A10	APC	637 | 670/30	Armenian Hamster	Biolegend	124212	1/200
CD4	RM4-5	Biotin	N/A	Rat	Biolegend	100508	1/100
CD43	1B11	PE-Cy7	561 | 780/60	Rat	Biolegend	121218	1/800
CD44	IM7	BUV737	355 | 740/35	Rat	BD Biosciences	612799	1/1000
CD44	IM7	BUV395	355 | 379/28	Rat	BD Biosciences	740215	1/1000
CD45.1	A20	Pacific Blue	405 | 450/50	Mouse IgG2ακ	Biolegend	110722	1/100; 1/200
CD45.1	A20	FITC	488 | 530/30	Mouse IgG2ακ	Biolegend	110706	1/100; 1/200
CD45.1	A20	BUV395	355 | 379/28	Mouse IgG2ακ	BD Biosciences	565212	1/200
CD45.1	A20	APC	637 | 670/30	Mouse IgG2ακ	BD Biosciences	561873	1/200
CD45.1	A20	BV605	405 | 605/40	Mouse IgG2ακ	Biolegend	110737	1/100
CD45.2	104	PE	561 | 586/15	Mouse IgG2ακ	Biolegend	109808	1/100
CD45.2	104	PerCP-Cy5.5	488 | 780/60	Mouse IgG2ακ	Biolegend	109828	1/100
CD62L	MEL-14	APC-Cy7	637 | 780/60	Rat	Biolegend	104428	1/200
CD62L	MEL-14	BUV737	355 | 740/35	Rat	Biolegend	565213	1/200

Target	Clone	Fluorophore /Conjugate	Laser | Filter	Isotype	Manufacturer	Reference Number	Dilution Factor
CD69	H12F3	FITC	488 | 530/30	Armenian Hamster	BD Biosciences	553236	1/100
CD71	C2	PE	561 | 586/15	Rat	BD Biosciences	553267	1/100
CD8	53-6.7	BUV395	355 | 379/28	Rat	BD Biosciences	563786	1/100; 1/200
CD8	53-6.7	BUV805	355 | 820/60	Rat	BD Biosciences	564920	1/200
CX3CR1	SA011F11	BV650	405 | 670/30	Mouse IgG2ακ	Biolegend	149033	1/100
F4/80	BM8	AF700	637 | 730/45	Rat	Biolegend	123130	1/100
FR4	EBIO12A5	PE-Cy7	561 | 780/60	Rat	eBioscience	25544582	1/100
KLRG1	2F1	FITC	488 | 780/60	Syrian Hamster	eBioscience	11589382	1/100
NK1.1	PK136	Biotin	N/A	Mouse	Biolegend	108704	1/100
NK1.1	PK136	AF700	637 | 730/45	Mouse IgG2ακ	BD Biosciences	550627	1/100
PD-1	29F1A12	BV785	405 | 780/60	Rat	Biolegend	135218	1/100
SLAMF6	13G3	BV421	405 | 450/50	Mouse IgG2ακ	BD Biosciences	740090	1/200
TIGIT	1G9	BV650	405 | 670/30	Mouse IgG2ακ	BD Biosciences	744213	1/100
TIM-3	RMT3-23	BV605	405 | 605/40	Rat	Biolegend	119721	1/100
Vα2	B20.1	PE	561 | 586/15	Rat	Biolegend	127808	1/100
Intracellular Antibodies							
BATF	D7C5	NA	NA	Rabbit	Cell Signalling Technologies	8638	1/400
BCL2	3F11	PE	561 | 586/15	Hamster	BD Pharmingen	556357	1/20
BIM	C34C5	NA	NA	Rabbit	Cell Signalling Technologies	2933	1/100
CD107a	1D4B	FITC	488 | 780/60	Rat	Biolegend	121606	1/400
cJun	60A8	NA	NA	Rabbit	Cell Signalling Technologies	9165	1/100
EGR2	ERONGR2	APC	637 | 670/30	Rat	eBioscience	17669182	1/50
EGR2	ERONGR2	PE	561 | 586/15	Rat	eBioscience	12669182	1/100
Eomesodermin	Dam11mag	AF488	488 | 530/30	Rat	eBioscience	53487582	1/200
Granzyme B	GB11	APC	637 | 670/30	Mouse IgG1	Invitrogen	GRC05	1/500
Helios	22F6	FITC	488 | 530/30	Armenian Hamster	Biolegend	137214	1/100
IFN-γ	XNG1.2	PE-Cy7	561 | 780/60	Rat	eBioscience	25731182	1/2000
IL-2	JES65H4	APC	637 | 670/30	Rat	eBioscience	17702182	1/100

Target	Clone	Fluorophore /Conjugate	Laser | Filter	Isotype	Manufacturer	Reference Number	Dilution Factor
IRF4	IRF4.3.E34	AF647	637 | 670/30	Rat	Biolegend	646408	1/100
JunB	C37F9	NA	NA	Rabbit	Cell Signalling Technologies	3753	1/100
JunD	EPR17365	NA	NA	Rabbit	Abcam	ab181615	1/800 1/1000 (Western Blot)
Ki67	B56	PerCP-Cy5.5	488 | 780/60	Mouse IgG1	BD Biosciences	561284	1/500
Tbet	EBIO4B10	PE-Cy7	561 | 780/60	Mouse IgG1 κ	eBioscience	25582582	1/100
TCF1	CD3D9	NA	NA	Rabbit	Cell Signalling Technologies	2203S	1/100
TNF-α	MP6-XT22	PE	561 | 586/15	Rat	Biolegend	506306	1/2000
TOX	TXRX10	PE	561 | 586/15	Rat	eBioscience	12650282	1/100
Secondary Antibodies							
Streptavidin	N/A	PE-Cy7	561 | 780/60	NA	BD Pharmingen	557598	1/1000
Anti-Rabbit 2º	Polyclonal	AF647	637 | 670/30	Goat	Invitrogen	A21245	1/1000
Anti-Rabbit 2º	Polyclonal	AF594	561 | 610/20	Goat	Invitrogen	A11012	1/1000
Antibodies for *in vitro* Activation							
CD28	37.51	NA	NA	Syrian Hamster	BD Biosciences	553295	1/100; 1/1000
CD3	145-2C11	NA	NA	Armenian Hamster	BD Biosciences	553058	1/50; 1/100; 1/1000
Antibodies for Western Blotting							
Beta Actin	AC-74	NA	NA	Mouse	Sigma Aldrich	A2228	1/10000
Anti-Mouse 2º	Polyclonal	HRP	NA	Rabbit	Dako	p0260	1/10000
Anti-Rabbit 2º	Polyclonal	HRP	NA	Goat			1/10000

2.1.4. Kits

Table 6. Summary of experimental kits

Kit	Manufacturer	Reference Number
EasySep™ Mouse Naïve CD8+ T Cell Isolation Kit	STEMCELL Technologies	19858
EasySep™ Mouse CD8+ T Cell Isolation Kit	STEMCELL Technologies	19853
EasySep™ Dead Cell Removal (Annexin V) Kit	STEMCELL Technologies	17899
P3 Primary Cell 4D-Nucleofector® X Kit S	Lonza	V4XP-3032
Qubit 1X dsDNA HS Assay Kit	Invitrogen	Q33231
CUTANA ChIC/ CUT&RUN Kit	Epicypher	14-1048
CUTANA CUT&RUN Library Prep Kit	Epicypher	14-1001
CaspGLOW Fluorescein Active Caspase Staining Kit	Invitrogen	88-7003-42
CellTrace Violet Cell Proliferation Kit	Invitrogen	C34557
DNeasy Blood & Tissue DNA Extraction Kit	QIAGEN	69504
eBioscience™ Foxp3 / Transcription Factor Staining Buffer Set	Invitrogen	00-5523-00
Zombie Aqua™ Fixable Viability Kit	Biolegend	423102

2.1.5. Bacterial and Viral Strains

All bacterial and viral stocks were stored at -80ºC and were periodically re-titred to confirm stable stock concentrations.

Table 7. Mouse pathogens used for infection studies

Pathogen	Source
LCMV-Armstrong Strain	Dutko & Oldstone, 1983[107]
LCMV-Clone 13 Strain	Ahmed et al, 1984[487]
Ovalbumin transgenic *Listeria monocytogenes*-OVA (LM-OVA)	Pope et al., 2001[488]
LCMV-glycoprotein (GP) 33-42 peptide transgenic *Listeria monocytogenes* (LM-33)	Manjunath et al., 2001[489]

2.1.6. Mouse Models

Table 8. Mouse strains utilised and their relevant information

Mouse Strain	Official Name	Source	Identifier
B6	C57BL/6J (B6)	Walter and Eliza Hall Institute (WEHI) Kew Animal Facility, VIC, Australia	IMSR_JAX:000664
P14	P14 TCR transgenic (B6.Cg-Tcratm1MomTg(TcrLCMV)327Sdz/TacMmjax)	Pircher et al., 1989[490]	MMRRC_037394-JAX
RIP-OVA	RIP-OVA^{hi} transgenic (C57BL/6-Tg(In2-OVA)59Wehi/WehiJ)	Kurts et al., 1998[224]	IMSR_JAX:005433
OT-I	OT-I TCR transgenic (C57BL/6-Tg(TcraTcrb)1100Mjb/J)	Hogquist et al., 1994[491]	IMSR_JAX:003831

CD45.1	CD45.1 (B6.SJL-*PtprcaPep3b/*BoyJ)	The Australian Phenomics Facility, ANU, Australia	IMSR_JAX:002014

2.2. Experimental Methods

2.2.1. General Lab Procedures

Laboratory procedures were performed in the research facilities (Physical Containment 2 certified laboratories) of the Peter MacCallum Cancer Centre (Peter Mac), following all mandated safety protocols and appropriately handling of chemicals, genetically modified organisms, and pathogens.

Cells were washed using PBS, FACS buffer, or 1% cRPMI depending on the experimental protocol. For the various cell isolation procedures and experimental assays, cells in FACS tubes and centrifuge tubes (10mL, 15mL, 50mL) were centrifuged in a benchtop centrifuge at 1500RPM for 5 mins at 4ºC. For 96-well round- and v-bottomed plates during flow cytometry staining, cells were centrifuged in a benchtop centrifuge at either 1500RPM or 1750RPM for 3-5mins at 4ºC. Finally, cells in microcentrifuge tubes were pelleted by centrifuging cells at 500-1000 X G for 3 mins at 4ºC using a microcentrifuge or 5-10 mins at RT using a mini centrifuge.

Cell counts were determined by taking a 10 µL aliquot from the cell suspension and diluting it in a volume of trypan blue (TB) to achieve a dilution factor (DF) that is appropriate for the expected cell count for each experiment (i.e. 1/100 for 10 million cells and above, 1/10 for 1– 10 million cells, and 1/2 for below 1 million cells). Except as specified, isolated cells were always kept on ice or in 4ºC to maximise cell viability.

2.2.2. Mouse techniques, procedures, and handling

2.2.2.1. Animal Ethics and General Procedures

All mice were cared for, managed, and housed according to guidelines approved by the Peter MacCallum Cancer Centre (PMCC) Animal Experimentation Ethics Committee under the approved ethics protocol E669 and the current guidelines from the Australian Code of Practice for the Care and Use of Animals for Scientific Purposes.

C57BL/6J (B6) mice were purchased from the Walter and Eliza Hall Institute (WEHI) Animal Facilities between 4-7 weeks of age and given at least one week to acclimate to the new facility before usage. All other mouse strains (listed in Section 2.1.6) were bred in-house and given at least 2 days to acclimate after room transfer before being utilised in any experiment. The OT-I and P14 mouse lines were continually back-crossed to the WEHI B6 background as part of routine colony maintenance to prevent OT-I and P14 cell rejection upon adoptive transfer due to genetic drift.

Mice were euthanised by either cervical dislocation for spleen harvest alone, or CO_2 asphyxiation when harvesting lymph nodes or conducting cardiac bleeds. Intraperitoneal and intravenous injections were performed with a 0.5mL or 1.0mL 27G syringe. Intravenous

injections for adoptive transfers and infections were conducted via retro-orbital injection (ROIV) on isoflurane-anaesthetised mice. The injection vehicle was PBS or media without FBS and injection volumes injected did not exceed 200µL.

2.2.2.2. Adoptive Transfer

All donor CD8+ T cells were resuspended in PBS and were stored on ice to minimise cell loss. The following numbers of wild-type or CRISPR-edited (Section 2.2.5) CD8+ T cell were utilised for adoptive transfer in the indicated experiments. As outlined in the relevant Results chapter sections, cells were labelled with CTV prior to transfer in some experiments (Section 2.2.3.1).

Table 9. Summary of adoptive transfer experiments

Donor CD8+ T cell	Cell Count (in 200µL PBS)	Recipient Mice	Experiment	Relevant Thesis Section
Naïve P14 cells	50,000 P14 cells	Uninfected B6	LCMV Armstrong Infection (Day 5, 8, 42, 112 takedowns)	5.2.2, 5.2.3, 5.2.6
		Uninfected B6 or CD45.1	Serial rechallenge experiments (i.e. LCMV Armstrong, LM-33, LCMV Cl.13)	5.2.7
	2,000,000 P14 cells	Uninfected B6	LCMV Armstrong Infection (24hr, 48hr, 72hr, Day 5 and 8 takedowns)	4.2.1, 5.2.2
	5,000 P14 cells	Uninfected B6	LCMV Cl.13 Infection (Day 8, 20, and Day takedown)	3.2, 5.2.4
Naïve OT-I cells	2,000,000 OT-I cells	Uninfected RIP-OVA	Tolerance induction experiments	3.2
	2,000,000 OT-I cells	Uninfected B6	LM-OVA infection (72hr takedown)	3.2
Day 42 “Memory” P14 cells	10,000 P14 cells	Uninfected B6	Secondary rechallenge experiments (i.e. LM-33 secondary infection)	5.2.7
Day 8 “Effector” P14 cells	10,000 P14 cells	Infection matched B6	Effector phase CRISPR experiments	5.2.3

Prior to adoptive transfer, a purity stain was performed by flow cytometry to confirm CD45.1 genotype and determine % OT-I or P14 cells (i.e. CD8+Vα2+ cells, or CD8+CD45.1+ cells in effector phase CRISPR or memory cell rechallenge experiments). Cells were then diluted accordingly to inject the appropriate numbers of P14 or OT-I cells per mouse. No more than 20 million cells were injected per day to avoid adverse effects (e.g. stroke downstream of increased blood viscosity).

2.2.2.3. Infections

Concentrated bacterial and viral stocks were thawed at RT and diluted in either PBS (*Listeria*) or plain RPMI (LCMV) to the appropriate concentration for infection. For LCMV infections, mice were infected intravenously with either $2x10^5$ plaque forming units (PFU) LCMV-Armstrong or $2x10^6$ PFU LCMV Cl.13. For *Listeria* infections, mice were intravenously infected either with $1x10^5$ colony forming units (CFU) LM-OVA (60hr phenotyping experiments) or $5x10^4$ CFU LM-33 (all other experiments). In specific experiments, mice were intraperitoneally infected with $2x10^6$ CFU LM-33 (see Section 3.2.4).

All procedures involving infectious agents and associated samples followed approved biosafety guidelines for the safe handling, disinfection, and disposal of contaminated labware.

2.2.2.4. Diabetes Testing and Peptide Injections

For tolerance diabetes experiments (Chapter 3), the onset of diabetes was monitored until day 42 after OT-I adoptive transfer through routine urine glucose measurements using Diastix urinalysis testing strips (Bayer). Animals were considered diabetic after three consecutive days of $\geq$28 mmol/L urine glucose. For the high-dose peptide tolerance experiment, 10µg ovalbumin peptide (SIINFEKL) in PBS was administered intravenously one day prior to adoptive transfer of OT-I cells and at days 1 and 2 post-adoptive transfer.

2.2.3. Cell Isolation

2.2.3.1. CD8+ T cell isolation and CTV labelling

Naïve CD8+ T cells were required for CRISPR experiments, adoptive transfer studies, and *in vitro* assays. To purify naïve CD8+ T cells, spleens and pooled lymph nodes (inguinal, axillary, brachial, cervical, mesenteric, pancreatic and sacral) from euthanised donor mice (P14, OT-I or B6 mice) were harvested into 5mL of 1% cRPMI in 15mL tubes and stored on ice. A single cell suspension was prepared by mashing the organs through a 70µm cell strainer and washing out the remaining cells from the strainer with 1% cRPMI prior to centrifugation. Cell pellets were resuspended in 2mL RBC lysis buffer and incubated at RT for 2mins to lyse RBCs, and then 10mL of 1% or 10% cRPMI was added to stop the lysis reaction. Cell suspensions were filtered through a 100µm nylon mesh to remove cell debris prior to centrifugation and resuspension in 500µL MACS buffer in a fresh FACS or centrifuge tube. Naive CD8+ T cells (CD3+CD8+CD44-CD62L+) were enriched through negative depletion using the EasySep Mouse Naïve CD8+ T Cell Isolation Kit (STEMCELL Technologies) following manufacturer's instructions. Briefly, 25µL of the EasySep Naïve CD8+ T cell Isolation cocktail was added to each sample prior to mixing by vortexing and incubation for 10 mins at RT. 50µL of EasySep Streptavidin RapidSpheres were then added to each sample, the sample was vortexed to mix, and then incubated for 5 minutes at RT. Tubes were then transferred to an EasySep Magnetic cell separation rack to magnetically pellet the RapidSpheres. Once

cleared, the supernatant was transferred to fresh tubes, centrifuged to pellet the cells, resuspended in 10% cRPMI, and kept on ice. The resulting naïve CD8+ T cells were counted and resuspended in media (either PBS or 10% cRPMI) appropriate for the specific downstream experimental procedure. For effector phase CRISPR experiments (described in Section 5.2.3, Fig. 5.4F), the above procedures were followed except that the EasySep Mouse CD8+ T cell Isolation Kit (STEMCELL Technologies) was used to enrich total (i.e. both naïve and antigen experienced) CD8+ T cells.

CD8+ T cells in specific experiments (Section 3.2, and 4.2.1) were CTV labelled using the CellTrace Violet Cell Proliferation Kit (Invitrogen). After naïve CD8+ T cell isolation, cells were resuspended in room temperature 10% cRPMI at $5.0x10^7$ cells/mL and transferred to a fresh centrifuge tube. 1µL of 10mM CTV stock per mL of cells (i.e. 10µM final concentration) was added to the side of the tube prior to vortexing, and incubation for 5 mins at RT in the dark. Cells were then washed three times with 10% cRPMI, counted and resuspended at the appropriate concentration in PBS for adoptive transfer.

2.2.3.2. Spleen and lymph node cell isolation and processing

Unless otherwise stated, all *in vivo* phenotyping and infection experiments involved analysis of splenic CD8+ T cells. Spleens were harvested after euthanasia and processed into an RBC lysed single cell suspension as in 2.2.1.1. (i.e. all steps prior to T cell enrichment). Cells were resuspended in 1mL 10% cRPMI and counted, then typically diluted to $1\text{-}3x10^7$ cells/mL depending on the cell number required for downstream analysis. 100µL of cells were aliquoted into 96-well round-bottom plates or FACS tubes for staining (Section 2.2.7.1), 96-well flat-bottomed plates for peptide restimulation (Section 2.2.4.3) or cell culture plates for other *in vitro* assays. In specific experiments with a low frequency of P14 or OT-I cells, such as day 42 tolerance induction experiments (Section 3.4) and day 8 LCMV Armstrong effector phase CRISPR studies (Section 5.2.2), lymph nodes were also harvested and pooled with spleens during tissue processing and cell isolation to maximise cell recovery. Sacral and pancreatic lymph nodes analysed for 60h tolerance timepoint RIP-OVA mouse experiments (Section 3.2) were similarly processed into a single cell suspension except that cells did not undergo RBC lysis, and cells were harvested and processed in MACS buffer to prevent cell clumping.

2.2.3.3. Peripheral Blood Mononuclear Cell (PBMC) Isolation

For PBMC isolation in memory and rechallenge experiments, 100-200µL of blood were collected into FACS tubes containing 1mL 4% sodium citrate by either serial retro-orbital bleeds using heparinised glass capillary tubes, or by cardiac bleed at experiment completion using 27G syringes. Samples were then mixed with 1mL RPMI by vortexing, and underlaid with 1mL of room-temperature Histopaque using a glass Pasteur pipette. Samples were centrifuged at 2000 RPM for 15mins at RT with no brake, and cells at (and immediately above

and below) the interphase were harvested with a plastic transfer pipette and transferred into a new FACS tube. Tubes were topped up with 1% cRPMI and cells pelleted via centrifugation at 2500 RPM for 9 mins at RT prior to resuspension in 1% cRPMI for downstream applications.

2.2.4. *In vitro* cultures

2.2.4.1. In vitro activation of CD8+ T cells

Naïve CD8+ T cells were activated *in vitro* to validate CRISPR KO by flow cytometry or for T cell phenotyping and molecular analysis. 0.1 – 2.0x10^6 naïve CD8+ T cells were aliquoted into 96-well flat-bottom plates and incubated for 24hrs at 37ºC, 5% CO_2 with the relevant stimulation conditions outlined in the table below.

Table 10. Summary of *in vitro* stimulation conditions according to each experiment

CD8+ T cell type	Stimulation Condition	Experiment
Wild-type CD8+ T cells	5 µg/mL anti-CD3 (plate-bound), 5 µg/mL anti-CD28, and 100 IU/mL rhIL-2 in 100µL 10%cRPMI	24hr activation molecular phenotyping: Co-IP MS (Section 2.2.8), CUT&RUN (Section 2.2.9)
CRISPR KO CD8+ T cells	5 µg/mL anti-CD3 (plate-bound), 5 µg/mL anti-CD28, and 100 IU/mL rhIL-2 in 100µL 10%cRPMI	MAC-Seq (Section 2.2.10) CRISPR KO Validation
	50 ng/mL PMA, 0.5 µg/mL Ionomycin in 200µL 10%cRPMI	CRISPR KO Validation
	4.0 µg /mL Ionomycin in 200µL 10%cRPMI	

2.2.4.2. IL-7 culture

In assays where CD8+ T cells are required to be naïve *in vitro*, wild-type or CRISPR KO cells were cultured in 5 ng/mL IL-7 in 10% cRPMI at 37ºC, 5% CO_2 for a maximum of 3 days.

2.2.4.3. Peptide Restimulation

For peptide restimulation assays to assess either cytokine production or Jun protein re-expression, 2x10^6 splenocytes in 10%cRPMI (isolated as in Section 2.2.3.1) were aliquoted into a 96-well flat bottom plate and incubated at 37ºC, 5% CO_2 in the presence or absence of the appropriate peptide (0.1µg/mL; Ovalbumin 257-264 (SIINFEKL) peptide for OT-I cells and LCMV-glycoprotein (GP) 33-41 (KAVYNFATM) (LCMV-GP_{33-41}) peptide for P14 cells). For intracellular cytokine staining assays, cells were cultured for 5hrs in 3µg/mL Brefeldin A and CD107a-FITC antibody (1/400 dilution), whereas for Jun re-expression, cells were incubated with peptide alone for 24hrs. Cells were then washed and stained for flow cytometry. Background cytokine staining was assessed by analysing cells cultured without peptide.

2.2.4.4. Cell line culture and maintenance

The 4T1.2 murine breast carcinoma cell line utilised for CRISPR KO optimisation was kindly provided by the Johnstone laboratory at PMCC. This cell line was maintained in MEMα without any supplements and passaged using TrypLE (Thermo Fisher). CRISPR-edited 4T1.2 cells were transferred to 6-well plates and kept for 72hrs at 37ºC, 5% CO_2 prior to assessment of protein expression via western blot and flow cytometry.

An ectopic retroviral packaging cell line, GP+E-86, used for retroviral transduction experiments (Section 2.2.8) was kindly provided by the Beavis laboratory at PMCC. The cells contained a murine stem cell retrovirus vector (LXSN-pMSCV-AP1:NFAT-GFP) that encoded a truncated human nerve growth factor receptor selection marker and an enhanced green fluorescent protein (GFP) reporter, which is driven by a minimal *IL2* promoter downstream of an AP-1:NFAT composite element. Cells were cultured in 10% cRPMI with 0.1 mM non-essential amino acids and 10 mM 4-(2-hydroxyethyl)-1-piperazineethanesulfonic acid (HEPES) at 37 °C with 5% CO_2, passaged via TrypLE and maintained for at least 2 weeks prior to acquisition of supernatants for retroviral transduction experiments.

2.2.5. CRISPR Gene Editing

2.2.5.1. Design of single guide RNAs (sgRNAs)

sgRNA design for electroporation-based CRISPR gene deletion was accomplished through a combination of online genome editing tools and molecular databases, such as CHOPCHOP, the UCSC Genome Browser database, and UniProt [492-494]. Multiple sgRNA sequences were designed and trialled for each mouse gene target (see table 8). sgRNA sequences that target an exonic region coding for a functional domain were prioritised where feasible, with sgRNAs selected based on high predicted KO efficiency and low off-target scores. A previously reported *Cd19* guide was utilised as a control for all experiments [495]. sgRNAs were manufactured by Integrated DNA Technologies via their Alt-R™ CRISPR-Cas9 System.

Prior to first use, lyophilised sgRNAs were resuspended at either 0.3 or 0.6nmol/μL in nuclease-free H_2O. Knock-out efficiency was evaluated by flow cytometry or Western Blotting for the target protein. High knock-out efficiency individual and combined sgRNAs used in this thesis are summarised below.

Table 11. Summary of sgRNAs used in this thesis

Target	Guide Name	Sequence (5'-3')	Selected for Experiments?
Cd19	Cd19	CCUGGCCUGGGAUUGCACGU	Yes
Jun	cJun #1	GCTCGTCGGTCACGTTCTTG	Yes
Jun	cJun #2	TGGGGCGCCCTCCTATGGCG	Yes
Jun	cJun #3	GAAGGUCCGAGUUCUUGGCG	No
Junb	JunB #1	UGAGCUCCCAGUCCCGACGG	Yes
Junb	JunB #2	TCACGACGACTCTTACGCAG	Yes
Jund	JunD #1	GAAGCUCGGCACGUCCGGCA	Yes
Jund	JunD #2	GCAGTTTCGCGGGTGGCGCC	No
Jund	JunD #3	AACGCCCTTCTATGGCGAGG	No
Tox	Tox #1	CGAAGATTGTGGCATCAATG	Yes
Tox	Tox #2	AGCGGCCTGCCTCTGATATG	Yes
Tox	Tox #3	AGGTCCCAGACAAGGAGCGG	No
Bim	Bim #1	GACAATTGCAGCCTGCTGAG	Yes
Bim	Bim #2	GCACAGGAGCTGCGGCGGAT	Yes
Batf	Batf	TGTGAAGTACTTGAGCTCCT	Yes
Designation for CRISPR KO Condition		**Guide Combination**	
AP-1 sgRNA		cJun#1 + cJun#2 + JunB#1 + JunB#2 + JunD#1	
cJun sgRNA		cJun#1 + cJun#2	
JunB sgRNA		JunB#1 + JunB#2	
JunD sgRNA		JunD #1	
cJun/JunD sgRNA		cJun#1 + cJun#2 + JunD #1	
Batf sgRNA		Batf	
JunB/Batf sgRNA		JunB#1 + JunB#2 + Batf	
AP-1/Bim sgRNA		cJun#1 + cJun#2 + JunB#1 + JunB#2 + JunD#1 + Bim#1 + Bim #2	
Tox sgRNA		Tox #1 + Tox#2	
Ctrl sgRNA		Cd19	

2.2.5.2. CRISPR/Cas9 ribonucleoprotein (RNP) Electroporation

The CRISPR-based electroporation protocol used in this project has been described previously [496]. Briefly, for each CRISPR reaction Cas9/sgRNA RNP complexes were prepared by combining 0.6µL of Cas9 protein (IDT) with 0.3nmol of sgRNA(s) before being topped up to 5µL with nuclease-free H_2O and incubated for 10mins at RT. For each reaction, 20µL P3 buffer was prepared separately by adding 3.6µL of Supplement 1 to 16.4µL P3 Primary Cell Solution (Lonza P3 Primary Cell 4D-Nucleofector Kit). 1 – 8x10^6 CD8+ T cells per reaction were washed with PBS, pelleted, resuspended in the 20µL of prepared P3 buffer, and combined with the Cas9/sgRNA RNP solution. The resulting 25µL cell/RNP mixture was transferred to a well of 16-well nucleocuvette strip (Lonza) and electroporated on a 4D-Nucleofector using the "mouse T cell, unstimulated" (Pulse DN100) program. Immediately after electroporation, 130µL pre-warmed 10% cRPMI was added to each sample and cells were rested for 10 mins at 37ºC, 5% CO_2. Electroporated cells were transferred to new tubes,

washed, pelleted, resuspended in PBS then counted. Cells were adjusted to their desired concentrations and either activated *in vitro*, or adoptively transferred into recipient mice for *in vivo* phenotyping studies.

2.2.6. Western Blotting

For western blotting of CRISPR edited 4T1.2 cells and primary mouse CD8+ T cells (activated for 24hrs), cells were washed with cold 1X PBS and lysed at 4ºC for 20 mins with periodic vortexing in radioimmunoprecipitation assay (RIPA) lysis buffer containing protease inhibitors. Lysed cells were centrifuged at 12,000 RPM for 20 mins at 4ºC to pellet cell debris. Supernatants were acquired and protein concentrations were quantified using the Pierce BCA Protein Assay Kit. 10µg of protein per sample were added to an equal volume of 2X Laemmli sample buffer, with proteins then denatured at 95ºC for 5 mins, and resolved on a Bolt Bis-Tris Plus 4–12% gel (Thermo Fisher) run in 1X 2-Morpholinoethanesulphonic acid-Sodium dodecyl sulphate (MES SDS) running buffer (Thermo Fisher) at 50V for 5 mins, then 180V for 30mins. Resolved gels were transferred to 0.45µM PVDF membranes (Thermo Fisher) through a Trans-Blot Semi-Dry electrophoretic transfer cell (Bio-Rad) at 25 V for 45mins. Membranes were incubated in 5% skim milk in PBST at RT for 1 hour, probed with primary antibodies (10ug/mL) at 4ºC overnight, washed three times with PBST, incubated with HRP-conjugated secondary antibodies for 1 h at room temperature, and finally washed three times again with PBST. Chemiluminescence was generated using Amersham ECL Western Blotting Detection Reagents (Cytiva) and detected using the ChemiDoc Imaging System (Bio-Rad).

2.2.7. Retroviral Transduction

Whole splenocytes from B6 mice were incubated for 24 hours in 10% cRPMI containing 0.5 µg/mL anti-CD3, 0.5 µg/mL anti-CD28, 600IU/mL rhIL-2, and 5ng/mL IL-7. All incubation steps were performed at 37ºC and 5% CO_2. Activated T cells were isolated via Ficoll density centrifugation and were resuspended at 1.5-2.0 x 10^6 cells/mL of GP+E-86 retroviral supernatants (Section 2.2.4.4.) with 600IU/mL rhIL-2 and 5ng/mL IL-7 in non-tissue culture treated plates coated with 1:100 Retronectin (TaKaRa). Cells in the retroviral supernatant solution were centrifuged for at 1200 x g for 1.5hrs at room temperature with minimal acceleration and deceleration for two rounds, with an overnight incubation at prior to the second round. Following centrifugation, cells were incubated for 4 hours, washed, resuspended at 2.0 x 10^6 cells/mL of 10% cRPMI with 0.1 mM non-essential amino acids, 10 mM 4-(2-hydroxyethyl)-1-piperazineethanesulfonic acid (HEPES), 5 ng/mL IL-7, and 1:1000 IL-15, and incubated for 2 days prior to CRISPR electroporation (Section 2.2.5.2), *in vitro* activation (Section 2.2.4.1), and FACS analysis. Live NGFR+ CD8+ T cells were considered as transduced cells (Fig. S2).

2.2.8. Flow Cytometry

2.2.8.1. Flow cytometric staining and analysis

When staining up to $2x10^6$ cells for flow cytometry, cells were transferred into the wells of a 96-well round- or V-bottomed plate and washed at least once with FACS buffer prior to staining. To stain $>2x10^6$ cells, cell staining was conducted in FACS tubes. For surface staining, cells were incubated for 25 mins RT in the dark with 50µL per $2x10^6$ cells of antibodies diluted in PBS or FACS buffer. To exclude dead cells, a fluorescent viability dye, such as the Zombie Aqua Fixable Viability Dye was included in the antibody cocktail. To prevent dye exchange between brilliant violet fluorophores, Brilliant Stain Buffer Plus (BD Horizon) was included in the staining cocktail. Samples were either washed and resuspended in FACS buffer for immediate analysis by flow cytometry, or subsequently fixed and permeabilised for intracellular staining of nuclear factors using the Foxp3 / Transcription Factor Staining Buffer Set (eBioscience) for ~1 hour at 4ºC in the dark. Alternatively, for cytoplasmic cytokine staining, cells were fixed with Fixation Buffer (Biolegend) for 10 minutes at RT then washed twice with 1X Permeabilization Wash Buffer ("Perm Wash"). Fixed cells were either stored in the dark at 4ºC for a maximum of 3 days, or immediately subjected to intracellular staining by incubating for ~1 hour at 4ºC in the dark with 50µL per $2x10^6$ cells of antibodies diluted in Perm Wash before being washed again. Cells stained with unconjugated rabbit primary antibodies for intracellular markers were then stained for 30 mins at 4ºC in the dark with a goat anti-rabbit secondary antibody (AlexaFluor 594 or AlexaFluor 647) in Perm Wash containing 10% normal goat serum. Stained cells were then washed with Perm Wash followed by FACS buffer before resuspension in 100-150µL FACS buffer for analysis on a flow cytometer in either FACS tubes or cluster tubes. Flow cytometric data were collected on the following flow cytometers: BD FACSymphony A5, BD FACSymphony A3, BD Fortessa and BD Canto II, using BD FACSDiva software v9.1 (BD Biosciences). Specific gating strategies to isolate transgenic TCR $CD45.1^+$ $CD8^+$ T cells from *ex vivo* samples across various experimental models (Fig. S1). A minimum of 1,000 CD45.1+ CD8+ T cell events were recorded per sample whenever possible.

2.2.8.2. CaspGLOW staining

To assess caspase activity, cells in specific experiments (Section 5.2.2) were stained with the CaspGLOW™ Fluorescein Active Caspase Staining Kit according to the manufacturer's instructions. After splenocyte isolation (Section 2.2.3.1), cells were transferred to U-bottom plates were pelleted and resuspended in 5uL/mL FITC-DEVD-FMK CaspGLOW stain in 10% cRPMI. Cells were incubated for 45-60mins at 37ºC, 5% CO_2, washed twice with CaspGLOW Wash, and then subjected to downstream flow cytometry procedures.

2.2.8.3. *Cell sorting*

FACS-based sorting was performed to isolate CRISPR-edited CD45.1$^+$ CD8$^+$ T cells (Section 2.2.9.1) from splenocytes of recipient B6 mice at either day 8 or day 42 of LCMV Armstrong infection. Isolated splenocytes (Section 2.2.3.1) were pooled according to each KO condition and resuspended at 1x10^8 cells/mL in MACS Buffer in FACS tubes. At the corresponding resuspension volume, cells were stained with the following surface antibodies for 30 minutes on ice: CD8 BUV395, CD45.1 Pacific Blue, Vα2 PE, B220 Biotin, CD11b Biotin, CD4 Biotin, and NK1.1 Biotin. Cells were washed with MACS buffer, filtered through a 35 µM nylon mesh, pelleted, followed by secondary staining with streptavidin PE-Cy7 for 20 mins on ice. Cells were washed, filtered, pelleted, and then resuspended at 5x10^7 cells/mL in MACS buffer containing 1/100 7AAD viability stain. Stained cells were filtered again and sorted (see Fig S3 for gating strategy) by the PMCC Flow Cytometry Facility through a 100µM nozzle on a BD FACSAria Fusion 5 Cytometer into a FACS tube with RPMI containing 20% FBS. Sorted cells were pelleted and resuspended in cold PBS for downstream processing (Section 2.2.9.1).

2.2.9. DNA Sequencing of KO genomic regions

2.2.9.1. Sample preparation and DNA extraction

Cells subjected to long-read sequencing were CRISPR-edited P14 cells either cultured in IL-7 for 24 hrs (Section 2.2.4.2) or sorted from splenocytes of LCMV-Armstrong infected mice (Section 2.2.7.3). Genomic DNA (gDNA) from these cells were isolated through column-based extraction using DNeasy Blood and Tissue DNA Extraction Kit (QIAGEN) following manufacturer's instructions. gDNA was eluted in TE buffer and was quantified using a NanoDrop spectrophotometer (Thermo Fisher) and/or the 1X dsDNA HS Assay Kit (Invitrogen) on a Qubit fluorometer. gDNA samples were stored in -20 ºC until use.

2.2.9.2. Polymerase Chain Reaction (PCR), DNA sequencing, and CRISPR variant analysis

Genomic regions for the gene KOs were PCR-amplified prior to long-read sequencing. DNA primers pairs for *Junb, Jun,* and *Jund* (Table 9) were designed using Primer3 to amplify a 1,000-1,200 base pair (bp) amplicon of the genomic region that covers the CRISPR target sites for each gene, with at least 100 bp away from the closest target site. All primers were obtained from IDT and were resuspended in nuclease-free water at a 10µM concentration and stored in -20 ºC until use.

Table 12 Primers used for PCR for DNA sequencing of KO regions

Primer	Target (size)	Sequence
JunB Forward	*Junb* (1175 bp)	GCCTTTACGCACAGCTGCCA
JunB Reverse		AGCAACTGGCAGCCGTTGCT
cJun Forward	*Jun* (1169 bp)	AGCGCACGCTCCTAAACAAA
cJun Reverse		ATTGCCCCTCAGCCCTGACA
JunD Forward	*Jund* (1172 bp)	GCTCCCGCCCCTTTATGCAA
JunD Reverse		TGTTTGAGCTGCGCCACCTG

The touchdown PCR protocol below (Table 10) was utilised, with each PCR reaction mixture containing the following: 12.5µL Q5 High-Fidelity 2X Master Mix (New England Biolabs), 1.25µL 10µM forward primer, 1.25µL 10µM reverse primer, the volume required for 50ng gDNA, and topped up to 25µL with nuclease-free water. PCR reactions were run on a T100 Thermal Cycler (BioRad), and the resulting PCR products were submitted to Plasmidsaurus for DNA cleanup and Premium PCR Sequencing using Oxford Nanopore Technology with custom analysis and annotation.

Table 13. Touchdown PCR Parameters for DNA sequencing of KO regions

Step	Temp. (°C)	Time (sec)	Cycles	Stage
1	98	30	1	Initial Denaturation
2	98	10	10	Denaturation
3	73 (-0.5/cycle)	30		Annealing (Touchdown step)
4	72	90		Extension
5	98	10	25	Denaturation
6	68	30		Annealing
7	72	90		Extension
8	72	120	1	Final extension
9	4	∞		Hold temperature

Genome editing outcomes for *Jun, Junb,* and *Jund* (modifications such as insertions, deletion, and/or substitutions) from raw FASTQ reads were analysed via CRIPResso2 utilising the sgRNAs and their corresponding amplicon reference sequences, using default parameters except for a minimum alignment threshold of 40%[497].

2.2.10. Co-immunoprecipitation / Mass Spectrometry (Co-IP MS)

2.2.10.1. Co-IP MS sample preparation

For Co-IP MS experiments (Section 4.2.2) OT-I CD8+ T cells were isolated and activated with CD3/CD28/IL2 as per Sections 2.2.3.1 and 2.2.4.1 respectively. ~4.5×10^7 activated OT-I cells were subjected to IP (n=2 biological replicates) using a previously

described protocol [498,499]. Cells were washed twice with PBS and sequentially lysed on ice using 2 cell pellet volumes each of i) hypotonic lysis buffer (40 minutes; 10mM HEPES pH 7.5, 10mM KCl, 1.5mM $MgCl_2$); ii) nucleoplasmic lysis buffer (20 minutes; 20mM HEPES pH 7.9, 1.5mM $MgCl_2$, 150mM potassium acetate, 10% (v/v) glycerol, 0.05% (v/v) NP-40); low salt chromatin digestion buffer (1 hour, 20mM HEPES pH 7.9, 1.5mM $MgCl_2$, 10% (v/v) glycerol, 150mM NaCl, 0.1% (v/v) NP-40, 250 U/mL Benzonase (Merck, 70746–4)) and; iv) high salt chromatin lysis buffer (20 minutes, 20mM HEPES pH 7.9, 3mM EDTA, 1.5mM $MgCl_2$, 10% (v/v) glycerol, 500mM NaCl, 0.1% (v/v) NP-40). High salt chromatin fractions were diluted with high salt dilution buffer (6 pellet volumes; 20mM HEPES pH 7.9, 3mM EDTA, 1.5mM $MgCl_2$, 10% (v/v) glycerol, 0.1% (v/v) NP-40). Nucleoplasmic, low salt chromatin and diluted high salt chromatin lysates were combined and tumbled for 2hrs at 4°C with 5µg antibody (JunB Cell Signalling, cJun Cell Signalling, JunD Abcam, purified rabbit IgG, Bethyl Laboratories P120–101) and 25µL Dynabeads™ Protein A. Beads were washed 5 times (20mM Tris-HCl pH 7.5, 150mM NaCl, 1.5mM $MgCl_2$, 3mM EDTA, 10% (v/v) glycerol, 0.1% (v/v) NP-40) and 2 times in 100mM ammonium bicarbonate. Beads were resuspended in 50µL 100mM ammonium bicarbonate and incubated overnight at 37°C with 400ng Trypsin (Promega V5280). Beads were supplemented with an additional 400ng Trypsin and incubated for a further 4hrs at 37°C. The peptide-containing supernatant was isolated from the beads and acidified through the addition of 10% formic acid. Peptides were isolated using C18 ultra micro-spin columns (Pierce #87782) which had been pre-conditioned (100% acetonitrile followed by 2 rounds of 80% acetonitrile) and equilibrated (0.5% formic acid). Columns were washed twice (0.1% formic acid) and peptides were eluted using 40µL 80% acetronitrile diluted in 0.1% formic acid. Excess acetonitrile was evaporated using a vacuum centrifuge and samples were analysed at the Bio21 Mass Spectrometry and Proteomics facility (Parkville, VIC 3052, Australia). LC MS/MS was carried out on a QExactive plus Orbitrap mass spectrometer (Thermo Scientific) with a nanoESI interface in conjunction with an Ultimate 3000 RSLC nanoHPLC (Dionex Ultimate 3000). The LC system was equipped with an Acclaim Pepmap nano-trap column (Dinoex-C18, 0 Å, 75µm × 2cm) and an Acclaim Pepmap RSLC analytical column (Dinoex-C18, 100 Å, 75µm × 50cm). The tryptic peptides were injected to the enrichment column at an isocratic flow of 5µL/min of 2% v/v CH_3CN containing 0.1% v/v formic acid for 5 min applied before the enrichment column was switched in-line with the analytical column. The eluents were 0.1% v/v formic acid (solvent A) and 100% v/v CH_3CN in 0.1% v/v formic acid (solvent B). The flow gradient was (i) 0–6min at 3% B, (ii) 6–40 min, 3–25% B (iii) 40–48 min, 25–45% B (iv) 48–50 min, 40–80% B (v) 50–53 min, 85–85% B (vi) 53–54 min 85–3% and equilibrated at 3% B for 10 minutes before the next sample injection. The QExactive plus mass spectrometer was operated in the data-dependent mode, whereby full MS1 spectra were acquired in positive mode, 70 000 resolution, AGC target of 3e6 and maximum IT time of

50ms. Fifteen of the most intense peptide ions with charge states ≥2 and intensity threshold of 1.7e4 were isolated for MSMS. The isolation window was set at 1.2m/z and precursors fragmented using normalized collision energy of 30, 17 500 resolution, AGC target of 1e5 and maximum IT time of 100ms. Dynamic exclusion was set to be 30sec. Label free quantification of detected peptides was carried out using the MaxQuant computational platform and biologically meaningful insights were gained using the Perseus bioinformatics platform (see Section 2.3.2 for more data analysis pipeline details).

2.2.10.2. Co-IP MS bioinformatic analysis

Results from the MaxQuant 1.6.2.3 program were processed in R version 4.4.1 to filter out potential contaminants, peptides in reverse directions and protein groups with max score larger than 40. Statistical tests were performed with the function stat_test from the package IPinquiry4 [500], with scaling factor from "DEseq" on nuclear genes (GO:0005634). Known protein binders were extracted from StringDB using R package STRINGdb [501] and visualised with ggplot2 v3.5.1[502].

Top candidate interaction partners for each individual Jun protein (JunB, cJun, and JunD) were defined as proteins exhibiting a $\log_2$ fold change >5 and a p-value <0.05 based on IPinquiry statistical testing. Pathway enrichment analysis was performed using STRING v12.0 (Search Tool for the Retrieval of Interacting Genes/Proteins; https://string-db.org) on each unique and shared candidate binding partners. Only the enriched pathways from Gene Ontology (Biological Processes) and Reactome pathway databases were recorded. To appraise biological connectivity and visualize enriched pathways, protein–protein interaction networks were generated also through STRING with a minimum required interaction score of 0.7, incorporating all available active interaction sources.

2.2.11. Cleavage Under Targets & Release Using Nuclease (CUT&RUN)

2.2.11.1. CUT&RUN sample preparation

Cleavage Under Targets & Release Using Nuclease (CUT&RUN) was performed using CD8+ T cells from B6 mice that were isolated and activated via CD3/CD28/IL2 stimulation *in vitro* for 24hrs as per described in Sections 2.2.3.1 and 2.2.4.1 respectively. In some repeats, dead cells post-activaion were removed using the EasySep Dead Cell Removal (Annexin V) Kit (STEMCELL Technologies) according to manufacturer's procedures. ~5×10^5 activated CD8+ T cells were subjected to CUT&RUN using the CUTANA ChIC/CUT&RUN Kit (Epicypher) following manufacturer's instructions. Activated cells were transferred to 8-strip PCR tubes, washed in a buffer containing spermidine and protease inhibitors, then bound to pre-activated Concanavalin A (ConA) conjugated paramagnetic beads through adsorption. Cell-bead suspensions were washed and isolated through magnetic separation. Antibody binding buffer containing 0.001% digitonin and 2mM EDTA was added to permeabilise the

cells, then 1µL of target antibody (JunB Cell Signalling, cJun Cell Signalling, JunD Abcam, see Section 2.1.3) was added per CUT&RUN reaction and cells were incubated overnight at 4ºC under constant rotation (60 RPM) on a 3D Nutating Mixer. Cell-bead suspensions were then washed, incubated with 2.5µL pAG-Mnase (20X) for 10 minutes at room temperature and washed again, before targeted chromatin digestion and release through incubation for 2hrs at 4ºC with constant rotation after addition of 1µL calcium chloride (100mM). pAG-Mnase activity was then halted with the addition of 33µL stop buffer and incubation for 10 mins at 37ºC in a thermocycler. The stop buffer chelates calcium ions and contains an *E.coli* Spike-in DNA for downstream NGS normalisation. Cell-bead suspensions were magnetically pelleted and the supernatant containing CUT&RUN enriched DNA was transferred to new tubes. DNA purification was then performed using nucleic acid purification spin-columns or SPRIselect beads. Purified CUT&RUN enriched DNA was quantified using the 1X dsDNA HS Assay Kit (Invitrogen) on a Qubit fluorometer.

2.2.11.2. Library Preparation and Quality Control

Illumina NGS libraries were prepared from 5ng of purified CUT&RUN enriched DNA using the CUTANA CUT&RUN Library Prep Kit (Epicypher) following a combinatorial dual indexing primer strategy. Briefly, the CUT&RUN enriched DNA was mixed with an End Repair Master Mix (comprised of End Prep Buffer and End Prep Enzyme) and incubated on a thermocycler initially for 20 mins at 20ºC, then for 30 mins at 65ºC, before being held at 4ºC until the next step. The reactions were added with Illumina Adapters, alongside a Ligation Master Mix, composed of a Ligation Mix and Ligation enhancer, and were incubated in a thermocycler at 20ºC for 15 minutes without a heated lid. U-Excision Enzyme was then added followed by incubation at 37ºC for 15 mins, with the lid temperature set to >47 ºC. CUT&RUN pre-indexing libraries for each reaction were purified through SPRIselect reagent clean-up procedures and eluted in 0.1X TE buffer. Each CUT&RUN reaction was assigned a unique pair of i5 and i7 indexing primers. Indexing PCR master mixes were prepared by adding the unique i5-i7 pair and HotStart 2x PCR Master Mix to the CUT&RUN pre-indexing libraries. PCR was then performed using the following PCR parameters:

Table 14. PCR Parameters for CUT&RUN Library Preparation

Step	Temp. (°C)	Time (sec)	Cycles	Stage
1	98	45	1	Hot Start activation of DNA Polymerase
2	98	15	14	DNA melting
3	60	10		Hybrid annealing/extension
4	72	60	1	Final extension
5	4	∞		Hold temperature

The resulting indexed libraries were again purified through SPRIselect reagent clean-up procedures and eluted in 0.1X TE buffer. Library quality was assessed on an Agilent Tapestation using the D1000 ScreenTape (Agilent) following manufacturer's instructions. Successful CUT&RUN Library preparation was indicated by fragment peaks at ~300 bp (i.e. the size of nucleosome bound DNA + sequencing adapter fragments). CUT&RUN libraries were quantified using the 1X dsDNA HS Assay Kit on a Qubit fluorometer, and paired-end DNA sequencing was performed on the NextSeq 2000 platform (Illumina) at the PMCC Molecular Genomics Core.

2.2.11.3. CUT&RUN bioinformatic analysis

2.2.11.3.1. Hybrid genome construction

To construct a custom hybrid genome for downstream alignment, the primary FASTA files for the *Mus musculus* reference genome, GRCm38 (mm10) and the *E. coli* K12-MG1655 genome were first obtained and then concatenated to generate a single hybrid reference genome FASTA, which was indexed with Bowtie2 version 2.3.4.1 with the bowtie2-build command.

2.2.11.4. CUT&RUN Data pre-processing and analysis

Raw CUT&RUN sequencing data from mouse samples (with K12-MG1655 *E. coli* spike-in) were processed using a series of bash scripts. Quality control of raw and trimmed reads was performed using FastQC version 0.11.5. Adapter and quality trimming was carried out with BBDuk (bbmap version 35.19). Screening for contamination and alignment rates against the *E. coli* spike-in was performed using FastQ Screen version 0.15.3. Reads were aligned to a custom hybrid genome (mouse mm10 + K12-MG1655) using Bowtie2 version 2.3.4.1, followed by SAM/BAM processing using SAMtools version 1.9 and Sambamba version 0.6.7. BAM files were filtered to remove mitochondrial reads, blacklisted regions (ENCODE mm10 version 2), PCR duplicates (marked with Picard version 3.0.0), and multimappers. Coverage tracks were generated using deepTools' bamCoverage version 3.5.0 and normalized to RPKM. Peak calling was conducted using MACS2 version 2.2.7.1 with IgG input controls. Fragment size and insert size distributions were assessed with Picard's CollectInsertSizeMetrics, and mapping statistics were compiled using SAMtools. MultiQC was used to generate quality control summaries.

Genomic signal tracks (bigWigs) were generated and viewed using the Integrative Genomics Viewer (IGV)[503]. Gene annotation of peaks and overlap analysis were performed via ChIPSeeker R package[504]. Motif enrichment analysis was performed via the Analysis of Motif Enrichment (AME) function of the Memes R package[505]. Enrichment analysis for the shared and unique target genes of the Jun members was performed through the online Enrichr tool, focusing on Gene Ontology (Biological Processes) and Reactome databases [506].

2.2.11.5. Peak overlap analysis with NFAT ChIP-Seq data

To validate Jun protein and NFAT co-occupancy, we utilised published NFAT ChIP-seq data (GSE64409) from wild-type CD8+ T cells *in vitro* stimulated with PMA/ionomycin for 1 hr[141]. The NFAT ChIP-seq bigWig file was lifted over to the mm10 reference genome via the liftOver R package[507]. Comparative analysis of JunB, cJun, JunD, and NFAT bigWig files was performed using the rtracklayer and GenomicRanges R packages[508,509]. Discrete peaks were defined by filtering signal scores $\geq$ 5, merging adjacent regions within 100bp, while removing fragments < 50bp. All peak sets were merged, resulting to a master consensus locus framework. Presence of each transcription factor and co-occupancy at each consensus locus was defined as a minimum threshold of $\geq$ 1 bp direct overlap between each individual factor peak and the consensus locus. Annotation of consensus regions against the mm10 mouse genome was performed using the following R annotation packages: ChIPSeeker[504], org.Mm.eg.db[510] and TxDb.Mmusculus.UCSC.mm10.knownGene[511]. Promoter targets were defined as those within ±3kbp of transcription start sites. Peak and peak-associated gene overlaps were visualised using the VennDiagram R package[512].

2.2.12. Multiplexed Analysis of Cells Sequencing (MAC-Seq)

2.2.12.1. MAC-Seq sample preparation

Multiplexed analysis of cells sequencing (MAC-Seq) was performed at the PMCC Molecular Genomics Core and the Victorian Centre of Functional Genomics (VCFG) as previously described [513]. Naïve B6 CD8+ T cells were isolated and edited by CRISPR/Cas9 RNP electroporation to generate the following CRISPR KO groups: AP-1 sgRNA, cJun sgRNA, JunB sgRNA, JunD sgRNA, cJun/JunD sgRNA, BATF sgRNA and Ctrl sgRNA (see Table 8, Section 2.2.3.1 and 2.2.5). $5x10^3$ CRISPR KO cells from 2 independent biological replicates prepared in parallel were then aliquoted in triplicate (3 technical replicates) across 6 separate 96-well V-bottom plates, with each plate allocated to a different timepoint (unstimulated, 1.5hrs, 3hrs, 6hrs, 12hrs, 24hrs). Cells were then activated with CD3/CD28/IL-2 (as in Section 2.2.4.1), or, in the case of the unstimulated condition, resuspended in 10% cRPMI alone and incubated in 37ºC, 5% CO_2 for 30 mins (i.e. harvested in parallel with the 30min stimulation timepoint). At each timepoint, plates were spun down, washed once with PBS, then pelleted again and immediately snap frozen on dry ice after removal of the supernatant. To account for potential batch effects at each timepoint, an unrelated set of purified naïve WT B6 CD8+ T cells, fixed via the FixNCut protocol[514], were added in triplicate to each plate as a normalisation control for downstream bioinformatic analysis. RNA extraction, library preparation and RNA sequencing was performed for each plate well by the PMCC Molecular Genomics Core according to an adapted MAC-Seq workflow [513]. Indexed libraries were sequenced on a NextSeq 500 instrument (Illumina) using a custom sequencing primer (i.e. MAC-seq Read

primer) and a High Output Kit v2.5 75 Cycles (Illumina) with paired-end configuration (25 base pairs for read 1 and 50 base pairs for read 2).

2.2.12.2. MAC-Seq bioinformatic analysis

2.2.12.2.1. Alignment, Quality Control, and Integration of MACSeq plates

Data pre-processing procedures were performed by the VCFG at the PMCC. Raw FASTQ files were obtained and aligned to the human reference FASTA file using STARsolo in an in-house Nextflow pipeline Dinoflow. MultiQC was used to provide a report of alignment outcomes and sequencing quality. A matrix of raw reads was generated for downstream analyses.

Sequencing quality in each well was examined to confirm reasonable numbers of genes and reads. Relative log expression was calculated for each sample to check the consistency of gene expression across different samples. Principal component analysis was performed to reveal relationships among samples, such as any unwanted effects like row or column effects. Standard deviations of RNA read counts were calculated for each treatment group (i.e. KO condition and activation timepoint) and for the entire plate. Treatment groups were flagged as potential outliers if their standard deviation was greater than the whole plate's standard deviation. Clustering analysis was initially done for each MAC-Seq plate to see if the plate control groups and empty wells could be separated from the treatment wells, signifying that the differences in gene expression are independent of batch effects. Three integration methods were used to integrate plates together: Canonical Correlation Analysis (CCA), Mutual Nearest Neighbour (MNN) and Harmony[515]. The integrated data was then clustered and visualised to check for batch effects or any other issues that might affect the downstream analysis.

2.2.12.2.2. Differential gene expression

Differential gene expression analysis was performed using the edgeR package on count matrices extracted from the pre-processed MACseq data [516]. Normalisation factors were estimated using the TMMwsp (Trimmed Mean of M-values with singleton pairing) method to correct for compositional differences across libraries. A design matrix without an intercept (i.e., ~ 0 + group) was used to model expression levels for each treatment group. Dispersion estimates were calculated, followed by fitting a quasi-likelihood negative binomial model using default settings of edgeR. A contrast matrix was created to evaluate pairwise comparisons between each knockout against a common control group (Ctrl sgRNA). Quasi-likelihood F-tests were applied to each contrast, and differential expression results were extracted applying Benjamini-Hochberg correction for multiple testing. The resulting gene-level statistics were then used as input for gene set enrichment analysis (GSEA) with the fgsea R package to calculate enrichment scores for specific human gene sets mapped to mouse orthologs [517,518],

along with a manually curated gene set from our research group[91]. Bubble plots and GSEA heatmaps of normalised enrichment scores (NES) were generated using the R packages ggplot2, tidyverse and ComplexHeatmap[519].

2.3. Statistical Analysis

Flow cytometric data (i.e. frequencies and mean/median fluorescence intensities (MFI)) and representative flow cytometry plots were generated using FlowJo Software (Treestar, version 10), and downstream calculations were conducted using Microsoft Excel (v16.71). Graphing of data and statistical analyses were conducted through Prism Software (GraphPad, version 10). For pairwise comparison, p values were calculated using either an unpaired T test when data passed normality tests, or otherwise a two-tailed Mann Whitney test. For comparison of 3 or more groups, p values were calculated using an ordinary one-way ANOVA with post-hoc Dunnett's multiple comparison's test or two-tailed Kruskal-Wallis test with post-hoc Dunn's multiple comparison's test to compare all groups against the control group. For timecourse data containing multiple groups (e.g. serial bleed experiments), p values were calculated using a restricted maximum likelihood (REML) analysis of mixed effects models followed by multiple comparisons analysis via an uncorrected Fisher's LSD test.

2.4. Data Availability

Raw datasets and processed bioinformatic data will be made available in public repositories. Sequencing reads and alignment files from CUT&RUN and MACSeq will be deposited to the NCBI Gene Expression Omnibus[520]. Raw Co-IP MS proteomics data will be submitted to the Proteomics Identifications Database[521].

CHAPTER 3

Measuring the influence of TOX on peripheral CD8+ T cell tolerance

3.1. INTRODUCTION

CD8+ T cells adopt distinct hypofunctional states in response to chronic antigen to limit both autoimmunity and infection-induced immunopathology. This includes important regulatory states such as peripheral tolerance and exhaustion, which both attenuate T cell effector function via a diversity of molecular mechanisms [284,286,378-380]. Peripheral tolerance is induced in lymphoid organs when naïve T cells encounter antigen in the absence of innate immune activation. Tolerant cells fail to acquire effector functions and rapidly exit cell cycle, preventing these cells from participating in an immune response. As T cells that recognise antigen in the steady-state are likely to be self-reactive, this prevents self-reactive T cells from differentiating into effector cells that could cause autoimmunity, although this process is also hijacked by cancer to evade immunity [201]. In contrast, exhaustion arises later in the immune response when cells that have already begun to differentiate into effector cells encounter persistent, elevated antigen in contexts such as chronic viral infection and cancer. Exhaustion is characterised by diminished cytokine production and muted T cell proliferative expansion, which is likely an evolutionary adaptation to reduce the risk of collateral immunopathology during a widely disseminated infection [286]. Consistent with these two states arising at fundamentally different points in the immune response, exhaustion and tolerance are transcriptionally and epigenetically distinct processes that trigger distinct differentiation trajectories[91]. Nevertheless, tolerance and exhaustion share some similarities, including deficiencies in cytokine production, restraint by checkpoint molecules such as PD-1, and induction of an NFAT-dependent regulatory gene program downstream of diminished AP-1 activity [141,339,378,522]. These overlapping features mean that peripheral tolerance and exhaustion are often assumed to be similar processes [217,378,522]. Resolving whether conserved molecular processes enforce both tolerance and exhaustion is crucial to enable therapeutic targeting of these regulatory checkpoints in contexts such as autoimmunity and cancer [98,201,306,353].

The transcription factor TOX is critically required for the transcriptional and epigenetic commitment of chronically stimulated cells towards an exhausted fate [311,349,350]. TOX expression is induced in exhausted cells by the NFAT homodimers that form in the absence of AP-1, meaning that NFAT may similarly induce TOX during tolerance induction. Indeed, TOX expression is up-regulated in tolerant CD8+ T cells [91,229], raising the possibility that a common TOX-driven gene regulatory program underpins both tolerance and exhaustion. In this chapter, we test this hypothesis by deleting TOX in CD8+ T cells undergoing peripheral

tolerance in an *in vivo* tolerance model. We find that TOX is fully dispensable for tolerance induction across a range of different contexts, providing functional evidence that tolerance and exhaustion are molecularly distinct processes.

3.2. RESULTS

3.2.1. TOX is upregulated in tolerance but not as much as in exhaustion

To compare TOX levels in tolerance versus exhaustion, we first assessed TOX protein expression in tolerant, exhausted and early effector CD8+ T cells (Fig. 3.1A). To generate tolerant or early effector cells, CD45.1+ ovalbumin (OVA)-specific TCR transgenic CD8+ (OT-I) cells were adoptively transferred into either RIP-OVA^{hi} mice, or wild-type C57BL/6 (B6) mice infected intravenously (i.v.) with OVA-transgenic *Listeria monocytogenes* (LM-OVA) respectively [224,488,491].

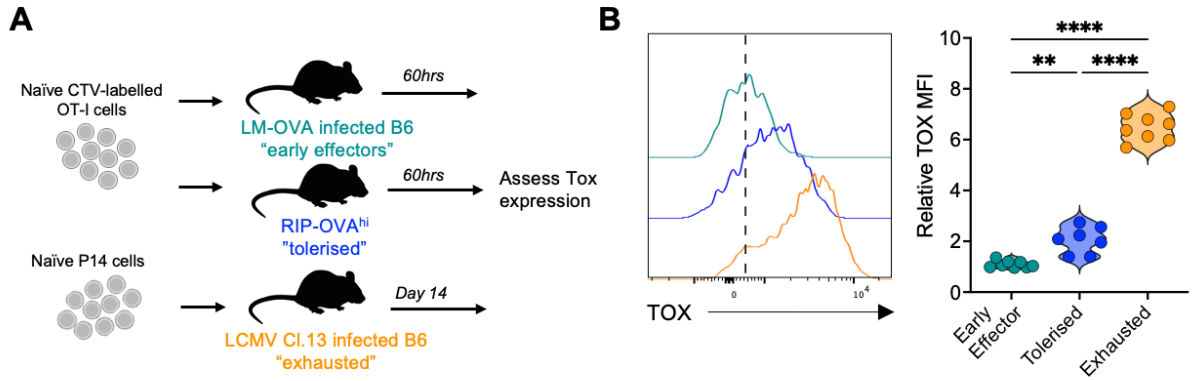


Figure 3.1. TOX expression of distinct differentiation states
(A) 2x10^6 CD45.1+ CTV-labelled OT-I cells were injected into RIP-OVA^{hi} mice, or B6 mice subsequently infected i.v. with LM-OVA. 5x10^3 CD45.1+ P14 cells were injected into B6 mice, and 2-3 days recipients were infected i.v. with LCMV Cl.13. Either 60hrs (tolerised; blue and early effector cells; teal) or 14 days later (exhausted; orange), CD8+ CD45.1+ cells were assessed for TOX expression in either the sacral and pancreatic LNs (tolerised) or spleens (early effectors, exhausted).
(B) Representative histogram plot (left) and pooled expression data (right) are shown from n=7-8 mice per condition from two experiments. A dotted vertical line in the histogram indicates TOX MFI of naïve OT-I cells transferred into an uninfected B6 control. MFI values are shown relative to the MFI of naïve OT-I cells; p-values were calculated using a Kruskal-Wallis test with a post-hoc Dunn's multiple comparisons test: ** = $p < 0.01$, **** = $p < 0.0001$

RIP-OVA^{hi} mice transgenically express OVA as a model self-antigen within their insulin producing pancreatic islet β cells. Islet-derived OVA is constitutively cross-presented in the draining pancreatic lymph node, and OT-I antigen engagement in this model triggers peripheral tolerance. To generate exhausted cells, CD45.1+ LCMV GP$_{33-41}$-specific TCR transgenic CD8+ (P14) cells were adoptively transferred into B6 infected i.v. with the chronic LCMV Cl.13 strain [487,490]. CD45.1+ CD8+ cells were then analysed for TOX expression by flow cytometry at either 60hrs for OT-I cells, which is when OT-I commit to a tolerant fate in the RIP-OVA^{hi} model [91] or at Day 14 for P14 cells, which is when cells begin to commit to an exhausted fate in the LCMV Cl.13 model [314]. In line with previously published RNA and protein

expression data [91,229], tolerised cells expressed TOX protein at ~2 fold higher levels than in early effector cells, however, TOX levels in tolerised cells were still significantly lower (~3 fold) than those found in exhausted cells (Fig. 3.1B). As this comparison may be confounded by intrinsic differences between TCR-transgenic cells (i.e. OT-I versus P14), future efforts to measure TOX expression of *in-vivo* exhausted OT-I cells such as those responding to OVA-expressing tumours[523] are essential. Altogether, our preliminary data indicate that while tolerant cells up-regulate TOX expression relative to functional effector cells, this increase is not to the levels seen in exhaustion.

3.2.2. TOX deletion via CRISPR functionally mimic established TOX-deficient phenotype in chronic infection

To functionally assess the importance of TOX in peripheral tolerance induction, we first optimised *Tox* deletion in naïve CD8+ T cells using an electroporation-based CRISPR/Cas9 gene knockout (KO) approach [496]. Two single guide RNAs (sgRNA) were designed to target the HMG-Box DNA binding domain and nuclear localisation signal respectively in exon 5 of the *Tox* gene (Fig. 3.2A). KO efficiency was validated *in vitro* in T cells stimulated with ionomycin to trigger NFAT-dependent *Tox* induction. *Tox* gene deletion with these sgRNAs ("Tox sgRNA") led to a 95% reduction in TOX protein levels relative to control cells treated with an sgRNA targeting an irrelevant gene (*Cd19*; "Ctrl sgRNA") (Fig. 3.2B) [383].

To validate that CRISPR editing resulted in a functional knockout of the *Tox* gene, we assessed whether CRISPR edited P14 cells could recapitulate the previously reported TOX deficient phenotype during LCMV Cl.13 infection [311,349,350,524]. At days 8 and 27 of chronic infection, Tox sgRNA edited P14 cells had reduced TOX expression compared to control cells (Fig. 3.2C, 3.2E). Importantly, relative to control cells, day 8 Tox sgRNA cells had a partial loss of PD-1 and TIGIT, alongside reduced frequencies of TCF1+ cells (Fig. 3.2D) that closely resembled the published Day 8 *Tox* knockout phenotype[349]. Moreover, *Tox* deletion dramatically skewed cells towards an intermediate exhausted phenotype (TCF1- CX3CR1+ CD101-) at the expense of CD101+ terminally exhausted cells at later timepoints post-infection (p.i.) (day 27) alongside an overall reduction in P14 numbers in line with prior reports using *Tox* knockout mice [292,349] (Fig. 3.1F-G). Thus, our CRISPR editing approach leads to a functional deletion of the *Tox* gene.

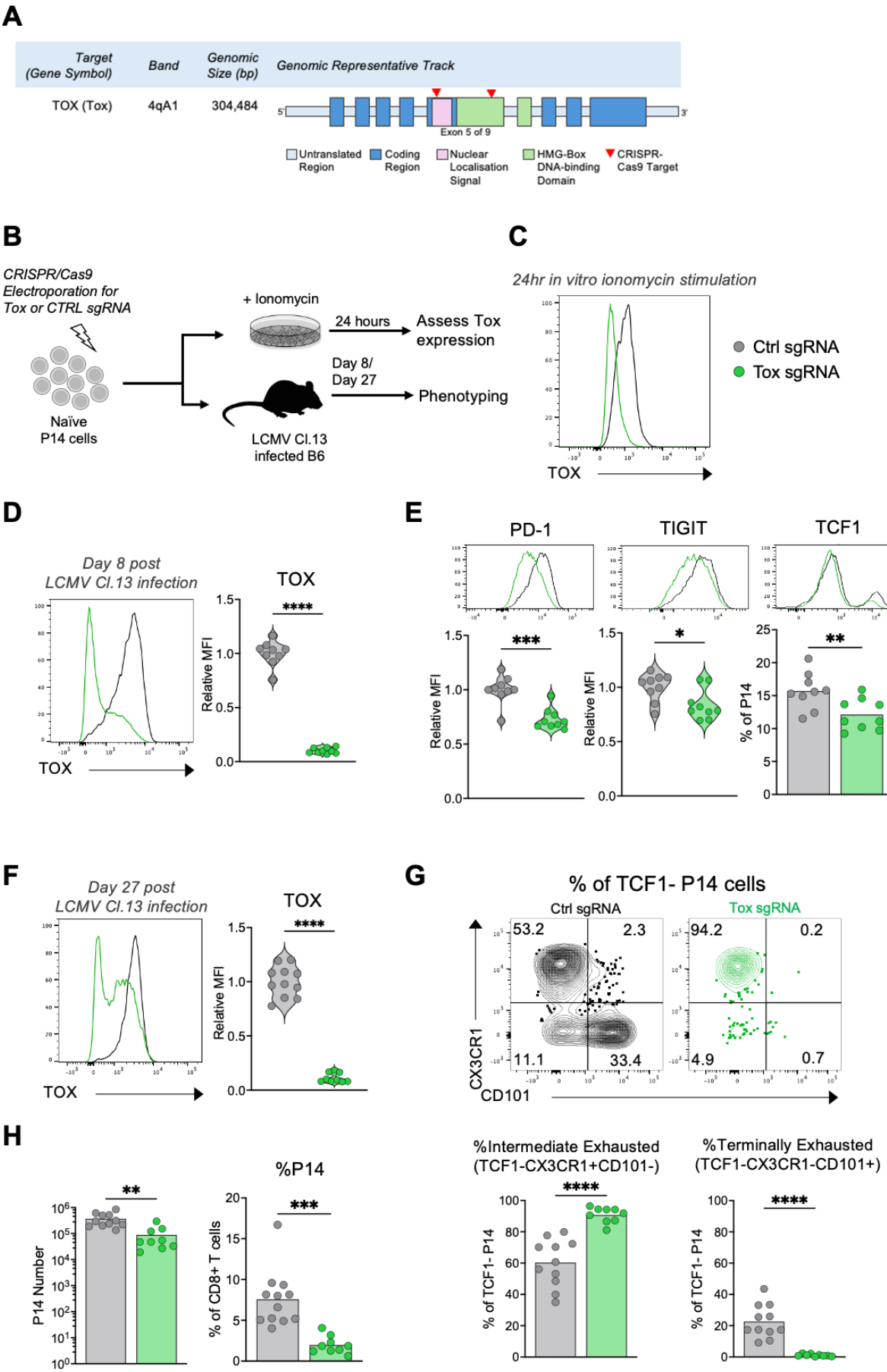

A
Target (Gene Symbol)
Band
Genomic Size (bp)
Genomic Representative Track
TOX (Tox)
4qA1
304,484
5'
3'
Exon 5 of 9
Untranslated Region
Coding Region
Nuclear Localisation Signal
HMG-Box DNA-binding Domain
CRISPR-Cas9 Target
B
CRISPR/Cas9 Electroporation for Tox or CTRL sgRNA
Naïve P14 cells
+ Ionomycin
24 hours
Assess Tox expression
Day 8/ Day 27
Phenotyping
LCMV Cl.13 infected B6
C
24hr in vitro ionomycin stimulation
TOX
Ctrl sgRNA
Tox sgRNA
D
Day 8 post LCMV Cl.13 infection
TOX
Relative MFI
****
E
PD-1
TIGIT
TCF1
Relative MFI
% of P14
***
*
**
F
Day 27 post LCMV Cl.13 infection
TOX
Relative MFI
****
G
% of TCF1- P14 cells
Ctrl sgRNA
Tox sgRNA
53.2
2.3
11.1
33.4
94.2
0.2
4.9
0.7
CX3CR1
CD101
H
P14 Number
**
%P14
% of CD8+ T cells
***
%Intermediate Exhausted (TCF1-CX3CR1+CD101-)
%Terminally Exhausted (TCF1-CX3CR1-CD101+)
% of TCF1- P14
****

Figure 3.2. Optimisation and functional validation of TOX gene deletion via CRISPR
(A) Location of CRISPR-Cas9 sgRNA target sites relative to the functional domains of the *Tox* gene coding regions.
(B) P14 cells were subjected to CRISPR-Cas9 nucleofection with either Tox sgRNA (green) or Ctrl sgRNA (grey) RNPs. *Tox* KO was validated by assessing TOX expression via flow cytometry 24hr after *in vitro* stimulation with ionomycin alone, or immune phenotyping of CRISPR-edited CD45.1+ P14 cells at days 8 and 27 p.i. after adoptive transfer into B6 mice subsequently infected with LCMV Cl.13.
(C) Representative histogram plot of TOX expression after *in vitro* stimulation.
(D) Representative histogram plot (left) of TOX expression within splenic CD45.1+ P14 cells at day 8 p.i. Pooled MFI data (right) are shown from three independent experiments (n=9 mice per group).
(E) PD-1, TIGIT, and TCF1 expression in splenic Tox sgRNA and Ctrl sgRNA P14 cells from LCMV Cl.13 infected B6 mice at day 8 p.i. Representative histograms (top) and pooled MFI data (bottom) are shown from three independent experiments (n=9 mice per group).
(F) Representative histogram plot (left) of TOX expression within splenic CD45.1+ P14 cells at day 21 p.i. Pooled MFI data (right) are shown from three independent experiments (n=9-11 mice per group).
(G) Representative flow cytometry plots (top) depicting the frequencies of TCF1-CX3CR1+CD101- "Intermediate Exhausted" and TCF1-CX3CR1-CD101+ "Terminally Exhausted" cells within TCF1- CD45.1 splenic Tox sgRNA or Ctrl sgRNA P14 cells at day 27 p.i. Pooled frequency data are shown (bottom graphs) from three independent experiments (n=9-11 mice per group).
(H) CD45.1+ P14 cells number (left) and frequency within CD8+ cells (right) for each sgRNA condition at day 27 p.i. from three independent experiments (n=9-11 mice per group).
When phenotyping the Tox sgRNA edited cells, unedited (TOX^{hi}) cells were excluded from the analysis. MFI values are expressed relative to the average MFI of the Ctrl sgRNA group; p-values were calculated using an unpaired t-test: * = $p < 0.05$ ** = $p < 0.01$, *** = $p < 0.001$, **** = $p < 0.0001$

3.2.3. TOX is not essential in early commitment of peripheral tolerance

We next examined whether *Tox* deletion impacts peripheral tolerance induction. Tox sgRNA and Ctrl sgRNA edited CD45.1+ OT-I cells were labelled with the cell division dye Cell Trace Violet (CTV) to enable tracking of proliferation, and adoptively transferred into RIP-OVA^{hi} mice (Fig. 3.3A). At 60hrs post-transfer, which is when commitment to tolerance occurs [91], dividing OT-I cells within the draining sacral and pancreatic lymph nodes (LNs) were assessed for tolerance and early effector marker expression. Despite diminished TOX expression (Fig 3.3B), Tox sgRNA cells failed to exhibit evidence of a tolerance breach. Relative to control cells, Tox sgRNA cells displayed comparable OT-I cell frequencies and number within the LNs, alongside normal induction of canonical anergy markers, such as EGR2, Helios and FR4 (Fig. 3.3C-D). Expression of effector markers (GzmB and CD25) and quiescence (TCF1 and CD62L) markers was unchanged (Fig. 3.3E-F). Moreover, TOX loss failed to rescue effector function, with no significant change in cytokine production (IFN-γ, TNF-α, IL-2) following peptide restimulation (Fig. 3.3G)[91]. More importantly, expression of inhibitory receptors (PD-1

and TIM3) and markers for exhausted cell subsets (CX3CR1 and CD101) were unaffected following *Tox* deletion. Thus, unlike its role in exhaustion, TOX likely does not impact early establishment of peripheral tolerance.

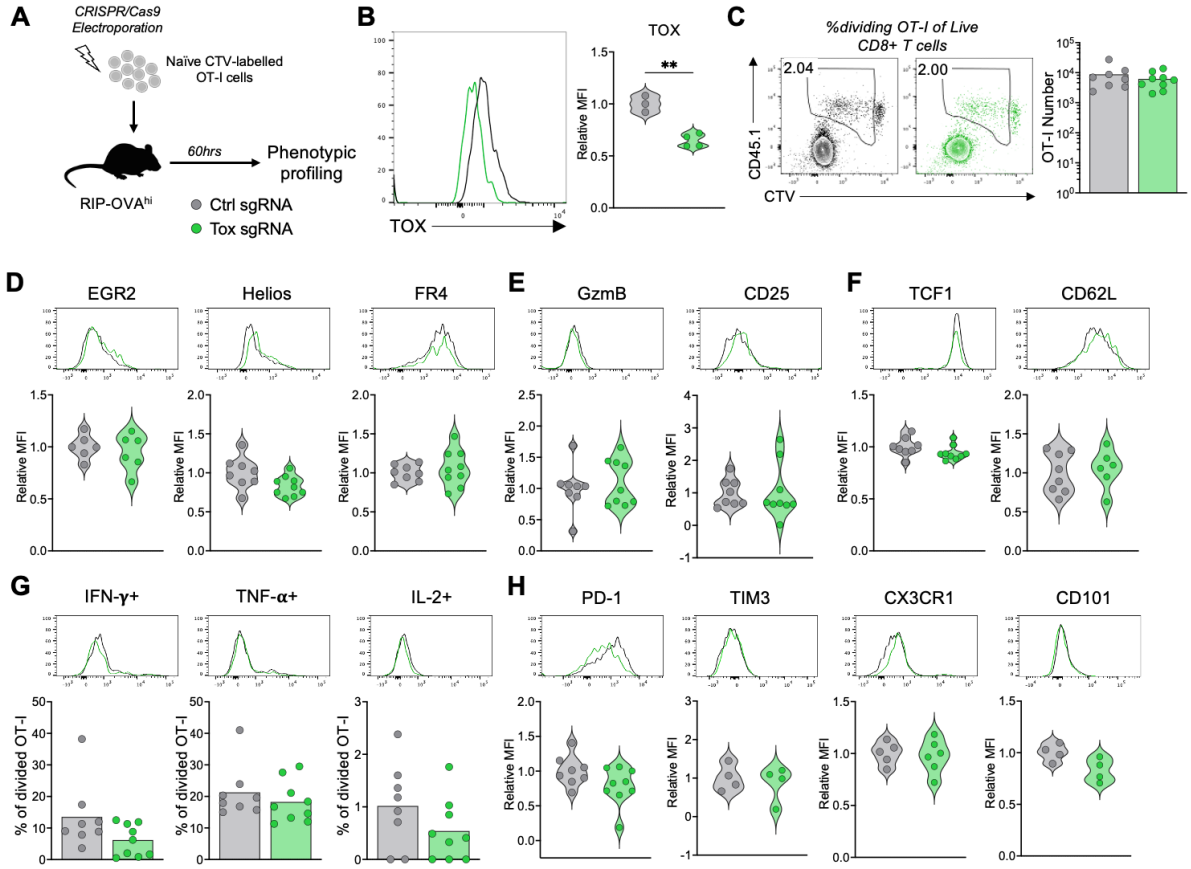


Figure 3.3. TOX loss does not impact early commitment to peripheral tolerance
(A) CD45.1+ OT-I cells were CTV-labelled, subjected to CRISPR-Cas9 nucleofection with either *Tox* (green) or Ctrl (grey) sgRNA RNPs, and adoptively transferred into RIP-OVA^{hi} mice, followed by immunophenotyping of recovered *Tox* or Ctrl sgRNA OT-I cells in sacral and pancreatic lymph nodes (LN) after 60 hrs.
(B) Representative histogram (left) and pooled data (right) showing TOX expression from two independent experiments (n=3-4 mice per group).
(C) Representative frequency (left) and pooled number (right) of dividing CD45.1+ OT-I cells from three independent experiments (n=9 mice/group).
(D-H) Expression of (D) anergy markers (EGR2, Helios and FR4), (E) effector markers (GzmB and CD25), (F) quiescence markers (TCF1 and CD62L), (G) peptide restimulation-induced cytokines (IFNγ, TNFα, and IL-2) and (H) exhaustion-related markers (PD-1, TIM3, CX3CR1, CD101). Representative histograms (top) and pooled data (bottom) are shown from four independent experiments (n=4-9 mice per group). MFI values are expressed relative to the average MFI of the Ctrl sgRNA group; p-values were calculated using an unpaired t-test: ** = $p < 0.01$.

3.2.4. TOX is not essential to the maintenance of peripheral tolerance

After initial commitment to tolerance, tolerised OT-I cells in the RIP-OVA^{hi} model are deleted by BIM-dependent apoptosis[207,232,233]. In contrast, tolerance disruption triggers OT-I cell effector differentiation, leading to diabetes downstream of islet cell destruction[224,272].Tox sgRNA cells failed to induce diabetes, indicating that peripheral tolerance was preserved throughout the 42-day monitoring period (Fig. 3.4A,C). Furthermore, similar to Ctrl sgRNA cells, Tox sgRNA cells were not detectable in the spleen and LNs at this late timepoint, indicating that the tolerance mechanisms were preserved in the RIP-OVA^{hi} model[232,233,525]. Therefore, TOX is dispensable for tolerance maintenance.

Breaching tolerance in the RIP-OVA^{hi} model requires the provision and infection-associated inflammation and additional antigen, with neither signal alone sufficient to breach tolerance [91]. Thus, we next investigated whether TOX deletion could lower the threshold for breaching tolerance by allowing cells to bypass tolerance when exposed to either increased antigen or bystander infection alone. RIP-OVA^{hi} mice given Ctrl or Tox sgRNA OT-I cells were either challenged with *Listeria* encoding an irrelevant LCMV-derived antigen (+LM-33), or repeatedly i.v. injected with the $OVA_{257-264}$ peptide antigen specific for the OT-I TCR (+OVA) (Fig. 3.4A). Additional antigenic exposure increases OT-I expansion[91], and this coincided with elevated TOX expression (Fig. 3.4B) to levels similar to those seen in exhaustion (Fig. 3.1B). Nonetheless, Tox sgRNA cells failed to induce diabetes in either +LM-33 and +OVA settings (Fig. 3.4C), with cells deleted normally in the +LM-33 condition. In contrast, cells in the +OVA condition were detectable within pooled spleen and pancreatic lymph node samples at day 42 p.i. likely due to systemic antigen-driven expansion (Fig. 3.4D). However, despite TOX loss still being evident in the Tox sgRNA group (Fig. 3.4F), OT-I cell number and marker expression were similar regardless of *Tox* deletion (Fig. 3.4E-I). Thus, despite TOX expression during tolerance, TOX is dispensable for peripheral tolerance induction and maintenance, even in the presence of additional signals that push cells closer to a breach in tolerance.

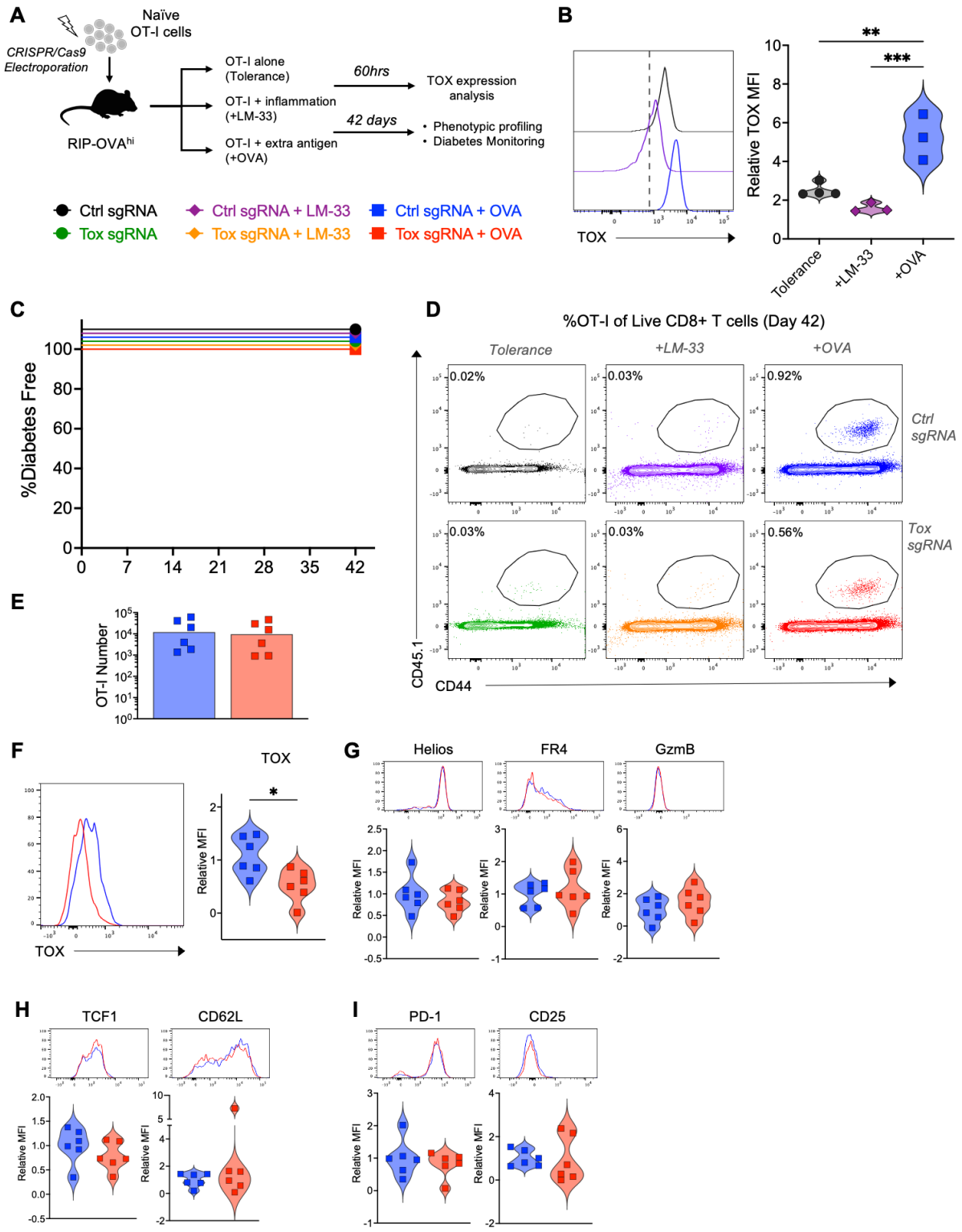


Figure 3.4. Tolerance maintenance and peripheral deletion remain intact in the absence of TOX

(A) CRISPR-edited OT-I cells were adoptively transferred into RIP-OVAhi mice that were either untreated ("Tolerance", circles), infected I.P. simultaneously with LM-33 (bystander infection; "+LM-33", diamonds), or injected I.V. with OVA peptide 1 day before OT-I transfer and days 1 and 2 post-transfer (extra antigen; "+OVA", squares).

(B) Representative histogram (left) and data (right) showing TOX expression of Ctrl sgRNA OT-I cells recovered from pooling sacral and pancreatic lymph nodes of RIP-OVA mice in the

Tolerance, +LM-33, and +OVA conditions after 60 hrs. data shown is from a single experiment (n=3-4 per group)
(C) Diabetes incidence in mice from (A) from 2 independent experiments (n=6 mice per group)
(D) Representative plots of recovered *Tox* or Ctrl sgRNA CD45.1+ CD44+ OT-I cells pooled from sacral and pancreatic lymph nodes, and spleens from each experimental group, 42 days post adoptive transfer
(E) Number of OT-I cells in each +OVA condition with from two independent experiments (n=6 per group).
(F) Representative histogram (left) and pooled data (right) showing TOX expression of Ctrl sgRNA +OVA (blue squares) and *Tox* sgRNA + OVA (red squares) from two independent experiments (n=6 mice per group)
Expression of **(G)** anergy-associated markers (Helios, FR4, and GzmB), **(H)** quiescence markers (TCF1 and CD62L) and **(I)** early activation markers, (PD-1 and CD25) of "Tox sgRNA + OVA" versus "Ctrl sgRNA + OVA" cells. Representative histograms (top) and pooled relative MFI data (bottom) are shown from two independent experiments (n=6 mice per group).
MFI values are expressed relative to the average MFI of Ctrl sgRNA + OVA group; p-values for all comparisons were calculated using an unpaired t-test: * = $p < 0.05$.

3.3. DISCUSSION

Shared phenotypes and molecular pathways between exhaustion and tolerance have made it challenging to determine if the underlying programs driving these two states are overlapping or distinct [141,217,350,378,522]. We confirm previous reports indicating TOX induction during tolerance [91,229], albeit at lower levels than those observed during exhaustion. However, TOX deficiency had no impact on the induction and maintenance of peripheral tolerance. Together, these data provide the first functional evidence that the molecular programs underpinning tolerance and exhaustion are distinct.

TOX induction during tolerance likely occurs downstream of the low affinity NFAT homodimers that form during both tolerance and exhaustion when NFAT is activated in the absence of AP-1 [141,339,526]. We previously identified that another NFAT-homodimer induced transcription factor, EGR2, was up-regulated in both tolerance and exhaustion, however the genes directly induced or repressed by EGR2 during exhaustion were completely distinct from previously reported EGR2 gene targets during T cell tolerance [341]. This suggests that despite similar upstream induction of EGR2, the downstream EGR2-dependent gene program in exhaustion vs tolerance was distinct. A caveat with this previous study though was that the EGR2 gene targets in tolerance had been defined in anergic CD4+ T cells, meaning that these differences could in part be due to differences between CD8+ and CD4+ T cells. In contrast, our current study provides more definitive functional proof that tolerance and exhaustion are molecularly distinct.

TOX is critically required for epigenetic and transcriptional commitment to exhaustion, where it promotes inhibitory receptor expression, suppresses T_{PEX} differentiation into exhausted effector subsets, and overall is required for persistence of exhausted T cells in the face of chronic antigen stimulation. In contrast, TOX deficiency during tolerance induction and maintenance has no impact on PD-1 and TIM3 expression, fails to rescue effector

differentiation, and is dispensable for cell persistence in contexts where deletion has been delayed by antigen supplementation during initial tolerance induction. The lack of TOX-dependent terminally differentiated TCF1- subsets might explain why *Tox* deletion fails to alter the tolerance phenotype, however TOX also influences less differentiated (TCF1+) T_{PEX} cells[524] by altering their chromatin state. In fact, TOX-deficient T_{PEX} cells adopt a less progenitor-like phenotype and display decreased levels of PD-1, Helios, and TCF1, alterations which we did not observe in tolerance[524]. Furthermore, additional antigen injection has been shown to reduce TCF1 gene expression by OT-I cells within the RIP-OVA^{hi} model[91], and yet we still did not observe a TOX KO phenotype after peptide injection. These data suggesting no functional TOX activity during tolerance are also consistent with prior findings that tolerant cells largely lack the epigenetic features of exhaustion that are in part known to be induced by TOX[91,312,524]. Thus, induction of TOX is likely a by-product of upstream antigen-induced NFAT signalling and is otherwise dispensable for the tolerance process. But because tolerance induction and, potentially, TOX upregulation mechanistically differ between various tolerance experimental models[220,527], examining whether TOX remains inessential during other tolerance contexts is also important.

It remains unclear why TOX up-regulation has minimal impact on tolerance induction, even in settings of increased antigen load. It is possible that genomic occupancy and target loci of TOX is inherently different between tolerance and exhaustion. Therefore, mapping TOX genomic binding via ChiPSeq or CUT&RUN in tolerant cells, either with or without increased antigen, would be necessary to test this possibility. Alternatively, investigating the effects of controlled TOX overexpression in antigen-naïve cells could clarify whether TOX alone, uncoupled from antigen, can at least induce some features of tolerance or whether external and internal factors contribute. These include a dysregulated immune microenvironment, an unfavourable epigenetic landscape (i.e. restricted accessibility to gene targets), or the presence or absence of essential co-factors[91,347,350]. Moreover, as these findings stemmed from a single tolerance model, examining whether TOX remains inessential in other tolerance contexts is warranted[220,527].

Our findings also imply that tolerance and exhaustion could be differentially targeted by immunotherapies[349,524]. For instance, modulation of TOX activity (and its downstream pathways) would be predicted to impact exhaustion while leaving peripheral tolerance intact. This could provide future avenues for more tailored and specific T cell immunotherapies.

Overall, this thesis chapter demonstrates that TOX is a selective regulator of exhaustion and not peripheral tolerance. Unlike during exhaustion, TOX up-regulation during tolerance is functionally dispensable for fate commitment and maintenance. These findings provide arguably the strongest functional evidence to date that tolerance and exhaustion are molecularly distinct regulatory processes.

CHAPTER 4 Assessing AP-1 Activity during early T cell differentiation

4.1. INTRODUCTION

During initial activation, CD8+ T cells integrate various activating and inhibitory signals to engage molecular programs that enable effector and memory differentiation (described in Section 1.2.2). However, persistent antigen encounter can divert cells towards regulatory states such as tolerance and exhaustion. Both regulatory checkpoints are thought to be driven by AP-1 diminished activity, either through insufficient induction during tolerance or direct repression in exhaustion[91,339,341,526]. The canonical view is that AP-1 forms a complex with NFAT, redirecting it away from regulatory genes that promote tolerance or exhaustion, and instead induce a gene program that enables CD8+ T cell differentiation towards effector and memory cell fates[141,379,427]. However, while the functional role of NFAT has been characterised extensively via through various functional disruption models[141,259,528], AP-1 function remains poorly defined. The *in vivo* expression patterns, interaction partners and genomic binding sites of the various AP-1 complexes during effector differentiation have not been comprehensively mapped.

In this chapter, we aimed to fill these knowledge gaps in AP-1 biology during T cell activation. We specifically focused on the biology of the Jun family of AP-1 factors as they were the target of our subsequent loss of function studies (see Chapter 5). While cJun is arguably the most well studied Jun family member due to its involvement in the “canonical” c-Fos/cJun AP-1 complex, JunB and JunD have also been implicated in facilitating aspects of T cell differentiation[468,529-533]. We find that all 3 Jun proteins are transiently expressed during the early stages of *in vivo* effector differentiation. Furthermore, we uncover unique and overlapping DNA binding patterns for JunB, cJun, and JunD during T cell activation, and confirm co-occupancy at known NFAT binding sites. While transient canonical complexes were not captured due to specific technical limitations (see discussion), we still uncovered novel and non-canonical protein interactions engaged by Jun family members in the nucleus. Collectively, our findings provide the first comprehensive molecular map of Jun protein expression, target genes and binding partners during functional effector cell differentiation

4.2. RESULTS

4.2.1. AP-1 Jun family members are transiently expressed during *in vivo* effector T cell differentiation

We first examined the temporal expression kinetics of the Jun family members during differentiation. While JunB, cJun, and JunD have all been documented to be rapidly induced and subsequently downregulated by *in vitro* stimulated CD8+ T cells, their *in vivo* expression dynamics remain poorly defined. To determine this, we adoptively transferred CTV-labelled CD45.1+ P14 cells into C57BL/6 recipients and infected them with acute LCMV Armstrong to induce effector differentiation. Mice were infected on days -8, -5, -3, -2, and -1 then harvested on day 0 to enable parallel staining and flow cytometric analysis of Jun protein expression across all timepoints, with uninfected mice included as baseline controls (Fig. 4.1A). To enable recovery of sufficient P14 cells at early timepoints, a large number ($2x10^6$) of P14 cells were transferred, including for later timepoints for consistency. Cells were also CTV-labelled prior to transfer to track cell division. We found that all Jun proteins were transiently expressed. Specifically, JunB and cJun peaked at day 1 post-infection (p.i.), while JunD peaked at day 2 p.i., with protein levels returning to baseline by day 5 (cJun, JunB) or 8 (JunD) p.i. (Fig. 4.1B-D). Thus, Jun proteins are only transiently expressed in a very narrow window spanning the first few days of T cell activation.

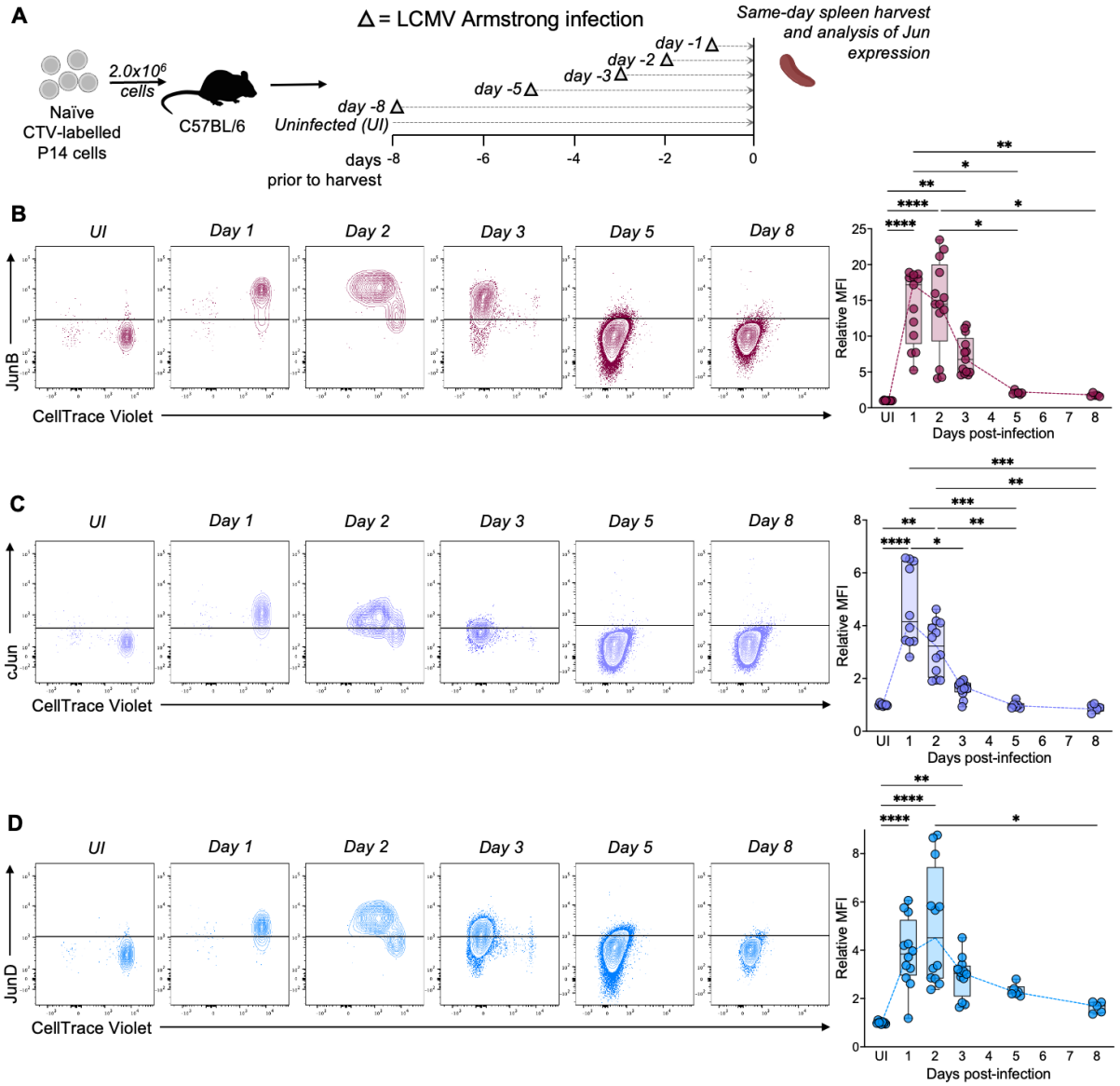


Figure 4.1. Transient expression of Jun family members during *in vivo* CD8+ T cell differentiation

(A) 2x10^6 CTV-labelled wild-type P14 cells were adoptively transferred into B6 mice that were either left uninfected, or infected with LCMV-Armstrong 1, 2, 3, 5, or 8 days prior to spleen harvest for analysis of Jun expression.

(B-D) Expression kinetics of JunB (maroon), cJun (light purple), and JunD (aqua) in splenic CD8+ P14 cells. Representative flow cytometry plots of Jun protein expression versus CTV signal of P14 cells at distinct infection timepoints are shown (left); horizontal line indicates Jun expression from naïve P14 cells in the uninfected (UI) group. Pooled relative MFI data (right) are shown from 4 independent experiments (n=5-12 mice per group). MFI values are expressed relative to the average MFI of undivided cells from the UI group. p-values were calculated using a Kruskal-Wallis test with post-hoc Dunn's multiple comparisons test: * = $p < 0.05$,** = $p < 0.01$,*** = $p < 0.001$,*** = $p < 0.0001$.

4.2.2. Different Jun proteins have distinct protein interactomes

Beyond their heterodimeric partners, the proteins that complex with each Jun protein during their transient induction are poorly defined. To address this, we performed co-immunoprecipitation mass spectrometry (Co-IP MS) on cJun, JunB and JunD isolated from the nuclear fraction of naïve CD8+ T cells stimulated *in vitro* with anti-CD3, anti-CD28 and IL-2 for 24hrs (Fig. 4.2).

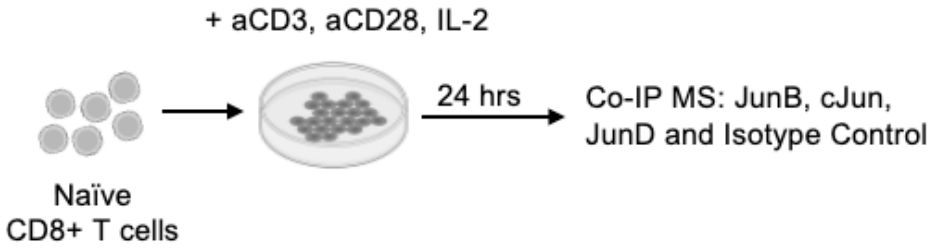


Figure 4.2 *In vitro* activation protocol for Co-IP MS analysis (described in Section 2.2.4.1)

By comparing the protein abundance values from each Jun IP condition versus the isotype control and ranking the putative hits according to fold change and p values (see Section 2.2.10.2), we identified n=136 JunB partners (86.7% novel), n=127 for cJun (74% novel) and n=70 for JunD (80% novel) (Table S1-3). All three of the Jun family members were found to interact with themselves, consistent with their well-characterised propensity to form homodimers [470], although this is also likely because these proteins are enriched by the IP antibodies. Notably, each Jun member also associated with members of other AP-1 subfamilies. Specifically, JunB interacted with cFos, Fosl2, and FosB; cJun with Fosl2; and JunD with cFos, Fosl2, FosB, and ATF7. Surprisingly, canonical AP-1 interactions, such as BATF with JunB, cFos with cJun, or NFAT with cJun, were not detected in this specific assay. As we have only evaluated cells activated *in vitro* at 24hrs, it is possible that these interactions were missed because they occur at earlier or later timepoints, and under more physiologic stimulation conditions.

Overlap analysis of the interaction partners revealed that JunB and cJun exclusively shared n=53 partners, while both had minimal overlap with JunD (i.e. n=5 shared with JunB and n=10 shared with cJun) (Fig. 4.3A). We also found that n=19 proteins were shared across all three Jun family members, which potentially converge on pathways associated with general RNA metabolism and gene expression, as well as to a lesser extent, RUNX expression and activity (Fig. 4.3B).Of note, pioneer factors such as IRF4 and RUNX3 were among the common interaction partners of all Jun members (Fig. 4.3C), consistent with prior evidence that these factors interact with AP-1 proteins [174,340,534,535]. Protein interaction partners unique only to JunB (n=59) were associated with chromatin modifying enzymes and mRNA processing factors (e.g. 3' end processing and mRNA splicing) (Fig. 4.4). JunB was also found to uniquely interact with transcription complex-associated TAF proteins, highlighting a

potentially stronger capacity for JunB to recruit the RNA polymerase machinery [536-538]. cJun-specific interaction partners (n=45) were heavily enriched for proteins critical for ribosomal and ribonucleoprotein biogenesis (Fig. 4.5). JunD uniquely associated with 36 proteins involved in a diverse set of molecular pathways, which include nucleocytoplasmic transport and vesicle trafficking, histone methylation, exoribonuclease-mediated mRNA decay, and mTORC1 regulation by amino acids (Fig. 4.6). These novel findings indicate that despite some core shared interaction partners, JunB, cJun, and JunD complex with non-overlapping and functionally unique classes of proteins, potentially hinting at non-redundant functions for each Jun protein.

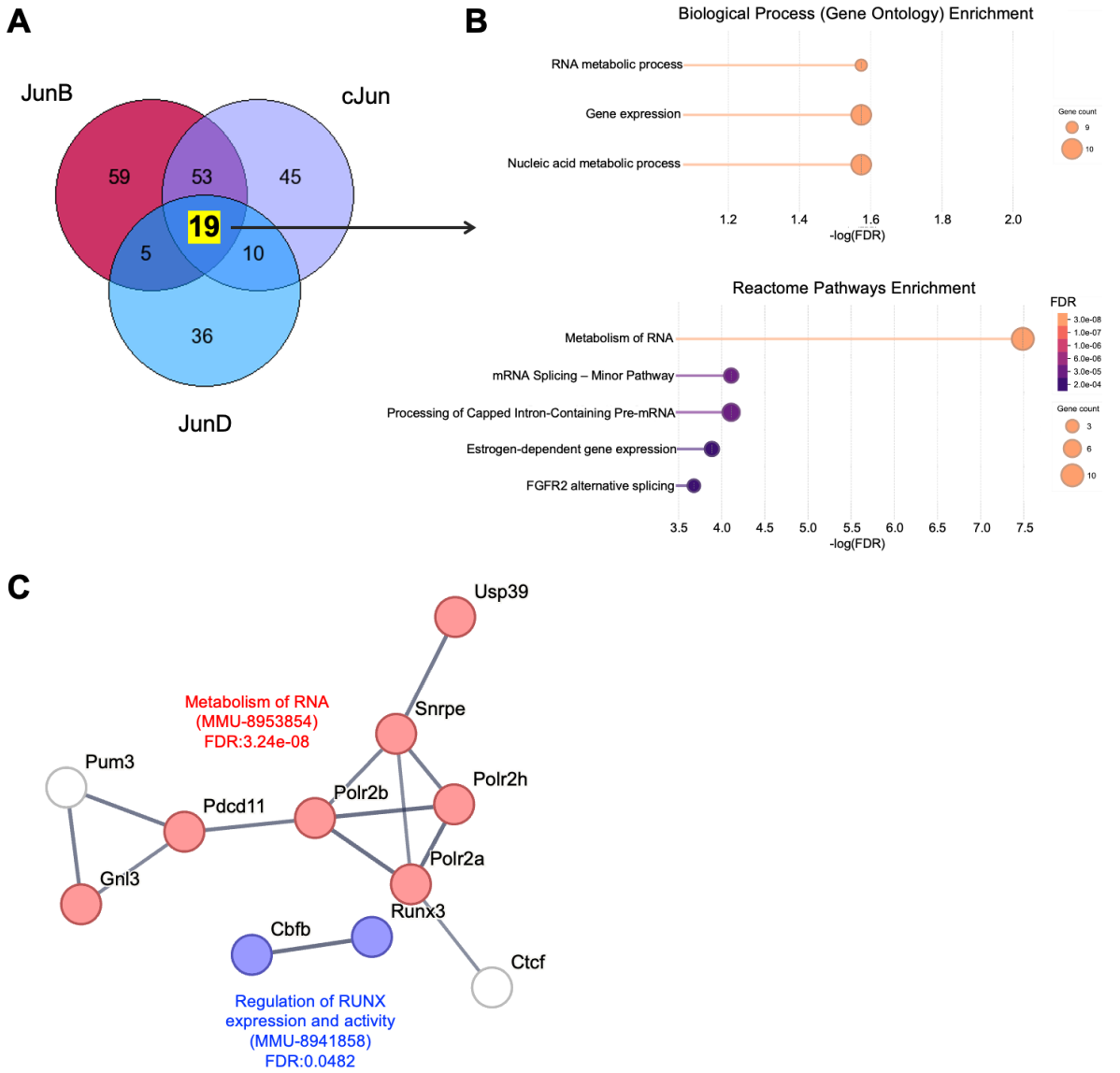


Figure 4.3 Shared protein interaction partners of all Jun family members
A) Venn diagram showing unique and overlapping protein interaction partners for JunB (maroon), cJun (light purple), and JunD (aqua) identified via Co-IP MS; n=19 protein partners are shared among all Jun members.
(B) Visualisation of top functionally enriched pathways (GO: Biological Processes and Reactome) of the shared protein interaction partners.
(C) Protein-protein interaction network of the shared protein interaction partners, with nodes colour-coded according to their relevant pathway.

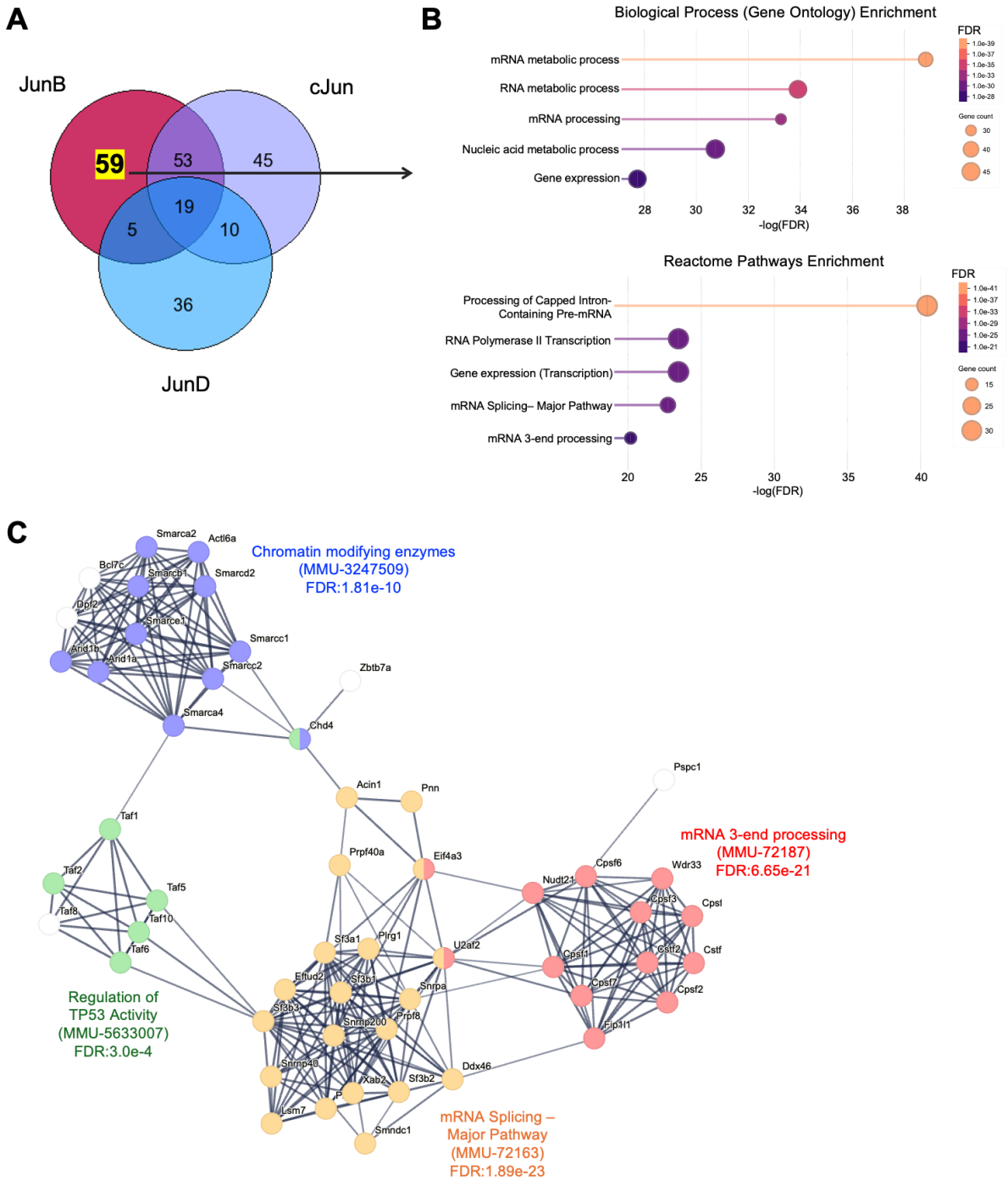


Figure 4.4 Protein interaction partners unique to JunB
(A) Venn diagram from Fig. 4.3A with the n=59 protein partners unique to JunB highlighted.
(B) Visualisation of top functionally enriched pathways (GO: Biological Processes and Reactome) of the JunB-specific protein interaction partners.
(C) Protein-protein interaction network of the JunB-specific protein interaction partners, with nodes colour-coded according to their relevant pathway.

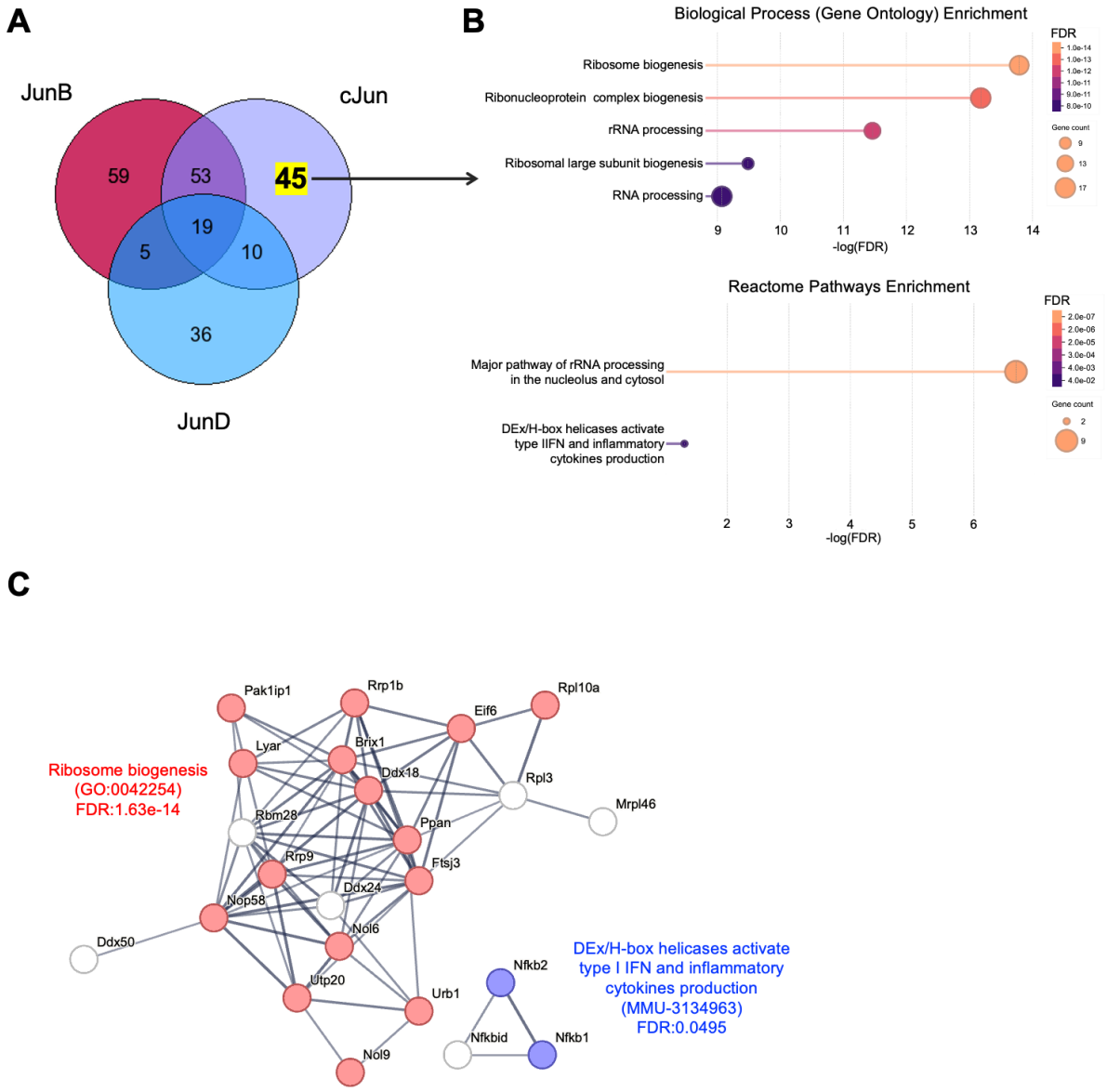


Figure 4.5 Protein interaction partners unique to cJun
(A) Venn diagram from Fig. 4.3A with the n=45 protein partners unique to cJun highlighted.
(B) Visualisation of top functionally enriched pathways (GO: Biological Processes and Reactome) of the cJun-specific protein interaction partners.
(C) Protein-protein interaction network of the cJun-specific protein interaction partners, with nodes colour-coded according to their relevant pathway.

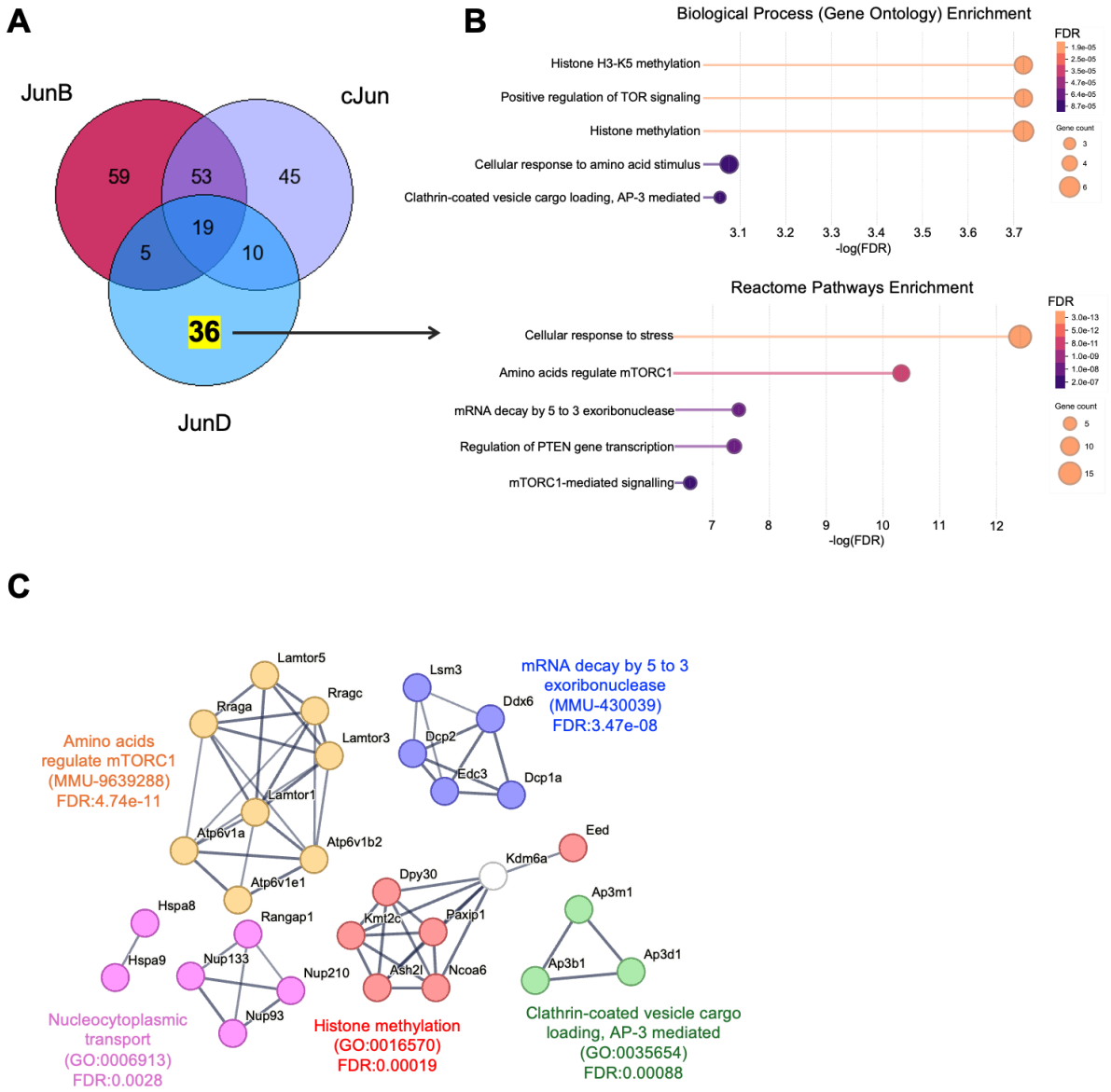


Figure 4.6 Protein interaction partners unique to JunD.
(A) Venn diagram from Fig. 4.3A with the n=36 protein partners unique to JunD highlighted.
(B) Visualisation of top functionally enriched pathways (GO: Biological Processes and Reactome) of the JunD-specific protein interaction partners.
(C) Protein-protein interaction network of the JunD-specific protein interaction partners, with nodes colour-coded according to their relevant pathway.

4.2.3. Jun proteins exhibit distinct but overlapping genomic binding profiles

Next, we mapped the genome-wide binding sites of each Jun family member in CD8+ T cells activated for 24h *in vitro* (as shown in Fig. 4.2) using the cleavage under targets and release using nuclease (CUT&RUN) assay. At a genome-wide level, Jun binding patterns were broadly similar across family members (Fig. 4.7A). Motif analysis identified enrichment of the consensus AP-1 binding motifs (i.e. 5'-TGA(C/G)TCA-3') within peaks that were occupied by JunB, cJun and JunD (Table S4). Annotation of these peaks then revealed distinct trends in binding preferences, with cJun and JunD preferentially binding to promoter regions, and JunB favouring both intronic and promoter regions at comparable frequencies (Fig. 4.7B). JunB bound the largest number of genomic sites (32,561), followed by JunD (19,126) and cJun (17,095). A significant number of these peaks were shared between all 3 Jun proteins (11,310), and consistent with its larger number of binding sites, JunB had the most unique binding sites (15,911; 49% of JunB peaks) followed by JunD (5,074; 27% of JunD peaks) and cJun (2,811; 16% of cJun peaks) (Fig. 4.7C). Similar trends were seen when profiling the peak adjacent genes (Fig. 4.7D).

Genes linked to peaks bound by all 3 Jun proteins were significantly enriched for core cellular pathways by pathway enrichment analysis, including cell cycle, RNA metabolism, protein translation, and ubiquitination (Tables 10-11). This may indicate overlapping roles for all Jun members in regulating core molecular processes necessary for T cell proliferation, differentiation and activation. Furthermore, all Jun members bound genomic loci associated with canonical effector-associated genes, such as *Il2ra, Id2, Gzmb,* and *Il2* (Fig. 4.7E). In contrast, pathway analysis of genes selectively bound by each individual Jun did not yield any significant pathway enrichment (Table S5-7). Nevertheless, genes that appear linked to certain aspects of T cell biology were preferentially bound by each Jun, including *Rps10*[539] (JunB), *Il4i1*[540] (cJun), *and Ei24*[541] (JunD) (Fig. 4.7F). While functional data is needed to prove that these pathways and/or genes are transcriptionally controlled by each Jun before any strong conclusions can be drawn, these data hint at both shared and non-redundant functions for each Jun protein in T cell transcriptional regulation.

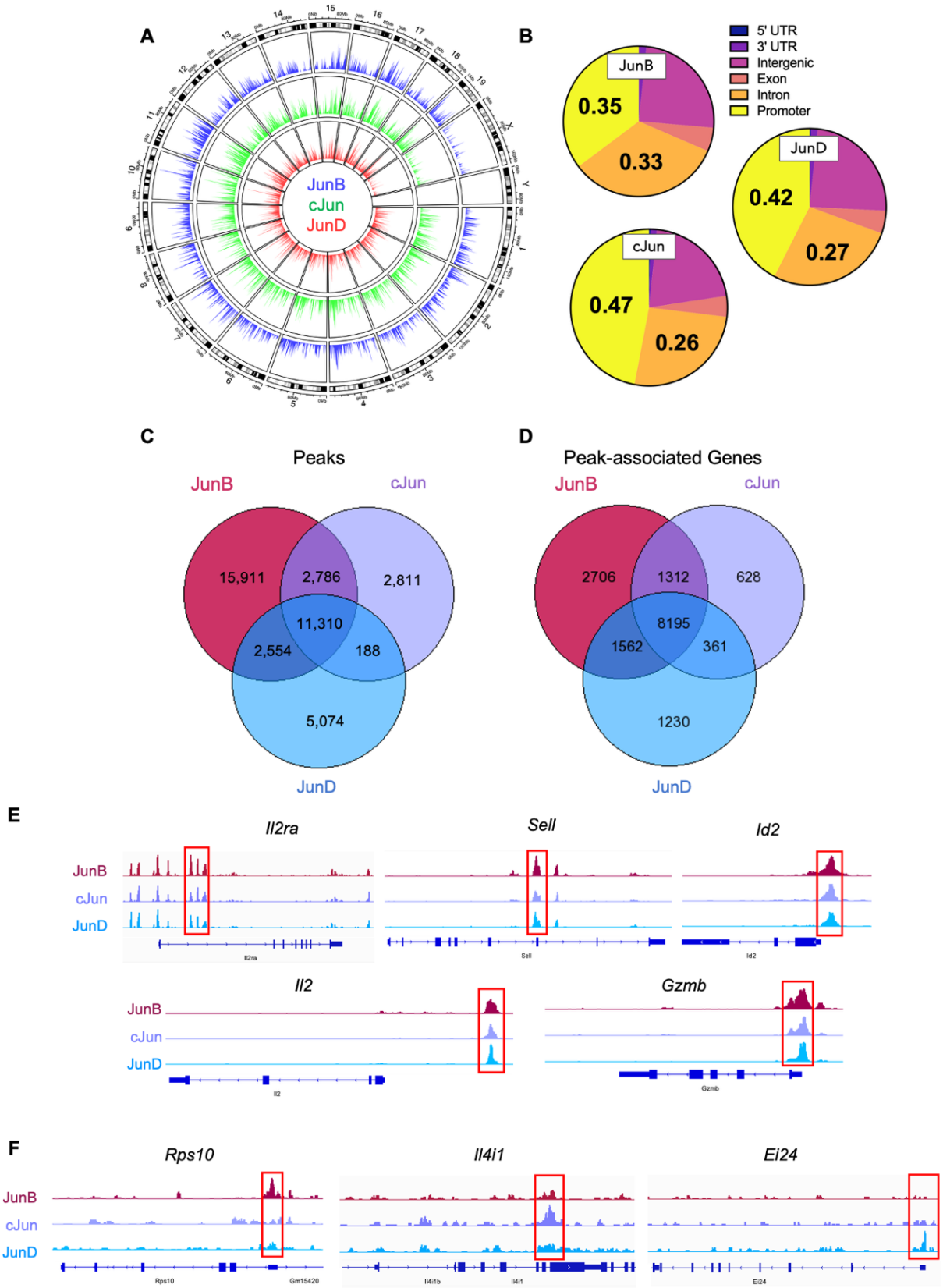


Figure 4.7 Genomic binding profiles of Jun family members
(A) Circle plot depicting genome-wide distribution of CUT&RUN peaks for JunB (blue), cJun (green), and JunD (red) from one independent experiment
(B) Pie charts with genomic distribution of JunB, cJun and JunD peaks. Proportion of peaks within promoters and introns for each Jun member are indicated.

(C-D) Venn diagrams of unique and overlapping peaks **(C)** and putative peak-associated genes **(D)** for JunB (maroon), cJun (light purple), and JunD (aqua).
(E-F) Representative genome browser tracks of JunB, cJun, and JunD CUT&RUN profiles at select gene loci that are shared among **(E)** and unique **(F)** to each Jun member. Red boxes highlight peaks of interest.

Table 15. Top enriched Reactome pathways of genes associated with CUT&RUN peaks shared among all Jun family members

Reactome Pathway	P-value	Adjusted P-value	Odds Ratio	Gene Overlap
Cell Cycle, Mitotic	2.53E-25	5.13E-22	2.554337	327/516
Cell Cycle	1.44E-24	1.46E-21	2.272433	393/649
Signaling by Rho GTPases, Miro GTPases and RHOBTB3	1.04E-20	7.03E-18	2.064806	401/688
Cellular Responses to Stimuli	3.41E-20	1.73E-17	1.880652	496/887
Signaling by Rho GTPases	4.86E-20	1.87E-17	2.054738	391/672
Cellular Responses to Stress	5.51E-20	1.87E-17	1.945419	447/787
RHO GTPase Cycle	3.22E-17	9.34E-15	2.242471	272/450
Diseases of Signal Transduction by Growth Factor Receptors and Second Messengers	4.84E-17	1.23E-14	2.229752	272/451
Metabolism of RNA	3.06E-16	6.91E-14	1.826134	421/761
M Phase	5.67E-16	1.15E-13	2.344403	229/372

Table 16. Top enriched GO Biological processes of genes associated with CUT&RUN peaks shared among all Jun family members

GO Biological Process	P-value	Adjusted P-value	Odds Ratio	Gene Overlap
Ubiquitin-Dependent Protein Catabolic Process (GO:0006511)	2.40E-20	1.26E-16	2.419154	283/455
Protein Ubiquitination (GO:0016567)	2.36E-19	6.19E-16	2.602239	236/369
Protein Modification by Small Protein Conjugation (GO:0032446)	1.43E-17	2.5E-14	2.665244	204/316
Proteasomal Protein Catabolic Process (GO:0010498)	9.94E-17	1.3E-13	2.399436	231/372
Proteasome-Mediated Ubiquitin-Dependent Protein Catabolic Process (GO:0043161)	1.32E-14	1.38E-11	2.332198	209/340
RNA Processing (GO:0006396)	1.66E-13	1.45E-10	2.401247	181/291
Positive Regulation of DNA-templated Transcription (GO:0045893)	7.52E-12	5.62E-09	1.482615	638/1274
Protein Polyubiquitination (GO:0000209)	9.48E-12	6.2E-09	2.495733	144/228
Modification-Dependent Protein Catabolic Process (GO:0019941)	1.64E-11	9.52E-09	2.580154	133/208
Regulation of Translation (GO:0006417)	5.89E-11	3.08E-08	2.550041	128/201

4.2.4. Jun proteins and NFAT share genomic targets related to T cell signalling

To validate whether Jun proteins occupy known NFAT genomic targets, we compared our Jun CUT&RUN data with published NFAT ChIP-Seq data from *in vitro* activated CD8+ T cells. While these datasets were acquired from separate assays and distinct activation contexts (see Section 2.2.11.5), peak overlap analysis still revealed n=1,136 shared peaks (Fig. 4.8A) which were associated to n=469 genes (Fig 4.8B). These overlapping genes included canonical regulators for T cell activation (e.g. *Il2* and *Il2ra)* and signalling (e.g. *Plcg1* and *Lck*, Fig. 4.8C). As expected, the gene overlap between the Jun proteins and NFAT was significantly enriched for T cell receptor and cytokine signalling pathways (Tables 14-15). We also observed regions uniquely occupied by Jun proteins in the absence of NFAT, which were enriched for effector differentiation-related genes such as *Ccr7* and *Prdm1* (Fig. 4.8D). In contrast, gene loci uniquely occupied by NFAT were associated with negative regulators of T cell differentiation, i.e. *Pdcd1*, *Eomes*, and *Tox* (Fig. 4.8E). We also found that among the Jun proteins, JunB alone can co-occupy genomic sites with NFAT, while cJun and JunD, independently, cannot. (Fig. 4.8A). This comparative analysis capturing canonical Jun and NFAT co-occupancy confirms that NFAT/AP-1 complexes are engaged during T cell activation.

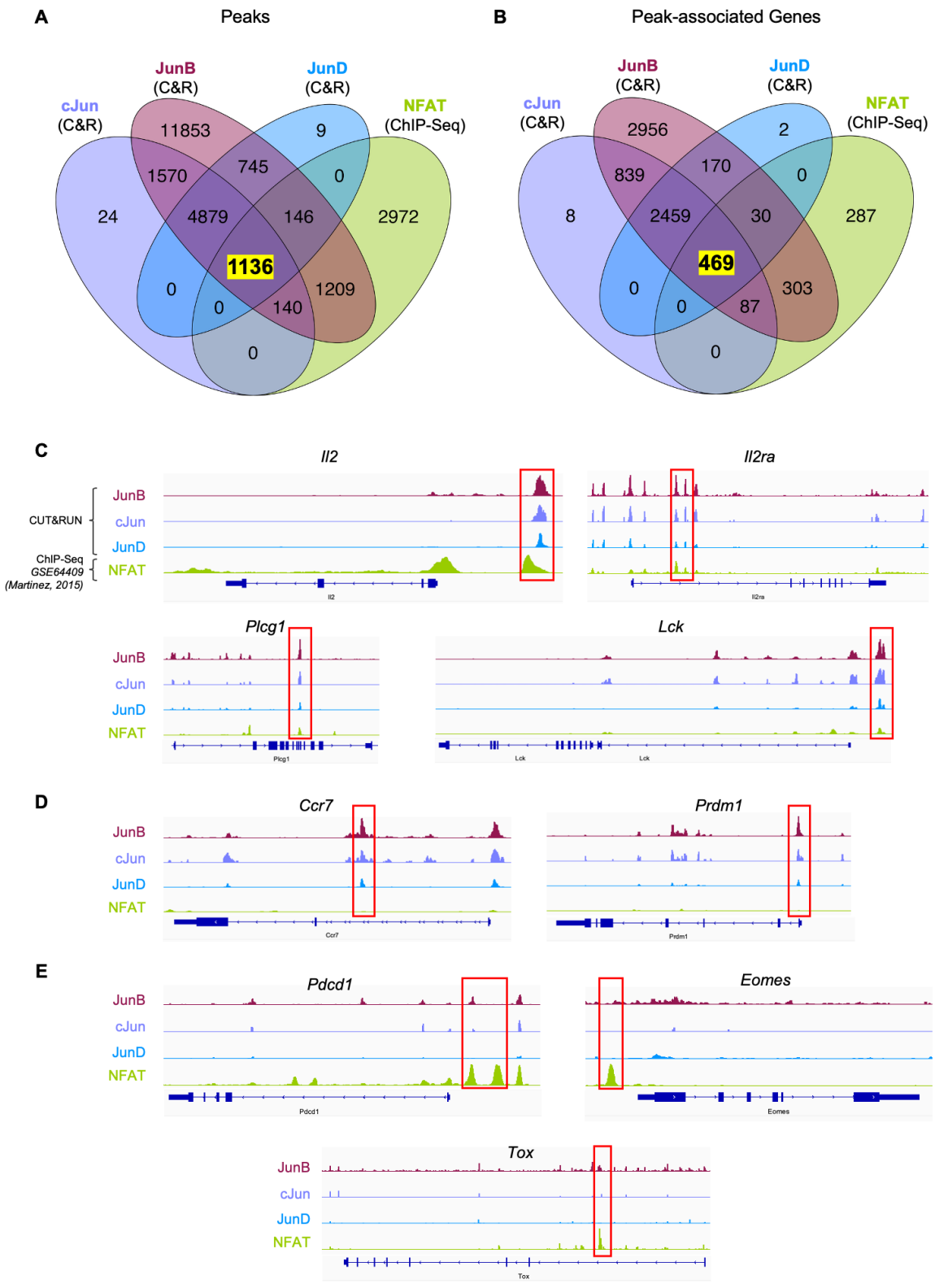


Figure 4.8 Genomic occupancy of Jun proteins at known NFAT binding sites
(A-B) Venn diagrams of unique and overlapping peaks **(A)** and putative peak-associated genes **(B)** for CUT&RUN data for JunB (maroon), cJun (light purple), JunD (aqua), and published ChIP-Seq data for NFAT (yellow green) from Martinez et al (2015).
(B) Representative genome browser tracks of JunB, cJun, and JunD CUT&RUN, and NFAT ChIP-Seq profiles at select gene loci that are shared among all **(C)**, unique to only Jun members (D), and unique only to NFAT (E). Red boxes highlight peaks of interest.

Table 17. Top enriched Reactome pathways of genes associated with peaks shared with all Jun family members (CUT&RUN) and NFAT (ChIP-Seq).

Reactome Pathway	P-value	Adjusted P-value	Odds Ratio	Gene Overlap
Signaling by Interleukins	9.26E-22	1.51E-18	3.528785	98/452
Cytokine Signaling in Immune System	1.10E-17	8.97E-15	2.556129	129/776
Signal Transduction	6.39E-17	3.48E-14	1.799618	310/2613
Immune System	7.58E-15	3.1E-12	1.801828	259/2150
Diseases of Signal Transduction by Growth Factor Receptors and Second Messengers	6.94E-13	2.27E-10	2.71174	80/451
Signaling by Receptor Tyrosine Kinases	2.54E-11	6.91E-09	2.402882	86/536
MAP Kinase Activation	5.20E-10	1.22E-07	6.604872	22/63
Interleukin-17 Signaling	9.08E-09	1.62E-06	5.413351	22/72
MyD88 Cascade Initiated on Plasma Membrane	1.16E-08	1.62E-06	4.449353	26/98
Toll Like Receptor 10 (TLR10) Cascade	1.16E-08	1.62E-06	4.449353	26/98

Table 18. Top enriched GO Biological processes of genes associated with peaks shared with all Jun family members (CUT&RUN) and NFAT (ChIP-Seq).

GO Biological Process	P-value	Adjusted P-value	Odds Ratio	Gene Overlap
Intracellular Signaling Cassette (GO:0141124)	8.61E-13	3.68E-09	2.95172	69/362
T Cell Receptor Signaling Pathway (GO:0050852)	4.2E-11	6.48E-08	5.426559	29/95
Antigen Receptor-Mediated Signaling Pathway (GO:0050851)	4.55E-11	6.48E-08	4.691765	33/120
T Cell Activation (GO:0042110)	1.18E-10	1.27E-07	4.484558	33/124
Regulation of Intracellular Signal Transduction (GO:1902531)	2.4E-10	2.06E-07	2.727505	61/340
T-helper Cell Lineage Commitment (GO:0002295)	1.45E-09	1.03E-06	40.78808	10/13
Positive Regulation of Cytokine Production (GO:0001819)	1.97E-09	1.2E-06	2.559668	61/358
Regulation of T Cell Receptor Signaling Pathway (GO:0050856)	3.27E-09	1.75E-06	7.075949	19/52
Negative Regulation of Cytokine Production (GO:0001818)	4.12E-09	1.96E-06	3.194241	41/200
Regulation of Apoptotic Process (GO:0042981)	2.36E-08	1.01E-05	1.947362	97/722

4.3. DISCUSSION

AP-1 and its Jun family members have long been proposed as critically required for T cell activation and differentiation [170,253,426,469,476,542]. However, current knowledge of the *in vivo* expression kinetics, interaction partners and genome-wide binding sites of each Jun family member is limited. In this chapter, we addressed these knowledge gaps during CD8+ T cell activation and differentiation. We reveal distinct but overlapping temporal patterns of Jun expression during *in vivo* effector differentiation, with JunB and cJun being upregulated early, with JunD being induced later. Although these findings are limited to the 24hr *in vitro* activation timepoint assessed, we find that despite a "core" interactome of factors common to all Juns, each Jun interacts with a distinct subset of nuclear proteins. Finally, we demonstrate different but overlapping genome-wide binding patterns for each Jun protein. Collectively, these data suggest that despite some evidence of redundancy, each Jun protein likely plays non-redundant roles in controlling T cell activation and differentiation.

In line with previous observations, [175,438,543-545], we find that induction of Jun expression is only transient, with expression largely returning to baseline by days 5-8 post-infection. Previous *in vitro* work has suggested that the different Jun proteins have different induction kinetics after T cell activation [175,546]. *In vivo*, these differences were less evident, with all 3 Jun proteins largely similar in expression kinetics, albeit with a slight delay in induction and loss of JunD relative to the other Jun proteins. It remains possible that early induction kinetics (i.e. within the first few hours of *in vivo* activation) are distinct, however our data suggest that the expression window of all 3 Jun proteins is otherwise largely similar and overlapping *in vivo*.

To define potential functional differences between the different Jun proteins, we mapped each Jun protein's interactome. Consistent with their gene regulatory role, all Jun proteins interacted with RNA Polymerase II and components of the splicing complex, alongside known AP-1 transcriptional interaction partners (RUNX3 and IRF4)[174,176,547].One of the main functions ascribed to AP-1 is chromatin remodelling during T cell activation[165,170,438,548]. Interestingly, the only Jun protein that interacted with chromatin remodelling complexes was JunB, suggesting that AP-1 driven chromatin remodelling may be predominantly JunB-dependent. In contrast, cJun uniquely interacted with NF-κB factors and factors linked to ribosome biogenesis, while JunD interacted with histone methylation complexes, components of the nuclear pore complex and, oddly, components of mTOR complex that are normally cytoplasmic (potentially indicating some cytoplasmic contamination in the assay). Some of the JunD interaction partners (EED and Nuclear Pore Complex) are associated with heterochromatin [549], which may indicate that at least some JunD complexes are repressive. Further validation and functional studies, such as downstream western blot analysis, proximity labelling, and reciprocal immunoprecipitation experiments, are needed to probe the biological relevance of these observed interactions[468].

The genome-wide binding patterns of the Jun proteins also support the concept that JunB is functionally distinct from the other Juns. All Jun proteins bound to an overlapping set of regions adjacent to genes linked to core functions, implying potentially redundant roles in T cell activation. And in line with canonical data, shared Jun co-occupancy at known NFAT binding sites were skewed towards genes critical for T cell signalling[141]. However, JunB bound to more sites overall, can co-bind with NFAT exclusively, and had more unique binding sites than the other Jun proteins. Coupled with its unique association with chromatin remodelling complexes, this may suggest that JunB has more non-redundant roles than the other two Jun proteins. This aligns with recent data demonstrating that JunB is essential for effector CD8+ T cell expansion, survival and differentiation during acute infection, with JunB deficient cells failing to properly acquire the transcriptional and epigenetic features of effector cells[438].

Unexpectedly, we were unable to detect canonical Jun interactions, such as cJun binding to cFos, JunB binding to BATF, or overall Jun/AP-1 interactions with NFAT. This may relate to the kinetics and strength of these interactions; cFos, BATF, and NFAT expression/activation kinetics in CD8+ T cells can differ from those of the Jun family members[91,175], and thus may be more evident at earlier or later timepoints. For example, JunB-BATF genomic co-occupancy in *ex vivo* CD8+ T cells is observed at day 3 post-acute infection[176]. Additionally, because the interaction between AP1 and NFAT is inherently dependent on DNA binding[550,551], standard Co-IP procedures could disrupt the stability of this protein heterodimer-DNA complex and therefore will not be captured in the proteomic analysis. Profiling the Jun protein interactome at different timepoints post activation with a cross-linking step in the Co-IP protocol, is thus likely required to better resolve these interactions. Finally, capturing these canonical complexes could be dependent on more physiological activation conditions, requiring the use of peptide-MHC ligands or *in vivo* experimental models.

While these descriptive findings provide deeper molecular insights into the possible functional roles of each Jun protein, gene knock-out data is needed to functionally test how Jun protein loss impacts these biological processes. To complement these findings, we conducted comprehensive gene knock-out studies in Chapter 5 to both determine the roles of each Jun protein, and to more broadly functionally test key paradigms around AP-1 biology.

CHAPTER 5 Evaluating the role of AP-1 in CD8+ T cell effector and memory cell differentiation

5.1. INTRODUCTION

The capacity of AP-1 to functionally repurpose NFAT into a factor that promotes the effector gene program is considered essential to insulate effector CD8+ T cells against both tolerance and exhaustion. However, given accumulating evidence that tolerance and exhaustion are molecularly distinct processes that emerge at different points of the immune response, it is unclear how AP-1 deficiency could simultaneously trigger both states. Resolving this question is important as AP-1 factors are being repurposed for immunotherapy despite our limited understanding of which regulatory processes AP-1 regulates [416,478-486]. Addressing this question is also critical to gain deeper insights into the pathways controlling the tolerance and exhaustion regulatory checkpoints.

The paradigm that AP-1 alters NFAT activity to prevent tolerance and/or exhaustion has mainly stemmed from studies perturbing NFAT rather than AP-1 activity [141]. Furthermore, previous studies examining the impact of AP-1 activity on effector CD8+ T cell differentiation have largely been correlative [91,341,476,552], with relatively few *in vivo* knock-out (KO) studies that have been limited to examining only a few AP-1 family members [176,437-439]. Therefore, the question of whether AP-1, as a whole or through its individual Jun subfamily members, is required to prevent the emergence of tolerance, exhaustion, or both must be functionally interrogated.

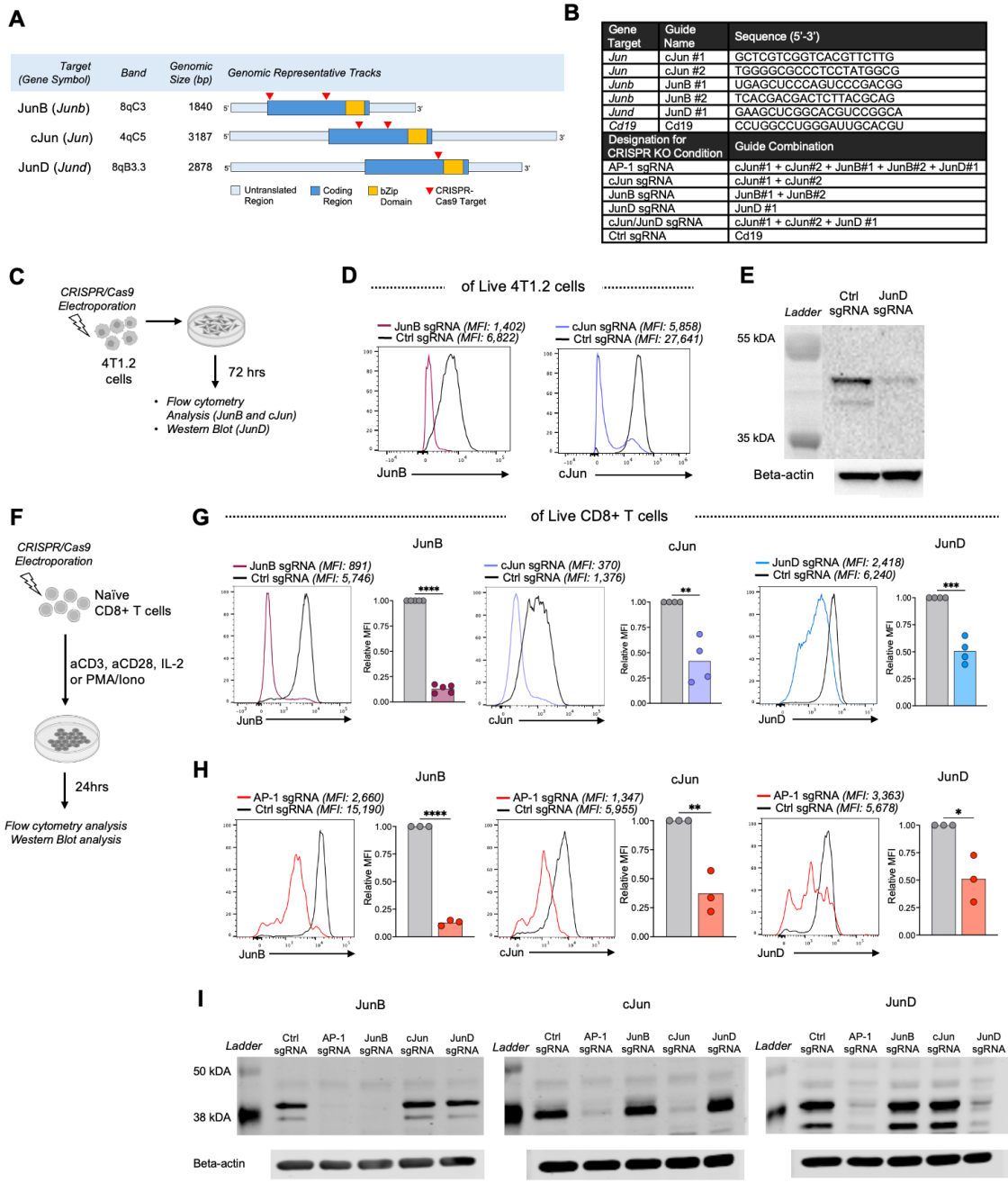
To this end, we genetically ablated AP-1 in CD8+ T cells by knocking out all Jun family members (i.e. JunB, cJun, and JunD) alone or in combination and measured their capacity to form effector and memory cells during acute infection. We discovered that AP-1, particularly JunB containing AP-1 complexes, are critically required for effector CD8+ T cell survival and expansion. AP-1 and JunB deficient cells acquired features of exhaustion but not tolerance, with AP-1 surprisingly being largely dispensable for early effector differentiation outside of a potential role in induction of protein translation capacity. Unexpectedly, JunD and cJun were fully dispensable for effector cell expansion and differentiation but instead played roles in memory CD8+ T cell persistence and functional recall respectively. These findings challenge current paradigms surrounding AP-1 biology.

5.2. RESULTS

5.2.1. Optimisation of AP-1 CRISPR knock-out

Given the large number of Fos or Fos-like proteins, and the capacity of Jun proteins to homodimerize, the shortest path to full ablation of canonical AP-1 complexes is deletion of the

3 Jun genes (*Junb, Jun,* and *Jund)*. We addressed this by electroporation of Cas9-sgRNA ribonucleoproteins (RNPs) targeting the sole exonic region of each mouse Jun gene to trigger CRISPR-mediated gene deletion (Fig. 5.1A). Various sgRNAs for each Jun member (see Table 8, Chapter 2) were tested and selected based on their knock-out efficacy of *Junb* ("JunB sgRNA"), *Jun* ("cJun sgRNA"), or *Jund* ("JunD sgRNA") versus control sgRNA treated cells (*Cd19* targeting sgRNA; "Ctrl sgRNA") in 4T1.2 mouse breast cancer cells, which constitutively and highly express AP-1 (Fig. 5.1B-C). Gene knockout (KO) was assessed by measuring protein loss using either flow cytometry (JunB and cJun; Fig. 5.1D) or western blotting (JunD; Fig. 5.1E), with potent sgRNAs identified against all targets using this approach.



Gene Target	Guide Name	Sequence (5'-3')
Jun	cJun #1	GCTCGTCGGTCACGTTCTTG
Jun	cJun #2	TGGGGCGCCCTCCTATGGCG
Junb	JunB #1	UGAGCUCCCAGUCCCGACGG
Junb	JunB #2	TCACGACGACTCTTACGCAG
Jund	JunD #1	GAAGCUCGGCACGUCCGGCA
Cd19	Cd19	CCUGGCCUGGGAUUGCACGU
Designation for CRISPR KO Condition	**Guide Combination**	
AP-1 sgRNA	cJun#1 + cJun#2 + JunB#1 + JunB#2 + JunD#1	
cJun sgRNA	cJun#1 + cJun#2	
JunB sgRNA	JunB#1 + JunB#2	
JunD sgRNA	JunD #1	
cJun/JunD sgRNA	cJun#1 + cJun#2 + JunD #1	
Ctrl sgRNA	Cd19	

Figure 5.1 Optimisation of CRISPR-mediated gene deletion of AP-1
(A) Location of sgRNA target sites relative to annotated domains in *Junb*, *Jun*, and *Jund*.
(B) Gene targets and sgRNA sequences used for CRISPR/Cas9 gene deletion.
(C) Schematic of initial CRISPR KO optimisation experiments with mouse 4T1.2 cells
(D) Representative histogram plots of JunB (left) and cJun (right) expression by JunB sgRNA (maroon), cJun sgRNA (light purple), and Ctrl sgRNA (grey) 4T1.2 cells.
(E) Representative Western Blot analysis for JunD expression in lysates from Ctrl sgRNA and JunD sgRNA 4T1.2 cells
(F) Schematic of CRISPR KO optimisation experiments on activated CD8+ T cells
(G-H) Representative histogram plots and pooled data showing expression of JunB (left), cJun (middle), and JunD (right) in activated JunB sgRNA (maroon), cJun sgRNA (light purple), JunD sgRNA (aqua), AP-1 sgRNA (red), and Ctrl sgRNA (grey) CD8+ T cells activated with either anti-CD3/CD28 and IL-2 **(G)**, or PMA/ionomycin **(H)**. MFI values are relative to the Ctrl sgRNA average.
(I) Representative Western Blot analysis for JunB, cJun, and JunD expression in lysates from activated Ctrl sgRNA, AP-1 sgRNA, JunB sgRNA, cJun sgRNA, and JunD sgRNA CD8+ T cells. p values for all comparisons were calculated using an unpaired t-test: * = $p < 0.05$, ** = $p < 0.01$, *** = $p < 0.001$, **** = $p < 0.0001$.

KO was next validated individually or in combination in CRISPR edited naïve primary mouse CD8+ T cells that were subsequently activated for 24hrs *in vitro* to induce Jun protein expression (Fig. 5.1F). High knock-out efficiency was observed when Jun sgRNAs were either delivered alone (Fig. 5.1G) or in combination ("AP-1 sgRNA"; Fig. 5.1H). Note that the high JunD antibody background staining in the JunD flow cytometry assay means that the calculated KO efficiency in T cells is likely a significant underestimate. Indeed, western blot analysis reveal substantial and specific depletion of Jun proteins (including JunD) across all targeted conditions (Fig. 5.I).

To confirm that our knock-out approach functionally inhibits AP-1-dependent transcription, we CRISPR-edited retrovirally transduced T cells with an NFAT/AP1-driven GFP reporter[553] (Fig.5.2A-B). After activation, transduced AP-1 sgRNA cells displayed attenuated GFP expression compared to controls (Fig. 5.2C), verifying that simultaneous targeting of *Junb, Jun,* and *Jund* directly hinders NFAT/AP-1 transcriptional activity.

Collectively, these data establish our CRISPR-based approach as an effective research tool to probe *in vivo* Jun and AP-1 function in CD8+ T cells.

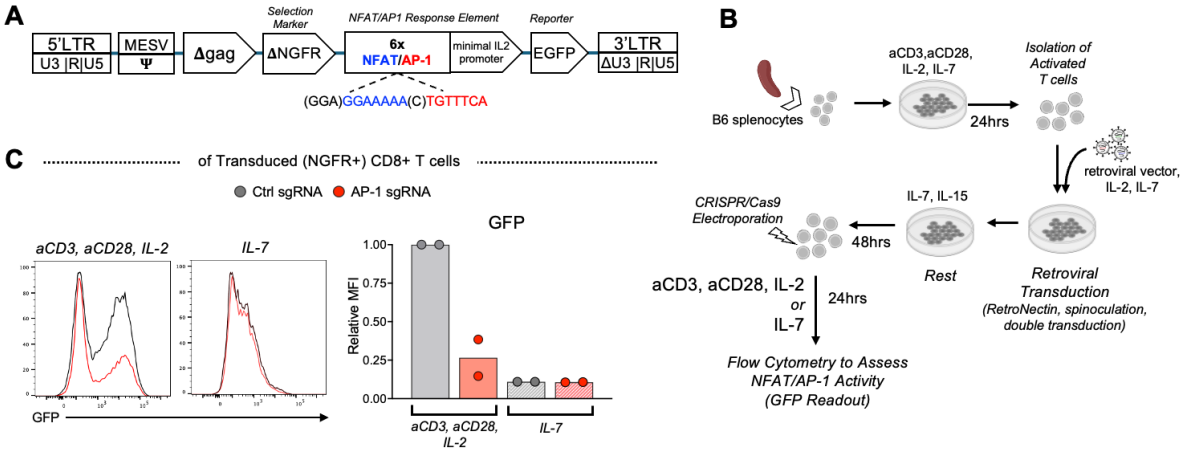


Figure 5.2 Reduced NFAT/AP-1 transcriptional activity following CRISPR-mediated deletion of AP-1
(A) Schematic of the retroviral vector comprising a constitutive ΔNGFR selection marker and an inducible 6X NFAT/AP1 composite element upstream of minimal IL2 promoter driving enhanced green fluorescent protein (EGFP) expression.
(B) Experimental schematic. Retroviral transduction of CD8+ T cells and subsequent CRISPR KO as described in Section 2.2.7
(C) Representative histogram plots and pooled data depicting GFP expression in transduced (NGFR+) AP-1 sgRNA (red) and Ctrl sgRNA (grey) CD8+ T cells either activated with anti-CD3/CD28 and IL-2 (left) or cultured in IL-7 (right). Data are from two independent experiments.

5.2.2. Loss of AP-1 triggers decreased survival and acquisition of exhausted-like features during effector differentiation

We next assessed the effects of AP-1 deletion in CD8+ T cell effector differentiation *in vivo*. Naïve AP-1 sgRNA or Ctrl sgRNA CD45.1+ P14 cells were adoptively transferred into B6 recipient mice prior to infection with acute LCMV Armstrong infection (Fig. 5.3A). AP-1 sgRNA P14 cells were consistently reduced in splenic frequency and number across all timepoints p.i. compared to control (Fig. 5.3B). This appeared due to impaired survival rather than proliferation, as, relative to control, AP-1 sgRNA cells had increased caspase activity in a preliminary experiment, especially at day 8 p.i., with no consistent decrease in the proportion of cycling (Ki67+) cells (Fig. 5.3C-D). While AP-1 sgRNA cells had increased pro-apoptotic BIM expression that skewed the ratio of BIM to the pro-survival protein BCL-2, a preliminary experiment examining CRISPR ablation of *Bim* ("Bim sgRNA") in AP-1 sgRNA cells ("AP-1/Bim sgRNA") did not rescue cell survival, indicating that elevated apoptosis was BIM-independent (Fig. 5.3E,F).

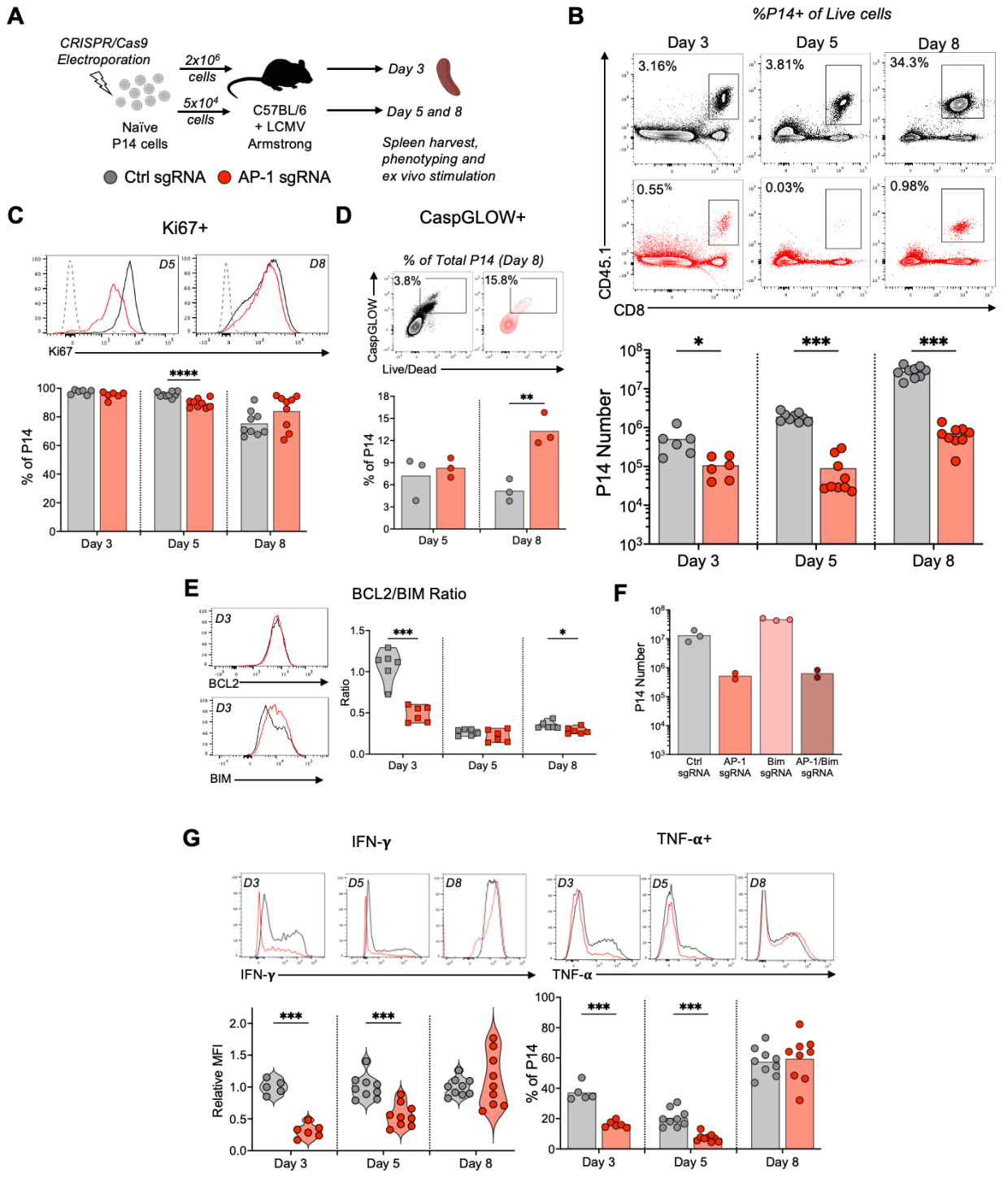


Figure 5.3 AP-1 deletion impairs effector CD8+ T cell survival and function

(A) Experimental schematic. P14 cells were subjected to CRISPR/Cas9 nucleofection with either AP-1 sgRNA (red) or Ctrl sgRNA (grey) RNPs and intravenously injected into B6 recipient mice, subsequently infected with acute LCMV Armstrong 2-3 days later. Either 2 x 10^6 or 5 x 10^4 cells were transferred for harvest and splenic P14 cell phenotyping at day 3, or days 5 and 8, p.i. respectively.

(B) Representative flow cytometry plots depicting the frequencies of live (top), and pooled cell numbers (bottom), of splenic CD45.1+ CD8+ P14 cells at days 3, 5, and 8 p.i.

(C) Representative Ki67 histogram at day 5 and 8 p.i. (top), and pooled frequencies of Ki67+ within P14 cells at days 3, 5, and 8 p.i. (bottom). Dashed line show Ki67 expression of total CD8+ CD44- T cells.
(D) Representative (top; day 8 p.i.) and pooled (day 5 and day 8) frequency of caspase+ (CaspGLOW+), live/dead+ cells within total P14 cells from a single experiment.
(E) Representative P14 cell BCL2 and BIM histograms (left; day 3 p.i.) and pooled BCL2/BIM ratios (right; BCL2 MFI divided by BIM MFI, days 3, 5, 8).
(F) Splenic number of AP-1 sgRNA P14 cells +/- *Bim* deletion at day 8 p.i. from a single experiment.
(G) Representative (top) and pooled (bottom) peptide restimulation-induced IFNγ (left) and TNFα (right) production by P14 cells at days 3, 5, and 8 p.i.
MFI values are expressed relative the average MFI of the Ctrl sgRNA group. Unless stated otherwise, data are from 2-3 independent experiments for each timepoint (n=6-9 mice per group), and p values for all day 3, 5, and 8 p.i. comparisons were calculated using unpaired t-tests:* = $p < 0.05$, ** = $p < 0.01$, *** = $p < 0.001$, **** = $p < 0.0001$.

We next assessed cytokine function within AP-1 deficient effector cells. At day 3 and 5 p.i., both IFNγ and TNFα production was diminished in the absence of AP-1 (Fig. 5.3G), consistent with prior work implicating AP-1 in transcriptional induction of cytokine expression[554,555]. Unexpectedly, though, AP-1 sgRNA cells had recovered normal cytokine expression by day 8 p.i. (Fig. 5.3G). Given the survival defect of AP-1 deficient cells, we speculated that this may be because the cells recovered at day 8 p.i. are those cells that failed to CRISPR delete the *Jun* genes.

As AP-1 expression peaks at days 1-2 p.i., decreases shortly after, then returns to baseline by day 8 p.i. (as discussed in Section 4.2.1), we assessed gene KO in P14 cells at days 3, 5, and 8 p.i. by *ex vivo* re-stimulation with LCMV-GP_{33-41} peptide for 24hrs to induce Jun protein expression in a preliminary experiment (Fig. 5.4A). Notably, day 3 p.i. AP-1 sgRNA cells had reduced capacity to re-express each Jun family member, while days 5 and 8 p.i. AP-1 sgRNA cells were comparable to controls (Fig. 5.4B-D). This indicates that there was a gradual loss of cells fully ablated of AP-1 deficient cells. While their survival defect makes it difficult to assess if AP-1 is required for cytokine production by day 8 effector cells, at least at early timepoints p.i., AP-1 is required for optimal cytokine production.

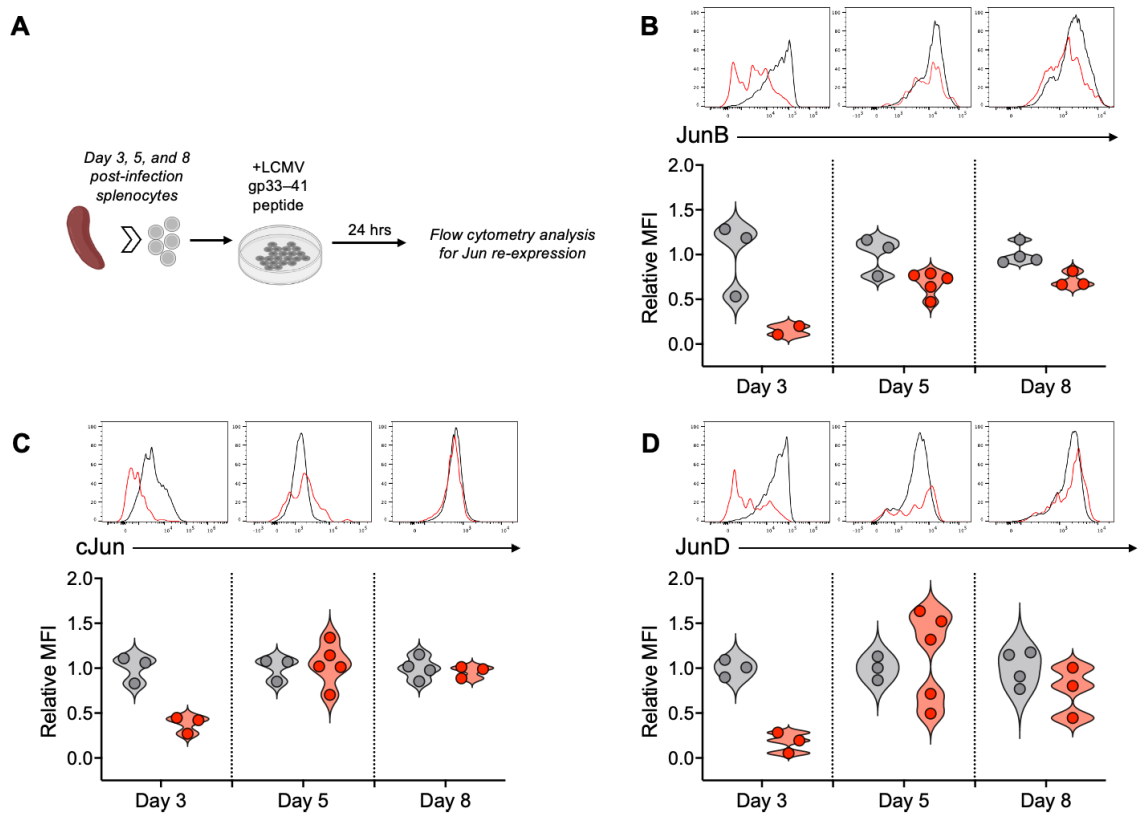


Figure 5.4 Re-expression of Jun proteins *ex vivo* at days 3, 5, and 8 p.i.
(A) Experimental schematic. *Ex vivo* stimulation assay to induce Jun expression at days 3, 5 and 8 p.i. for assessment of gene KO in CRISPR-edited P14 cells. Representative histograms (top) and pooled relative MFIs (bottom) of JunB **(B)**, cJun **(C)**, and JunD **(D)** after 24 h peptide restimulation. Data is from a single experiment (n=2-5 mice per group).

Despite not being bona fide AP-1 knockout cells, the remaining AP-1 sgRNA cells exhibited phenotypic features more consistent with exhaustion than tolerance. Unlike tolerant cells, AP-1 sgRNA cells induced GzmB, T-bet, and KLRG1 expression relatively normally (Fig 5.5A-C), and at best minimally up-regulated the tolerance markers, FR4 and Helios, which it should be noted are also expressed at low levels in exhausted cells (Fig. 5.5D-E). The exhaustion markers PD-1, and to a lesser extent TOX, were up-regulated in the AP-1 sgRNA cells at day 8 p.i., albeit not at the levels seen in chronic LCMV Cl.13 infection (Fig. 5.5F-G). Inhibitory receptors, TIM-3 and TIGIT, which are typically not expressed at all in tolerance[91] were also similarly upregulated (Fig 5.5H-I). Thus, AP-1 ablation dramatically impairs effector cell survival and cytokine production, without appearing to impact GzmB induction or proliferation. AP-1 deficient cells acquired a mild phenotype more reminiscent of exhaustion than tolerance. Overall, AP-1 deficiency does not appear to arrest cells in a classical non-proliferative, GzmB deficient tolerant or anergic state, arguing that AP-1 is not required to insulate effector cells against tolerance induction.

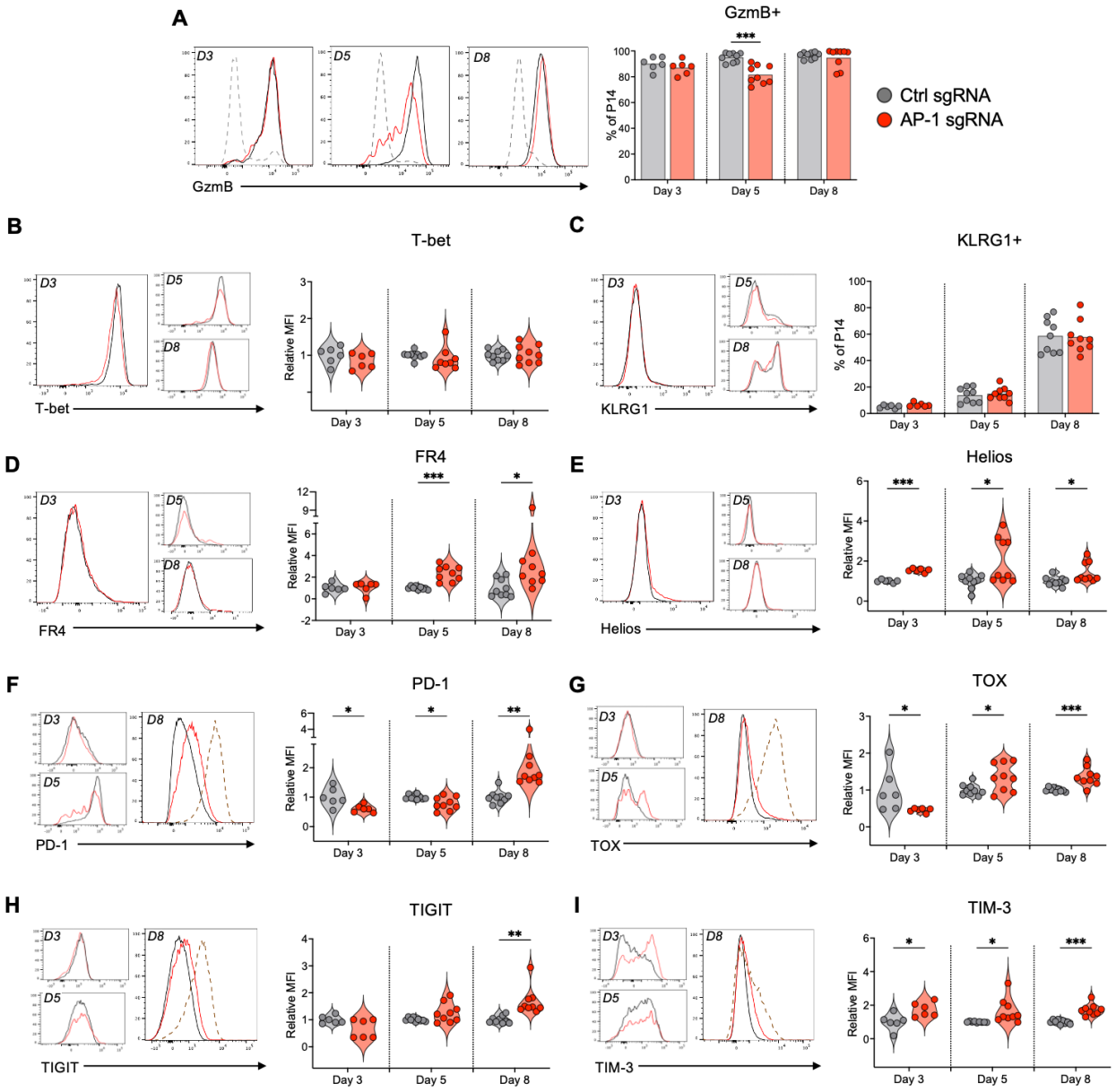


Figure 5.5 Expression of canonical markers associated with tolerance or exhaustion by residual AP-1 sgRNA cells

Representative histograms (left) and pooled data (right) from splenic Ctrl or AP-1 sgRNA P14 cells at various timepoints post-acute LCMV infection showing GzmB **(A)**, T-bet **(B)**, KLRG1 **(C)**, FR4 **(D),** Helios **(E),** PD-1 **(F),** TOX **(G),** TIGIT **(H),** and TIM-3 **(I)** expression. Dashed line shows marker expression in total CD8+ CD44- T cells in **(A)** and exhausted P14 cells isolated from chronic LCMV infection at day 8 p.i. in **(F-I)**. MFI values are expressed relative to the average MFI of the Ctrl sgRNA group. All data are from 2-3 independent experiments for each timepoint (n=6-9 mice per group), and p values for comparisons at days 3, 5, and 8 p.i. were calculated using unpaired t-tests:* = $p < 0.05$, ** = $p < 0.01$, *** = $p < 0.001$, **** = $p < 0.0001$.

5.2.3. JunB deletion is sufficient to phenocopy AP-1 deficiency

Given our strategy to functionally knockout AP-1 was to simultaneously delete all Jun family members, we next tested whether individual Jun knockouts could result in similar phenotypic effects. Surprisingly, JunB deficiency alone could almost fully phenocopy the AP-1 sgRNA cells in terms of cell numbers and PD-1 expression at day 8 p.i. (Fig. 5.6-B,D). In contrast, cells deficient for either cJun or JunD alone (cJun sgRNA and JunD sgRNA) or in combination (cJun/JunD sgRNA) did not display these features and were phenotypically comparable with control cells (Fig. 5.6A-B,D). As with AP-1 sgRNA cells, JunB sgRNA cells recovered at day 8 p.i. were cells that failed to CRISPR edit the *Junb* gene, highlighting the survival deficiency upon JunB loss (Fig. 5.6E). Conversely, cJun/JunD sgRNA cells were still cJun and JunD deficient at day 8 p.i. consistent with normal expansion (Fig. 5.6F). To further demonstrate that residual P14 cells in both the AP-1 and JunB sgRNA conditions were enriched for unedited alleles, we utilised long-read DNA sequencing to assess frequencies of DNA mutations (i.e. insertions, deletions, and/or substitutions) in cells recovered at day 8 p.i. Despite high initial editing efficiencies on the *Junb* locus prior to adoptive transfer (Fig. 5.7B), AP-1 and JunB sgRNA cells at day 8 p.i. were enriched for unmodified alleles (Fig. 5.7C), confirming the loss of *bona fide* KO cells. A minor fraction of AP-1 sgRNA cells did retain modifications but only in *Jun* and *Jund*. cJun and JunD sgRNA cells largely maintained, or even became slightly more enriched, for modified alleles at their targeted gene loci (Fig. 5.7B-C). Background mutations detected in Ctrl sgRNA cells were likely due to PCR or sequencing artifacts.

JunB heterodimerises with BATF, another AP-1 family member known to be required for effector CD8+ T cell expansion [176,437,475]. Utilising sgRNAs optimised to delete *Batf* (Fig. 5.6C), we generated P14 cells deficient for BATF, either alone (“Batf sgRNA”) or together with JunB (“JunB/Batf sgRNA”), and assessed effector differentiation at day 8 p.i.. Both Batf sgRNA and JunB/Batf sgRNA cells showed diminished persistence and elevated PD-1 expression, recapitulating the defects observed in AP-1 and JunB sgRNA cells (Fig. 5.6 A-B, D). Interestingly, an interaction partner of the BATF/JunB heterodimer, IRF4[340,472,479], was elevated in expression in all conditions where either JunB and/or BATF were deleted, in line with previous observations in BATF deficient cells[437] (Fig. 5.6G). However, unlike the AP-1/JunB deficient conditions, Batf sgRNA cells had normal levels of CD127+ KLRG1- memory precursor cells and normal Eomes expression (Fig. 5.6H-I). These data suggest that JunB may also influence aspects of effector differentiation through BATF-independent mechanisms. Together, our findings demonstrate that the functional role of AP-1 in CD8+ T cell effector differentiation is predominantly mediated by JunB, partially through its coordination with BATF. Surprisingly, cJun and JunD appear to be dispensable in this process, as there were no discernible effects when both were knocked out alone or in combination.

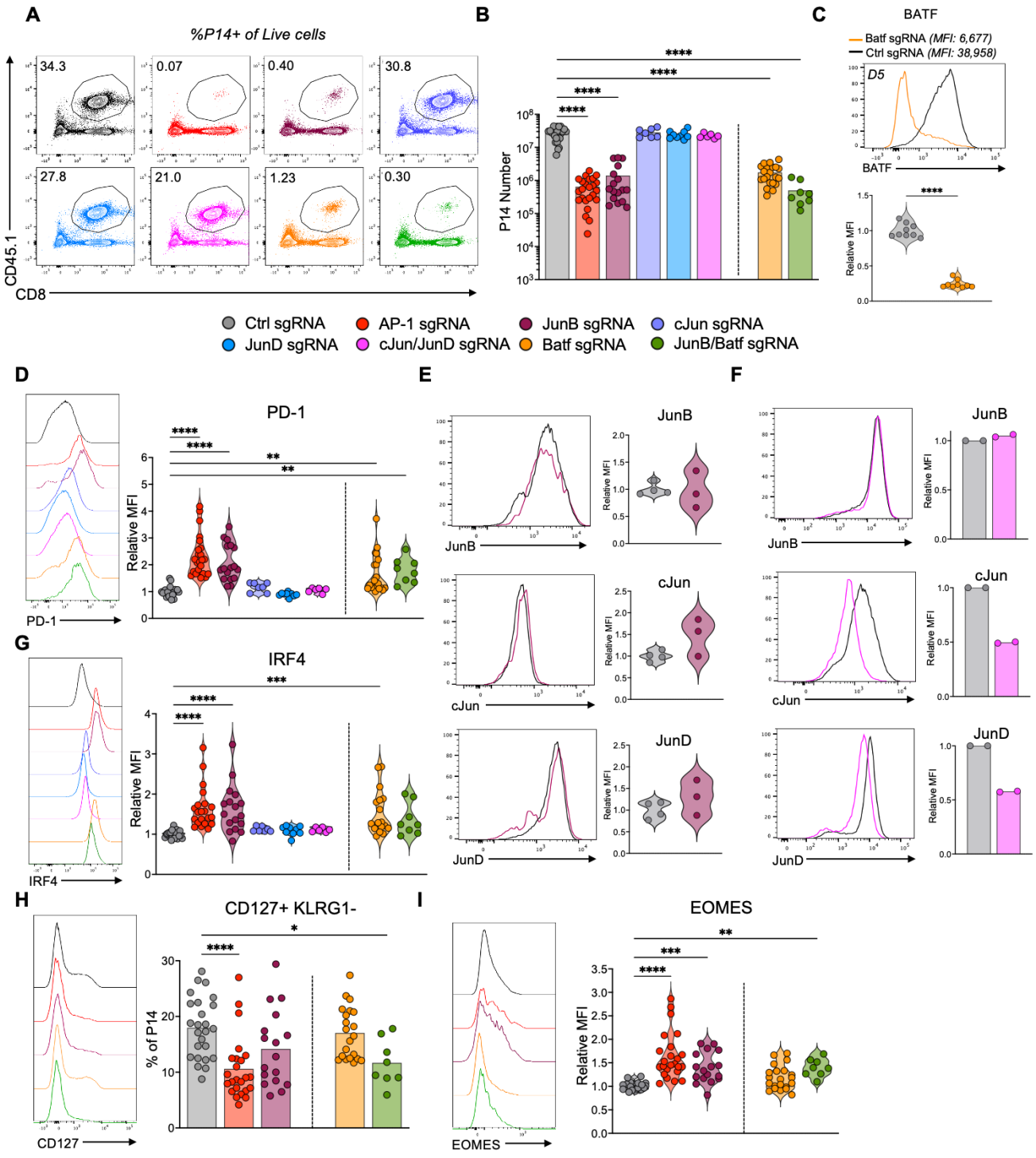

A
%P14+ of Live cells
34.3
0.07
0.40
30.8
27.8
21.0
1.23
0.30
CD45.1
CD8
B
P14 Number
C
BATF
Batf sgRNA (MFI: 6,677)
Ctrl sgRNA (MFI: 38,958)
D5
BATF
Relative MFI
Ctrl sgRNA
AP-1 sgRNA
JunB sgRNA
cJun sgRNA
JunD sgRNA
cJun/JunD sgRNA
Batf sgRNA
JunB/Batf sgRNA
D
PD-1
Relative MFI
E
JunB
cJun
JunD
F
JunB
cJun
JunD
G
IRF4
Relative MFI
H
CD127+ KLRG1-
% of P14
CD127
I
EOMES
Relative MFI

Figure 5.6 Phenotypic effects of individual and combined gene deletion of AP-1 family members during effector differentiation

(A-B) Representative frequency **(A)** and pooled numbers **(B)** at day 8 p.i. of CD45.1+ CD8+ P14 cells across the following different CRISPR conditions: Ctrl sgRNA (grey), AP-1 sgRNA (red), JunB sgRNA (maroon), cJun sgRNA (light purple), JunD sgRNA (aqua), cJun/JunD sgRNA (magenta), Batf sgRNA (orange), and JunB/Batf sgRNA (green).

(C) Representative (top) and pooled (bottom) BATF expression at day 5 p.i. in Batf sgRNA and Ctrl sgRNA cells.

(D) Representative (left) and pooled (right) PD-1 expression at day 8 p.i. across the different CRISPR conditions.

(E,F) Representative (left) and pooled (right) JunB (top), cJun (middle), and JunD (bottom) re-expression at day 8 p.i. upon peptide restimulation of JunB sgRNA versus Ctrl sgRNA **(E)** or cJun/JunD sgRNA versus Ctrl sgRNA **(F)** P14 cells. Pooled relative MFI (right) of JunB, cJun, and JunD expression from a single experiment (n=2-4 mice per group).

(G) Representative (left) and pooled (right) IRF4 expression at day 8 p.i. across the different CRISPR conditions.

(H,I) Representative (left) and pooled (right) CD127 expression/CD127+KLRG1- cell frequencies **(H)** or Eomes expression **(I)** at day 8 p.i. in the indicated CRISPR edited P14 conditions.

MFI values are expressed relative to the average MFI of the Ctrl sgRNA group. Data is from eight independent experiments (n=6-27 mice per group), and p values for all comparisons were calculated using Ordinary one-way ANOVA with post-hoc Dunnett's multiple comparisons test (against Ctrl sgRNA cells only):* = $p < 0.05$, ** = $p < 0.01$, *** = $p < 0.001$, **** = $p < 0.0001$.

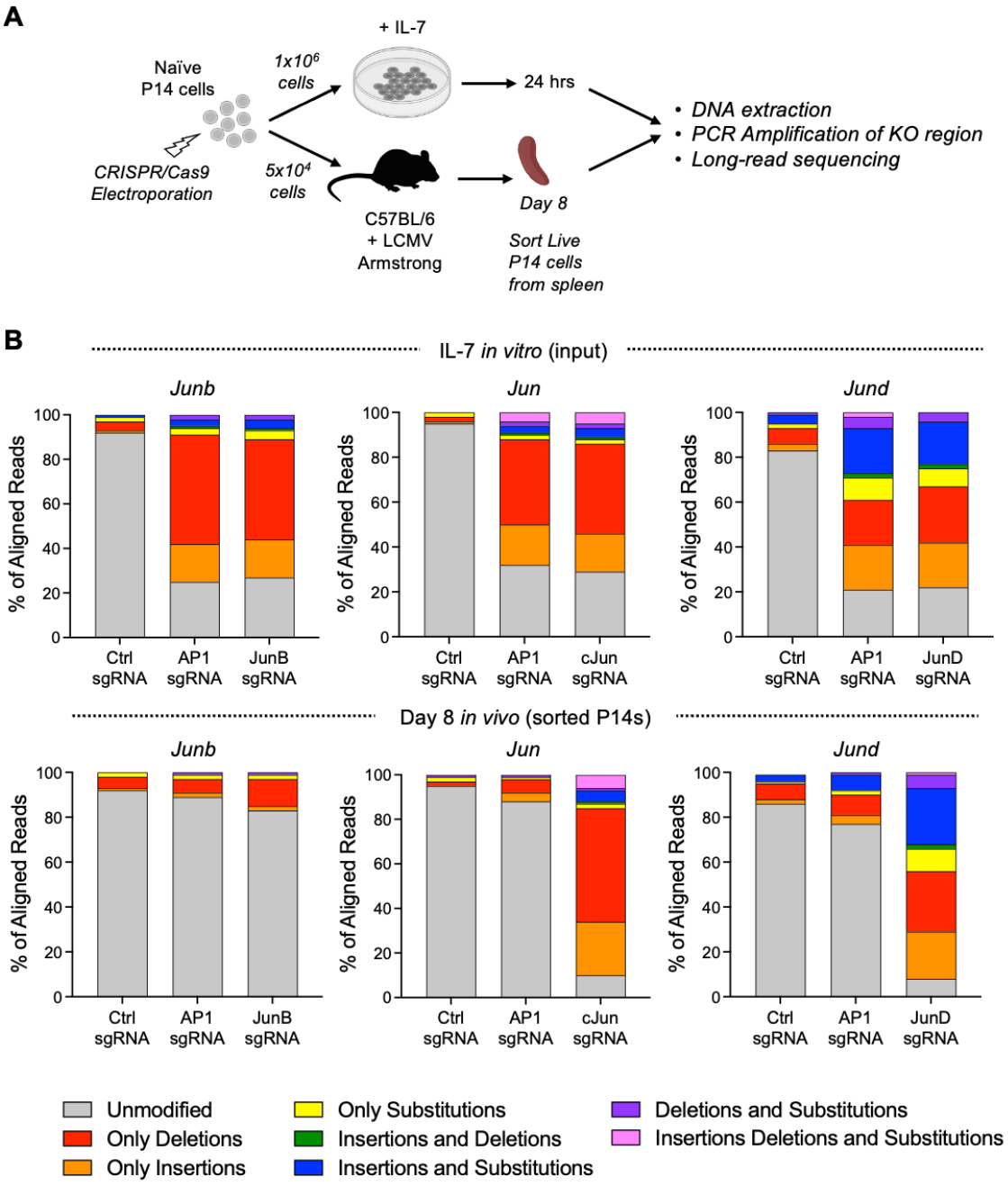


Figure 5.7 DNA mutations in CRISPR-edited cells pre- and post-adoptive transfer and infection

(A) Experimental schematic. CRISPR-edited P14 cells were analysed for mutations by DNA sequencing as outlined in Section 2.2.9

(B) Representative stacked bar graphs showing the frequencies of editing outcomes at *Junb* (left), *Jun* (middle), and *Jund* (right) genomic loci relative to aligned sequencing reads from Ctrl sgRNA (left bars), AP-1 sgRNA (middle bars), and individual Jun sgRNA cells (i.e. JunB, cJun, JunD; right bars). CRISPR-edited cells from the same P14 donor were either cultured in IL-7 (input; top row) or sorted from n=3-5 mice at day 8 p.i. (sorted P14; bottom row). Data is from a single experiment.

5.2.4. Different Jun proteins play analogous roles in CD8+ T cell exhaustion

Given the lack of an observed function for cJun and JunD in effector differentiation, we next investigated whether these proteins may instead play roles in CD8+ T cell exhaustion (Fig. 5.8A). AP-1 and JunB deficient cells were also included in these experiments to assess if AP-1/JunB plays comparable roles in exhaustion. AP-1 and JunB sgRNA cells displayed a survival defect at 20 p.i. with LCMV Cl.13, analogous to the phenotypes seen in acute infection, however again cJun/JunD sgRNA cell numbers were normal (Fig. 5.8B). Surprisingly, expression of the exhaustion markers, TOX and TCF1, and the proportions of CX3CR1+ intermediate and CD101+ terminally exhausted cell subsets were largely unaffected following deletion of AP-1 or its individual Jun members (Fig. 5.8C-E). Thus, JunB containing AP-1 complexes similarly control cell survival in both exhausted and effector populations, although interestingly, unlike in acute infection, JunB loss does not impact exhausted cell phenotypes or subsets. Both cJun and JunD appear dispensable for cell persistence and differentiation in exhaustion, again analogous to the results at day 8 p.i. with acute LCMV.

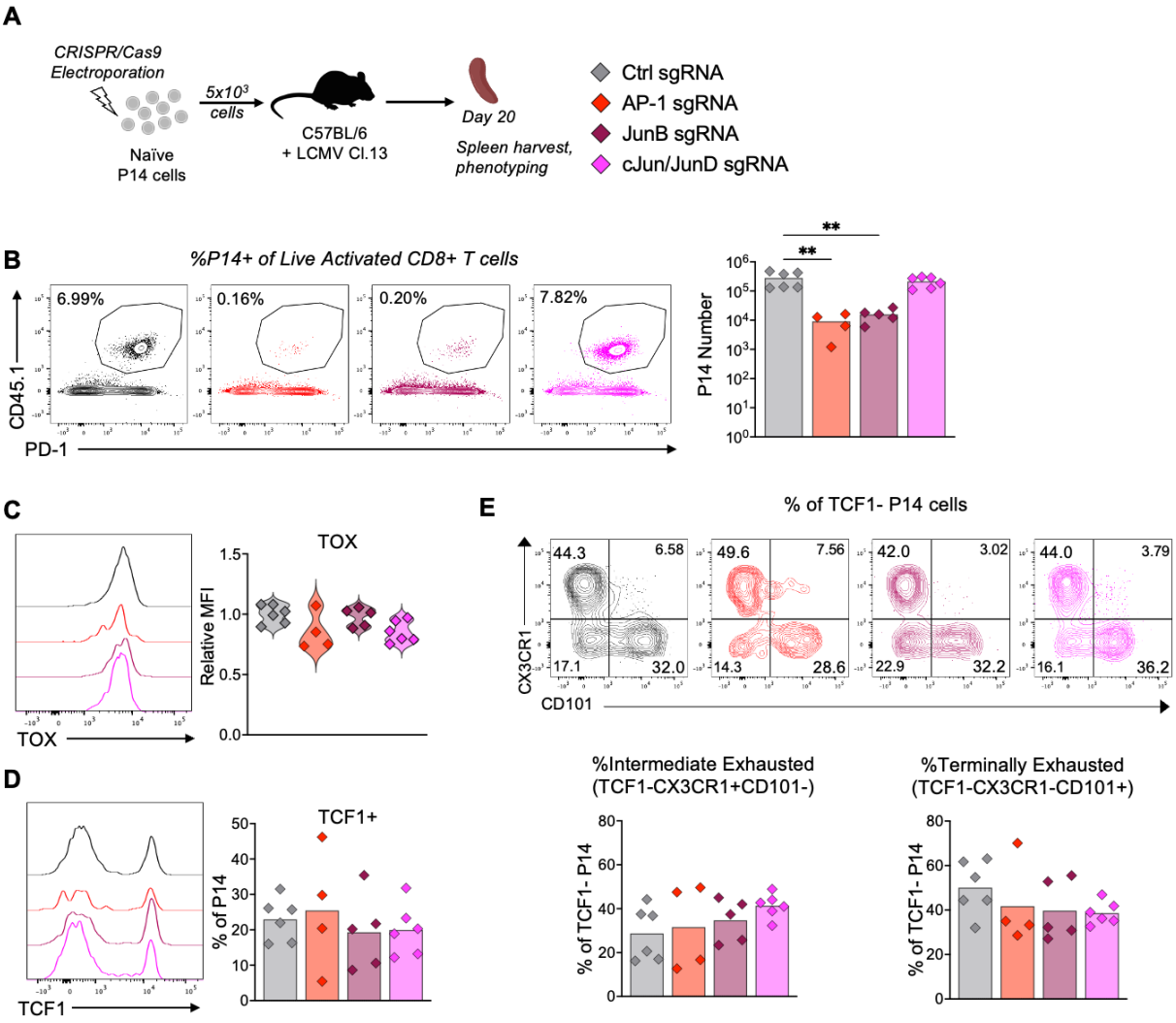


Figure 5.8 Influence of AP-1 deletion on exhausted cell differentiation

(A) Experimental schematic. CD45.1+ P14 cells were CRISPR edited to generate AP-1 sgRNA (red), Ctrl sgRNA (grey), JunB sgRNA (maroon), or cJun/JunD sgRNA (magenta) conditions, and 5,000 cells were i.v. injected into B6 recipient mice infected with LCMV Cl.13 2-3 days later. At day 20 p.i., spleens were harvested and processed for immunophenotyping.

(B) Splenic P14 representative frequencies (left) and pooled numbers (right) at day 20 p.i. across all CRISPR conditions.

(C-D) Representative (left) and pooled (right) TOX **(C)** and TCF1 **(D)** expression in P14 cells at day 20 p.i.

(E) Representative (top) and pooled (bottom) frequencies of CX3CR1+CD101- "Intermediate Exhausted" and CX3CR1-CD101+ "Terminally Exhausted" cells within TCF1- P14 cells at day 20 p.i.

MFI values are expressed relative to the average MFI of the Ctrl sgRNA group. Data are from two independent experiments (n=4-11 mice per group); p-values were calculated using Ordinary one-way ANOVA with post hoc Dunnett's multiple comparisons test; ** = $p < 0.01$

5.2.5. Little to no impact on transcriptional induction of the early effector gene program upon AP-1 deletion

Based on prior work, typically in cell lines, AP-1 transcription factors are regarded as essential for early induction of effector and activation genes within stimulated T cells [253,279,427,545,550]. To examine the impact of AP-1 and individual Jun deficiency on initial gene induction during effector T cell differentiation, we performed a high throughput and high temporal resolution bulk RNAseq timecourse of all CRISPR KO conditions across the first 24hrs of *in vitro* T cell activation using multiplexed analysis of cell sequencing (MAC-Seq) (Fig. 5.9A). MAC-Seq is a high throughput bulk RNA-seq workflow that allows simultaneous transcriptional analysis of various cell perturbations and timepoints in a 384 well plate format[513]. Unexpectedly, there were no differences in the global transcriptional profiles across all KO conditions for each time point of activation using UMAP clustering (Fig. 5.9B). Next, we measured the expression kinetics of early effector cytokines such as *Gzmb, Ifng, Il2, Il2ra, and Tnf*, and observed no major differences across all conditions (Fig. 5.9C), suggesting that AP-1 is dispensable for early induction of key effector genes. To globally examine transcriptional changes in the different KO conditions, we performed pathway enrichment analysis of differentially expressed genes relative to control. Surprisingly, there was no significant enrichment in canonical pathways related to TCR signalling, chromatin remodelling, apoptosis, or effector differentiation, and no strong evidence of aberrant exhaustion or tolerance gene expression (Fig. 5.9D). Interestingly, though, AP-1 and JunB sgRNA cells had significantly downregulated ribosomal gene sets and pathways associated with protein synthesis within the first hours of activation. While further work is needed to functionally prove that AP-1 and JunB deficient cells have translation defects, these data suggest that the compromised effector cell survival and differentiation seen in the absence of JunB may in part be due defects in protein translation rather than simply deficiencies in effector gene expression.

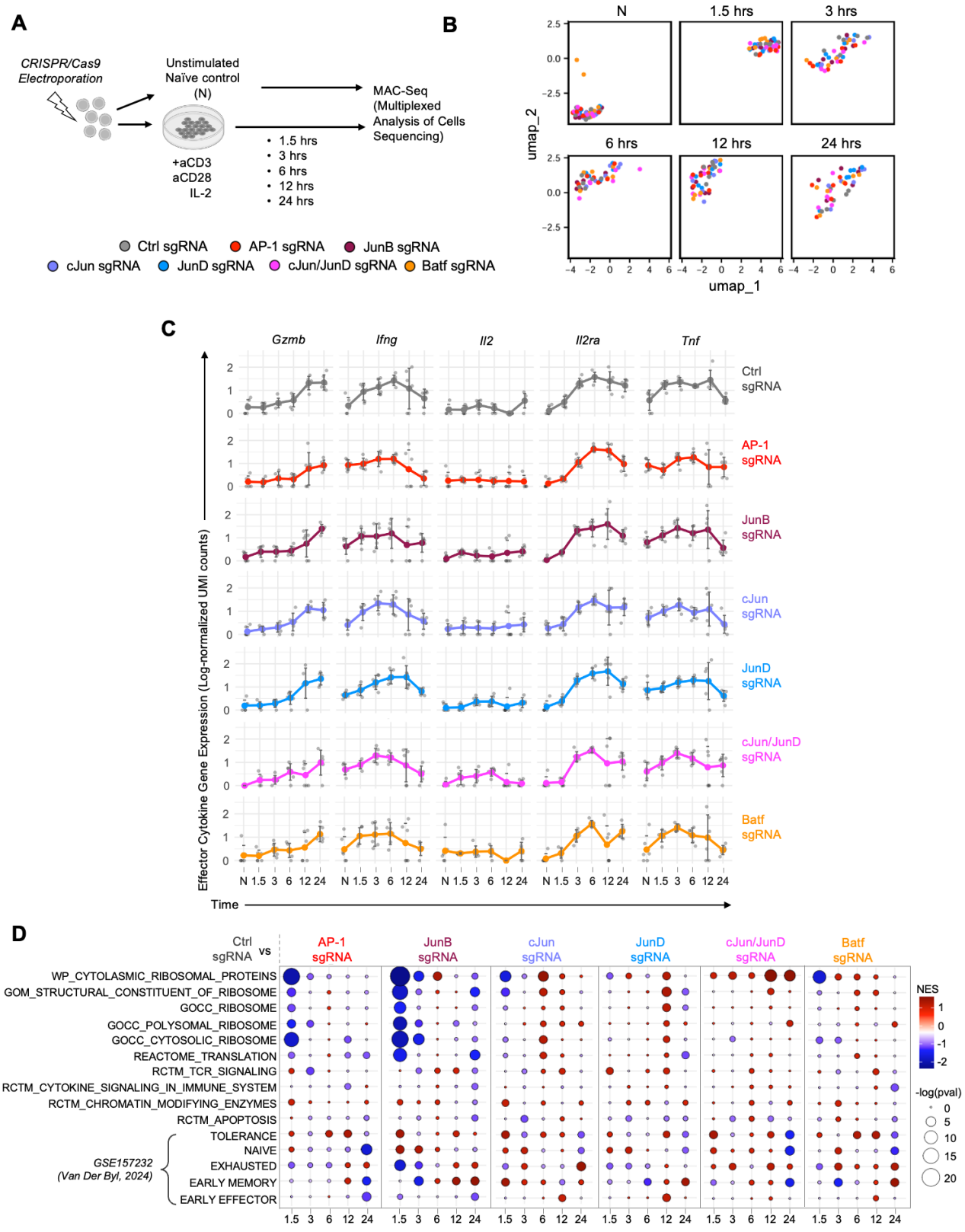

A
CRISPR/Cas9
Electroporation
Unstimulated
Naïve control
(N)
+aCD3
aCD28
IL-2
• 1.5 hrs
• 3 hrs
• 6 hrs
• 12 hrs
• 24 hrs
MAC-Seq
(Multiplexed
Analysis of Cells
Sequencing)
Ctrl sgRNA
AP-1 sgRNA
JunB sgRNA
cJun sgRNA
JunD sgRNA
cJun/JunD sgRNA
Batf sgRNA
B
N
1.5 hrs
3 hrs
6 hrs
12 hrs
24 hrs
umap_2
umap_1
C
Gzmb
Ifng
Il2
Il2ra
Tnf
Ctrl sgRNA
AP-1 sgRNA
JunB sgRNA
cJun sgRNA
JunD sgRNA
cJun/JunD sgRNA
Batf sgRNA
Effector Cytokine Gene Expression (Log-normalized UMI counts)
N 1.5 3 6 12 24
Time
D
Ctrl sgRNA vs
AP-1 sgRNA
JunB sgRNA
cJun sgRNA
JunD sgRNA
cJun/JunD sgRNA
Batf sgRNA
WP_CYTOLASMIC_RIBOSOMAL_PROTEINS
GOM_STRUCTURAL_CONSTITUENT_OF_RIBOSOME
GOCC_RIBOSOME
GOCC_POLYSOMAL_RIBOSOME
GOCC_CYTOSOLIC_RIBOSOME
REACTOME_TRANSLATION
RCTM_TCR_SIGNALING
RCTM_CYTOKINE_SIGNALING_IN_IMMUNE_SYSTEM
RCTM_CHROMATIN_MODIFYING_ENZYMES
RCTM_APOPTOSIS
GSE157232
(Van Der Byl, 2024)
TOLERANCE
NAIVE
EXHAUSTED
EARLY MEMORY
EARLY EFFECTOR
1.5 3 6 12 24
NES
-log(pval)

Figure 5.9 Transcriptomic profiling of AP-1 deficient cells during early activation by MAC-seq
(A) Experimental schematic. B6 CD8+ T cells (n=2 biological replicates) were CRISPR edited to generate Ctrl sgRNA (grey), AP-1 sgRNA (red), JunB sgRNA (maroon), cJun sgRNA (light purple), JunD sgRNA (aqua), cJun/JunD sgRNA (magenta) and Batf sgRNA (orange) cells. n=3 technical replicates per CRISPR condition were then activated with anti-CD3/CD28 and IL-2, harvested at unstimulated (N), 1.5, 3, 6, 12, and 24hrs post-activation, and then RNA-sequenced.
(B) Uniform Manifold Approximation and Projection (UMAP) plots showing transcriptomic clustering of each CRISPR condition across each activation timepoint. Each point represents one of the 6 technical and biological replicates from each CRISPR condition.
(C) Log-normalised Unique Molecular Identifier (UMI) counts of *Gzmb, Ifng, Il2, Il2ra*, and *Tnf* (left to right) at each activation timepoint, for each CRISPR condition. Points and error bars represent mean and standard deviation, respectively.
(D) Gene set enrichment analysis of each CRISPR condition relative to Ctrl sgRNA cells across activation timepoints. GO:Biological Processes and Reactome gene-sets relevant to early T cell activation, together with differentiation-related gene sets (i.e., tolerance, naive, exhausted, early memory, and early effector) from Van Der Byl et al (2024) are shown. Bubble size reflects -log10 (p value), and colour denotes normalised enrichment score (NES, red: positive, blue=negative)

5.2.6. JunD deficiency selectively disrupts memory cell persistence

While cJun and JunD appeared dispensable for effector differentiation, exhaustion and early activation, it was possible that they might play roles in memory differentiation. To assess memory formation, we tracked the persistence and phenotype of cJun, JunD, and cJun/JunD sgRNA cells during acute LCMV Armstrong infection in blood (days 8, 18, 25, 32, 42, 60, 90, 112 p.i.) and spleen (days 42 and 112 p.i.) (Fig. 5.10A). As cells contracted from day 8 p.i., both JunD and cJun/JunD sgRNA cells exhibited a more pronounced decline compared to cJun sgRNA and Ctrl sgRNA cells in both blood (Fig. 5.10B) and spleen (Fig. 5.10C-D). Interestingly, and in contrast to previous splenic results (Fig. 5.10B), cJun/JunD sgRNA cells were diminished in the blood at day 8.p.i. potentially hinting at migration defects in these cells. When we quantified the degree of contraction between the effector phase (day 8 p.i.) and early memory phase (day 42 p.i.), we found that the JunD sgRNA and cJun/JunD sgRNA groups contracted significantly more than Ctrl sgRNA and cJun sgRNA cells (Fig. 5.10E). Collectively, these findings indicate that JunD is required for normal T cell persistence during memory.

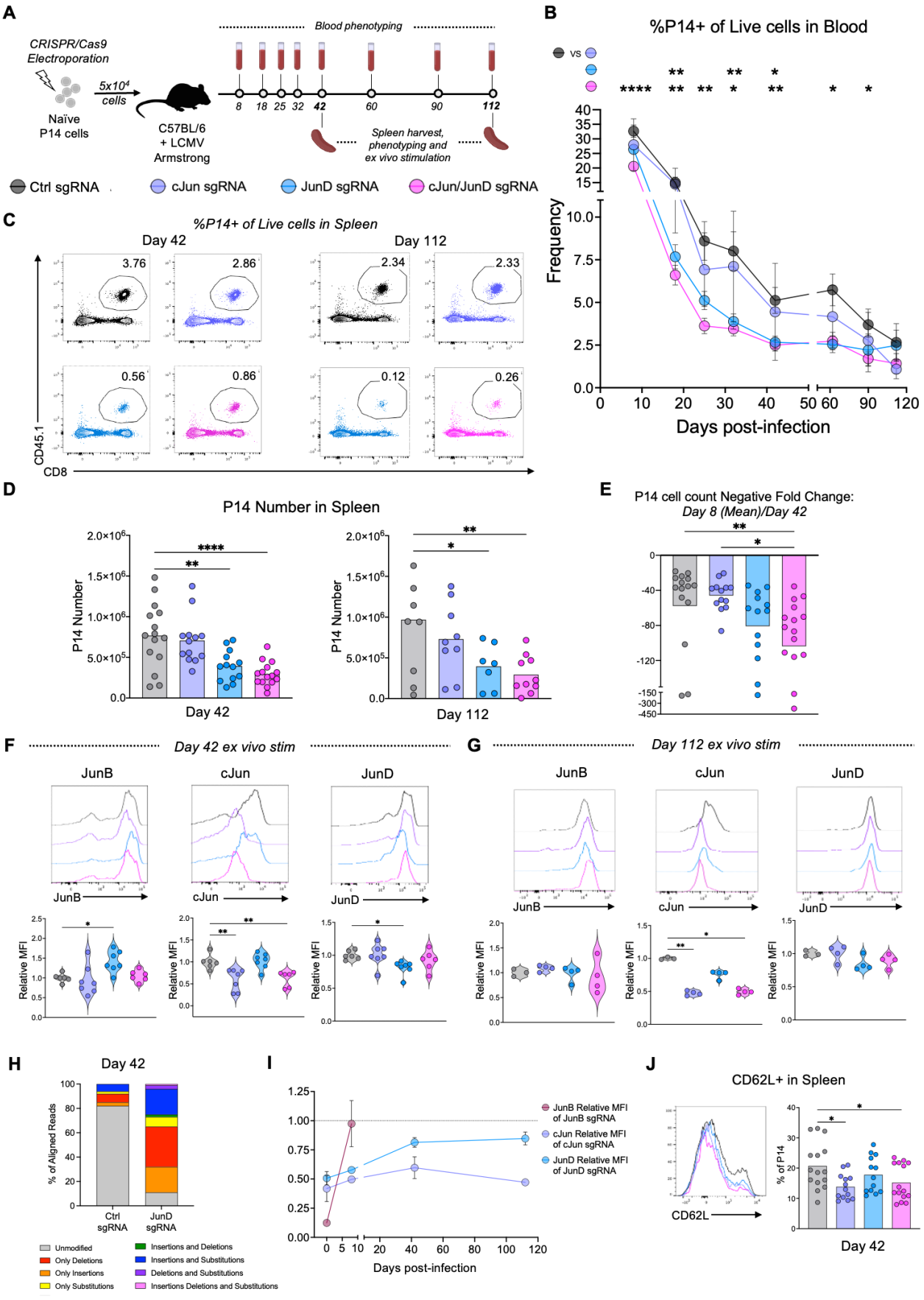

A
CRISPR/Cas9
Electroporation
5x10⁴ cells
Naïve P14 cells
C57BL/6 + LCMV Armstrong
Blood phenotyping
8 18 25 32 42 60 90 112
Spleen harvest, phenotyping and ex vivo stimulation
Ctrl sgRNA
cJun sgRNA
JunD sgRNA
cJun/JunD sgRNA
B
%P14+ of Live cells in Blood
vs
Frequency
Days post-infection
C
%P14+ of Live cells in Spleen
Day 42
Day 112
3.76
2.86
2.34
2.33
0.56
0.86
0.12
0.26
CD45.1
CD8
D
P14 Number in Spleen
P14 Number
Day 42
Day 112
E
P14 cell count Negative Fold Change:
Day 8 (Mean)/Day 42
F
Day 42 ex vivo stim
JunB
cJun
JunD
Relative MFI
G
Day 112 ex vivo stim
H
Day 42
% of Aligned Reads
Ctrl sgRNA
JunD sgRNA
Unmodified
Only Deletions
Only Insertions
Only Substitutions
Insertions and Deletions
Insertions and Substitutions
Deletions and Substitutions
Insertions Deletions and Substitutions
I
JunB Relative MFI of JunB sgRNA
cJun Relative MFI of cJun sgRNA
JunD Relative MFI of JunD sgRNA
Days post-infection
J
CD62L+ in Spleen
CD62L
% of P14
Day 42

Figure 5.10 Memory formation and maintenance following cJun and/or JunD deletion
(A) Experimental schematic. CD45.1+ P14 cells were CRISPR edited to generate Ctrl sgRNA (grey), cJun sgRNA (light purple), JunD sgRNA (aqua) and cJun/JunD sgRNA (magenta) cells. 50,000 cells were i.v. injected into B6 recipient mice infected with LCMV Armstrong 2-3 days later. Blood was collected at days 8, 18, 25, 32, 42, 60, 90, and 112 p.i., and spleens were harvested at days 42 and 112 p.i. for immunophenotyping.
(B) CD45.1+ P14 cells frequency in blood over time in acute infection. Individual points and error bars represent the mean and standard error of the mean (SEM), respectively. Statistical comparisons against Ctrl sgRNA were calculated using Restricted Maximum Likelihood (REML) and post-hoc Uncorrected Fisher's LSD analysis.
(C-D) Representative splenic P14 frequencies **(C)** and pooled numbers **(D)** at day 42 p.i. (left) and day 112 p.i. (right) across CRISPR conditions.
(E) Fold change in mean P14 cell counts at day 42 p.i. relative to day 8 p.i. (i.e. day 8 counts divided by day 42 counts then expressed as a negative value).
(F-G) Representative (top) and pooled (bottom) JunB (left), cJun (middle), and JunD (right) re-expression upon peptide restimulation of CRISPR-edited P14 cells at days 42 p.i. **(F)** and 112 p.i. **(G)** Data from two independent experiments (n=6 mice per group).
(H) Representative histogram (left) and pooled frequencies (right) of CD62L expression in P14 cells from each CRISPR condition at day 42 p.i.
(I) Representative stacked bar graph showing genome editing outcomes at *Jund* loci relative to aligned sequencing reads for Ctrl sgRNA (left) and JunD sgRNA cells (right) sorted from n=3 mice at day 42 p.i. Data is from a single experiment.
(J) Re-expression of each Jun within each KO condition across time. Individual points and error bars represent the mean and standard error of the mean (SEM), respectively.
Unless specified, data are from 8 independent experiments (n=3-19 mice per group for each timepoint) and p values were calculated using Kruskal-Wallis test with post-hoc Dunnett's multiple comparisons test. * = $p < 0.05$, ** = $p < 0.01$, *** = $p < 0.001$, **** = $p < 0.0001$

Given that JunD deficient cells have a survival deficiency during memory, we speculated that cells that failed to CRISPR edit the JunD gene would become enriched over time. Interestingly, the surviving splenic JunD sgRNA and cJun/JunD sgRNA P14 cells at day 42 p.i, had slight reductions in *ex vivo* JunD levels (Fig. 5.10F) and were enriched for modified *Jund* alleles, with a notable fraction being insertions and substitutions (Fig. 5.10H). However, by day 112 p.i, *ex vivo* JunD expression by these cells became indistinguishable from Ctrl sgRNA cells (Fig. 5.10G, I). Interestingly, JunB expression was slightly increased in JunD sgRNA cells, although only at day 42 p.i. In contrast, deficient cJun expression was preserved in the cJun and cJun/JunD sgRNA cells at days 42 and 112 p.i. consistent with cJun deletion having no impact on memory cell persistence.

In terms of memory cell phenotype, we did not observe substantial differences in all the features we assessed in any of the CRISPR KO conditions (data not shown). There was a modest trend toward cJun sgRNA cells having a lower CD62L+ cell proportion at day 42 p.i. in the spleen (Fig 5.10J), however this difference was not maintained at later timepoints in the blood (data not shown). Overall, these data suggest that JunD is required for memory cell persistence, but that cJun is dispensable for memory cell differentiation and persistence.

5.2.7. Deleting cJun may affect memory responses in subsequent immune challenges

We next assessed if cJun is required for memory cell expansion upon rechallenge. Day 42 p.i. cJun sgRNA or Ctrl sgRNA cells were transferred into naïve B6 recipients prior to rechallenge by LM-33 infection, which is recombinant *Listeria monocytogenes* expressing the LCMV GP_{33-41} epitope recognised by P14 cells (Fig. 5.8A). At day 7 p.i., cJun sgRNA cell numbers and Ki67+ cell proportions were comparable to control cells, indicating normal re-expansion (Fig. 5.8 B-C). However, there was a mild phenotypic difference, with slightly increase effector-like CD127-KLRG1+ cells, and slightly reduced memory-associated CD127+ cells, in the cJun sgRNA group (Fig. 5.8D). We also confirmed that the cJun sgRNA cells recovered after re-expansion are still bona fide knockout cells (Fig. 5.8E). Thus, cJun loss has no impact on re-expansion and, at best a mild impact on memory cell phenotype.

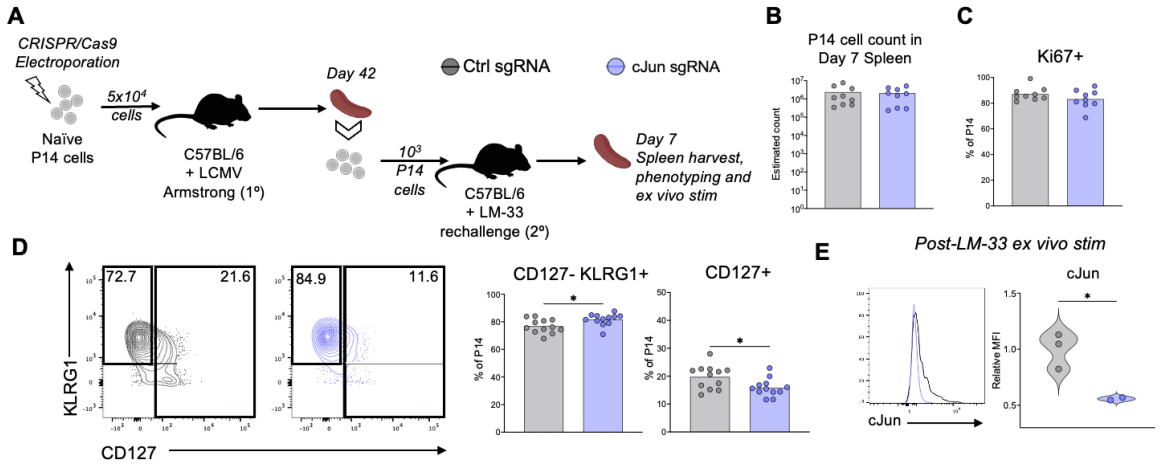


Figure 5.11 Effects of cJun deletion on memory recall
(A) Experimental schematic. Ctrl sgRNA (grey) and cJun sgRNA (light purple) were generated as per Fig. 5.7A, and at day 42 p.i. 10,000 P14 cells were transferred into B6 mice, which were then infected i.v. with *Listeria monocytogenes*–gp33 (LM-33). At day 7 p.i., spleens were harvested for immunophenotyping.
(B-D) Pooled P14 numbers **(B)** and frequencies of Ki67+ **(C),** CD127-KLRG1 and CD127+ (**D,** right) P14 cells in cJun sgRNA versus Ctrl sgRNA cells at day 7 p.i. Representative CD127 and KLRG1 expression is shown (**D**, left). Data are from three independent experiments (n=9 mice per group)
(E) Representative (left) and pooled (right) cJun re-expression upon peptide re-stimulation of cJun sgRNA versus Ctrl sgRNA P14 cells at day 7 p.i. n=2–3 mice per condition from a single experiment. MFI values are relative to the average MFI of the Ctrl sgRNA group. p-values for all comparisons were calculated using an unpaired t-test,* = $p < 0.05$;

We speculated that the observed mild memory cell phenotypes seen in the absence of cJun might impact memory cell fitness in the context of long-term serial rechallenge. To assess this, we transferred a 1:1 mixture of cJun sgRNA and Ctrl sgRNA P14 $CD8^+$ T cells that were differentially congenically marked (CD45.2/CD45.2 and CD45.1/CD45.2 respectively) into uninfected CD45.1/CD45.1 recipients (Fig. 5.9A). Mice were first infected with acute LCMV Armstrong, and then rechallenged with LM-33 once memory was established

at day 61 p.i. The resulting secondary memory cells were then challenged again with LCMV-Cl.13 81 days later (i.e. day 142 after the initial LCMV Armstrong infection) (Fig. 5.9A).

In contrast to all of our prior experiments, we observed decreased cJun sgRNA cell expansion in the blood at day 8 post-primary infection relative to control cells (Fig. 5.9B), however this was likely due to the proliferative/expansion advantage conferred by CD45.1 expression in the control cells[556] (I.A. Parish, unpublished observations). This was a confounding effect in these experiments, meaning that the experiment will need to be repeated with CD45.1/CD45.1 and CD45.1/CD45.2 P14 cells transferred into CD45.2/CD45.2 recipients to rule out any impact of CD45.1 on the observed phenotypes. Nevertheless, by normalising Ctrl to KO ratios at later timepoints to this initial day 8 ratio, we were able to gain preliminary insights into the role of cJun in memory cell fitness. These data suggested that there was a slight deficiency in cJun sgRNA frequency that increased over time across the course of the experiment, particularly after the final LCMV-Cl13 challenge (Fig. 5.9B,C). We again observed a slight skewing in splenic memory subsets at the completion of the experiment, although in this case there was a skewing towards memory-associated populations (CD127+ cells) at the expense of more differentiated effector populations (CD127-KLRG1+) (Fig. 5.9D). Finally, we confirmed that the cJun sgRNA cells recovered after tertiary challenge remained cJun deficient (Fig. 5.9E). This data may suggest a mild role for cJun in long-term memory cell fitness after serial re-challenge, although these experiments need to be repeated to rule out the confounding effects of CD45.1 in the observed phenotypes.

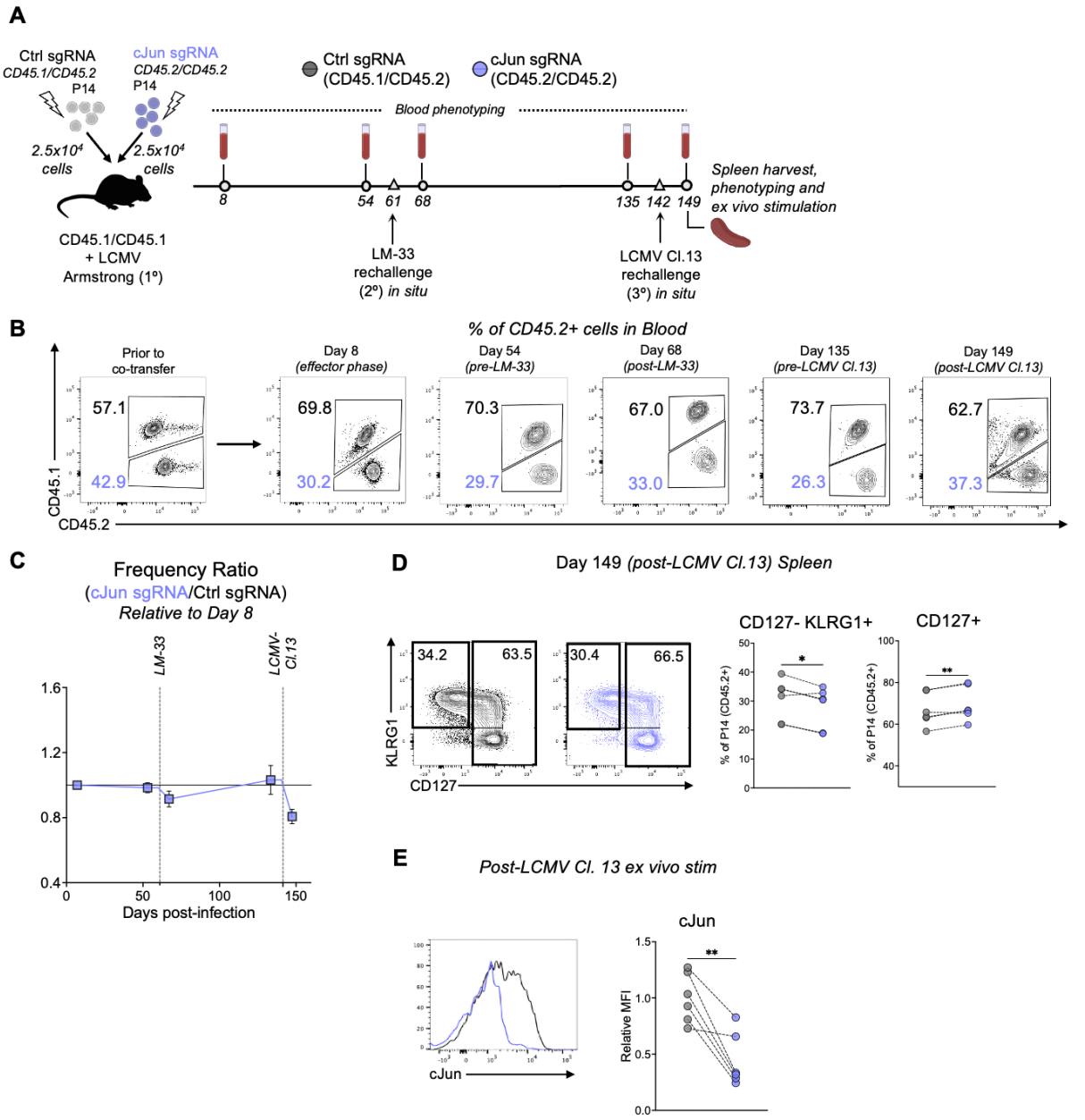


Figure 5.12 cJun deficient memory cell fitness after repeated immune challenge
(A) Experimental schematic. Ctrl sgRNA (grey) and cJun sgRNA (light purple) were generated from congenically distinct donor P14 mice (CD45.1/CD45.2 and CD45.2/CD45.2 respectively) and then co-transferred at equal amounts (i.e., 2.5 x 10^4 per condition) into uninfected CD45.1/CD45.1 mice, followed by primary infection with LCMV Armstrong (1°). Mice were rechallenged in situ with *Listeria monocytogenes–gp33* at day 61 post-LCMV Armstrong infection (2°), and with LCMV Cl.13 81 days later (day 142 post-LCMV Armstrong infection) (3°). Blood was collected at day 8 p.i. and 7 days before and after each rechallenge. At day 149 of the experiment (7 days after LCMV Cl.13), spleens were harvested for analysis.
(B) Representative Ctrl sgRNA and cJun sgRNA frequencies prior to cotransfer, and 8, 68, 135, and 149 post-LCMV Armstrong infection (left to right).
(C) Ctrl sgRNA:cJun sgRNA ratios (divided by the ratio at day 8) over time. Individual points and error bars represent the mean and standard error of the mean (SEM), respectively.
(D) Representative (left) and pooled (right) CD127-KLRG1+ and CD127+ subset frequencies at day 149 (i.e., 7 days post LCMV Cl.13 infection).

(E) Representative (left) and pooled (right) cJun re-expression upon peptide restimulation of splenic cJun sgRNA and Ctrl sgRNA P14 cells at day 149. MFI values are relative to the Ctrl sgRNA group.
Data are from two independent experiments (n=6 mice/group). Connecting lines (D,E) indicate paired values from the same mouse. p-values for all comparisons were calculated using a paired t-test,* = $p < 0.05$, ** = $p < 0.01$.

5.3. DISCUSSION

In this chapter, we examined the impact of full AP-1 ablation, and deletion of individual Jun proteins, on effector, exhausted and memory T cell differentiation. By simultaneously deleting *Junb, Jun,* and *Jund*, we generated functionally AP-1 deficient cells characterised by restricted AP1:NFAT-dependent transcriptional activity. Because our reporter assay likely underestimated loss of AP-1 activity due to the pre-activation required for transduction, we will be generating retrogenic mice using the NFAT/AP-1-driven GFP reporter to enable assessment of AP-1 function in CRISPR edited naïve CD8+ T cells. Notably, while AP-1 deficient cells had a pronounced survival defect and evidence of cytokine production deficiencies, many aspects of effector differentiation remained intact, and there was little to no evidence of aberrant differentiation of effector cells into a tolerance state. Instead, AP-1 deficient cells exhibited mild features more consistent with exhaustion rather than tolerance. The bulk of these phenotypes were driven by JunB deficiency, with functional studies indicating that BATF/JunB heterodimers may be responsible for most of these phenotypes. Surprisingly, AP-1 and JunB deficiency had little impact of effector cell gene induction during initial activation, suggesting that the observed phenotypes maybe due to transcriptional effects later in the immune response, or downstream of other deficiencies (e.g. protein translation deficiencies). In contrast, cJun and JunD deficiency, either alone or in combination, had no discernible impact on effector differentiation or exhaustion. Instead, JunD was required for memory cell persistence, while cJun appeared largely dispensable for memory differentiation outside of mild phenotypic alterations and a potential slight deficiency in long-term fitness after serial rechallenge. Collectively, these data challenge many of the assumptions around AP-1 function in CD8+ T cell biology.

We highlight a previously unappreciated role of AP-1 in regulating the survival of differentiating CD8+ T cells across both effector and exhausted cell fates. The mechanistic basis of this effect on survival remains unclear. Interestingly, early gene expression during the first 24h of T cell activation, including survival genes, was largely unaltered outside of a potential deficiency in protein translation that needs to be functionally validated. This could imply that the survival defect is due to protein translation defects, however prior work in the context of BATF and JunB deficiency, which we found were the primary drivers of the AP-1 phenotype, failed to demonstrate survival deficiencies and transcriptional changes until later

timepoints[437,438].Further molecular profiling is needed at these later timepoints to better define the cause of this survival defect.

Unexpectedly, AP-1 deficient cells exhibited relatively normal early induction of the effector gene program, at least within the first 24hrs of activation *in vitro*. This directly challenges assumptions around AP-1 function based predominantly on over-expression studies in cell lines, as AP-1 is currently assumed to be essential for early T cell gene induction within the initial hours of activation. Our data suggest that other factors can compensate for AP-1 loss in induction of these genes. Interestingly, despite no changes in initial cytokine gene expression, we still observed reduced cytokine production in AP-1 deficient cells at later time points of infection. Again, further mechanistic work is required to define the molecular basis of this disparity, but it could either be because AP-1 is required for sustained cytokine transcription, or potentially because of impaired translational capacity (i.e. a transcription-independent effect). AP-1 may also trigger early epigenetic changes that don't functionally impact transcription until a later point in infection[95, 184, 529]. RNA-seq profiling of AP-1 deficient effector T cells at later points of infection, alongside ATAC-seq experiments to probe the early epigenetic impact of AP-1 loss, is required to resolve some of these questions. Nevertheless, assessing these questions beyond the first few days of activation will be challenging given the profound survival defect of AP-1 deficient cells from day 3 onwards. Rescuing the AP-1 deficient cells from apoptosis through a compound gene KO approach could help to resolve this problem. Alternatively, working with pure AP-1 deficient cells through gene disruption by CRISPR knock-in of a reporter gene[553] to enable KO cell purification prior to adoptive transfer would at least mean that the recovered cells are not contaminated with/enriched for unedited cells. Our lab is currently optimising CRISPR knock-in within P14 cells, although we have yet to achieve high efficiency knock-in to naïve cells, which would be required to use this approach in the study of AP-1.

As might be expected, the strong selective pressure against AP-1 deficiency meant that the "AP-1 KO" cells recovered at day 8 p.i. were enriched for cells with normal Jun expression that failed to CRISPR edit the Jun loci. Nevertheless, these residual cells displayed mild features of exhaustion, such as enhanced expression of inhibitory receptors and exhaustion-associated transcription factors. While our sequencing data revealed enrichment of cells with unmodified Jun loci, a fraction of these cells may still possess phenotype-altering hypomorphic alleles downstream of monoallelic edits or in-frame indels[557-559], the detection of which may have been obscured due to PCR amplification bias that favours wild-type alleles[560]. Alternative strategies to accurately detect CRISPR variants such as polymerase-free targeted long-read nanopore sequencing will be explored in further confirmatory experiments[561]. Regardless, the loss of bona fide AP-1 deficient cells suggests that the observed induction of exhaustion-associated features is likely a significant under-estimate of the full AP-1 KO

phenotype. Pure AP-1 KO cells (via CRISPR knock-in reporters, see above) could help resolve this problem. These data do provide mild support to the hypothesis that AP-1 is required to suppress features of exhaustion. In contrast, AP-1 deficient cells did not display features of tolerance. Unlike exhausted cells, which first diverge from functional effector cells at day 5 p.i., tolerant cells transcriptionally diverge from effector cells within the first 24hr of antigen encounter[91]. We failed to observe aberrant induction of the tolerance gene program in AP-1 deficient cells activated for 24hrs *in vitro*. Furthermore, while tolerant cells prematurely exit cell cycle, undergo BIM-dependent death and do not express GzmB[91,229,562-564], AP-1 deficient cells proliferated and expressed GzmB normally, and underwent BIM-independent apoptosis. Thus, our data support a role for AP-1 as a suppressor of exhaustion but not tolerance.

We then uncovered context-specific roles for JunB, cJun and JunD in CD8+ T cell differentiation. JunB was the dominant AP-1 member responsible for the AP-1 KO survival deficiency and mild exhaustion phenotype. This finding is consistent with emerging evidence that JunB is essential for epigenetic and transcriptional programming of effector CD8+ T cell differentiation [438]. The bulk of the JunB-dependent phenotypes overlap with the BATF KO phenotype, with compound deficiency of both factors failing to meaningfully exacerbate most phenotypes. This aligns with a model whereby BATF and JUNB heterodimers, potentially in combination with IRF4[340,472,565] are the key AP-1 complex required for CD8+ T cell differentiation. Nevertheless, some JunB effects appeared BATF-independent, in line with recent studies showing that JunB can control effector cell differentiation through both BATF-dependent and -independent mechanisms[176,438]. Given that the AP-1 phenotype is largely BATF/JunB dependent, it is interesting to note that BATF and JunB deficient cells do not display obvious survival defects or differential gene expression until 3-4 days post-activation[437,438]. This aligns with our findings that AP-1 deficiency does not overtly impact initial T cell activation.

Our most unexpected finding was that cJun and JunD were fully dispensable for T cell activation and effector differentiation, particularly given the common focus in the T cell field on cFos/cJun as the “canonical” T cell AP-1 factor. Instead, both Jun members contributed to aspects of T cell memory. JunD deficient cells had a pronounced defect in memory T cell persistence. This persistence phenotype appears to be exclusive to the antigen-independent persistence of stem-like T cell populations, as stem-like exhausted T cells were not impacted by JunD loss. Interestingly, our sequencing results did not reveal selective loss of KO cells, although more analysis is needed to see if less damaging mutations (e.g. in-frame indels) are enriched at memory timepoints. Still, our data expands upon prior limited evidence implicating JunD as a factor downstream of IL-7 signalling in T cells *in vitro*, and more recently, as a competitive transcription factor of BATF to shape early memory-like populations during CD8+ T cell differentiation[176,469,566]. Our prior data indicated that JunD is only transiently expressed

during the first few days of effector differentiation prior to returning to baseline levels of expression (see Chapter 4). Thus, it is currently unclear whether JunD programs long-term memory T survival during the early stages of T cell activation or promotes survival through continuous low-level expression during memory below the flow cytometry level of detection. Distinguishing between these possibilities requires temporal genetic ablation systems that enable JunD ablation after effector differentiation/during memory (e.g. inducible knockout transgenic mouse models or ex-vivo CRISPR-editing of effector or memory cells) [567,568]. Resolving when JunD is acting to promote long-term memory cell survival is required before any downstream mechanism/relevant gene targets responsible for the Jund deficient phenotype can be identified.

In contrast, cJun deficient cells had at best a very mild memory phenotype characterised by mild alterations in subset proportions/marker expression and long-term persistence upon serial rechallenge. Furthermore, this latter phenotype is questionable due to confounding effects associated with the CD45.1 congenic marker. These largely negative results are interesting given that overexpression of cJun confers improved functionality/persistence in the context of adoptive cell therapy [416,478], highlighting that gene over-expression does not always give reliable insights into normal gene function. As Jun family members have also been implicated in T_{RM}[467,569], the effect of cJun deficiency on T_{RM} differentiation, persistence and tissue maintenance should be assessed in future. It remains possible that cJun plays roles in T cell differentiation in other contexts that we have not assessed, but at best cJun plays a limited and highly specialised role in T cell differentiation.

Collectively, our data challenge many assumptions and dogmas surrounding AP-1 function in CD8+ T cells. While AP-1 may play some in insulating effector cells against exhaustion, it does not appear to insulate cells against tolerance. Given that the classical NFAT homodimer gene program is induced during tolerance, this may indicate that factors beyond canonical AP-1 factors can prevent NFAT homodimer formation. Further studies during early T cell activation (e.g. NFAT Co-IP MS) are required to resolve these questions. Additionally, we find that different AP-1 complexes have different roles in effector and memory T cell differentiation. While further research is required to resolve the molecular basis of these observations, these data demonstrate that AP-1 biology is significantly more complicated and nuanced than currently appreciated.

CHAPTER 6 Final Discussion

6.1. OVERVIEW

CD8+ T cells engage immunoregulatory processes to control their responses and maintain immune balance across different biological contexts. Peripheral tolerance inactivates self-reactive cells to prevent autoimmunity, while exhaustion limits immunopathology during persistent stimulation. Because next-generation immunotherapies aim to enhance CD8+ T cell functionality, gaining a better understanding of where both differentiation states molecularly overlap and diverge is essential.

Although tolerant and exhausted cells arise from different immune contexts, they share phenotypic features, such as inhibitory receptor expression and restrained effector function. Both states are also influenced by NFAT homodimer activity in the absence of AP-1. This has often led to the assumption that tolerance and exhaustion are similar processes, despite accumulating evidence of molecular differences between these states. A comprehensive functional comparison of the pathways required to enforce both states is lacking.

To this end, we functionally re-evaluated whether NFAT-dependent pathways are similarly regulated in both contexts by interrogating two critical aspects of the NFAT homodimer model. First, in Chapter 3, we tested whether TOX, a critical effector of the NFAT homodimer regulatory gene program in exhaustion, plays an equally significant role in peripheral tolerance. Second, in Chapters 4 and 5, we investigated whether AP-1-dependent NFAT regulation was equally important in preventing both tolerance and exhaustion, in addition to more broadly examining AP-1 function. By interrogating the responses of cell-specific gene knockouts in various *in vivo* models, we demonstrated that TOX was dispensable for tolerance, and that AP-1 loss alone was insufficient to cause effector T cells to become tolerant, with cells instead acquiring mild features of exhaustion (Fig. 6.1). Thus, despite some similarities, our data suggest that tolerance and exhaustion are molecularly separable processes (Table 19).

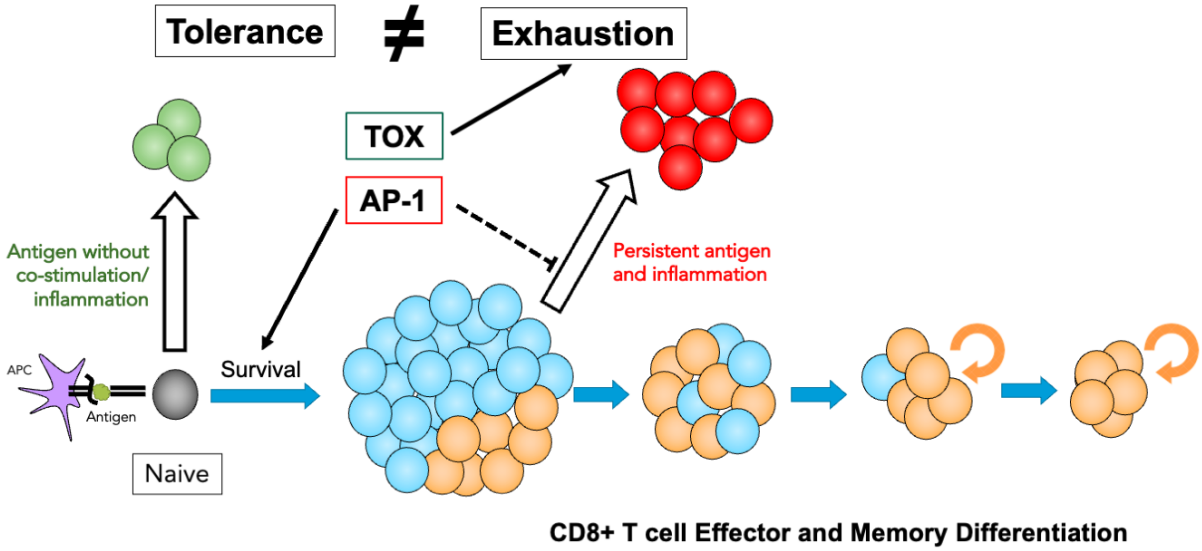


Figure 6.1. Interrogating the function of TOX and AP-1 in tolerance and exhaustion
This thesis has demonstrated that TOX and AP-1 operate differently in the context of exhaustion and tolerance. While TOX is upregulated in both states, TOX only regulates exhaustion and is dispensable for tolerance. AP-1 ablation disrupted conventional effector and memory differentiation through non-canonical mechanisms, with cells failing to adopt a tolerant state and instead acquiring mild features of exhaustion.

Table 19. Comparison of phenotypic and molecular features between T cell tolerance and exhaustion

Tolerance		Exhaustion
Phenotypic Features		
+	Induced by TCR stimulation	+++
+	PD-1 expression	++
+++	Impaired effector function	+
+	Persistence in chronic antigen	+
-	Proliferation	+
?	Immune checkpoint blockade response	+
Molecular Regulation		
+	NFAT homodimer gene regulation	+
+	TOX expression *	+++
-	Molecularly controlled by TOX? *	+++
-	Suppressed by AP-1 (JunB) during effector differentiation? *	+

"+": positive association, repeats indicate stronger association "-": no association, "?": association unclear
** derived from thesis findings*

6.2. Evidence of differences in how NFAT regulates tolerance and exhaustion

Prior evidence demonstrating that NFAT regulates both tolerance and exhaustion has sometimes led to the assumption that these two processes are molecularly similar[141,339,427].

However, prior work from our lab showed that an NFAT-induced transcription factor, EGR2, which is required for both tolerance and exhaustion, regulates completely different genes in each context[341]. In this thesis, we extend this notion by demonstrating that the NFAT-induced exhaustion master regulator, TOX, is functionally irrelevant in tolerance. Furthermore, while AP-1 ablation induces mild features of exhaustion that need to be interrogated further (see next section), it fails to trigger early divergence towards a tolerant state. Therefore, the mechanics of the NFAT regulatory gene program are differentially wired in tolerance versus exhaustion.

Further work is needed to define if other shared regulatory operate differently in both states. For example, other NFAT homodimer-induced transcription factors, such as the NR4A family of transcription factors, are also induced in tolerance and exhaustion and have been implicated in both processes[350,384]. IKZF2 is another transcription factor induced in both tolerance and exhaustion[229,570,571], although its functional role in these processes is currently unclear. It remains to be seen whether these factors operate similarly or differently in both contexts or whether NFAT itself functions in the same way across both tolerance and exhaustion. The NFAT homodimer transcriptional program only overlaps with less than half of either the exhaustion or tolerance gene signatures[141]. While this may be explained by NFAT-independent factors, this could also be related to differences in the binding partners of NFAT in tolerance versus exhaustion. Beyond AP-1, NFAT has been shown to bind to and partner with many other transcription factors (e.g. IRF4, FOXP3, GATA3, and SP1 [340,427]), which may explain how it differentially regulates distinct differentiation trajectories[464]. Further work is needed in the context of exhaustion and tolerance to resolve these questions.

Our results further highlight the risks in using individual markers as proxies to define CD8+ T cell fates. Just as PD-1 or CD69 alone do not define either exhaustion or tissue residency, respectively[572-574], factors such as EGR2 and TOX (or even cytokine production deficiencies) are insufficient to define a cell as tolerant or exhausted. Our data instead argue that more comprehensive functional profiling, marker analysis, and transcriptional and epigenetic profiling are needed.

In addition to our previous EGR2 paper[341], this to our knowledge is one of the few studies to functionally interrogate the molecular differences between tolerance and exhaustion. These data build upon our previous phenotypic analyses demonstrating distinct epigenetic and transcriptional profiles in tolerance versus exhaustion [91].

6.3. Full AP-1 ablation challenges assumptions about AP-1 function

Arguably the most surprising aspect of our AP-1 ablation experiments is how many aspects of T cell activation and differentiation were unaffected by AP-1 loss. AP-1 is classically regarded as a factor required for the induction of most key genes linked to the T cell

activation[427]. In contrast, we find that AP-1 deficient cells have relatively normal early gene induction outside of hints of protein translation deficiencies that need to be verified. AP-1 KO cells appear capable of proliferation and some degree of expansion and differentiation (including GzmB expression), with the main phenotype observed being diminished survival by a yet undetermined pathway. While AP-1 KO cells did have deficiencies in cytokine production, which aligns with current assumptions about AP-1 activity, this was not due to defects in initial induction of cytokine gene expression. It remains unclear if this cytokine defect is due to an inability to sustain cytokine transcription, or whether this phenotype is downstream of dysregulated cellular pathways (e.g. defective protein translation). In the former case, an inability to sustain cytokine transcription could be due to indirect effects of AP-1 on transcription via epigenetic changes. These changes could still occur early during differentiation, meaning further work is needed to investigate the epigenetic effects of AP-1. These data align with previous work suggesting that JunB and BATF, the key AP-1 complex mediating these phenotypes (see next section), are largely dispensable for the first few days of early T cell activation[176,437,438]. Thus, AP-1 may predominantly be important in stabilising differentiation states and cell survival at later stages of the immune response and be largely dispensable for early T cell activation, which goes against current assumptions of AP-1 function.

The other unexpected finding was that cells failed to aberrantly become tolerant in the absence of AP-1. Tolerant cells diverge very early from effector cells (within 12h *in vivo*), fail to acquire effector functions and rapidly drop out of cycle, likely downstream of diminished TCR signalling capacity [91]. In contrast, AP-1 deficient cells did not acquire the tolerance gene program, continued to proliferate, and acquired many features of effector cells, including GzmB protein expression. This contradicts the current dogma that NFAT induction in the absence of AP-1 during early T cell activation will induce a classical anergy gene program[252,379]. In contrast, there were hints that AP-1 might insulate against exhaustion, although further work is needed to prove this. By day 8 of infection, AP-1 deficient cells had acquired some mild features of exhaustion, however the cells recovered at this timepoint were largely those cells that failed to fully delete AP-1. This phenotype may thus be an underestimate of the degree to which AP-1 suppresses the exhaustion gene program. Addressing this problem is challenging as AP-1 KO cells begin to die at the point during the immune response when exhausted cells first emerge (~day 5 p.i.). As already discussed in Chapter 5, additional approaches are needed to counter this problem and address whether bona fide AP-1 KO do enter an exhausted state.

The fact that these findings so emphatically contradict current assumptions raises questions around why our understanding of AP-1 biology was so inaccurate. Current paradigms may be correct, but at least *in vivo* there could be more redundancy with non-

canonical AP-1 subfamilies (e.g. MAF factors[575,576]) that can compensate for loss of Jun family members. Alternatively, it's possible that current models are not applicable *in vivo*, and that we need to revisit our understanding of NFAT and AP-1 biology.

6.4. Distinct roles for different AP-1 complexes in T cell differentiation

AP-1 is not a single transcriptional regulator. It represents a wide array of diverse dimeric complexes with distinct functions. Our findings demonstrate non-redundant roles for different Jun proteins in CD8+ T cell differentiation. In contrast to the assumption that cJun is the main AP-1 member that controls T cell activation and effector differentiation [443-445,529,544,577], we find, instead, that JunB plays the prominent role in this process. Surprisingly, we were unable to identify a definitive function for cJun, other than a potential minor role in supporting memory. These findings, along with JunD's role in memory homeostasis, emphasize the distinct functions of Jun family members in directing CD8+ T cell differentiation.

The heterogeneity of AP-1 likely evolved to enable repurposing of shared regulatory elements and molecular partners to generate context-specific transcriptional outcomes [412,434,578]. While JunB, cJun, and JunD bind to the same AP-1 motifs with overlapping protein interaction partners, they execute divergent functions. Competition for binding at shared gene loci, and for interactions with various protein partners, might enable fine-tuning of genes and pathways during T cell differentiation. Nevertheless, given the modest number of transcriptional changes observed in cells deficient for AP-1 and the individual Jun proteins thus far, more comprehensive transcriptomic profiling at later timepoints, alongside epigenetic profiling, is needed to determine to what degree competition at shared binding sites contribute to the Jun-specific phenotypes that we have observed.

Considering how JunB and JunD interact with proteins related to chromatin remodelling and histone modifications, respectively, Jun proteins likely shape epigenetic priming and maintenance in line with the known chromatin remodelling function of AP-1 factors[165,170,172,548]. JunB may serve as a pioneer factor that primes chromatin for early effector responses, however, as alluded to in the last section, the transcriptional impact of these epigenetic changes may not be evident until later stages of the response. In contrast, JunD might function to strengthen or modulate memory responses. This idea is supported by recent evidence showing that JunD might compete with BATF for JunB binding during differentiation, which was proposed to limit terminal effector differentiation[176]. However, we did not observe alterations in short-lived effector cell or memory precursor cell proportions in the absence of JunD, arguing against this mechanism and indicating that further work is needed. To conclusively determine when these Jun proteins are acting, targeted experiments such as temporal gene knock-outs (e.g., AP-1 deletion in effector cells) and multiomic profiling at different timepoints during differentiation are required.

Functional compensation among the AP-1 proteins remains possible. This might explain the modest phenotype seen following deletion of cJun, as other AP-1 factors could be compensating for its role, although compound loss of JunD and cJun at least did not markedly change the KO phenotype. Moreover, the memory defect after JunD loss might reflect a shift toward an effector-like state, possibly driven by increased activity of JunB. Given that JunB KO cells fail to survive initial expansion, though, we cannot rule out a role for JunB in memory, potentially in combination with cJun. These possible interactions among Jun family members introduce another layer of complexity in understanding how AP-1 regulates T cell fate decisions.

Finally, investigating the roles of AP-1 members beyond the Jun family is important. Growing evidence points to other AP-1 members playing distinct roles in T cell biology: BATF3 in memory programming[439], MAF in exhaustion[575], and FOS family members in T_{RM} differentiation[164,579]. A comprehensive systems-level analysis combined with *in vivo* functional studies are essential to fully decipher the complex molecular roles of the AP-1 family.

CHAPTER 7 Appendix

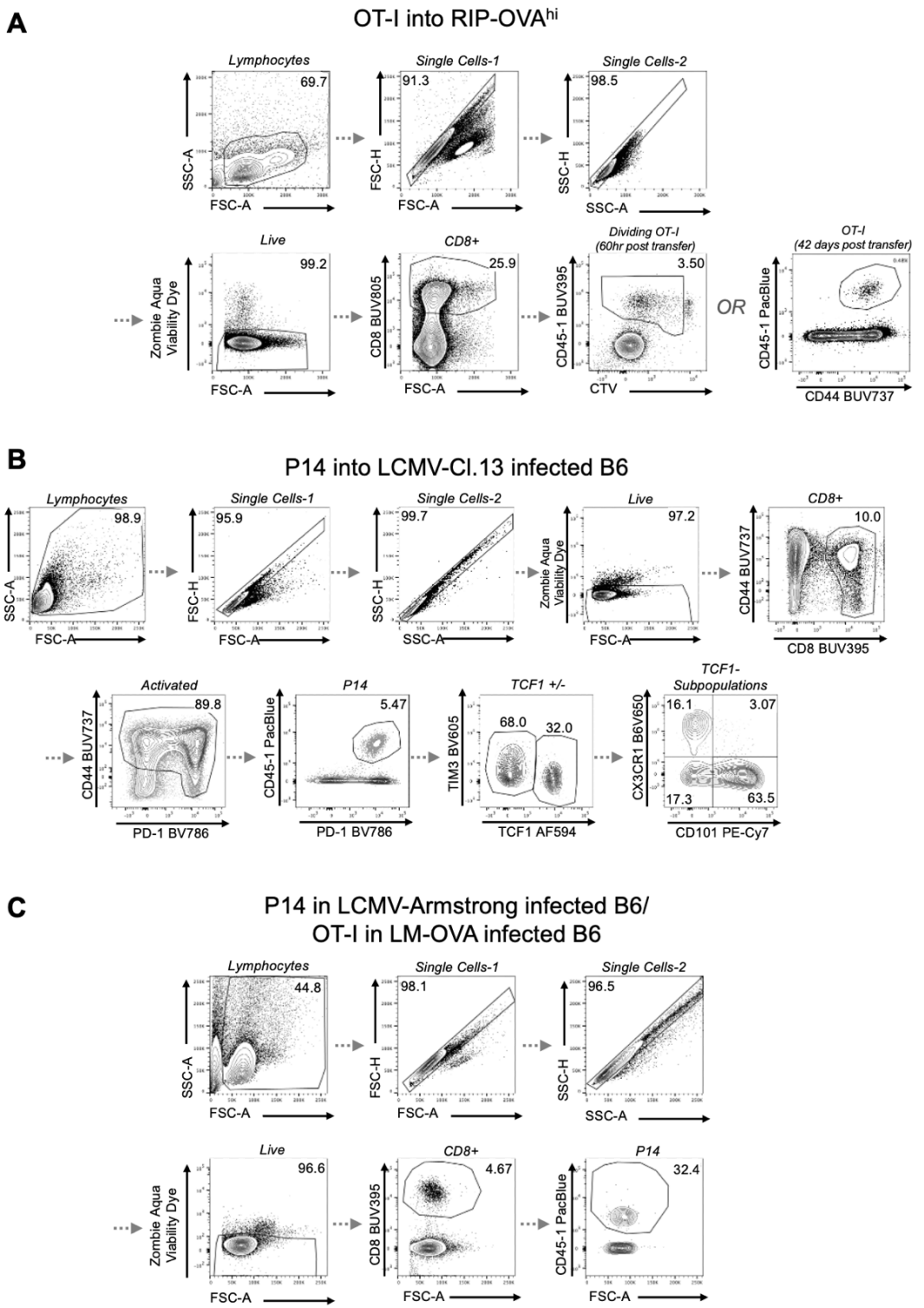


Figure S1. Gating strategies to identify TCR transgenic CD45.1+ CD8+ T cells within different *in vivo* models
Representative flow cytometry plots illustrating sequential gating to identify transgenic TCR CD45.1+ CD8+ T cells (P14 or OT-I).

(A) OT-I cells adoptively transferred into RIP-OVA mice for peripheral tolerance **(B)** P14 cells into B6 mice infected with LCMV-Cl13 for exhaustion (at day 20 post-infection) **(C)** P14 cells or OT-I cells into B6 mice infected with either LCMV-Armstrong or LM-OVA, respectively, for effector and memory differentiation. The example above shows day 42 post-LCMV Armstrong infection.

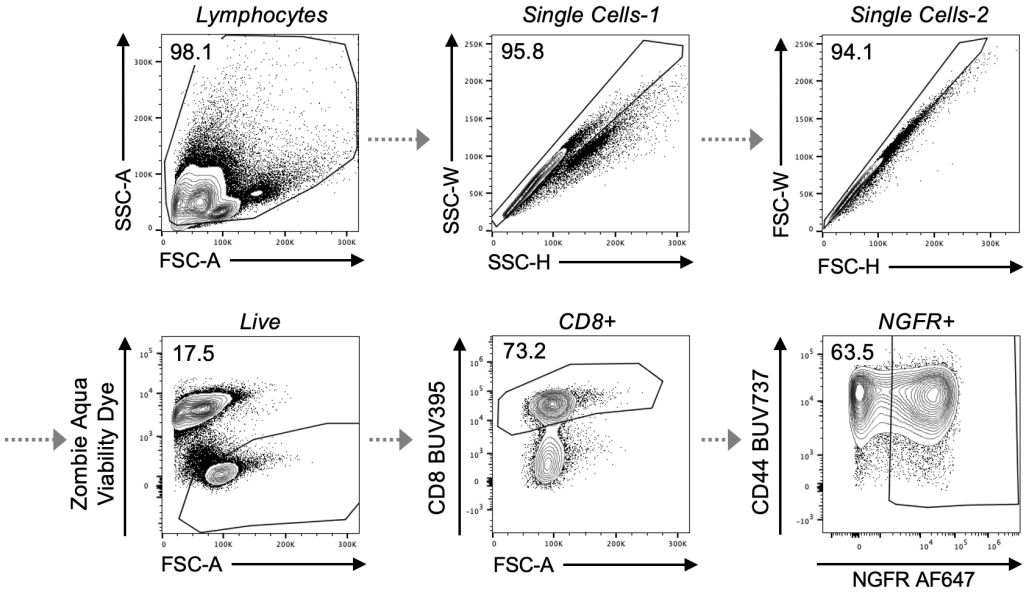


Figure S2. Gating strategy to identify CD8+ T cells transduced with NFAT/AP1-driven GFP reporter
Representative flow cytometry plots to show sequential gating to identify activated transduced (NGFR+) CD8+ T cells with NFAT/AP1-driven GFP reporter

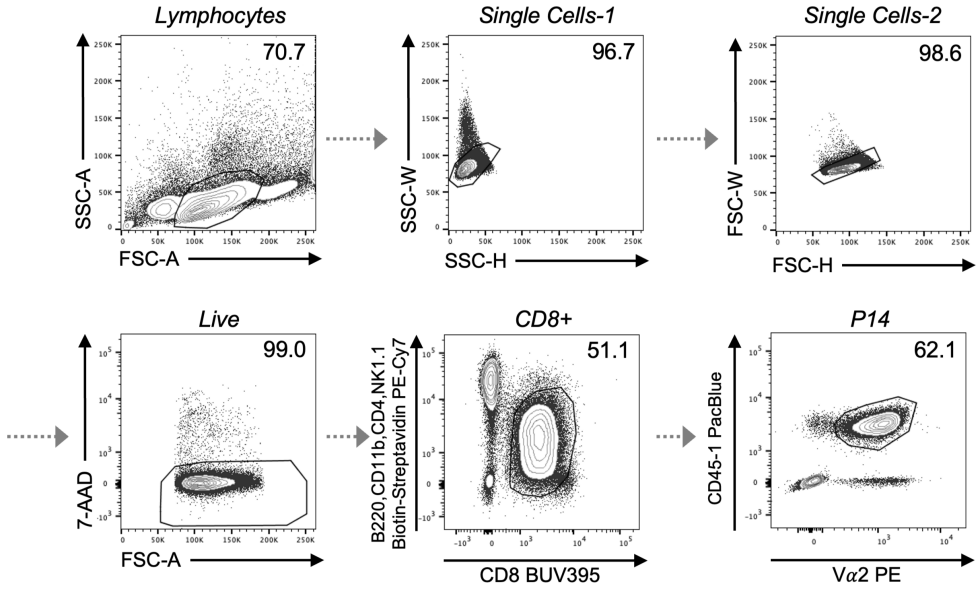


Figure S3. Gating strategy for sort
Representative flow cytometry plots to show sequential gating for sorting of P14 cells from spleens of LCMV-infected mice.

Table S1. Significant protein interaction partners of JunB (LogFC>0, p. value<0.05, n=136) in CD8+ T cells activated *in vitro* for 24hrs

Protein Name	LogFC	F.statistic	p.value	adj p.value
SMARCA4	8.98855	117.256	1.75E-25	8.17E-24
SMARCC2	8.971556	117.2952	1.72E-25	8.17E-24
ARID1A	8.691844	114.8314	5.03E-25	1.88E-23
CPSF6	4.35161	88.60472	7.20E-20	1.92E-18
SMARCD2	7.974137	106.2982	4.81E-16	8.60E-15
CPSF1	4.500508	87.47494	9.38E-16	1.52E-14
JUNB	7.755551	102.8636	5.42E-14	7.80E-13
NUDT21	3.172185	66.26401	6.07E-14	8.41E-13
SMARCC1	7.632368	98.49096	5.78E-13	6.97E-12
TAF1	7.566635	94.87578	1.89E-12	2.14E-11
ACTL6A	7.400494	85.30239	3.01E-11	2.96E-10
TAF6	7.296145	80.25814	1.47E-10	1.41E-09
CPSF7	7.268857	79.08983	2.18E-10	2.04E-09
TAF5	7.241031	77.90094	3.24E-10	2.96E-09
TFIP11	7.183693	75.29346	7.17E-10	6.39E-09
WDR33	7.154157	73.88145	1.07E-09	9.28E-09
CPSF3	7.093196	70.94726	2.36E-09	1.84E-08
CPSF2	3.080001	60.55263	3.51E-09	2.68E-08
IRF4	6.996608	66.6603	7.81E-09	5.84E-08
SMARCE1	6.928478	64.00388	1.73E-08	1.25E-07
FOSL2	6.819781	60.74561	5.74E-08	3.58E-07
RBBP6	6.81977	60.74532	5.74E-08	3.58E-07
SMARCA2	6.81976	60.74503	5.74E-08	3.58E-07
WWP2	6.819781	60.74561	5.74E-08	3.58E-07
ARID1B	6.742498	58.66095	1.28E-07	7.71E-07
PSPC1	6.742498	58.66095	1.28E-07	7.71E-07
AQR	6.660806	56.37848	2.85E-07	1.62E-06
MAP4K2	6.618174	55.0517	4.26E-07	2.31E-06
POLR2A	6.618163	55.05141	4.26E-07	2.31E-06
SMARCB1	6.618152	55.05113	4.26E-07	2.31E-06
TAF2	6.574233	53.75799	6.36E-07	3.31E-06
NCBP1	6.433794	48.37872	2.13E-06	1.08E-05
DPF2	6.383758	45.97195	3.19E-06	1.53E-05
POLR2B	6.383737	45.97132	3.19E-06	1.53E-05
SART1	3.928435	44.75031	3.19E-06	1.53E-05
ZNF638	6.331892	44.09523	4.78E-06	2.23E-05
THOC2	2.236378	38.87236	5.97E-06	2.76E-05

Protein Name	LogFC	F.statistic	p.value	adj p.value
SRRM2	1.328336	20.76462	6.06E-06	2.77E-05
CSTF3	6.164219	37.06691	1.61E-05	7.02E-05
EML3	6.164219	37.06691	1.61E-05	7.02E-05
FIP1L1	2.730997	36.96924	1.61E-05	7.02E-05
SRRT	6.164241	37.06753	1.61E-05	7.02E-05
SNW1	3.675733	37.70629	3.04E-05	0.000126
HNRNPUL2	6.040526	32.65241	3.64E-05	0.000148
RBM10	6.040515	32.65213	3.64E-05	0.000148
CDC5L	2.366643	32.21436	5.55E-05	0.000223
BCAS2	5.905223	28.48561	8.25E-05	0.000325
TAF8	5.905223	28.48561	8.25E-05	0.000325
SON	1.979667	28.55309	0.00012	0.000464
CHD4	5.832461	26.64463	0.000124	0.00047
SSB	5.832461	26.64463	0.000124	0.00047
U2SURP	2.824479	30.22671	0.000171	0.000639
PRPF31	5.755891	24.92418	0.000188	0.000696
PRPF4B	3.424992	29.22112	0.000196	0.00072
PRPF6	1.922318	26.56586	0.000215	0.000782
FAM208A	5.674993	23.31925	0.000284	0.001011
KIAA1429	5.675025	23.31976	0.000284	0.001011
BCLAF1	1.892768	25.58065	0.000287	0.001014
PURB	5.589266	21.65341	0.00043	0.001487
RUNX3	5.589299	21.65392	0.00043	0.001487
PTBP1	2.362268	25.68869	0.000444	0.001523
THOC5	2.31968	24.67096	0.000613	0.002067
CSTF2	5.498158	19.9086	0.000651	0.002155
SCAF4	5.498212	19.90941	0.000651	0.002155
CWC22	2.275693	23.6156	0.000846	0.002777
SF3B2	1.346443	19.27314	0.000917	0.002956
CBFB	5.400916	18.14016	0.000988	0.003106
RBM22	5.400916	18.14016	0.000988	0.003106
ZBTB7A	5.400895	18.13986	0.000988	0.003106
CPSF4	3.12127	19.93526	0.001254	0.003908
EFTUD2	0.958916	11.56806	0.001421	0.004393
PRPF8	0.893724	10.23481	0.001436	0.004403
PDCD11	5.296609	16.37799	0.001503	0.004463
PLRG1	5.296641	16.3784	0.001503	0.004463
RRBP1	5.296598	16.37786	0.001503	0.004463
USP39	5.296609	16.37799	0.001503	0.004463
SF3B3	0.916699	10.78374	0.001646	0.004846
SF3B1	0.865524	9.950912	0.001672	0.004885

Protein Name	LogFC	F.statistic	p.value	adj p.value
SF1	3.05203	18.23282	0.001813	0.005257
FOS	5.184214	14.7567	0.002292	0.00635
GNL3	5.184214	14.7567	0.002292	0.00635
NXF1	5.184214	14.7567	0.002292	0.00635
SAFB	5.184224	14.75682	0.002292	0.00635
SNRPE	5.184224	14.75682	0.002292	0.00635
THOC1	1.923058	19.3837	0.002279	0.00635
NCOA5	2.979304	16.64096	0.00262	0.007206
MATR3	1.8791	18.43059	0.003067	0.008372
PNN	1.518271	17.26764	0.003139	0.008507
RFWD2	5.062291	13.22129	0.003504	0.009361
SF3A2	5.062291	13.22129	0.003504	0.009361
CLK3	2.353947	17.15139	0.003695	0.009802
PRPF3	2.902701	15.17318	0.003783	0.009895
RBBP4	2.90269	15.17302	0.003783	0.009895
PABPC1	1.696379	16.89096	0.003883	0.010045
SNRNP40	1.654974	16.01035	0.005129	0.013139
CTR9	4.929093	11.69506	0.005373	0.013577
POLR2E	4.929071	11.69487	0.005373	0.013577
PRPF40A	1.259439	13.70981	0.007852	0.01971
ACIN1	0.897208	9.953489	0.008091	0.020174
PQBP1	4.782336	10.23667	0.008268	0.020477
EIF4A3	0.82346	8.689278	0.008556	0.021053
SNRNP200	0.716049	6.837206	0.009108	0.022118
KIAA0020	4.618965	8.720717	0.012778	0.030056
RPS17	4.618933	8.720508	0.012778	0.030056
CHTOP	2.082704	11.35125	0.013845	0.032363
PRPF4	2.547702	9.886135	0.016278	0.037349
XAB2	2.547737	9.8865	0.016278	0.037349
CCAR1	4.434667	7.079004	0.019854	0.043424
CTCF	4.434677	7.079084	0.019854	0.043424
HNRNPH2	4.434667	7.079004	0.019854	0.043424
LAS1L	4.434677	7.079084	0.019854	0.043424
SEC61A1	4.434677	7.079084	0.019854	0.043424
SLTM	4.434677	7.079084	0.019854	0.043424
TAF10	4.434656	7.078925	0.019854	0.043424
UBR4	4.434688	7.079163	0.019854	0.043424
SF3A1	0.970205	9.731878	0.024242	0.052713
PGAM5	1.377894	10.72448	0.025599	0.055341
RALY	1.925217	8.919976	0.026399	0.056418
SNRPA	1.925274	8.920611	0.026399	0.056418

Protein Name	LogFC	F.statistic	p.value	adj p.value
DDX46	1.267547	10.09956	0.02763	0.058713
DDX1	4.223344	5.457811	0.031059	0.063824
POLR2C	4.223355	5.457874	0.031059	0.063824
POLR2H	4.223355	5.457874	0.031059	0.063824
SUPT6H	4.223344	5.457811	0.031059	0.063824
ZC3H13	4.223355	5.457874	0.031059	0.063824
DHX30	2.331013	7.347554	0.033507	0.068479
U2AF2	0.911664	8.460346	0.035863	0.072895
BCL7C	3.975691	4.053029	0.049017	0.094987
CACTIN	3.975691	4.053029	0.049017	0.094987
FOSB	3.97568	4.052982	0.049017	0.094987
HNRNPA0	3.97568	4.052982	0.049017	0.094987
LSM7	3.97568	4.052982	0.049017	0.094987
SAFB2	2.209079	6.206798	0.047954	0.094987
SMNDC1	3.97568	4.052982	0.049017	0.094987
WDR61	3.975691	4.053029	0.049017	0.094987
WDR82	3.97568	4.052982	0.049017	0.094987

Table S2. Significant protein interaction partners of cJun (LogFC>0, p. value<0.05, n=127) in CD8+ T cells activated *in vitro* for 24hrs

Protein Name	LogFC	F.statistic	p.value	adj p.value
NFKB1	7.802476	89.1255	1.60E-10	2.50E-09
GOLGA5	8.891862	94.92796	7.42E-10	9.93E-09
ZNF638	7.383768	68.00183	3.15E-09	3.69E-08
PDCD11	7.784929	76.28637	5.95E-09	6.77E-08
FBXO38	7.966058	72.88085	9.09E-09	1.00E-07
SAFB2	4.362041	57.55338	1.56E-08	1.58E-07
CUX1	7.075558	52.87176	6.60E-08	5.76E-07
SAFB	7.046583	51.53764	8.93E-08	7.61E-07
RRBP1	6.986888	46.46973	1.63E-07	1.30E-06
FAM172A	6.826101	40.19759	7.40E-07	5.55E-06
UTP20	6.956061	38.93506	1.82E-06	1.31E-05
NCOA5	3.949635	38.48618	1.97E-06	1.39E-05
CLCC1	6.826137	35.55511	3.59E-06	2.45E-05
POLR2A	6.75618	34.07852	4.90E-06	3.23E-05
GNL3	6.524171	35.5582	8.42E-06	5.35E-05
SSB	6.524171	35.5582	8.42E-06	5.35E-05
MNDAL	6.48164	31.2039	1.14E-05	6.91E-05
TEX10	6.481567	34.41291	1.14E-05	6.91E-05
RASAL3	6.437685	33.14345	1.55E-05	9.23E-05
SLTM	6.392408	31.72181	2.11E-05	1.22E-04

Protein Name	LogFC	F.statistic	p.value	adj p.value
TFIP11	6.437593	27.00108	2.46E-05	1.40E-04
DDX24	6.345664	30.09727	2.86E-05	1.58E-04
KIAA0020	6.345664	30.09727	2.86E-05	1.58E-04
SATB1	6.29741	28.29085	3.89E-05	2.12E-04
SART1	3.601942	28.11726	4.41E-05	2.36E-04
BCLAF1	2.020557	29.24865	4.56E-05	2.41E-04
CEBPZ	6.247374	26.00753	5.30E-05	2.76E-04
DOCK2	1.377658	21.71472	5.75E-05	2.95E-04
FAM208A	6.195618	24.69563	7.21E-05	3.56E-04
HNRNPUL2	6.195673	25.00315	7.21E-05	3.56E-04
POLR2B	6.195618	24.69563	7.21E-05	3.56E-04
NOL6	6.141898	21.52693	9.81E-05	4.78E-04
DHX30	3.4905	23.098	1.02E-04	4.93E-04
PCF11	6.247319	21.19514	1.11E-04	5.22E-04
URB1	6.247319	21.19514	1.11E-04	5.22E-04
FKBP15	6.028175	20.39051	1.82E-04	8.34E-04
NFKB2	6.028157	20.07705	1.82E-04	8.34E-04
ELMO1	2.821521	18.57657	2.19E-04	9.90E-04
LACTB	3.369816	22.50995	2.38E-04	1.06E-03
BRIX1	5.967761	19.16632	2.49E-04	1.10E-03
LAS1L	5.904632	17.84989	3.40E-04	1.46E-03
DDX1	5.904595	16.17666	4.25E-04	1.81E-03
DDX50	5.838672	16.90633	4.64E-04	0.001913
MOGS	5.838653	16.41621	4.64E-04	0.001913
NO66	5.838653	16.41621	4.64E-04	0.001913
SRRM2	1.020041	14.88252	5.37E-04	0.002189
AQR	6.028083	15.47286	6.15E-04	0.002479
JUN	5.838763	14.87674	6.91E-04	0.002755
KIAA1429	5.696931	15.0319	0.000869	0.003292
NFKBID	5.697004	14.23481	0.000869	0.003292
RBM10	5.696912	14.52	0.000869	0.003292
SRPK1	5.696949	15.25953	0.000869	0.003292
PRPF4B	3.143081	18.16451	0.00096	0.003601
NCBP1	5.620444	13.30272	0.001191	0.004337
PRPF31	5.620462	13.9981	0.001191	0.004337
USP7	3.093166	14.8857	0.001268	0.004574
DDX18	1.568137	19.47761	0.001468	0.005243
PPP1R10	5.769477	12.69043	0.001562	0.005527
NXF1	5.539768	13.71112	0.001635	0.005676
RBM28	5.53975	13.74241	0.001635	0.005676
CHTOP	2.453217	15.30766	0.001663	0.00572

Protein Name	LogFC	F.statistic	p.value	adj p.value
EDC4	5.454177	11.61469	0.002246	0.007388
RPS17	5.454214	12.85558	0.002246	0.007388
SNRPE	5.454232	12.99584	0.002246	0.007388
USP39	5.454232	12.99584	0.002246	0.007388
CBFB	5.363341	11.88374	0.00309	0.009658
IKZF5	5.363304	12.16193	0.00309	0.009658
NOL9	5.363268	11.22916	0.00309	0.009658
PPAN	5.363268	11.22916	0.00309	0.009658
RUNX3	5.363323	12.16975	0.00309	0.009658
PGAM5	1.676756	15.04717	0.003306	0.010162
SNW1	2.873827	11.59228	0.003844	0.011624
BCAS2	5.266278	11.47245	0.00426	0.012193
IRF4	5.266296	11.34752	0.00426	0.012193
LYAR	5.266278	11.47245	0.00426	0.012193
PAK1IP1	5.26626	11.28967	0.00426	0.012193
POLR2E	5.266241	10.80477	0.00426	0.012193
SON	1.534144	15.05625	0.004068	0.012193
ZC3H13	5.266241	10.80477	0.00426	0.012193
CDC5L	1.764194	13.64904	0.004883	0.013873
PABPC1	1.615794	14.32977	0.005033	0.01419
CTCF	5.162215	10.37314	0.005882	0.01646
THOC2	1.477921	11.03166	0.006065	0.016847
THRAP3	0.922071	9.92035	0.006961	0.019193
RALY	2.1765	12.72168	0.007538	0.020484
SUPT6H	5.162178	8.513914	0.007493	0.020484
MRPL46	5.050099	9.88658	0.008139	0.021646
RBM22	5.050117	10.12329	0.008139	0.021646
WDR82	5.050136	10.03273	0.008139	0.021646
FOSL2	5.162325	8.027784	0.009139	0.024134
CTR9	4.928511	8.953516	0.01129	0.029607
MATR3	1.578383	10.22223	0.014354	0.037379
HACD3	2.542638	7.946157	0.015183	0.038998
PELP1	2.542649	7.848079	0.015183	0.038998
CCAR1	4.795727	7.579402	0.015706	0.039265
SEC61A1	4.795745	8.292107	0.015706	0.039265
SF3A2	4.795763	8.582951	0.015706	0.039265
SP110	4.795745	8.292107	0.015706	0.039265
PRPF6	1.327157	10.24897	0.015993	0.039717
CWC22	1.718707	10.09591	0.017503	0.042899
RANBP2	4.795708	6.505213	0.017486	0.042899
GLYR1	2.466162	7.17031	0.019943	0.048563

Protein Name	LogFC	F.statistic	p.value	adj p.value
CACTIN	4.649491	6.977292	0.021922	0.050745
HNRNPA0	4.64951	7.462424	0.021922	0.050745
ISG20L2	4.649546	7.414862	0.021922	0.050745
POLR2H	4.649528	7.600261	0.021922	0.050745
RBBP6	4.64951	7.462424	0.021922	0.050745
RRP1B	4.64951	7.462424	0.021922	0.050745
RRP9	4.649491	6.977292	0.021922	0.050745
ILF3	1.262155	9.503046	0.023273	0.053543
CLK3	1.896821	6.830372	0.025647	0.058288
SF1	2.385395	6.215509	0.026174	0.059129
EIF6	4.486778	6.649659	0.030722	0.066982
HNRNPH2	4.48676	6.654839	0.030722	0.066982
SCAF4	4.486778	6.649659	0.030722	0.066982
U2SURP	1.833721	6.858199	0.032604	0.070673
PRPF4	2.299914	6.010328	0.034321	0.073545
RPL3	0.686733	6.026195	0.036139	0.077
FTSJ3	4.303286	5.619161	0.043269	0.088613
NOP58	0.79549	7.119066	0.04348	0.088613
POLR2C	4.303268	5.454305	0.043269	0.088613
PQBP1	4.303268	5.454305	0.043269	0.088613
SRRT	4.303286	5.619161	0.043269	0.088613
THOC5	1.514912	6.490449	0.042215	0.088613
TRIM28	1.51493	6.811048	0.042215	0.088613
WDR61	4.303286	5.619161	0.043269	0.088613
RPL10A	0.737724	6.490679	0.047399	0.096079

Table S3. Significant protein interaction partners of JunD (LogFC>0, p. value<0.05, n=70) in CD8+ T cells activated *in vitro* for 24hrs

Protein Name	LogFC	F.statistic	p.value	adj p.value
EDC4	9.598892	184.1468	1.93E-37	1.70E-35
CAD	9.451141	180.6515	7.79E-37	5.50E-35
RANBP2	8.517854	131.6342	1.04E-27	6.13E-26
KMT2C	8.489513	130.3328	3.38E-27	1.70E-25
HMHA1	2.96446	79.55513	3.98E-18	1.41E-16
AP3B1	7.778995	98.76111	3.27E-17	9.62E-16
JUND	7.54985	94.59853	6.74E-15	1.59E-13
ATP6V1A	7.521943	94.33278	1.22E-14	2.69E-13
DCP1A	7.243549	87.0478	2.55E-12	4.29E-11
AP3D1	7.137321	83.06224	1.52E-11	2.44E-10
EDC3	7.02272	78.62663	9.11E-11	1.29E-09

FOSL2	6.940874	76.09836	3.01E-10	3.93E-09
IRF4	6.761914	70.21023	3.29E-09	3.75E-08
DCP2	6.663342	66.25044	1.09E-08	1.07E-07
DDX6	6.663291	66.24876	1.09E-08	1.07E-07
KDM6A	6.663325	66.24988	1.09E-08	1.07E-07
ATP6V1B2	4.474985	61.03849	1.38E-08	1.28E-07
AP3M1	6.611358	63.99382	1.99E-08	1.80E-07
ASH2L	6.557502	62.15775	3.63E-08	3.13E-07
PAXIP1	6.443282	58.6524	1.21E-07	1.02E-06
LAMTOR1	6.319289	55.68202	4.05E-07	3.11E-06
PTBP1	3.117038	45.46678	6.54E-07	4.81E-06
JUN	6.253009	53.67603	7.42E-07	5.35E-06
NUP210	6.110539	47.08819	2.50E-06	1.63E-05
RANGAP1	6.110556	47.72977	2.50E-06	1.63E-05
NXF1	6.03372	44.73985	4.59E-06	2.89E-05
NUP93	5.775071	33.86563	2.87E-05	1.69E-04
ATF7	5.677475	30.66674	5.31E-05	2.93E-04
DPY30	5.677475	30.66674	5.31E-05	2.93E-04
RRAGC	5.677475	30.66674	5.31E-05	2.93E-04
RRAGA	5.572734	26.9759	9.83E-05	5.34E-04
NCOA6	5.459754	23.95845	1.83E-04	9.77E-04
FOS	5.337207	20.17883	3.40E-04	1.74E-03
LAMTOR3	5.337241	20.17961	3.40E-04	1.74E-03
NUP133	5.33719	20.17845	3.40E-04	1.74E-03
RUNX3	5.203276	16.9182	6.36E-04	3.16E-03
CBFB	5.055624	13.90254	1.19E-03	5.69E-03
MNDAL	5.055607	13.90228	1.19E-03	5.69E-03
PDCD11	5.055607	13.90228	1.19E-03	5.69E-03
RBBP4	3.106782	18.01486	1.95E-03	8.94E-03
RRBP1	4.891085	11.23442	2.25E-03	1.00E-02
DOCK2	1.088406	11.61529	2.29E-03	1.01E-02
CTCF	4.70541	8.701754	4.26E-03	0.017712
FOSB	4.705427	8.701888	4.26E-03	0.017712
GNL3	4.705393	8.70162	4.26E-03	0.017712
PCF11	4.705359	8.701353	4.26E-03	0.017712
POLR2A	4.705359	8.701353	4.26E-03	0.017712
PYHIN1	1.112592	11.02955	5.01E-03	0.020574
ATP6V1E1	2.87129	12.97665	0.005891	0.02363
LAMTOR5	2.87129	12.97665	0.005891	0.02363
STOML2	1.855134	15.94638	0.006355	0.024926
HSPA8	0.727968	7.452094	0.006494	0.025192
RFWD2	4.492195	7.119566	0.008148	0.031263

KIAA0020	4.241899	5.805002	0.016236	0.057891
LAS1L	4.241899	5.805002	0.016236	0.057891
NO66	4.241899	5.805002	0.016236	0.057891
RPS17	4.241916	5.805052	0.016235	0.057891
LSM3	2.425151	6.206462	0.030371	0.106148
PELP1	2.425128	6.206305	0.030371	0.106148
CEBPZ	3.938949	4.421463	0.035843	0.114001
EED	3.938915	4.421323	0.035846	0.114001
MATR3	1.519623	9.706715	0.034364	0.114001
PIAS1	3.938932	4.421393	0.035845	0.114001
POLR2B	3.938898	4.421253	0.035847	0.114001
POLR2H	3.938898	4.421253	0.035847	0.114001
SLTM	3.938915	4.421323	0.035846	0.114001
SNRPE	3.938932	4.421393	0.035845	0.114001
TEX10	3.938932	4.421393	0.035845	0.114001
USP39	3.938915	4.421323	0.035846	0.114001
HSPA9	0.890402	6.930126	0.042538	0.134071

Table S4. Top enriched transcription factor binding motifs among bound genomic regions shared by all Jun family members

Sequence Logo	Motif ID (JASPAR2024 Database)	Alternative Motif Name	length	p value	e value	True Positive Threshold	True Positive (%)	False Positive (%)
	MA1141.2	FOS::JUND	9	2.04E-204	4.31E-201	1.52	1326 (32.4%)	264 (6.4%)
	MA1128.2	FOSL1::JUN	9	3.53E-204	7.44E-201	2.16	1329 (32.4%)	266 (6.5%)
	MA0099.4	FOS::JUN	9	1.99E-202	4.19E-199	2.41	1325 (32.3%)	267 (6.5%)
	MA1132.2	JUN::JUNB	8	6.76E-202	1.42E-198	2.67	1449 (35.4%)	339 (8.3%)
	MA1130.2	FOSL2::JUN	9	1.68E-199	3.54E-196	3.22	1237 (30.2%)	225 (5.5%)
	MA1633.2	BACH1	9	2E-196	4.22E-193	1.06	1277 (31.2%)	252 (6.2%)
	MA1134.2	FOS::JUNB	9	3.04E-196	6.41E-193	1.09	1269 (31.0%)	248 (6.1%)
	MA1144.2	FOSL2::JUND	9	4.15E-196	8.74E-193	1.09	1332 (32.5%)	283 (6.9%)
	MA1135.2	FOSB::JUNB	9	1.53E-194	3.23E-191	2.21	1199 (29.3%)	214 (5.2%)
	MA1137.2	FOSL1::JUNB	9	1.49E-193	3.14E-190	3.80	1242 (30.3%)	238 (5.8%)
	MA1142.2	FOSL1::JUND	8	8.55E-193	1.8E-189	3.71	1341 (32.7%)	294 (7.2%)
	MA1138.2	FOSL2::JUNB	9	2.88E-190	6.07E-187	3.23	1113 (27.2%)	178 (4.3%)
	MA0477.3	FOSL1	9	1.04E-188	2.19E-185	2.44	1189 (29.0%)	219 (5.3%)
	MA0491.3	JUND	9	1.87E-188	3.94E-185	1.95	1209 (29.5%)	230 (5.6%)

Table S5. Top enriched Reactome pathways and GO Biological processes of genes associated with the unique CUT&RUN peaks of JunB

Reactome Pathway	P-value	Adjusted P-value	Odds Ratio	Overlap
Collagen Formation	1.60E-02	0.999996	1.832146	20/90
Ciprofloxacin ADME	2.00E-02	0.999996	9.596004	3/5
NR1H2 & NR1H3 Regulate Gene Expression Linked to Triglyceride Lipolysis in Adipose	2.00E-02	0.999996	9.596004	3/5
Cellular Hexose Transport	2.20E-02	0.999996	2.9876	7/22
Hormone Ligand-Binding Receptors	2.27E-02	0.999996	3.999907	5/13
Smooth Muscle Contraction	2.94E-02	0.999996	2.134941	11/44
Neurotransmitter Clearance	3.57E-02	0.999996	4.265482	4/10
Organic Cation Transport	3.57E-02	0.999996	4.265482	4/10
p75NTR Regulates Axonogenesis	3.57E-02	0.999996	4.265482	4/10
MET Receptor Activation	3.60E-02	0.999996	6.396966	3/6

GO Biological Process	P-value	Adjusted P-value	Odds Ratio	Overlap
AV Node Cell Action Potential (GO:0086016)	2.41E-04	0.972674	32.01222	5/6
Positive Regulation of Vitamin D Receptor Signaling Pathway (GO:0070564)	1.49E-03	0.999995	25.6003	4/5
Regulation of Mitochondrial mRNA Stability (GO:0044528)	3.99E-03	0.999995	12.79941	4/6
Regulation of Vitamin D Receptor Signaling Pathway (GO:0070562)	8.32E-03	0.999995	8.532445	4/7
Regulation of Protein Polymerization (GO:0032271)	1.21E-02	0.999995	2.669078	10/34
Calcium-Dependent Cell-Cell Adhesion via Plasma Membrane Cell Adhesion Molecules (GO:0016339)	1.47E-02	0.999995	2.429979	11/40
Response to Vitamin (GO:0033273)	1.49E-02	0.999995	6.398964	4/8
Response to Vitamin D (GO:0033280)	1.49E-02	0.999995	6.398964	4/8
Positive Regulation of Smoothened Signaling Pathway (GO:0045880)	1.70E-02	0.999995	3.201186	7/21
Protein Autoprocessing (GO:0016540)	1.99E-02	0.999995	3.491515	6/17

Table S6. Top enriched Reactome pathways and GO Biological processes of genes associated with the unique CUT&RUN peaks of cJun

Reactome Pathway	P-value	Adjusted P-value	Odds Ratio	Overlap
Synthesis of PI	9.24E-03	0.999995	20.62726	2/5
Negative Regulation of TCF-dependent Signaling by WNT Ligand Antagonists	1.06E-02	0.999995	7.744	3/15
Amine Ligand-Binding Receptors	1.08E-02	0.999995	4.083383	5/43
Collagen Chain Trimerization	1.19E-02	0.999995	3.978475	5/44
mRNA Decay by 3' to 5' Exoribonuclease	1.27E-02	0.999995	7.147938	3/16
Acrosome Reaction and Sperm Oocyte Membrane Binding	1.36E-02	0.999995	15.46965	2/6
Collagen Biosynthesis and Modifying Enzymes	1.85E-02	0.999995	3.053766	6/67
Collagen Formation	2.31E-02	0.999995	2.619619	7/90
Terminal Pathway of Complement	2.43E-02	0.999995	10.31203	2/8
Synthesis, Secretion, and Inactivation of Glucagon-like Peptide-1 (GLP-1)	2.69E-02	0.999995	5.161067	3/21

GO Biological Process	P-value	Adjusted P-value	Odds Ratio	Overlap
Adenylate Cyclase-Inhibiting Serotonin Receptor Signaling Pathway (GO:0007198)	0.002246	0.90478	15.4928	3/9
Icosanoid Secretion (GO:0032309)	0.003135	0.90478	13.27886	3/10
Adenylate Cyclase-Inhibiting G Protein-Coupled Receptor Signaling Pathway (GO:0007193)	0.008026	0.90478	3.727717	6/56
G Protein-Coupled Serotonin Receptor Signaling Pathway (GO:0098664)	0.008659	0.90478	8.448436	3/14
Regulation of Tooth Mineralization (GO:0070170)	0.009242	0.90478	20.62726	2/5
Regulation of Monoatomic Ion Transmembrane Transport (GO:0034765)	0.012259	0.90478	4.960769	4/29
TRAMP-dependent tRNA Surveillance Pathway (GO:0071038)	0.013576	0.90478	15.46965	2/6
Exonucleolytic Trimming to Gen Mat 3'-End of 5.8S rRNA Frm Tricistronic rRNA Trnscpt (GO:0000467)	0.013576	0.90478	15.46965	2/6
Vascular Associated Smooth Muscle Contraction (GO:0014829)	0.013576	0.90478	15.46965	2/6
Nuclear Polyadenylation-Dependent rRNA Catabolic Process (GO:0071035)	0.013576	0.90478	15.46965	2/6

Table S7. Top enriched Reactome pathways and GO Biological processes of genes associated with the unique CUT&RUN peaks of JunD

Reactome Pathway	P-value	Adjusted P-value	Odds Ratio	Overlap
Regulation of Gene Expression in Endocrine-Committed (NEUROG3+) Progenitor Cells	2.11E-03	0.999996	22.94377	3/5
Synaptic Adhesion-Like Molecules	7.76E-03	0.999996	4.784184	5/21
WNT Ligand Biogenesis and Trafficking	1.95E-02	0.999996	3.644121	5/26
PI3K Events in ERBB4 Signaling	2.01E-02	0.999996	6.553615	3/10
Formation of the Nephric Duct	2.18E-02	0.999996	4.371009	4/18
Assembly of Active LPL and LIPC Lipase Complexes	2.63E-02	0.999996	4.079391	4/19
Defective B3GALTL Causes PpS	2.72E-02	0.999996	2.870404	6/38
O-glycosylation of TSR Domain-Containing Proteins	3.06E-02	0.999996	2.783274	6/39
FGFR3 Mutant Receptor Activation	3.36E-02	0.999996	5.096713	3/12
Signaling by Activated Point Mutants of FGFR3	3.36E-02	0.999996	5.096713	3/12

GO Biological Process	P-value	Adjusted P-value	Odds Ratio	Overlap
Venous Blood Vessel Development (GO:0060841)	0.000429	0.64826	20.41001	4/7
Cardiac Atrium Morphogenesis (GO:0003209)	0.000522	0.64826	7.662582	6/18
Negative Regulation of Cartilage Development (GO:0061037)	0.001094	0.64826	8.50839	5/14
Negative Regulation of Chondrocyte Differentiation (GO:0032331)	0.001558	0.64826	7.657143	5/15
Secondary Heart Field Specification (GO:0003139)	0.002112	0.64826	22.94377	3/5
Venous Blood Vessel Morphogenesis (GO:0048845)	0.002112	0.64826	22.94377	3/5
Heart Field Specification (GO:0003128)	0.002112	0.64826	22.94377	3/5
Negative Regulation of Insulin-Like Growth Factor Receptor Signaling Pathway (GO:0043569)	0.002112	0.64826	22.94377	3/5
Regulation of ATPase-coupled Calcium Transmembrane Transporter Activity (GO:1901894)	0.002112	0.64826	22.94377	3/5
Regulation of Digestive System Process (GO:0044058)	0.004032	0.795368	15.29503	3/6

REFERENCES

1 Muller, V., de Boer, R. J., Bonhoeffer, S. & Szathmary, E. An evolutionary perspective on the systems of adaptive immunity. *Biol Rev Camb Philos Soc* **93**, 505–528 (2018). https://doi.org/10.1111/brv.12355

2 Cooper, M. D. & Herrin, B. R. How did our complex immune system evolve? *Nat Rev Immunol* **10**, 2–3 (2010). https://doi.org/10.1038/nri2686

3 Mueller, E. A. & Levin, P. A. Bacterial Cell Wall Quality Control during Environmental Stress. *mBio* **11** (2020). https://doi.org/10.1128/mBio.02456-20

4 Janeway, C. A., Jr. Approaching the asymptote? Evolution and revolution in immunology. *Cold Spring Harb Symp Quant Biol* **54 Pt 1**, 1–13 (1989). https://doi.org/10.1101/sqb.1989.054.01.003

5 Wang, R. *et al.* The interaction of innate immune and adaptive immune system. *MedComm (2020)* **5**, e714 (2024). https://doi.org/10.1002/mco2.714

6 Murphy, K. M. & Weaver, C. *Janeway's immunobiology*. 9th ed. edn, (New York : Garland Science, 2017).

7 Chaplin, D. D. Overview of the immune response. *J Allergy Clin Immunol* **125**, S3–23 (2010). https://doi.org/10.1016/j.jaci.2009.12.980

8 Medzhitov, R. Recognition of microorganisms and activation of the immune response. *Nature* **449**, 819–826 (2007). https://doi.org/10.1038/nature06246

9 Davis, M. M. & Bjorkman, P. J. T-cell antigen receptor genes and T-cell recognition. *Nature* **334**, 395–402 (1988). https://doi.org/10.1038/334395a0

10 Bancroft, G. J., Schreiber, R. D., Bosma, G. C., Bosma, M. J. & Unanue, E. R. A T cell-independent mechanism of macrophage activation by interferon-gamma. *J Immunol* **139**, 1104–1107 (1987).

11 Zimecki, M., Abruzzini, A. F., Pierce, C. W. & Kapp, J. A. Antigen presentation to T cell lines and clones by peritoneal macrophages, peritoneal B cells and antigen-specific B cell hybridomas. *Arch Immunol Ther Exp (Warsz)* **36**, 409–422 (1988).

12 Fujii, S., Liu, K., Smith, C., Bonito, A. J. & Steinman, R. M. The linkage of innate to adaptive immunity via maturing dendritic cells in vivo requires CD40 ligation in addition to antigen presentation and CD80/86 costimulation. *J Exp Med* **199**, 1607–1618 (2004). https://doi.org/10.1084/jem.20040317

13 Puleston, D. J. *et al.* Autophagy is a critical regulator of memory CD8(+) T cell formation. *Elife* **3** (2014). https://doi.org/10.7554/eLife.03706

14 Ziegler, K. & Unanue, E. R. Identification of a macrophage antigen-processing event required for I-region-restricted antigen presentation to T lymphocytes. *J Immunol* **127**, 1869–1875 (1981).

15 Zinkernagel, R. M. & Doherty, P. C. Restriction of in vitro T cell-mediated cytotoxicity in lymphocytic choriomeningitis within a syngeneic or semiallogeneic system. *Nature* **248**, 701–702 (1974). https://doi.org/10.1038/248701a0

16 Townsend, A. R. *et al.* The epitopes of influenza nucleoprotein recognized by cytotoxic T lymphocytes can be defined with short synthetic peptides. *Cell* **44**, 959–968 (1986). https://doi.org/10.1016/0092-8674(86)90019-x

17 Townsend, A. *et al.* Association of class I major histocompatibility heavy and light chains induced by viral peptides. *Nature* **340**, 443–448 (1989). https://doi.org/10.1038/340443a0

18 Townsend, A. R., Gotch, F. M. & Davey, J. Cytotoxic T cells recognize fragments of the influenza nucleoprotein. *Cell* **42**, 457–467 (1985). https://doi.org/10.1016/0092-8674(85)90103-5

19 Jones, E. Y. MHC class I and class II structures. *Curr Opin Immunol* **9**, 75–79 (1997). https://doi.org/10.1016/s0952-7915(97)80162-8

20 Trowsdale, J. *et al.* Sequences encoded in the class II region of the MHC related to the 'ABC' superfamily of transporters. *Nature* **348**, 741–744 (1990). https://doi.org/10.1038/348741a0

21 Bevan, M. J. Cross-priming for a secondary cytotoxic response to minor H antigens with H-2 congenic cells which do not cross-react in the cytotoxic assay. *J Exp Med* **143**, 1283–1288 (1976). https://doi.org/10.1084/jem.143.5.1283
22 Bevan, M. J. The major histocompatibility complex determines susceptibility to cytotoxic T cells directed against minor histocompatibility antigens. *J Exp Med* **142**, 1349–1364 (1975). https://doi.org/10.1084/jem.142.6.1349
23 Doyle, C. & Strominger, J. L. Interaction between CD4 and class II MHC molecules mediates cell adhesion. *Nature* **330**, 256–259 (1987). https://doi.org/10.1038/330256a0
24 Glick, B., Chang, T. S. & Jaap, R. G. The Bursa of Fabricius and Antibody Production. *Poultry Science* **35**, 224–225 (1956). https://doi.org/https://doi.org/10.3382/ps.0350224
25 Miller, J. F. & Mitchell, G. F. The thymus and the precursors of antigen reactive cells. *Nature* **216**, 659–663 (1967). https://doi.org/10.1038/216659a0
26 Burnet, F. M. A modification of Jerne's theory of antibody production using the concept of clonal selection. *CA Cancer J Clin* **26**, 119–121 (1976). https://doi.org/10.3322/canjclin.26.2.119
27 Burnet, F. M. The immunological significance of the thymus: an extension of the clonal selection theory of immunity. *Australas Ann Med* **11**, 79–91 (1962). https://doi.org/10.1111/imj.1962.11.2.79
28 Hesslein, D. G. & Schatz, D. G. Factors and forces controlling V(D)J recombination. *Adv Immunol* **78**, 169–232 (2001). https://doi.org/10.1016/s0065-2776(01)78004-2
29 Tonegawa, S. Somatic generation of antibody diversity. *Nature* **302**, 575–581 (1983). https://doi.org/10.1038/302575a0
30 Volpe, J. M. & Kepler, T. B. Large-scale analysis of human heavy chain V(D)J recombination patterns. *Immunome Res* **4**, 3 (2008). https://doi.org/10.1186/1745-7580-4-3
31 Murugan, A., Mora, T., Walczak, A. M. & Callan, C. G., Jr. Statistical inference of the generation probability of T-cell receptors from sequence repertoires. *Proc Natl Acad Sci U S A* **109**, 16161–16166 (2012). https://doi.org/10.1073/pnas.1212755109
32 Sender, R. *et al.* The total mass, number, and distribution of immune cells in the human body. *Proc Natl Acad Sci U S A* **120**, e2308511120 (2023). https://doi.org/10.1073/pnas.2308511120
33 de Greef, P. C. *et al.* The naive T-cell receptor repertoire has an extremely broad distribution of clone sizes. *Elife* **9** (2020). https://doi.org/10.7554/eLife.49900
34 Mason, D. A very high level of crossreactivity is an essential feature of the T-cell receptor. *Immunol Today* **19**, 395–404 (1998). https://doi.org/10.1016/s0167-5699(98)01299-7
35 Viola, A. & Lanzavecchia, A. T cell activation determined by T cell receptor number and tunable thresholds. *Science* **273**, 104–106 (1996). https://doi.org/10.1126/science.273.5271.104
36 Butz, E. A. & Bevan, M. J. Massive expansion of antigen-specific CD8+ T cells during an acute virus infection. *Immunity* **8**, 167–175 (1998). https://doi.org/10.1016/s1074-7613(00)80469-0
37 Blattman, J. N. *et al.* Estimating the precursor frequency of naive antigen-specific CD8 T cells. *J Exp Med* **195**, 657–664 (2002). https://doi.org/10.1084/jem.20001021
38 Moon, J. J. *et al.* Naive CD4(+) T cell frequency varies for different epitopes and predicts repertoire diversity and response magnitude. *Immunity* **27**, 203–213 (2007). https://doi.org/10.1016/j.immuni.2007.07.007
39 Marzo, A. L. *et al.* Initial T cell frequency dictates memory CD8+ T cell lineage commitment. *Nat Immunol* **6**, 793–799 (2005). https://doi.org/10.1038/ni1227
40 Murugan, R. *et al.* Clonal selection drives protective memory B cell responses in controlled human malaria infection. *Sci Immunol* **3** (2018). https://doi.org/10.1126/sciimmunol.aap8029
41 Mold, J. E. *et al.* Divergent clonal differentiation trajectories establish CD8(+) memory T cell heterogeneity during acute viral infections in humans. *Cell Rep* **35**, 109174 (2021). https://doi.org/10.1016/j.celrep.2021.109174

42 Cerottini, J. C., Nordin, A. A. & Brunner, K. T. Specific in vitro cytotoxicity of thymus-derived lymphocytes sensitized to alloantigens. *Nature* **228**, 1308–1309 (1970). https://doi.org/10.1038/2281308a0
43 Cantor, H. & Boyse, E. A. Functional subclasses of T lymphocytes bearing different Ly antigens. II. Cooperation between subclasses of Ly+ cells in the generation of killer activity. *J Exp Med* **141**, 1390–1399 (1975). https://doi.org/10.1084/jem.141.6.1390
44 Evans, R. L., Lazarus, H., Penta, A. C. & Schlossman, S. F. Two functionally distinct subpopulations of human T cells that collaborate in the generation of cytotoxic cells responsible for cell-mediated lympholysis. *J Immunol* **120**, 1423–1428 (1978).
45 Kisielow, P. *et al.* Ly antigens as markers for functionally distinct subpopulations of thymus-derived lymphocytes of the mouse. *Nature* **253**, 219–220 (1975). https://doi.org/10.1038/253219a0
46 Nossal, G. J., Cunningham, A., Mitchell, G. F. & Miller, J. F. Cell to cell interaction in the immune response. 3. Chromosomal marker analysis of single antibody-forming cells in reconstituted, irradiated, or thymectomized mice. *J Exp Med* **128**, 839–853 (1968). https://doi.org/10.1084/jem.128.4.839
47 Howard, M. *et al.* Identification of a T cell-derived b cell growth factor distinct from interleukin 2. *J Exp Med* **155**, 914–923 (1982). https://doi.org/10.1084/jem.155.3.914
48 Sakaguchi, S., Yamaguchi, T., Nomura, T. & Ono, M. Regulatory T cells and immune tolerance. *Cell* **133**, 775–787 (2008). https://doi.org/10.1016/j.cell.2008.05.009
49 Golstein, P., Wigzell, H., Blomgren, H. & Svedmyr, E. A. Cells mediating specific in vitro cytotoxicity. II. Probable autonomy of thymus-processed lymphocytes (T cells) for the killing of allogeneic target cells. *J Exp Med* **135**, 890–906 (1972). https://doi.org/10.1084/jem.135.4.890
50 Sun, J., Leahy, D. J. & Kavathas, P. B. Interaction between CD8 and major histocompatibility complex (MHC) class I mediated by multiple contact surfaces that include the alpha 2 and alpha 3 domains of MHC class I. *J Exp Med* **182**, 1275–1280 (1995). https://doi.org/10.1084/jem.182.5.1275
51 Srinivasan, S., Zhu, C. & McShan, A. C. Structure, function, and immunomodulation of the CD8 co-receptor. *Front Immunol* **15**, 1412513 (2024). https://doi.org/10.3389/fimmu.2024.1412513
52 Purbhoo, M. A. *et al.* The human CD8 coreceptor effects cytotoxic T cell activation and antigen sensitivity primarily by mediating complete phosphorylation of the T cell receptor zeta chain. *J Biol Chem* **276**, 32786–32792 (2001). https://doi.org/10.1074/jbc.M102498200
53 Chapman, N. M., Boothby, M. R. & Chi, H. Metabolic coordination of T cell quiescence and activation. *Nat Rev Immunol* **20**, 55–70 (2020). https://doi.org/10.1038/s41577-019-0203-y
54 Qi, Q. *et al.* Diversity and clonal selection in the human T-cell repertoire. *Proc Natl Acad Sci U S A* **111**, 13139–13144 (2014). https://doi.org/10.1073/pnas.1409155111
55 Gerlach, C. *et al.* Heterogeneous differentiation patterns of individual CD8+ T cells. *Science* **340**, 635–639 (2013). https://doi.org/10.1126/science.1235487
56 Lynch, A. C. *et al.* A Dapl1(+) subpopulation of naive CD8 T cells is enriched for memory-lineage precursors. *Sci Adv* **11**, eadx5687 (2025). https://doi.org/10.1126/sciadv.adx5687
57 Steinman, R. M., Gutchinov, B., Witmer, M. D. & Nussenzweig, M. C. Dendritic cells are the principal stimulators of the primary mixed leukocyte reaction in mice. *J Exp Med* **157**, 613–627 (1983). https://doi.org/10.1084/jem.157.2.613
58 Austyn, J. M., Steinman, R. M., Weinstein, D. E., Granelli-Piperno, A. & Palladino, M. A. Dendritic cells initiate a two-stage mechanism for T lymphocyte proliferation. *J Exp Med* **157**, 1101–1115 (1983). https://doi.org/10.1084/jem.157.4.1101
59 Horgan, K. J., Van Seventer, G. A., Shimizu, Y. & Shaw, S. Hyporesponsiveness of "naive" (CD45RA+) human T cells to multiple receptor-mediated stimuli but augmentation of responses by co-stimuli. *Eur J Immunol* **20**, 1111–1118 (1990). https://doi.org/10.1002/eji.1830200525

60 Lafferty, K. J., Warren, H. S., Woolnough, J. A. & Talmage, D. W. Immunological induction of T lymphocytes: role of antigen and the lymphocyte costimulator. *Blood Cells* **4**, 395–406 (1978).
61 Vasilevko, V., Ghochikyan, A., Holterman, M. J. & Agadjanyan, M. G. CD80 (B7-1) and CD86 (B7-2) are functionally equivalent in the initiation and maintenance of CD4+ T-cell proliferation after activation with suboptimal doses of PHA. *DNA Cell Biol* **21**, 137–149 (2002). https://doi.org/10.1089/10445490252925404
62 Reis e Sousa, C. Dendritic cells in a mature age. *Nat Rev Immunol* **6**, 476–483 (2006). https://doi.org/10.1038/nri1845
63 Hendriks, J., Xiao, Y. & Borst, J. CD27 promotes survival of activated T cells and complements CD28 in generation and establishment of the effector T cell pool. *J Exp Med* **198**, 1369–1380 (2003). https://doi.org/10.1084/jem.20030916
64 Chen, L. & Flies, D. B. Molecular mechanisms of T cell co-stimulation and co-inhibition. *Nat Rev Immunol* **13**, 227–242 (2013). https://doi.org/10.1038/nri3405
65 Larsen, C. P., Knechtle, S. J., Adams, A., Pearson, T. & Kirk, A. D. A new look at blockade of T-cell costimulation: a therapeutic strategy for long-term maintenance immunosuppression. *Am J Transplant* **6**, 876–883 (2006). https://doi.org/10.1111/j.1600-6143.2006.01259.x
66 Curtsinger, J. M. & Mescher, M. F. Inflammatory cytokines as a third signal for T cell activation. *Curr Opin Immunol* **22**, 333–340 (2010). https://doi.org/10.1016/j.coi.2010.02.013
67 Wilfahrt, D. & Delgoffe, G. M. Metabolic waypoints during T cell differentiation. *Nat Immunol* **25**, 206–217 (2024). https://doi.org/10.1038/s41590-023-01733-5
68 Raynor, J. L. & Chi, H. Nutrients: Signal 4 in T cell immunity. *J Exp Med* **221** (2024). https://doi.org/10.1084/jem.20221839
69 Giles, J. R., Globig, A. M., Kaech, S. M. & Wherry, E. J. CD8(+) T cells in the cancer-immunity cycle. *Immunity* **56**, 2231–2253 (2023). https://doi.org/10.1016/j.immuni.2023.09.005
70 Budagian, V. *et al.* Reverse signaling through membrane-bound interleukin-15. *J Biol Chem* **279**, 42192–42201 (2004). https://doi.org/10.1074/jbc.M403182200
71 Wang, X., Lupardus, P., Laporte, S. L. & Garcia, K. C. Structural biology of shared cytokine receptors. *Annu Rev Immunol* **27**, 29–60 (2009). https://doi.org/10.1146/annurev.immunol.24.021605.090616
72 Dustin, M. L. The immunological synapse. *Cancer Immunol Res* **2**, 1023–1033 (2014). https://doi.org/10.1158/2326-6066.CIR-14-0161
73 Nel, A. E. T-cell activation through the antigen receptor. Part 1: signaling components, signaling pathways, and signal integration at the T-cell antigen receptor synapse. *J Allergy Clin Immunol* **109**, 758–770 (2002). https://doi.org/10.1067/mai.2002.124259
74 Gascoigne, N. R., Casas, J., Brzostek, J. & Rybakin, V. Initiation of TCR phosphorylation and signal transduction. *Front Immunol* **2**, 72 (2011). https://doi.org/10.3389/fimmu.2011.00072
75 Konig, R. & Zhou, W. Signal transduction in T helper cells: CD4 coreceptors exert complex regulatory effects on T cell activation and function. *Curr Issues Mol Biol* **6**, 1–15 (2004).
76 Oh-hora, M. & Rao, A. Calcium signaling in lymphocytes. *Curr Opin Immunol* **20**, 250–258 (2008). https://doi.org/10.1016/j.coi.2008.04.004
77 Tsuchida, M., Manthei, E. R., Alam, T., Knechtle, S. J. & Hamawy, M. M. T cell activation up-regulates the expression of the focal adhesion kinase Pyk2: opposing roles for the activation of protein kinase C and the increase in intracellular Ca2+. *J Immunol* **163**, 6640–6650 (1999).
78 Jayaraman, T., Ondriasova, E., Ondrias, K., Harnick, D. J. & Marks, A. R. The inositol 1,4,5-trisphosphate receptor is essential for T-cell receptor signaling. *Proc Natl Acad Sci U S A* **92**, 6007–6011 (1995). https://doi.org/10.1073/pnas.92.13.6007

79 Vaeth, M. *et al.* Store-Operated Ca(2+) Entry Controls Clonal Expansion of T Cells through Metabolic Reprogramming. *Immunity* **47**, 664–679 e666 (2017). https://doi.org/10.1016/j.immuni.2017.09.003
80 Jain, J. *et al.* The T-cell transcription factor NFATp is a substrate for calcineurin and interacts with Fos and Jun. *Nature* **365**, 352–355 (1993). https://doi.org/10.1038/365352a0
81 Khalaf, H., Jass, J. & Olsson, P. E. Differential cytokine regulation by NF-kappaB and AP-1 in Jurkat T-cells. *BMC Immunol* **11**, 26 (2010). https://doi.org/10.1186/1471-2172-11-26
82 Brignall, R. *et al.* Integration of Kinase and Calcium Signaling at the Level of Chromatin Underlies Inducible Gene Activation in T Cells. *J Immunol* **199**, 2652–2667 (2017). https://doi.org/10.4049/jimmunol.1602033
83 Stark, R., Hartung, A., Zehn, D., Frentsch, M. & Thiel, A. IL-12-mediated STAT4 signaling and TCR signal strength cooperate in the induction of CD40L in human and mouse CD8+ T cells. *Eur J Immunol* **43**, 1511–1517 (2013). https://doi.org/10.1002/eji.201243218
84 Park, W. R. *et al.* A mechanism underlying STAT4-mediated up-regulation of IFN-gamma induction inTCR-triggered T cells. *Int Immunol* **16**, 295–302 (2004). https://doi.org/10.1093/intimm/dxh034
85 Mognol, G. P., Carneiro, F. R., Robbs, B. K., Faget, D. V. & Viola, J. P. Cell cycle and apoptosis regulation by NFAT transcription factors: new roles for an old player. *Cell Death Dis* **7**, e2199 (2016). https://doi.org/10.1038/cddis.2016.97
86 Rivas, F. V., O'Keefe, J. P., Alegre, M. L. & Gajewski, T. F. Actin cytoskeleton regulates calcium dynamics and NFAT nuclear duration. *Mol Cell Biol* **24**, 1628–1639 (2004). https://doi.org/10.1128/MCB.24.4.1628-1639.2004
87 Carr, E. L. *et al.* Glutamine uptake and metabolism are coordinately regulated by ERK/MAPK during T lymphocyte activation. *J Immunol* **185**, 1037–1044 (2010). https://doi.org/10.4049/jimmunol.0903586
88 Schmidl, C., Delacher, M., Huehn, J. & Feuerer, M. Epigenetic mechanisms regulating T-cell responses. *J Allergy Clin Immunol* **142**, 728–743 (2018). https://doi.org/10.1016/j.jaci.2018.07.014
89 Russ, B. E. *et al.* Distinct epigenetic signatures delineate transcriptional programs during virus-specific CD8(+) T cell differentiation. *Immunity* **41**, 853–865 (2014). https://doi.org/10.1016/j.immuni.2014.11.001
90 Zehn, D., King, C., Bevan, M. J. & Palmer, E. TCR signaling requirements for activating T cells and for generating memory. *Cell Mol Life Sci* **69**, 1565–1575 (2012). https://doi.org/10.1007/s00018-012-0965-x
91 Van Der Byl, W. *et al.* The CD8(+) T cell tolerance checkpoint triggers a distinct differentiation state defined by protein translation defects. *Immunity* **57**, 1324–1344 e1328 (2024). https://doi.org/10.1016/j.immuni.2024.04.026
92 Sallusto, F., Lenig, D., Forster, R., Lipp, M. & Lanzavecchia, A. Two subsets of memory T lymphocytes with distinct homing potentials and effector functions. *Nature* **401**, 708–712 (1999). https://doi.org/10.1038/44385
93 Kaech, S. M. & Cui, W. Transcriptional control of effector and memory CD8+ T cell differentiation. *Nat Rev Immunol* **12**, 749–761 (2012). https://doi.org/10.1038/nri3307
94 Chang, J. T., Wherry, E. J. & Goldrath, A. W. Molecular regulation of effector and memory T cell differentiation. *Nat Immunol* **15**, 1104–1115 (2014). https://doi.org/10.1038/ni.3031
95 Xu, T., Pereira, R. M. & Martinez, G. J. An Updated Model for the Epigenetic Regulation of Effector and Memory CD8(+) T Cell Differentiation. *J Immunol* **207**, 1497–1505 (2021). https://doi.org/10.4049/jimmunol.2100633
96 Chen, Y., Zander, R., Khatun, A., Schauder, D. M. & Cui, W. Transcriptional and Epigenetic Regulation of Effector and Memory CD8 T Cell Differentiation. *Front Immunol* **9**, 2826 (2018). https://doi.org/10.3389/fimmu.2018.02826

97 Kaech, S. M. & Wherry, E. J. Heterogeneity and cell-fate decisions in effector and memory CD8+ T cell differentiation during viral infection. *Immunity* **27**, 393–405 (2007). https://doi.org/10.1016/j.immuni.2007.08.007
98 Philip, M. & Schietinger, A. CD8(+) T cell differentiation and dysfunction in cancer. *Nat Rev Immunol* **22**, 209–223 (2022). https://doi.org/10.1038/s41577-021-00574-3
99 Oliaro, J. *et al.* Asymmetric cell division of T cells upon antigen presentation uses multiple conserved mechanisms. *J Immunol* **185**, 367–375 (2010). https://doi.org/10.4049/jimmunol.0903627
100 Chang, J. T. *et al.* Asymmetric T lymphocyte division in the initiation of adaptive immune responses. *Science* **315**, 1687–1691 (2007). https://doi.org/10.1126/science.1139393
101 Chung, H. K., McDonald, B. & Kaech, S. M. The architectural design of CD8+ T cell responses in acute and chronic infection: Parallel structures with divergent fates. *J Exp Med* **218** (2021). https://doi.org/10.1084/jem.20201730
102 Youngblood, B. *et al.* Effector CD8 T cells dedifferentiate into long-lived memory cells. *Nature* **552**, 404–409 (2017). https://doi.org/10.1038/nature25144
103 Henning, A. N., Roychoudhuri, R. & Restifo, N. P. Epigenetic control of CD8(+) T cell differentiation. *Nat Rev Immunol* **18**, 340–356 (2018). https://doi.org/10.1038/nri.2017.146
104 Zehn, D., Thimme, R., Lugli, E., de Almeida, G. P. & Oxenius, A. 'Stem-like' precursors are the fount to sustain persistent CD8(+) T cell responses. *Nat Immunol* **23**, 836–847 (2022). https://doi.org/10.1038/s41590-022-01219-w
105 Parish, I. A. & Kaech, S. M. Diversity in CD8(+) T cell differentiation. *Curr Opin Immunol* **21**, 291–297 (2009). https://doi.org/10.1016/j.coi.2009.05.008
106 McManus, D. T. *et al.* An early precursor CD8(+) T cell that adapts to acute or chronic viral infection. *Nature* **640**, 772–781 (2025). https://doi.org/10.1038/s41586-024-08562-y
107 Dutko, F. J. & Oldstone, M. B. Genomic and biological variation among commonly used lymphocytic choriomeningitis virus strains. *J Gen Virol* **64 (Pt 8)**, 1689–1698 (1983). https://doi.org/10.1099/0022-1317-64-8-1689
108 Wherry, E. J. & Ahmed, R. Memory CD8 T-cell differentiation during viral infection. *J Virol* **78**, 5535–5545 (2004). https://doi.org/10.1128/JVI.78.11.5535-5545.2004
109 Turner, D. L., Cauley, L. S., Khanna, K. M. & Lefrancois, L. Persistent antigen presentation after acute vesicular stomatitis virus infection. *J Virol* **81**, 2039–2046 (2007). https://doi.org/10.1128/JVI.02167-06
110 Kakaradov, B. *et al.* Early transcriptional and epigenetic regulation of CD8(+) T cell differentiation revealed by single-cell RNA sequencing. *Nat Immunol* **18**, 422–432 (2017). https://doi.org/10.1038/ni.3688
111 Abadie, K. *et al.* Reversible, tunable epigenetic silencing of TCF1 generates flexibility in the T cell memory decision. *Immunity* **57**, 271–286 e213 (2024). https://doi.org/10.1016/j.immuni.2023.12.006
112 Pandit, A. & De Boer, R. J. Stochastic Inheritance of Division and Death Times Determines the Size and Phenotype of CD8(+) T Cell Families. *Front Immunol* **10**, 436 (2019). https://doi.org/10.3389/fimmu.2019.00436
113 Buchholz, V. R. *et al.* Disparate individual fates compose robust CD8+ T cell immunity. *Science* **340**, 630–635 (2013). https://doi.org/10.1126/science.1235454
114 Gattinoni, L. *et al.* Wnt signaling arrests effector T cell differentiation and generates CD8+ memory stem cells. *Nat Med* **15**, 808–813 (2009). https://doi.org/10.1038/nm.1982
115 Kaech, S. M. *et al.* Selective expression of the interleukin 7 receptor identifies effector CD8 T cells that give rise to long-lived memory cells. *Nat Immunol* **4**, 1191–1198 (2003). https://doi.org/10.1038/ni1009
116 Rutishauser, R. L. *et al.* Transcriptional repressor Blimp-1 promotes CD8(+) T cell terminal differentiation and represses the acquisition of central memory T cell properties. *Immunity* **31**, 296–308 (2009).

117 Joshi, N. S. *et al.* Inflammation directs memory precursor and short-lived effector CD8(+) T cell fates via the graded expression of T-bet transcription factor. *Immunity* **27**, 281–295 (2007). https://doi.org/10.1016/j.immuni.2007.07.010
118 Huster, K. M. *et al.* Selective expression of IL-7 receptor on memory T cells identifies early CD40L-dependent generation of distinct CD8+ memory T cell subsets. *Proc Natl Acad Sci U S A* **101**, 5610–5615 (2004). https://doi.org/10.1073/pnas.0308054101
119 Silva, J. G. *et al.* Emergence and fate of stem cell-like Tcf7(+) CD8(+) T cells during a primary immune response to viral infection. *Sci Immunol* **8**, eadh3113 (2023). https://doi.org/10.1126/sciimmunol.adh3113
120 Johnnidis, J. B. *et al.* Inhibitory signaling sustains a distinct early memory CD8(+) T cell precursor that is resistant to DNA damage. *Sci Immunol* **6** (2021). https://doi.org/10.1126/sciimmunol.abe3702
121 Pais Ferreira, D. *et al.* Central memory CD8(+) T cells derive from stem-like Tcf7(hi) effector cells in the absence of cytotoxic differentiation. *Immunity* **53**, 985–1000 e1011 (2020). https://doi.org/10.1016/j.immuni.2020.09.005
122 Remmerswaal, E. B. M. *et al.* Expression of IL-7Ralpha and KLRG1 defines functionally distinct CD8(+) T-cell populations in humans. *Eur J Immunol* **49**, 694–708 (2019). https://doi.org/10.1002/eji.201847897
123 Sandu, I. & Oxenius, A. T-cell heterogeneity, progenitor-progeny relationships, and function during latent and chronic viral infections. *Immunol Rev* **316**, 136–159 (2023). https://doi.org/10.1111/imr.13203
124 Wojciechowski, S. *et al.* Bim mediates apoptosis of CD127(lo) effector T cells and limits T cell memory. *Eur J Immunol* **36**, 1694–1706 (2006). https://doi.org/10.1002/eji.200635897
125 Soerens, A. G. *et al.* Functional T cells are capable of supernumerary cell division and longevity. *Nature* **614**, 762–766 (2023). https://doi.org/10.1038/s41586-022-05626-9
126 Rai, D., Martin, M. D. & Badovinac, V. P. The longevity of memory CD8 T cell responses after repetitive antigen stimulations. *J Immunol* **192**, 5652–5659 (2014). https://doi.org/10.4049/jimmunol.1301063
127 Moioffer, S. J. *et al.* Inefficient Recovery of Repeatedly Stimulated Memory CD8 T Cells after Polymicrobial Sepsis Induction Leads to Changes in Memory CD8 T Cell Pool Composition. *J Immunol* **210**, 168–179 (2023). https://doi.org/10.4049/jimmunol.2200676
128 Badovinac, V. P., Porter, B. B. & Harty, J. T. Programmed contraction of CD8(+) T cells after infection. *Nat Immunol* **3**, 619–626 (2002). https://doi.org/10.1038/ni804
129 Porter, B. B. & Harty, J. T. The onset of CD8+-T-cell contraction is influenced by the peak of Listeria monocytogenes infection and antigen display. *Infect Immun* **74**, 1528–1536 (2006). https://doi.org/10.1128/IAI.74.3.1528-1536.2006
130 Jameson, S. C. & Masopust, D. Understanding Subset Diversity in T Cell Memory. *Immunity* **48**, 214–226 (2018). https://doi.org/10.1016/j.immuni.2018.02.010
131 Aktas, E., Kucuksezer, U. C., Bilgic, S., Erten, G. & Deniz, G. Relationship between CD107a expression and cytotoxic activity. *Cell Immunol* **254**, 149–154 (2009). https://doi.org/10.1016/j.cellimm.2008.08.007
132 Trapani, J. A. & Smyth, M. J. Functional significance of the perforin/granzyme cell death pathway. *Nat Rev Immunol* **2**, 735–747 (2002). https://doi.org/10.1038/nri911
133 Betts, M. R. & Koup, R. A. Detection of T-cell degranulation: CD107a and b. *Methods Cell Biol* **75**, 497–512 (2004). https://doi.org/10.1016/s0091-679x(04)75020-7
134 Thomas, D. A., Scorrano, L., Putcha, G. V., Korsmeyer, S. J. & Ley, T. J. Granzyme B can cause mitochondrial depolarization and cell death in the absence of BID, BAX, and BAK. *Proc Natl Acad Sci U S A* **98**, 14985–14990 (2001). https://doi.org/10.1073/pnas.261581498
135 Suzuki, I. & Fink, P. J. The dual functions of fas ligand in the regulation of peripheral CD8+ and CD4+ T cells. *Proc Natl Acad Sci U S A* **97**, 1707–1712 (2000). https://doi.org/10.1073/pnas.97.4.1707

136 Li, H., Zhu, H., Xu, C. J. & Yuan, J. Cleavage of BID by caspase 8 mediates the mitochondrial damage in the Fas pathway of apoptosis. *Cell* **94**, 491–501 (1998). https://doi.org/10.1016/s0092-8674(00)81590-1
137 Fujimoto, I., Takizawa, T., Ohba, Y. & Nakanishi, Y. Co-expression of Fas and Fas-ligand on the surface of influenza virus-infected cells. *Cell Death Differ* **5**, 426–431 (1998). https://doi.org/10.1038/sj.cdd.4400362
138 Gerlach, C. *et al.* The Chemokine Receptor CX3CR1 Defines Three Antigen-Experienced CD8 T Cell Subsets with Distinct Roles in Immune Surveillance and Homeostasis. *Immunity* **45**, 1270–1284 (2016). https://doi.org/10.1016/j.immuni.2016.10.018
139 Duckworth, B. C. *et al.* Effector and stem-like memory cell fates are imprinted in distinct lymph node niches directed by CXCR3 ligands. *Nat Immunol* **22**, 434–448 (2021). https://doi.org/10.1038/s41590-021-00878-5
140 Choi, H., Song, H. & Jung, Y. W. The Roles of CCR7 for the Homing of Memory CD8+ T Cells into Their Survival Niches. *Immune Netw* **20**, e20 (2020). https://doi.org/10.4110/in.2020.20.e20
141 Martinez, G. J. *et al.* The transcription factor NFAT promotes exhaustion of activated CD8(+) T cells. *Immunity* **42**, 265–278 (2015). https://doi.org/10.1016/j.immuni.2015.01.006
142 Kalia, V. *et al.* Prolonged interleukin-2Ralpha expression on virus-specific CD8+ T cells favors terminal-effector differentiation in vivo. *Immunity* **32**, 91–103 (2010). https://doi.org/10.1016/j.immuni.2009.11.010
143 Chang, J. T. *et al.* Asymmetric proteasome segregation as a mechanism for unequal partitioning of the transcription factor T-bet during T lymphocyte division. *Immunity* **34**, 492–504 (2011). https://doi.org/10.1016/j.immuni.2011.03.017
144 Gago da Graca, C. *et al.* Stem-like memory and precursors of exhausted T cells share a common progenitor defined by ID3 expression. *Sci Immunol* **10**, eadn1945 (2025). https://doi.org/10.1126/sciimmunol.adn1945
145 Chu, T. *et al.* Precursors of exhausted T cells are preemptively formed in acute infection. *Nature* (2025). https://doi.org/10.1038/s41586-024-08451-4
146 Crompton, J. G. *et al.* Lineage relationship of CD8(+) T cell subsets is revealed by progressive changes in the epigenetic landscape. *Cell Mol Immunol* **13**, 502–513 (2016). https://doi.org/10.1038/cmi.2015.32
147 Jarjour, N. N. *et al.* Collaboration between IL-7 and IL-15 enables adaptation of tissue-resident and circulating memory CD8(+) T cells. *bioRxiv* (2024). https://doi.org/10.1101/2024.05.31.596695
148 Rubinstein, M. P. *et al.* IL-7 and IL-15 differentially regulate CD8+ T-cell subsets during contraction of the immune response. *Blood* **112**, 3704–3712 (2008). https://doi.org/10.1182/blood-2008-06-160945
149 Kimura, M. Y. *et al.* IL-7 signaling must be intermittent, not continuous, during CD8(+) T cell homeostasis to promote cell survival instead of cell death. *Nat Immunol* **14**, 143–151 (2013). https://doi.org/10.1038/ni.2494
150 Nolz, J. C. & Richer, M. J. Control of memory CD8(+) T cell longevity and effector functions by IL-15. *Mol Immunol* **117**, 180–188 (2020). https://doi.org/10.1016/j.molimm.2019.11.011
151 Fann, M. *et al.* Histone acetylation is associated with differential gene expression in the rapid and robust memory CD8(+) T-cell response. *Blood* **108**, 3363–3370 (2006). https://doi.org/10.1182/blood-2006-02-005520
152 Araki, Y., Fann, M., Wersto, R. & Weng, N. P. Histone acetylation facilitates rapid and robust memory CD8 T cell response through differential expression of effector molecules (eomesodermin and its targets: perforin and granzyme B). *J Immunol* **180**, 8102–8108 (2008). https://doi.org/10.4049/jimmunol.180.12.8102
153 Chen, G. *et al.* Ezh2 Regulates Activation-Induced CD8(+) T Cell Cycle Progression via Repressing Cdkn2a and Cdkn1c Expression. *Front Immunol* **9**, 549 (2018). https://doi.org/10.3389/fimmu.2018.00549

154 Scott-Browne, J. P. *et al.* Dynamic Changes in Chromatin Accessibility Occur in CD8(+) T Cells Responding to Viral Infection. *Immunity* **45**, 1327–1340 (2016). https://doi.org/10.1016/j.immuni.2016.10.028
155 Bottcher, J. P. *et al.* Functional classification of memory CD8(+) T cells by CX3CR1 expression. *Nat Commun* **6**, 8306 (2015). https://doi.org/10.1038/ncomms9306
156 Gebhardt, T. *et al.* Memory T cells in nonlymphoid tissue that provide enhanced local immunity during infection with herpes simplex virus. *Nat Immunol* **10**, 524–530 (2009). https://doi.org/10.1038/ni.1718
157 Masopust, D. *et al.* Dynamic T cell migration program provides resident memory within intestinal epithelium. *J Exp Med* **207**, 553–564 (2010). https://doi.org/10.1084/jem.20090858
158 Schenkel, J. M., Fraser, K. A. & Masopust, D. Cutting edge: resident memory CD8 T cells occupy frontline niches in secondary lymphoid organs. *J Immunol* **192**, 2961–2964 (2014). https://doi.org/10.4049/jimmunol.1400003
159 Mackay, L. K. *et al.* Cutting edge: CD69 interference with sphingosine-1-phosphate receptor function regulates peripheral T cell retention. *J Immunol* **194**, 2059–2063 (2015). https://doi.org/10.4049/jimmunol.1402256
160 Park, S. L., Mackay, L. K. & Gebhardt, T. Distinct recirculation potential of CD69(+)CD103(-) and CD103(+) thymic memory CD8(+) T cells. *Immunol Cell Biol* **94**, 975–980 (2016). https://doi.org/10.1038/icb.2016.60
161 Mackay, L. K. *et al.* Hobit and Blimp1 instruct a universal transcriptional program of tissue residency in lymphocytes. *Science* **352**, 459–463 (2016). https://doi.org/10.1126/science.aad2035
162 Park, S. L. *et al.* Divergent molecular networks program functionally distinct CD8(+) skin-resident memory T cells. *Science* **382**, 1073–1079 (2023). https://doi.org/10.1126/science.adi8885
163 Wakim, L. M. *et al.* The molecular signature of tissue resident memory CD8 T cells isolated from the brain. *J Immunol* **189**, 3462–3471 (2012). https://doi.org/10.4049/jimmunol.1201305
164 Crowl, J. T. *et al.* Tissue-resident memory CD8(+) T cells possess unique transcriptional, epigenetic and functional adaptations to different tissue environments. *Nat Immunol* **23**, 1121–1131 (2022). https://doi.org/10.1038/s41590-022-01229-8
165 Bevington, S. L. *et al.* Inducible chromatin priming is associated with the establishment of immunological memory in T cells. *EMBO J* **35**, 515–535 (2016). https://doi.org/10.15252/embj.201592534
166 McDonald, B., Chick, B. Y., Hargreaves, D. C. & Kaech, S. M. Early Chromatin Remodeling Events in Acutely Stimulated CD8(+) T Cells. *Yale J Biol Med* **96**, 467–473 (2023). https://doi.org/10.59249/AXGU7370
167 Russ, B. E. *et al.* Active maintenance of CD8(+) T cell naivety through regulation of global genome architecture. *Cell Rep* **42**, 113301 (2023). https://doi.org/10.1016/j.celrep.2023.113301
168 Bennett, T. J., Udupa, V. A. V. & Turner, S. J. Running to Stand Still: Naive CD8(+) T Cells Actively Maintain a Program of Quiescence. *Int J Mol Sci* **21** (2020). https://doi.org/10.3390/ijms21249773
169 Turner, M. Regulation and function of poised mRNAs in lymphocytes. *Bioessays* **45**, e2200236 (2023). https://doi.org/10.1002/bies.202200236
170 Yukawa, M. *et al.* AP-1 activity induced by co-stimulation is required for chromatin opening during T cell activation. *J Exp Med* **217** (2020). https://doi.org/10.1084/jem.20182009
171 Bevington, S. L., Cauchy, P. & Cockerill, P. N. Chromatin priming elements establish immunological memory in T cells without activating transcription: T cell memory is maintained by DNA elements which stably prime inducible genes without activating steady state transcription. *Bioessays* **39** (2017). https://doi.org/10.1002/bies.201600184

172 Wolf, B. K. *et al.* Cooperation of chromatin remodeling SWI/SNF complex and pioneer factor AP-1 shapes 3D enhancer landscapes. *Nat Struct Mol Biol* **30**, 10–21 (2023). https://doi.org/10.1038/s41594-022-00880-x
173 Tsao, H. W. *et al.* Batf-mediated epigenetic control of effector CD8(+) T cell differentiation. *Sci Immunol* **7**, eabi4919 (2022). https://doi.org/10.1126/sciimmunol.abi4919
174 Wang, D. *et al.* The Transcription Factor Runx3 Establishes Chromatin Accessibility of cis-Regulatory Landscapes that Drive Memory Cytotoxic T Lymphocyte Formation. *Immunity* **48**, 659–674 e656 (2018). https://doi.org/10.1016/j.immuni.2018.03.028
175 Brenes, A. J., Lamond, A. I. & Cantrell, D. A. The Immunological Proteome Resource. *Nat Immunol* **24**, 731 (2023). https://doi.org/10.1038/s41590-023-01483-4
176 Fujisawa, S. *et al.* The transcription factor BATF pioneers the differentiation program of effector CD8(+) T cells through the interaction with IRF4. *Cell Rep* **44**, 116129 (2025). https://doi.org/10.1016/j.celrep.2025.116129
177 Intlekofer, A. M. *et al.* Effector and memory CD8+ T cell fate coupled by T-bet and eomesodermin. *Nat Immunol* **6**, 1236–1244 (2005). https://doi.org/10.1038/ni1268
178 Intlekofer, A. M. *et al.* Anomalous type 17 response to viral infection by CD8+ T cells lacking T-bet and eomesodermin. *Science* **321**, 408–411 (2008). https://doi.org/10.1126/science.1159806
179 Li, G. *et al.* T-Bet and Eomes Regulate the Balance between the Effector/Central Memory T Cells versus Memory Stem Like T Cells. *PLoS One* **8**, e67401 (2013). https://doi.org/10.1371/journal.pone.0067401
180 Sullivan, B. M., Juedes, A., Szabo, S. J., von Herrath, M. & Glimcher, L. H. Antigen-driven effector CD8 T cell function regulated by T-bet. *Proc Natl Acad Sci U S A* **100**, 15818–15823 (2003). https://doi.org/10.1073/pnas.2636938100
181 Beima, K. M. *et al.* T-bet binding to newly identified target gene promoters is cell type-independent but results in variable context-dependent functional effects. *J Biol Chem* **281**, 11992–12000 (2006). https://doi.org/10.1074/jbc.M513613200
182 Banerjee, A. *et al.* Cutting edge: The transcription factor eomesodermin enables CD8+ T cells to compete for the memory cell niche. *J Immunol* **185**, 4988–4992 (2010). https://doi.org/10.4049/jimmunol.1002042
183 Takemoto, N., Intlekofer, A. M., Northrup, J. T., Wherry, E. J. & Reiner, S. L. Cutting Edge: IL-12 inversely regulates T-bet and eomesodermin expression during pathogen-induced CD8+ T cell differentiation. *J Immunol* **177**, 7515–7519 (2006). https://doi.org/10.4049/jimmunol.177.11.7515
184 Kallies, A., Xin, A., Belz, G. T. & Nutt, S. L. Blimp-1 transcription factor is required for the differentiation of effector CD8(+) T cells and memory responses. *Immunity* **31**, 283–295 (2009). https://doi.org/10.1016/j.immuni.2009.06.021
185 Shin, H. M. *et al.* Epigenetic modifications induced by Blimp-1 Regulate CD8(+) T cell memory progression during acute virus infection. *Immunity* **39**, 661–675 (2013). https://doi.org/10.1016/j.immuni.2013.08.032
186 Kwon, H. *et al.* Analysis of interleukin-21-induced Prdm1 gene regulation reveals functional cooperation of STAT3 and IRF4 transcription factors. *Immunity* **31**, 941–952 (2009). https://doi.org/10.1016/j.immuni.2009.10.008
187 Xin, G. *et al.* A Critical Role of IL-21-Induced BATF in Sustaining CD8-T-Cell-Mediated Chronic Viral Control. *Cell Rep* **13**, 1118–1124 (2015). https://doi.org/10.1016/j.celrep.2015.09.069
188 Crotty, S., Johnston, R. J. & Schoenberger, S. P. Effectors and memories: Bcl-6 and Blimp-1 in T and B lymphocyte differentiation. *Nat Immunol* **11**, 114–120 (2010). https://doi.org/10.1038/ni.1837
189 Johnston, R. J. *et al.* Bcl6 and Blimp-1 are reciprocal and antagonistic regulators of T follicular helper cell differentiation. *Science* **325**, 1006–1010 (2009). https://doi.org/10.1126/science.1175870

190 Yang, C. Y. *et al.* The transcriptional regulators Id2 and Id3 control the formation of distinct memory CD8+ T cell subsets. *Nat Immunol* **12**, 1221–1229 (2011). https://doi.org/10.1038/ni.2158
191 Gong, D. & Malek, T. R. Cytokine-dependent Blimp-1 expression in activated T cells inhibits IL-2 production. *J Immunol* **178**, 242–252 (2007). https://doi.org/10.4049/jimmunol.178.1.242
192 Martins, G. A., Cimmino, L., Liao, J., Magnusdottir, E. & Calame, K. Blimp-1 directly represses Il2 and the Il2 activator Fos, attenuating T cell proliferation and survival. *J Exp Med* **205**, 1959–1965 (2008). https://doi.org/10.1084/jem.20080526
193 Nurieva, R. I. *et al.* Bcl6 mediates the development of T follicular helper cells. *Science* **325**, 1001–1005 (2009). https://doi.org/10.1126/science.1176676
194 Cui, W., Liu, Y., Weinstein, J. S., Craft, J. & Kaech, S. M. An interleukin-21-interleukin-10-STAT3 pathway is critical for functional maturation of memory CD8+ T cells. *Immunity* **35**, 792–805 (2011). https://doi.org/10.1016/j.immuni.2011.09.017
195 Ciucci, T., Vacchio, M. S. & Bosselut, R. A STAT3-dependent transcriptional circuitry inhibits cytotoxic gene expression in T cells. *Proc Natl Acad Sci U S A* **114**, 13236–13241 (2017). https://doi.org/10.1073/pnas.1711160114
196 Doherty, P. C. & Zinkernagel, R. M. T-cell-mediated immunopathology in viral infections. *Transplant Rev* **19**, 89–120 (1974). https://doi.org/10.1111/j.1600-065x.1974.tb00129.x
197 Duan, S. & Thomas, P. G. Balancing Immune Protection and Immune Pathology by CD8(+) T-Cell Responses to Influenza Infection. *Front Immunol* **7**, 25 (2016). https://doi.org/10.3389/fimmu.2016.00025
198 Wherry, E. J. & Kurachi, M. Molecular and cellular insights into T cell exhaustion. *Nat Rev Immunol* **15**, 486–499 (2015). https://doi.org/10.1038/nri3862
199 Liblau, R. S., Wong, F. S., Mars, L. T. & Santamaria, P. Autoreactive CD8 T cells in organ-specific autoimmunity: emerging targets for therapeutic intervention. *Immunity* **17**, 1–6 (2002). https://doi.org/10.1016/s1074-7613(02)00338-2
200 Walter, U. & Santamaria, P. CD8+ T cells in autoimmunity. *Curr Opin Immunol* **17**, 624–631 (2005). https://doi.org/10.1016/j.coi.2005.09.014
201 Nussing, S., Trapani, J. A. & Parish, I. A. Revisiting T Cell Tolerance as a Checkpoint Target for Cancer Immunotherapy. *Front Immunol* **11**, 589641 (2020). https://doi.org/10.3389/fimmu.2020.589641
202 Nossal, G. J. Negative selection of lymphocytes. *Cell* **76**, 229–239 (1994). https://doi.org/10.1016/0092-8674(94)90331-x
203 Xing, Y. & Hogquist, K. A. T-cell tolerance: central and peripheral. *Cold Spring Harb Perspect Biol* **4** (2012). https://doi.org/10.1101/cshperspect.a006957
204 Klein, L., Hinterberger, M., Wirnsberger, G. & Kyewski, B. Antigen presentation in the thymus for positive selection and central tolerance induction. *Nat Rev Immunol* **9**, 833–844 (2009). https://doi.org/10.1038/nri2669
205 Yates, A. J. Theories and quantification of thymic selection. *Front Immunol* **5**, 13 (2014). https://doi.org/10.3389/fimmu.2014.00013
206 Bouillet, P. *et al.* BH3-only Bcl-2 family member Bim is required for apoptosis of autoreactive thymocytes. *Nature* **415**, 922–926 (2002). https://doi.org/10.1038/415922a
207 Gray, D. H. *et al.* The BH3-only proteins Bim and Puma cooperate to impose deletional tolerance of organ-specific antigens. *Immunity* **37**, 451–462 (2012). https://doi.org/10.1016/j.immuni.2012.05.030
208 Enouz, S., Carrie, L., Merkler, D., Bevan, M. J. & Zehn, D. Autoreactive T cells bypass negative selection and respond to self-antigen stimulation during infection. *J Exp Med* **209**, 1769–1779 (2012). https://doi.org/10.1084/jem.20120905
209 Yu, W. *et al.* Clonal Deletion Prunes but Does Not Eliminate Self-Specific alphabeta CD8(+) T Lymphocytes. *Immunity* **42**, 929–941 (2015). https://doi.org/10.1016/j.immuni.2015.05.001
210 Bouneaud, C., Kourilsky, P. & Bousso, P. Impact of negative selection on the T cell repertoire reactive to a self-peptide: a large fraction of T cell clones escapes clonal

deletion. *Immunity* **13**, 829–840 (2000). https://doi.org/10.1016/s1074-7613(00)00080-7
211 Klein, L., Klugmann, M., Nave, K. A., Tuohy, V. K. & Kyewski, B. Shaping of the autoreactive T-cell repertoire by a splice variant of self protein expressed in thymic epithelial cells. *Nat Med* **6**, 56–61 (2000). https://doi.org/10.1038/71540
212 Anderson, A. C. *et al.* High frequency of autoreactive myelin proteolipid protein-specific T cells in the periphery of naive mice: mechanisms of selection of the self-reactive repertoire. *J Exp Med* **191**, 761–770 (2000). https://doi.org/10.1084/jem.191.5.761
213 Allen, S. *et al.* Promiscuous thymic expression of an autoantigen gene does not result in negative selection of pathogenic T cells. *J Immunol* **175**, 5759–5764 (2005). https://doi.org/10.4049/jimmunol.175.9.5759
214 Kedmi, R. & Littman, D. R. Antigen-presenting cells as specialized drivers of intestinal T cell functions. *Immunity* **57**, 2269–2279 (2024). https://doi.org/10.1016/j.immuni.2024.09.011
215 Nagler-Anderson, C. Man the barrier! Strategic defences in the intestinal mucosa. *Nat Rev Immunol* **1**, 59–67 (2001). https://doi.org/10.1038/35095573
216 Stamnaes, J. & Sollid, L. M. Celiac disease: Autoimmunity in response to food antigen. *Semin Immunol* **27**, 343–352 (2015). https://doi.org/10.1016/j.smim.2015.11.001
217 ElTanbouly, M. A. & Noelle, R. J. Rethinking peripheral T cell tolerance: checkpoints across a T cell's journey. *Nat Rev Immunol* **21**, 257–267 (2021). https://doi.org/10.1038/s41577-020-00454-2
218 Deeths, M. J., Kedl, R. M. & Mescher, M. F. CD8+ T cells become nonresponsive (anergic) following activation in the presence of costimulation. *J Immunol* **163**, 102–110 (1999).
219 Jenkins, M. K. & Schwartz, R. H. Antigen presentation by chemically modified splenocytes induces antigen-specific T cell unresponsiveness in vitro and in vivo. *J Exp Med* **165**, 302–319 (1987). https://doi.org/10.1084/jem.165.2.302
220 Kurts, C. *et al.* CD8 T cell ignorance or tolerance to islet antigens depends on antigen dose. *Proc Natl Acad Sci U S A* **96**, 12703–12707 (1999). https://doi.org/10.1073/pnas.96.22.12703
221 Parish, I. A. & Heath, W. R. Too dangerous to ignore: self-tolerance and the control of ignorant autoreactive T cells. *Immunol Cell Biol* **86**, 146–152 (2008). https://doi.org/10.1038/sj.icb.7100161
222 Forrester, J. V., Xu, H., Lambe, T. & Cornall, R. Immune privilege or privileged immunity? *Mucosal Immunol* **1**, 372–381 (2008). https://doi.org/10.1038/mi.2008.27
223 Zehn, D. & Bevan, M. J. T cells with low avidity for a tissue-restricted antigen routinely evade central and peripheral tolerance and cause autoimmunity. *Immunity* **25**, 261–270 (2006). https://doi.org/10.1016/j.immuni.2006.06.009
224 Kurts, C., Miller, J. F., Subramaniam, R. M., Carbone, F. R. & Heath, W. R. Major histocompatibility complex class I-restricted cross-presentation is biased towards high dose antigens and those released during cellular destruction. *J Exp Med* **188**, 409–414 (1998). https://doi.org/10.1084/jem.188.2.409
225 Salaman, M. R. & Gould, K. G. Breakdown of T-cell ignorance: The tolerance failure responsible for mainstream autoimmune diseases? *J Transl Autoimmun* **3**, 100070 (2020). https://doi.org/10.1016/j.jtauto.2020.100070
226 Ohashi, P. S. *et al.* Ablation of "tolerance" and induction of diabetes by virus infection in viral antigen transgenic mice. *Cell* **65**, 305–317 (1991). https://doi.org/10.1016/0092-8674(91)90164-t
227 Rojas, M. *et al.* Molecular mimicry and autoimmunity. *J Autoimmun* **95**, 100–123 (2018). https://doi.org/10.1016/j.jaut.2018.10.012
228 Suliman, B. A. Potential clinical implications of molecular mimicry-induced autoimmunity. *Immun Inflamm Dis* **12**, e1178 (2024). https://doi.org/10.1002/iid3.1178
229 Parish, I. A. *et al.* The molecular signature of CD8+ T cells undergoing deletional tolerance. *Blood* **113**, 4575–4585 (2009). https://doi.org/10.1182/blood-2008-10-185223

230 Hernandez, J., Aung, S., Redmond, W. L. & Sherman, L. A. Phenotypic and functional analysis of CD8(+) T cells undergoing peripheral deletion in response to cross-presentation of self-antigen. *J Exp Med* **194**, 707–717 (2001). https://doi.org/10.1084/jem.194.6.707
231 Schwartz, R. H. T Cell Anergy. *Annual Review of Immunology* **21**, 305–334 (2003). https://doi.org/10.1146/annurev.immunol.21.120601.141110
232 Davey, G. M. *et al.* Peripheral deletion of autoreactive CD8 T cells by cross presentation of self-antigen occurs by a Bcl-2-inhibitable pathway mediated by Bim. *J Exp Med* **196**, 947–955 (2002). https://doi.org/10.1084/jem.20020827
233 Kurts, C., Kosaka, H., Carbone, F. R., Miller, J. F. & Heath, W. R. Class I-restricted cross-presentation of exogenous self-antigens leads to deletion of autoreactive CD8(+) T cells. *J Exp Med* **186**, 239–245 (1997). https://doi.org/10.1084/jem.186.2.239
234 Marodon, G. & Rocha, B. Activation and 'deletion' of self-reactive mature and immature T cells during ontogeny of Mls-1a mice: implications for neonatal tolerance induction. *Int Immunol* **6**, 1899–1904 (1994). https://doi.org/10.1093/intimm/6.12.1899
235 Redmond, W. L., Marincek, B. C. & Sherman, L. A. Distinct requirements for deletion versus anergy during CD8 T cell peripheral tolerance in vivo. *J Immunol* **174**, 2046–2053 (2005). https://doi.org/10.4049/jimmunol.174.4.2046
236 Redmond, W. L., Hernandez, J. & Sherman, L. A. Deletion of naive CD8 T cells requires persistent antigen and is not programmed by an initial signal from the tolerogenic APC. *J Immunol* **171**, 6349–6354 (2003). https://doi.org/10.4049/jimmunol.171.12.6349
237 Pape, K. A., Merica, R., Mondino, A., Khoruts, A. & Jenkins, M. K. Direct evidence that functionally impaired CD4+ T cells persist in vivo following induction of peripheral tolerance. *J Immunol* **160**, 4719–4729 (1998).
238 Ardouin, L. *et al.* Broad and Largely Concordant Molecular Changes Characterize Tolerogenic and Immunogenic Dendritic Cell Maturation in Thymus and Periphery. *Immunity* **45**, 305–318 (2016). https://doi.org/10.1016/j.immuni.2016.07.019
239 Marchingo, J. M. *et al.* T cell signaling. Antigen affinity, costimulation, and cytokine inputs sum linearly to amplify T cell expansion. *Science* **346**, 1123–1127 (2014). https://doi.org/10.1126/science.1260044
240 Sakaguchi, S., Sakaguchi, N., Asano, M., Itoh, M. & Toda, M. Immunologic self-tolerance maintained by activated T cells expressing IL-2 receptor alpha-chains (CD25). Breakdown of a single mechanism of self-tolerance causes various autoimmune diseases. *J Immunol* **155**, 1151–1164 (1995).
241 Wildin, R. S. *et al.* X-linked neonatal diabetes mellitus, enteropathy and endocrinopathy syndrome is the human equivalent of mouse scurfy. *Nat Genet* **27**, 18–20 (2001). https://doi.org/10.1038/83707
242 Klawon, D. E. J. *et al.* Regulatory T cells constrain T cells of shared specificity to enforce tolerance during infection. *Science* **387**, eadk3248 (2025). https://doi.org/10.1126/science.adk3248
243 McNally, A., Hill, G. R., Sparwasser, T., Thomas, R. & Steptoe, R. J. CD4+CD25+ regulatory T cells control CD8+ T-cell effector differentiation by modulating IL-2 homeostasis. *Proc Natl Acad Sci U S A* **108**, 7529–7534 (2011). https://doi.org/10.1073/pnas.1103782108
244 Liu, Z. *et al.* Immune homeostasis enforced by co-localized effector and regulatory T cells. *Nature* **528**, 225–230 (2015). https://doi.org/10.1038/nature16169
245 Wong, H. S. *et al.* A local regulatory T cell feedback circuit maintains immune homeostasis by pruning self-activated T cells. *Cell* **184**, 3981–3997 e3922 (2021). https://doi.org/10.1016/j.cell.2021.05.028
246 Waithman, J., Gebhardt, T., Davey, G. M., Heath, W. R. & Carbone, F. R. Cutting edge: Enhanced IL-2 signaling can convert self-specific T cell response from tolerance to autoimmunity. *J Immunol* **180**, 5789–5793 (2008). https://doi.org/10.4049/jimmunol.180.9.5789

247 Qureshi, O. S. *et al.* Trans-endocytosis of CD80 and CD86: a molecular basis for the cell-extrinsic function of CTLA-4. *Science* **332**, 600–603 (2011). https://doi.org/10.1126/science.1202947
248 Fletcher, A. L., Malhotra, D. & Turley, S. J. Lymph node stroma broaden the peripheral tolerance paradigm. *Trends Immunol* **32**, 12–18 (2011). https://doi.org/10.1016/j.it.2010.11.002
249 Cao, P. *et al.* Myeloid-derived suppressor cells in transplantation tolerance induction. *Int Immunopharmacol* **83**, 106421 (2020). https://doi.org/10.1016/j.intimp.2020.106421
250 Schurich, A. *et al.* Dynamic regulation of CD8 T cell tolerance induction by liver sinusoidal endothelial cells. *J Immunol* **184**, 4107–4114 (2010). https://doi.org/10.4049/jimmunol.0902580
251 Guerder, S., Rincon, M. & Schmitt-Verhulst, A. M. Regulation of activator protein-1 and NF-kappa B in CD8+ T cells exposed to peripheral self-antigens. *J Immunol* **166**, 4399–4407 (2001). https://doi.org/10.4049/jimmunol.166.7.4399
252 Macian, F. *et al.* Transcriptional mechanisms underlying lymphocyte tolerance. *Cell* **109**, 719–731 (2002). https://doi.org/10.1016/s0092-8674(02)00767-5
253 Kang, S. M. *et al.* Transactivation by AP-1 is a molecular target of T cell clonal anergy. *Science* **257**, 1134–1138 (1992). https://doi.org/10.1126/science.257.5073.1134
254 Hugues, S. Dynamics of dendritic cell-T cell interactions: a role in T cell outcome. *Semin Immunopathol* **32**, 227–238 (2010). https://doi.org/10.1007/s00281-010-0211-2
255 Hugues, S. *et al.* Distinct T cell dynamics in lymph nodes during the induction of tolerance and immunity. *Nat Immunol* **5**, 1235–1242 (2004). https://doi.org/10.1038/ni1134
256 Tadokoro, C. E. *et al.* Regulatory T cells inhibit stable contacts between CD4+ T cells and dendritic cells in vivo. *J Exp Med* **203**, 505–511 (2006). https://doi.org/10.1084/jem.20050783
257 Tang, Q. *et al.* Visualizing regulatory T cell control of autoimmune responses in nonobese diabetic mice. *Nat Immunol* **7**, 83–92 (2006). https://doi.org/10.1038/ni1289
258 Marangoni, F. *et al.* The transcription factor NFAT exhibits signal memory during serial T cell interactions with antigen-presenting cells. *Immunity* **38**, 237–249 (2013). https://doi.org/10.1016/j.immuni.2012.09.012
259 Soto-Nieves, N. *et al.* Transcriptional complexes formed by NFAT dimers regulate the induction of T cell tolerance. *J Exp Med* **206**, 867–876 (2009). https://doi.org/10.1084/jem.20082731
260 Zheng, Y., Zha, Y., Driessens, G., Locke, F. & Gajewski, T. F. Transcriptional regulator early growth response gene 2 (Egr2) is required for T cell anergy in vitro and in vivo. *J Exp Med* **209**, 2157–2163 (2012). https://doi.org/10.1084/jem.20120342
261 Safford, M. *et al.* Egr-2 and Egr-3 are negative regulators of T cell activation. *Nat Immunol* **6**, 472–480 (2005). https://doi.org/10.1038/ni1193
262 Jeon, M. S. *et al.* Essential role of the E3 ubiquitin ligase Cbl-b in T cell anergy induction. *Immunity* **21**, 167–177 (2004). https://doi.org/10.1016/j.immuni.2004.07.013
263 Heissmeyer, V. *et al.* Calcineurin imposes T cell unresponsiveness through targeted proteolysis of signaling proteins. *Nat Immunol* **5**, 255–265 (2004). https://doi.org/10.1038/ni1047
264 Wiede, F. *et al.* T cell protein tyrosine phosphatase attenuates T cell signaling to maintain tolerance in mice. *J Clin Invest* **121**, 4758–4774 (2011). https://doi.org/10.1172/JCI59492
265 Zha, Y. *et al.* T cell anergy is reversed by active Ras and is regulated by diacylglycerol kinase-alpha. *Nat Immunol* **7**, 1166–1173 (2006). https://doi.org/10.1038/ni1394
266 Chen, J. *et al.* NR4A transcription factors limit CAR T cell function in solid tumours. *Nature* **567**, 530–534 (2019). https://doi.org/10.1038/s41586-019-0985-x
267 Liu, X. *et al.* Genome-wide analysis identifies NR4A1 as a key mediator of T cell dysfunction. *Nature* **567**, 525–529 (2019). https://doi.org/10.1038/s41586-019-0979-8
268 Goldberg, M. V. *et al.* Role of PD-1 and its ligand, B7-H1, in early fate decisions of CD8 T cells. *Blood* **110**, 186–192 (2007). https://doi.org/10.1182/blood-2006-12-062422

269 Tsushima, F. *et al.* Interaction between B7-H1 and PD-1 determines initiation and reversal of T-cell anergy. *Blood* **110**, 180–185 (2007). https://doi.org/10.1182/blood-2006-11-060087
270 Probst, H. C., McCoy, K., Okazaki, T., Honjo, T. & van den Broek, M. Resting dendritic cells induce peripheral CD8+ T cell tolerance through PD-1 and CTLA-4. *Nat Immunol* **6**, 280–286 (2005). https://doi.org/10.1038/ni1165
271 Okazaki, T. *et al.* PD-1 and LAG-3 inhibitory co-receptors act synergistically to prevent autoimmunity in mice. *J Exp Med* **208**, 395–407 (2011). https://doi.org/10.1084/jem.20100466
272 Keir, M. E., Freeman, G. J. & Sharpe, A. H. PD-1 regulates self-reactive CD8+ T cell responses to antigen in lymph nodes and tissues. *J Immunol* **179**, 5064–5070 (2007). https://doi.org/10.4049/jimmunol.179.8.5064
273 Sheppard, K. A. *et al.* PD-1 inhibits T-cell receptor induced phosphorylation of the ZAP70/CD3zeta signalosome and downstream signaling to PKCtheta. *FEBS Lett* **574**, 37–41 (2004). https://doi.org/10.1016/j.febslet.2004.07.083
274 Parry, R. V. *et al.* CTLA-4 and PD-1 receptors inhibit T-cell activation by distinct mechanisms. *Mol Cell Biol* **25**, 9543–9553 (2005). https://doi.org/10.1128/MCB.25.21.9543-9553.2005
275 Hui, E. *et al.* T cell costimulatory receptor CD28 is a primary target for PD-1-mediated inhibition. *Science* **355**, 1428–1433 (2017). https://doi.org/10.1126/science.aaf1292
276 Freeman, G. J. *et al.* Engagement of the PD-1 immunoinhibitory receptor by a novel B7 family member leads to negative regulation of lymphocyte activation. *J Exp Med* **192**, 1027–1034 (2000). https://doi.org/10.1084/jem.192.7.1027
277 Sharpe, A. H. & Pauken, K. E. The diverse functions of the PD1 inhibitory pathway. *Nat Rev Immunol* **18**, 153–167 (2018). https://doi.org/10.1038/nri.2017.108
278 Fife, B. T. *et al.* Interactions between PD-1 and PD-L1 promote tolerance by blocking the TCR-induced stop signal. *Nat Immunol* **10**, 1185–1192 (2009). https://doi.org/10.1038/ni.1790
279 Bevington, S. L. *et al.* Chromatin Priming Renders T Cell Tolerance-Associated Genes Sensitive to Activation below the Signaling Threshold for Immune Response Genes. *Cell Rep* **31**, 107748 (2020). https://doi.org/10.1016/j.celrep.2020.107748
280 Schietinger, A., Delrow, J. J., Basom, R. S., Blattman, J. N. & Greenberg, P. D. Rescued tolerant CD8 T cells are preprogrammed to reestablish the tolerant state. *Science* **335**, 723–727 (2012). https://doi.org/10.1126/science.1214277
281 Nelson, C. E. *et al.* Reprogramming responsiveness to checkpoint blockade in dysfunctional CD8 T cells. *Proc Natl Acad Sci U S A* **116**, 2640–2645 (2019). https://doi.org/10.1073/pnas.1810326116
282 Preston, G. C. *et al.* Single cell tuning of Myc expression by antigen receptor signal strength and interleukin-2 in T lymphocytes. *EMBO J* **34**, 2008–2024 (2015). https://doi.org/10.15252/embj.201490252
283 Baessler, A. & Vignali, D. A. A. T Cell Exhaustion. *Annu Rev Immunol* **42**, 179–206 (2024). https://doi.org/10.1146/annurev-immunol-090222-110914
284 Zajac, A. J. *et al.* Viral immune evasion due to persistence of activated T cells without effector function. *J Exp Med* **188**, 2205–2213 (1998). https://doi.org/10.1084/jem.188.12.2205
285 Moskophidis, D., Lechner, F., Pircher, H. & Zinkernagel, R. M. Virus persistence in acutely infected immunocompetent mice by exhaustion of antiviral cytotoxic effector T cells. *Nature* **362**, 758–761 (1993). https://doi.org/10.1038/362758a0
286 Blank, C. U. *et al.* Defining 'T cell exhaustion'. *Nat Rev Immunol* **19**, 665–674 (2019). https://doi.org/10.1038/s41577-019-0221-9
287 Philip, M. & Schietinger, A. Heterogeneity and fate choice: T cell exhaustion in cancer and chronic infections. *Curr Opin Immunol* **58**, 98–103 (2019). https://doi.org/10.1016/j.coi.2019.04.014

288 Hashimoto, M. *et al.* CD8 T Cell Exhaustion in Chronic Infection and Cancer: Opportunities for Interventions. *Annu Rev Med* **69**, 301–318 (2018). https://doi.org/10.1146/annurev-med-012017-043208
289 McKinney, E. F., Lee, J. C., Jayne, D. R., Lyons, P. A. & Smith, K. G. T-cell exhaustion, co-stimulation and clinical outcome in autoimmunity and infection. *Nature* **523**, 612–616 (2015). https://doi.org/10.1038/nature14468
290 Wiedeman, A. E. *et al.* Autoreactive CD8+ T cell exhaustion distinguishes subjects with slow type 1 diabetes progression. *J Clin Invest* **130**, 480–490 (2020). https://doi.org/10.1172/JCI126595
291 Wherry, E. J. *et al.* Molecular signature of CD8+ T cell exhaustion during chronic viral infection. *Immunity* **27**, 670–684 (2007). https://doi.org/10.1016/j.immuni.2007.09.006
292 Sen, D. R. *et al.* The epigenetic landscape of T cell exhaustion. *Science* **354**, 1165–1169 (2016). https://doi.org/10.1126/science.aae0491
293 Ma, R., Sun, J. H. & Wang, Y. Y. The role of transforming growth factor-beta (TGF-beta) in the formation of exhausted CD8 + T cells. *Clin Exp Med* **24**, 128 (2024). https://doi.org/10.1007/s10238-024-01394-0
294 Utzschneider, D. T. *et al.* High antigen levels induce an exhausted phenotype in a chronic infection without impairing T cell expansion and survival. *J Exp Med* **213**, 1819–1834 (2016). https://doi.org/10.1084/jem.20150598
295 Barber, D. L. *et al.* Restoring function in exhausted CD8 T cells during chronic viral infection. *Nature* **439**, 682–687 (2006). https://doi.org/10.1038/nature04444
296 Day, C. L. *et al.* PD-1 expression on HIV-specific T cells is associated with T-cell exhaustion and disease progression. *Nature* **443**, 350–354 (2006). https://doi.org/10.1038/nature05115
297 Blackburn, S. D. *et al.* Coregulation of CD8+ T cell exhaustion by multiple inhibitory receptors during chronic viral infection. *Nat Immunol* **10**, 29–37 (2009). https://doi.org/10.1038/ni.1679
298 Walunas, T. L. *et al.* CTLA-4 can function as a negative regulator of T cell activation. *Immunity* **1**, 405–413 (1994). https://doi.org/10.1016/1074-7613(94)90071-x
299 Fuertes Marraco, S. A., Neubert, N. J., Verdeil, G. & Speiser, D. E. Inhibitory Receptors Beyond T Cell Exhaustion. *Front Immunol* **6**, 310 (2015). https://doi.org/10.3389/fimmu.2015.00310
300 Bengsch, B. *et al.* Coexpression of PD-1, 2B4, CD160 and KLRG1 on exhausted HCV-specific CD8+ T cells is linked to antigen recognition and T cell differentiation. *PLoS Pathog* **6**, e1000947 (2010). https://doi.org/10.1371/journal.ppat.1000947
301 Chew, G. M. *et al.* TIGIT Marks Exhausted T Cells, Correlates with Disease Progression, and Serves as a Target for Immune Restoration in HIV and SIV Infection. *PLoS Pathog* **12**, e1005349 (2016). https://doi.org/10.1371/journal.ppat.1005349
302 Jones, R. B. *et al.* Tim-3 expression defines a novel population of dysfunctional T cells with highly elevated frequencies in progressive HIV-1 infection. *J Exp Med* **205**, 2763–2779 (2008). https://doi.org/10.1084/jem.20081398
303 Kaufmann, D. E. *et al.* Upregulation of CTLA-4 by HIV-specific CD4+ T cells correlates with disease progression and defines a reversible immune dysfunction. *Nat Immunol* **8**, 1246–1254 (2007). https://doi.org/10.1038/ni1515
304 Sakuishi, K. *et al.* Targeting Tim-3 and PD-1 pathways to reverse T cell exhaustion and restore anti-tumor immunity. *J Exp Med* **207**, 2187–2194 (2010). https://doi.org/10.1084/jem.20100643
305 Fourcade, J. *et al.* Upregulation of Tim-3 and PD-1 expression is associated with tumor antigen-specific CD8+ T cell dysfunction in melanoma patients. *J Exp Med* **207**, 2175–2186 (2010). https://doi.org/10.1084/jem.20100637
306 Scott, A. C. *et al.* TOX is a critical regulator of tumour-specific T cell differentiation. *Nature* **571**, 270–274 (2019). https://doi.org/10.1038/s41586-019-1324-y
307 Hor, J. L. *et al.* PD-1 controls differentiation, survival, and TCR affinity evolution of stem-like CD8+ T cells. *bioRxiv*, 2024.2008.2002.606241 (2024). https://doi.org/10.1101/2024.08.02.606241

308 Odorizzi, P. M., Pauken, K. E., Paley, M. A., Sharpe, A. & Wherry, E. J. Genetic absence of PD-1 promotes accumulation of terminally differentiated exhausted CD8+ T cells. *J Exp Med* **212**, 1125–1137 (2015). https://doi.org/10.1084/jem.20142237
309 Jin, X. *et al.* Dramatic rise in plasma viremia after CD8(+) T cell depletion in simian immunodeficiency virus-infected macaques. *J Exp Med* **189**, 991–998 (1999). https://doi.org/10.1084/jem.189.6.991
310 Schmitz, J. E. *et al.* Control of viremia in simian immunodeficiency virus infection by CD8+ lymphocytes. *Science* **283**, 857–860 (1999). https://doi.org/10.1126/science.283.5403.857
311 Alfei, F. *et al.* TOX reinforces the phenotype and longevity of exhausted T cells in chronic viral infection. *Nature* **571**, 265–269 (2019). https://doi.org/10.1038/s41586-019-1326-9
312 Beltra, J. C. *et al.* Developmental Relationships of Four Exhausted CD8(+) T Cell Subsets Reveals Underlying Transcriptional and Epigenetic Landscape Control Mechanisms. *Immunity* **52**, 825–841 e828 (2020). https://doi.org/10.1016/j.immuni.2020.04.014
313 Zhang, Z. *et al.* Pan-cancer landscape of T-cell exhaustion heterogeneity within the tumor microenvironment revealed a progressive roadmap of hierarchical dysfunction associated with prognosis and therapeutic efficacy. *EBioMedicine* **83**, 104207 (2022). https://doi.org/10.1016/j.ebiom.2022.104207
314 Giles, J. R. *et al.* Shared and distinct biological circuits in effector, memory and exhausted CD8(+) T cells revealed by temporal single-cell transcriptomics and epigenetics. *Nat Immunol* **23**, 1600–1613 (2022). https://doi.org/10.1038/s41590-022-01338-4
315 Daniel, B. *et al.* Divergent clonal differentiation trajectories of T cell exhaustion. *Nat Immunol* **23**, 1614–1627 (2022). https://doi.org/10.1038/s41590-022-01337-5
316 Kasmani, M. Y. *et al.* Clonal lineage tracing reveals mechanisms skewing CD8+ T cell fate decisions in chronic infection. *J Exp Med* **220** (2023). https://doi.org/10.1084/jem.20220679
317 Utzschneider, D. T. *et al.* Early precursor T cells establish and propagate T cell exhaustion in chronic infection. *Nat Immunol* **21**, 1256–1266 (2020). https://doi.org/10.1038/s41590-020-0760-z
318 Im, S. J. *et al.* Defining CD8+ T cells that provide the proliferative burst after PD-1 therapy. *Nature* **537**, 417–421 (2016). https://doi.org/10.1038/nature19330
319 Siddiqui, I. *et al.* Intratumoral Tcf1(+)PD-1(+)CD8(+) T Cells with Stem-like Properties Promote Tumor Control in Response to Vaccination and Checkpoint Blockade Immunotherapy. *Immunity* **50**, 195–211 e110 (2019). https://doi.org/10.1016/j.immuni.2018.12.021
320 Utzschneider, D. T. *et al.* T Cell Factor 1-Expressing Memory-like CD8(+) T Cells Sustain the Immune Response to Chronic Viral Infections. *Immunity* **45**, 415–427 (2016). https://doi.org/10.1016/j.immuni.2016.07.021
321 Tsui, C. *et al.* MYB orchestrates T cell exhaustion and response to checkpoint inhibition. *Nature* **609**, 354–360 (2022). https://doi.org/10.1038/s41586-022-05105-1
322 Paley, M. A. *et al.* Progenitor and terminal subsets of CD8+ T cells cooperate to contain chronic viral infection. *Science* **338**, 1220–1225 (2012). https://doi.org/10.1126/science.1229620
323 Leong, Y. A. *et al.* CXCR5(+) follicular cytotoxic T cells control viral infection in B cell follicles. *Nat Immunol* **17**, 1187–1196 (2016). https://doi.org/10.1038/ni.3543
324 He, R. *et al.* Follicular CXCR5- expressing CD8(+) T cells curtail chronic viral infection. *Nature* **537**, 412–428 (2016). https://doi.org/10.1038/nature19317
325 Hudson, W. H. *et al.* Proliferating Transitory T Cells with an Effector-like Transcriptional Signature Emerge from PD-1(+) Stem-like CD8(+) T Cells during Chronic Infection. *Immunity* **51**, 1043–1058 e1044 (2019). https://doi.org/10.1016/j.immuni.2019.11.002
326 Zander, R. & Cui, W. Exhausted CD8(+) T cells face a developmental fork in the road. *Trends Immunol* **44**, 276–286 (2023). https://doi.org/10.1016/j.it.2023.02.006

327 Raju, S. *et al.* Identification of a T-bet(hi) Quiescent Exhausted CD8 T Cell Subpopulation That Can Differentiate into TIM3(+)CX3CR1(+) Effectors and Memory-like Cells. *J Immunol* **206**, 2924–2936 (2021). https://doi.org/10.4049/jimmunol.2001348
328 Miller, B. C. *et al.* Subsets of exhausted CD8(+) T cells differentially mediate tumor control and respond to checkpoint blockade. *Nat Immunol* **20**, 326–336 (2019). https://doi.org/10.1038/s41590-019-0312-6
329 Zander, R. *et al.* CD4(+) T Cell Help Is Required for the Formation of a Cytolytic CD8(+) T Cell Subset that Protects against Chronic Infection and Cancer. *Immunity* **51**, 1028–1042 e1024 (2019). https://doi.org/10.1016/j.immuni.2019.10.009
330 Philip, M. *et al.* Chromatin states define tumour-specific T cell dysfunction and reprogramming. *Nature* **545**, 452–456 (2017). https://doi.org/10.1038/nature22367
331 Vignali, P. D. A. *et al.* Hypoxia drives CD39-dependent suppressor function in exhausted T cells to limit antitumor immunity. *Nat Immunol* **24**, 267–279 (2023). https://doi.org/10.1038/s41590-022-01379-9
332 Abdel-Hakeem, M. S. *et al.* Epigenetic scarring of exhausted T cells hinders memory differentiation upon eliminating chronic antigenic stimulation. *Nat Immunol* **22**, 1008–1019 (2021). https://doi.org/10.1038/s41590-021-00975-5
333 Yates, K. B. *et al.* Epigenetic scars of CD8(+) T cell exhaustion persist after cure of chronic infection in humans. *Nat Immunol* **22**, 1020–1029 (2021). https://doi.org/10.1038/s41590-021-00979-1
334 Tonnerre, P. *et al.* Differentiation of exhausted CD8(+) T cells after termination of chronic antigen stimulation stops short of achieving functional T cell memory. *Nat Immunol* **22**, 1030–1041 (2021). https://doi.org/10.1038/s41590-021-00982-6
335 Hensel, N. *et al.* Memory-like HCV-specific CD8(+) T cells retain a molecular scar after cure of chronic HCV infection. *Nat Immunol* **22**, 229–239 (2021). https://doi.org/10.1038/s41590-020-00817-w
336 Wieland, D. *et al.* TCF1(+) hepatitis C virus-specific CD8(+) T cells are maintained after cessation of chronic antigen stimulation. *Nat Commun* **8**, 15050 (2017). https://doi.org/10.1038/ncomms15050
337 Galletti, G. *et al.* Two subsets of stem-like CD8(+) memory T cell progenitors with distinct fate commitments in humans. *Nat Immunol* **21**, 1552–1562 (2020). https://doi.org/10.1038/s41590-020-0791-5
338 Utzschneider, D. T. *et al.* T cells maintain an exhausted phenotype after antigen withdrawal and population reexpansion. *Nat Immunol* **14**, 603–610 (2013). https://doi.org/10.1038/ni.2606
339 Vaeth, M. & Feske, S. NFAT control of immune function: New Frontiers for an Abiding Trooper. *F1000Res* **7**, 260 (2018). https://doi.org/10.12688/f1000research.13426.1
340 Man, K. *et al.* Transcription Factor IRF4 Promotes CD8(+) T Cell Exhaustion and Limits the Development of Memory-like T Cells during Chronic Infection. *Immunity* **47**, 1129–1141 e1125 (2017). https://doi.org/10.1016/j.immuni.2017.11.021
341 Wagle, M. V. *et al.* Antigen-driven EGR2 expression is required for exhausted CD8(+) T cell stability and maintenance. *Nat Commun* **12**, 2782 (2021). https://doi.org/10.1038/s41467-021-23044-9
342 Chen, Z. *et al.* TCF-1-Centered Transcriptional Network Drives an Effector versus Exhausted CD8 T Cell-Fate Decision. *Immunity* **51**, 840–855 e845 (2019). https://doi.org/10.1016/j.immuni.2019.09.013
343 Wu, T. *et al.* The TCF1-Bcl6 axis counteracts type I interferon to repress exhaustion and maintain T cell stemness. *Sci Immunol* **1** (2016). https://doi.org/10.1126/sciimmunol.aai8593
344 Staron, M. M. *et al.* The transcription factor FoxO1 sustains expression of the inhibitory receptor PD-1 and survival of antiviral CD8(+) T cells during chronic infection. *Immunity* **41**, 802–814 (2014). https://doi.org/10.1016/j.immuni.2014.10.013
345 Chen, Y. *et al.* BATF regulates progenitor to cytolytic effector CD8(+) T cell transition during chronic viral infection. *Nat Immunol* **22**, 996–1007 (2021). https://doi.org/10.1038/s41590-021-00965-7

346 McLane, L. M. *et al.* Role of nuclear localization in the regulation and function of T-bet and Eomes in exhausted CD8 T cells. *Cell Rep* **35**, 109120 (2021). https://doi.org/10.1016/j.celrep.2021.109120
347 Beltra, J. C. *et al.* Stat5 opposes the transcription factor Tox and rewires exhausted CD8(+) T cells toward durable effector-like states during chronic antigen exposure. *Immunity* **56**, 2699–2718 e2611 (2023). https://doi.org/10.1016/j.immuni.2023.11.005
348 Lukhele, S. *et al.* The transcription factor IRF2 drives interferon-mediated CD8(+) T cell exhaustion to restrict anti-tumor immunity. *Immunity* **55**, 2369–2385 e2310 (2022). https://doi.org/10.1016/j.immuni.2022.10.020
349 Khan, O. *et al.* TOX transcriptionally and epigenetically programs CD8(+) T cell exhaustion. *Nature* **571**, 211–218 (2019). https://doi.org/10.1038/s41586-019-1325-x
350 Seo, H. *et al.* TOX and TOX2 transcription factors cooperate with NR4A transcription factors to impose CD8(+) T cell exhaustion. *Proc Natl Acad Sci U S A* **116**, 12410–12415 (2019). https://doi.org/10.1073/pnas.1905675116
351 Kang, T. G. *et al.* Epigenetic regulators of clonal hematopoiesis control CD8 T cell stemness during immunotherapy. *Science* **386**, eadl4492 (2024). https://doi.org/10.1126/science.adl4492
352 Crispin, J. C. & Tsokos, G. C. Cancer immunosurveillance by CD8 T cells. *F1000Res* **9** (2020). https://doi.org/10.12688/f1000research.21150.1
353 Gebhardt, T., Park, S. L. & Parish, I. A. Stem-like exhausted and memory CD8(+) T cells in cancer. *Nat Rev Cancer* **23**, 780–798 (2023). https://doi.org/10.1038/s41568-023-00615-0
354 Schreiber, R. D., Old, L. J. & Smyth, M. J. Cancer immunoediting: integrating immunity's roles in cancer suppression and promotion. *Science* **331**, 1565–1570 (2011). https://doi.org/10.1126/science.1203486
355 Gallagher, M. P. *et al.* Long-term cancer risk of immunosuppressive regimens after kidney transplantation. *J Am Soc Nephrol* **21**, 852–858 (2010). https://doi.org/10.1681/ASN.2009101043
356 Alasfar, S. *et al.* Contemporary incidence and risk factors of post transplant Erythrocytosis in deceased donor kidney transplantation. *BMC Nephrol* **22**, 26 (2021). https://doi.org/10.1186/s12882-021-02231-2
357 Hanahan, D. & Weinberg, R. A. Hallmarks of cancer: the next generation. *Cell* **144**, 646–674 (2011). https://doi.org/10.1016/j.cell.2011.02.013
358 Bruni, D., Angell, H. K. & Galon, J. The immune contexture and Immunoscore in cancer prognosis and therapeutic efficacy. *Nat Rev Cancer* **20**, 662–680 (2020). https://doi.org/10.1038/s41568-020-0285-7
359 Salehi, S. *et al.* Disrupted priming within draining lymph nodes drives immune quiescence in gastric cancer. *bioRxiv* (2025). https://doi.org/10.1101/2025.05.05.651897
360 Zagorulya, M. *et al.* Tissue-specific abundance of interferon-gamma drives regulatory T cells to restrain DC1-mediated priming of cytotoxic T cells against lung cancer. *Immunity* **56**, 386–405 e310 (2023). https://doi.org/10.1016/j.immuni.2023.01.010
361 Horton, B. L. *et al.* Lack of CD8(+) T cell effector differentiation during priming mediates checkpoint blockade resistance in non-small cell lung cancer. *Sci Immunol* **6**, eabi8800 (2021). https://doi.org/10.1126/sciimmunol.abi8800
362 Rudloff, M. W. *et al.* Hallmarks of CD8(+) T cell dysfunction are established within hours of tumor antigen encounter before cell division. *Nat Immunol* **24**, 1527–1539 (2023). https://doi.org/10.1038/s41590-023-01578-y
363 Wicks, E. E. & Semenza, G. L. Hypoxia-inducible factors: cancer progression and clinical translation. *J Clin Invest* **132** (2022). https://doi.org/10.1172/JCI159839
364 Doedens, A. L. *et al.* Hypoxia-inducible factors enhance the effector responses of CD8(+) T cells to persistent antigen. *Nat Immunol* **14**, 1173–1182 (2013). https://doi.org/10.1038/ni.2714

365 Galon, J. *et al.* Type, density, and location of immune cells within human colorectal tumors predict clinical outcome. *Science* **313**, 1960–1964 (2006). https://doi.org/10.1126/science.1129139
366 Huang, Q. *et al.* The primordial differentiation of tumor-specific memory CD8(+) T cells as bona fide responders to PD-1/PD-L1 blockade in draining lymph nodes. *Cell* **185**, 4049–4066 e4025 (2022). https://doi.org/10.1016/j.cell.2022.09.020
367 Kallies, A., Zehn, D. & Utzschneider, D. T. Precursor exhausted T cells: key to successful immunotherapy? *Nat Rev Immunol* **20**, 128–136 (2020). https://doi.org/10.1038/s41577-019-0223-7
368 Fransen, M. F. *et al.* Tumor-draining lymph nodes are pivotal in PD-1/PD-L1 checkpoint therapy. *JCI Insight* **3** (2018). https://doi.org/10.1172/jci.insight.124507
369 Connolly, K. A. *et al.* A reservoir of stem-like CD8(+) T cells in the tumor-draining lymph node preserves the ongoing antitumor immune response. *Sci Immunol* **6**, eabg7836 (2021). https://doi.org/10.1126/sciimmunol.abg7836
370 Prokhnevska, N. *et al.* CD8(+) T cell activation in cancer comprises an initial activation phase in lymph nodes followed by effector differentiation within the tumor. *Immunity* **56**, 107–124 e105 (2023). https://doi.org/10.1016/j.immuni.2022.12.002
371 Jansen, C. S. *et al.* An intra-tumoral niche maintains and differentiates stem-like CD8 T cells. *Nature* **576**, 465–470 (2019). https://doi.org/10.1038/s41586-019-1836-5
372 Rahim, M. K. *et al.* Dynamic CD8(+) T cell responses to cancer immunotherapy in human regional lymph nodes are disrupted in metastatic lymph nodes. *Cell* **186**, 1127–1143 e1118 (2023). https://doi.org/10.1016/j.cell.2023.02.021
373 Kurtulus, S. *et al.* Checkpoint Blockade Immunotherapy Induces Dynamic Changes in PD-1(-)CD8(+) Tumor-Infiltrating T Cells. *Immunity* **50**, 181–194 e186 (2019). https://doi.org/10.1016/j.immuni.2018.11.014
374 Liu, B. *et al.* Temporal single-cell tracing reveals clonal revival and expansion of precursor exhausted T cells during anti-PD-1 therapy in lung cancer. *Nat Cancer* **3**, 108–121 (2022). https://doi.org/10.1038/s43018-021-00292-8
375 Caushi, J. X. *et al.* Transcriptional programs of neoantigen-specific TIL in anti-PD-1-treated lung cancers. *Nature* **596**, 126–132 (2021). https://doi.org/10.1038/s41586-021-03752-4
376 Oliveira, G. *et al.* Phenotype, specificity and avidity of antitumour CD8(+) T cells in melanoma. *Nature* **596**, 119–125 (2021). https://doi.org/10.1038/s41586-021-03704-y
377 Sade-Feldman, M. *et al.* Defining T Cell States Associated with Response to Checkpoint Immunotherapy in Melanoma. *Cell* **176**, 404 (2019). https://doi.org/10.1016/j.cell.2018.12.034
378 Schietinger, A. & Greenberg, P. D. Tolerance and exhaustion: defining mechanisms of T cell dysfunction. *Trends Immunol* **35**, 51–60 (2014). https://doi.org/10.1016/j.it.2013.10.001
379 Bandyopadhyay, S., Soto-Nieves, N. & Macian, F. Transcriptional regulation of T cell tolerance. *Semin Immunol* **19**, 180–187 (2007). https://doi.org/10.1016/j.smim.2007.02.006
380 Waugh, K. A., Leach, S. M. & Slansky, J. E. Targeting Transcriptional Regulators of CD8+ T Cell Dysfunction to Boost Anti-Tumor Immunity. *Vaccines (Basel)* **3**, 771–802 (2015). https://doi.org/10.3390/vaccines3030771
381 Schietinger, A. *et al.* Tumor-Specific T Cell Dysfunction Is a Dynamic Antigen-Driven Differentiation Program Initiated Early during Tumorigenesis. *Immunity* **45**, 389–401 (2016). https://doi.org/10.1016/j.immuni.2016.07.011
382 Pereira, R. M., Hogan, P. G., Rao, A. & Martinez, G. J. Transcriptional and epigenetic regulation of T cell hyporesponsiveness. *J Leukoc Biol* **102**, 601–615 (2017). https://doi.org/10.1189/jlb.2RI0317-097R
383 Aliahmad, P. *et al.* TOX provides a link between calcineurin activation and CD8 lineage commitment. *J Exp Med* **199**, 1089–1099 (2004). https://doi.org/10.1084/jem.20040051

384 Hiwa, R., Nielsen, H. V., Mueller, J. L., Mandla, R. & Zikherman, J. NR4A family members regulate T cell tolerance to preserve immune homeostasis and suppress autoimmunity. *JCI Insight* **6** (2021). https://doi.org/10.1172/jci.insight.151005
385 Hogan, P. G., Villalobos Reveles, B. & Arteaga Vazquez, L. J. TOX, through a glass, darkly. *Front Immunol* **16**, 1576468 (2025). https://doi.org/10.3389/fimmu.2025.1576468
386 Aliahmad, P., Seksenyan, A. & Kaye, J. The many roles of TOX in the immune system. *Curr Opin Immunol* **24**, 173–177 (2012). https://doi.org/10.1016/j.coi.2011.12.001
387 Yanai, H., Ban, T. & Taniguchi, T. Essential role of high-mobility group box proteins in nucleic acid-mediated innate immune responses. *J Intern Med* **270**, 301–308 (2011). https://doi.org/10.1111/j.1365-2796.2011.02433.x
388 Schilham, M. W. & Clevers, H. HMG box containing transcription factors in lymphocyte differentiation. *Semin Immunol* **10**, 127–132 (1998). https://doi.org/10.1006/smim.1998.0114
389 Carr, T. M., Wheaton, J. D., Houtz, G. M. & Ciofani, M. JunB promotes Th17 cell identity and restrains alternative CD4(+) T-cell programs during inflammation. *Nat Commun* **8**, 301 (2017). https://doi.org/10.1038/s41467-017-00380-3
390 Wilkinson, B. *et al.* TOX: an HMG box protein implicated in the regulation of thymocyte selection. *Nat Immunol* **3**, 272–280 (2002). https://doi.org/10.1038/ni767
391 Karlsson, M. *et al.* A single-cell type transcriptomics map of human tissues. *Sci Adv* **7** (2021). https://doi.org/10.1126/sciadv.abh2169
392 Lobbardi, R. *et al.* TOX Regulates Growth, DNA Repair, and Genomic Instability in T-cell Acute Lymphoblastic Leukemia. *Cancer Discov* **7**, 1336–1353 (2017). https://doi.org/10.1158/2159-8290.CD-17-0267
393 O'Flaherty, E. & Kaye, J. TOX defines a conserved subfamily of HMG-box proteins. *BMC Genomics* **4**, 13 (2003). https://doi.org/10.1186/1471-2164-4-13
394 Wang, L. & Bosselut, R. CD4-CD8 lineage differentiation: Thpok-ing into the nucleus. *J Immunol* **183**, 2903–2910 (2009). https://doi.org/10.4049/jimmunol.0901041
395 Liu, S. *et al.* TOX promotes follicular helper T cell differentiation in patients with primary Sjogren's syndrome. *Rheumatology (Oxford)* **62**, 946–957 (2023). https://doi.org/10.1093/rheumatology/keac304
396 Canaria, D. A. *et al.* Tox induces T cell IL-10 production in a BATF-dependent manner. *Front Immunol* **14**, 1275423 (2023). https://doi.org/10.3389/fimmu.2023.1275423
397 Xu, W. *et al.* The Transcription Factor Tox2 Drives T Follicular Helper Cell Development via Regulating Chromatin Accessibility. *Immunity* **51**, 826–839 e825 (2019). https://doi.org/10.1016/j.immuni.2019.10.006
398 Wu, C. J. *et al.* MiR-23~27~24-mediated control of humoral immunity reveals a TOX-driven regulatory circuit in follicular helper T cell differentiation. *Sci Adv* **5**, eaaw1715 (2019). https://doi.org/10.1126/sciadv.aaw1715
399 Seehus, C. R. & Kaye, J. The Role of TOX in the Development of Innate Lymphoid Cells. *Mediators Inflamm* **2015**, 243868 (2015). https://doi.org/10.1155/2015/243868
400 Yun, S. *et al.* TOX regulates the differentiation of human natural killer cells from hematopoietic stem cells in vitro. *Immunol Lett* **136**, 29–36 (2011). https://doi.org/10.1016/j.imlet.2010.11.008
401 Bordon, Y. TOX for tired T cells. *Nature Reviews Immunology* **19**, 476–476 (2019). https://doi.org/10.1038/s41577-019-0193-9
402 Yao, C. *et al.* Single-cell RNA-seq reveals TOX as a key regulator of CD8(+) T cell persistence in chronic infection. *Nat Immunol* **20**, 890–901 (2019). https://doi.org/10.1038/s41590-019-0403-4
403 Kim, C. G. *et al.* VEGF-A drives TOX-dependent T cell exhaustion in anti-PD-1-resistant microsatellite stable colorectal cancers. *Sci Immunol* **4** (2019). https://doi.org/10.1126/sciimmunol.aay0555
404 Maurice, N. J., Berner, J., Taber, A. K., Zehn, D. & Prlic, M. Inflammatory signals are sufficient to elicit TOX expression in mouse and human CD8+ T cells. *JCI Insight* **6** (2021). https://doi.org/10.1172/jci.insight.150744

405 Brenes, A. J. *et al.* Tissue environment, not ontogeny, defines murine intestinal intraepithelial T lymphocytes. *Elife* **10** (2021). https://doi.org/10.7554/eLife.70055
406 Sekine, T. *et al.* TOX is expressed by exhausted and polyfunctional human effector memory CD8(+) T cells. *Sci Immunol* **5** (2020). https://doi.org/10.1126/sciimmunol.aba7918
407 Aliahmad, P., de la Torre, B. & Kaye, J. Shared dependence on the DNA-binding factor TOX for the development of lymphoid tissue-inducer cell and NK cell lineages. *Nat Immunol* **11**, 945–952 (2010). https://doi.org/10.1038/ni.1930
408 Lee, W., Mitchell, P. & Tjian, R. Purified transcription factor AP-1 interacts with TPA-inducible enhancer elements. *Cell* **49**, 741–752 (1987). https://doi.org/10.1016/0092-8674(87)90612-x
409 Shaulian, E. & Karin, M. AP-1 as a regulator of cell life and death. *Nat Cell Biol* **4**, E131–136 (2002). https://doi.org/10.1038/ncb0502-e131
410 Shaulian, E. & Karin, M. AP-1 in cell proliferation and survival. *Oncogene* **20**, 2390–2400 (2001). https://doi.org/10.1038/sj.onc.1204383
411 Hess, J., Angel, P. & Schorpp-Kistner, M. AP-1 subunits: quarrel and harmony among siblings. *J Cell Sci* **117**, 5965–5973 (2004). https://doi.org/10.1242/jcs.01589
412 Eferl, R. & Wagner, E. F. AP-1: a double-edged sword in tumorigenesis. *Nat Rev Cancer* **3**, 859–868 (2003). https://doi.org/10.1038/nrc1209
413 Young, M. R. *et al.* Transgenic mice demonstrate AP-1 (activator protein-1) transactivation is required for tumor promotion. *Proc Natl Acad Sci U S A* **96**, 9827–9832 (1999). https://doi.org/10.1073/pnas.96.17.9827
414 Milde-Langosch, K. The Fos family of transcription factors and their role in tumourigenesis. *Eur J Cancer* **41**, 2449–2461 (2005). https://doi.org/10.1016/j.ejca.2005.08.008
415 Watt, A. C. *et al.* CDK4/6 inhibition reprograms the breast cancer enhancer landscape by stimulating AP-1 transcriptional activity. *Nat Cancer* **2**, 34–48 (2021). https://doi.org/10.1038/s43018-020-00135-y
416 Lynn, R. C. *et al.* c-Jun overexpression in CAR T cells induces exhaustion resistance. *Nature* **576**, 293–300 (2019). https://doi.org/10.1038/s41586-019-1805-z
417 Angel, P. *et al.* Phorbol ester-inducible genes contain a common cis element recognized by a TPA-modulated trans-acting factor. *Cell* **49**, 729–739 (1987). https://doi.org/10.1016/0092-8674(87)90611-8
418 Halazonetis, T. D., Georgopoulos, K., Greenberg, M. E. & Leder, P. c-Jun dimerizes with itself and with c-Fos, forming complexes of different DNA binding affinities. *Cell* **55**, 917–924 (1988). https://doi.org/10.1016/0092-8674(88)90147-x
419 Schutte, J. *et al.* jun-B inhibits and c-fos stimulates the transforming and trans-activating activities of c-jun. *Cell* **59**, 987–997 (1989). https://doi.org/10.1016/0092-8674(89)90755-1
420 Chen, M. *et al.* Emerging roles of activating transcription factor (ATF) family members in tumourigenesis and immunity: Implications in cancer immunotherapy. *Genes Dis* **9**, 981–999 (2022). https://doi.org/10.1016/j.gendis.2021.04.008
421 Kurokawa, H. *et al.* Structural basis of alternative DNA recognition by Maf transcription factors. *Mol Cell Biol* **29**, 6232–6244 (2009). https://doi.org/10.1128/MCB.00708-09
422 Foletta, V. C., Segal, D. H. & Cohen, D. R. Transcriptional regulation in the immune system: all roads lead to AP-1. *J Leukoc Biol* **63**, 139–152 (1998). https://doi.org/10.1002/jlb.63.2.139
423 Oughtred, R. *et al.* The BioGRID database: A comprehensive biomedical resource of curated protein, genetic, and chemical interactions. *Protein Sci* **30**, 187–200 (2021). https://doi.org/10.1002/pro.3978
424 Lee, W., Haslinger, A., Karin, M. & Tjian, R. Activation of transcription by two factors that bind promoter and enhancer sequences of the human metallothionein gene and SV40. *Nature* **325**, 368–372 (1987). https://doi.org/10.1038/325368a0

425 Jain, J., McCaffrey, P. G., Valge-Archer, V. E. & Rao, A. Nuclear factor of activated T cells contains Fos and Jun. *Nature* **356**, 801–804 (1992). https://doi.org/10.1038/356801a0
426 Ullman, K. S., Northrop, J. P., Admon, A. & Crabtree, G. R. Jun family members are controlled by a calcium-regulated, cyclosporin A-sensitive signaling pathway in activated T lymphocytes. *Genes Dev* **7**, 188–196 (1993). https://doi.org/10.1101/gad.7.2.188
427 Macian, F., Lopez-Rodriguez, C. & Rao, A. Partners in transcription: NFAT and AP-1. *Oncogene* **20**, 2476–2489 (2001). https://doi.org/10.1038/sj.onc.1204386
428 Phanstiel, D. H. *et al.* Static and Dynamic DNA Loops form AP-1-Bound Activation Hubs during Macrophage Development. *Mol Cell* **67**, 1037–1048 e1036 (2017). https://doi.org/10.1016/j.molcel.2017.08.006
429 Qiao, Y. *et al.* AP-1-mediated chromatin looping regulates ZEB2 transcription: new insights into TNFalpha-induced epithelial-mesenchymal transition in triple-negative breast cancer. *Oncotarget* **6**, 7804–7814 (2015). https://doi.org/10.18632/oncotarget.3158
430 St-Arnaud, R. & Quelo, I. Transcriptional coactivators potentiating AP-1 function in bone. *Front Biosci* **3**, d838–848 (1998). https://doi.org/10.2741/a327
431 Ogawa, S. *et al.* A nuclear receptor corepressor transcriptional checkpoint controlling activator protein 1-dependent gene networks required for macrophage activation. *Proc Natl Acad Sci U S A* **101**, 14461–14466 (2004). https://doi.org/10.1073/pnas.0405786101
432 Ng, K. W., Ridgway, P., Cohen, D. R. & Tremethick, D. J. The binding of a Fos/Jun heterodimer can completely disrupt the structure of a nucleosome. *EMBO J* **16**, 2072–2085 (1997). https://doi.org/10.1093/emboj/16.8.2072
433 Sheffield, N. C. *et al.* Patterns of regulatory activity across diverse human cell types predict tissue identity, transcription factor binding, and long-range interactions. *Genome Res* **23**, 777–788 (2013). https://doi.org/10.1101/gr.152140.112
434 Bejjani, F., Evanno, E., Zibara, K., Piechaczyk, M. & Jariel-Encontre, I. The AP-1 transcriptional complex: Local switch or remote command? *Biochim Biophys Acta Rev Cancer* **1872**, 11–23 (2019). https://doi.org/10.1016/j.bbcan.2019.04.003
435 Karin, M., Liu, Z. & Zandi, E. AP-1 function and regulation. *Curr Opin Cell Biol* **9**, 240–246 (1997). https://doi.org/10.1016/s0955-0674(97)80068-3
436 Cippitelli, M. *et al.* Negative transcriptional regulation of the interferon-gamma promoter by glucocorticoids and dominant negative mutants of c-Jun. *J Biol Chem* **270**, 12548–12556 (1995). https://doi.org/10.1074/jbc.270.21.12548
437 Kurachi, M. *et al.* The transcription factor BATF operates as an essential differentiation checkpoint in early effector CD8+ T cells. *Nat Immunol* **15**, 373–383 (2014). https://doi.org/10.1038/ni.2834
438 Sarkar, S. *et al.* JunB is required for CD8+ T cell responses to acute infections. *Int Immunol* (2024). https://doi.org/10.1093/intimm/dxae063
439 Ataide, M. A. *et al.* BATF3 programs CD8(+) T cell memory. *Nat Immunol* **21**, 1397–1407 (2020). https://doi.org/10.1038/s41590-020-0786-2
440 Maki, Y., Bos, T. J., Davis, C., Starbuck, M. & Vogt, P. K. Avian sarcoma virus 17 carries the jun oncogene. *Proc Natl Acad Sci U S A* **84**, 2848–2852 (1987). https://doi.org/10.1073/pnas.84.9.2848
441 Angel, P. *et al.* Oncogene jun encodes a sequence-specific trans-activator similar to AP-1. *Nature* **332**, 166–171 (1988). https://doi.org/10.1038/332166a0
442 Angel, P., Hattori, K., Smeal, T. & Karin, M. The jun proto-oncogene is positively autoregulated by its product, Jun/AP-1. *Cell* **55**, 875–885 (1988). https://doi.org/10.1016/0092-8674(88)90143-2
443 Vogt, P. K. Fortuitous convergences: the beginnings of JUN. *Nat Rev Cancer* **2**, 465–469 (2002). https://doi.org/10.1038/nrc818
444 Glover, J. N. & Harrison, S. C. Crystal structure of the heterodimeric bZIP transcription factor c-Fos-c-Jun bound to DNA. *Nature* **373**, 257–261 (1995). https://doi.org/10.1038/373257a0

445 Gentz, R., Rauscher, F. J., 3rd, Abate, C. & Curran, T. Parallel association of Fos and Jun leucine zippers juxtaposes DNA binding domains. *Science* **243**, 1695–1699 (1989). https://doi.org/10.1126/science.2494702
446 Chiu, R. *et al.* The c-Fos protein interacts with c-Jun/AP-1 to stimulate transcription of AP-1 responsive genes. *Cell* **54**, 541–552 (1988). https://doi.org/10.1016/0092-8674(88)90076-1
447 Ryder, K., Lau, L. F. & Nathans, D. A gene activated by growth factors is related to the oncogene v-jun. *Proc Natl Acad Sci U S A* **85**, 1487–1491 (1988). https://doi.org/10.1073/pnas.85.5.1487
448 Ryder, K., Lanahan, A., Perez-Albuerne, E. & Nathans, D. jun-D: a third member of the jun gene family. *Proc Natl Acad Sci U S A* **86**, 1500–1503 (1989). https://doi.org/10.1073/pnas.86.5.1500
449 Hirai, S. I., Ryseck, R. P., Mechta, F., Bravo, R. & Yaniv, M. Characterization of junD: a new member of the jun proto-oncogene family. *EMBO J* **8**, 1433–1439 (1989). https://doi.org/10.1002/j.1460-2075.1989.tb03525.x
450 Nakabeppu, Y., Ryder, K. & Nathans, D. DNA binding activities of three murine Jun proteins: stimulation by Fos. *Cell* **55**, 907–915 (1988). https://doi.org/10.1016/0092-8674(88)90146-8
451 Wisniewska, M. B. *et al.* Dimer composition and promoter context contribute to functional cooperation between AP-1 and NFAT. *J Mol Biol* **371**, 569–576 (2007). https://doi.org/10.1016/j.jmb.2007.05.079
452 Yazgan, O. & Pfarr, C. M. Regulation of two JunD isoforms by Jun N-terminal kinases. *J Biol Chem* **277**, 29710–29718 (2002). https://doi.org/10.1074/jbc.M204552200
453 Mechta-Grigoriou, F., Gerald, D. & Yaniv, M. The mammalian Jun proteins: redundancy and specificity. *Oncogene* **20**, 2378–2389 (2001). https://doi.org/10.1038/sj.onc.1204381
454 Kallunki, T., Deng, T., Hibi, M. & Karin, M. c-Jun can recruit JNK to phosphorylate dimerization partners via specific docking interactions. *Cell* **87**, 929–939 (1996). https://doi.org/10.1016/s0092-8674(00)81999-6
455 Bogoyevitch, M. A. & Kobe, B. Uses for JNK: the many and varied substrates of the c-Jun N-terminal kinases. *Microbiol Mol Biol Rev* **70**, 1061–1095 (2006). https://doi.org/10.1128/MMBR.00025-06
456 Ryseck, R. P. & Bravo, R. c-JUN, JUN B, and JUN D differ in their binding affinities to AP-1 and CRE consensus sequences: effect of FOS proteins. *Oncogene* **6**, 533–542 (1991).
457 Hilberg, F., Aguzzi, A., Howells, N. & Wagner, E. F. c-jun is essential for normal mouse development and hepatogenesis. *Nature* **365**, 179–181 (1993). https://doi.org/10.1038/365179a0
458 Schorpp-Kistner, M., Wang, Z. Q., Angel, P. & Wagner, E. F. JunB is essential for mammalian placentation. *EMBO J* **18**, 934–948 (1999). https://doi.org/10.1093/emboj/18.4.934
459 Thepot, D. *et al.* Targeted disruption of the murine junD gene results in multiple defects in male reproductive function. *Development* **127**, 143–153 (2000). https://doi.org/10.1242/dev.127.1.143
460 Passegue, E., Jochum, W., Behrens, A., Ricci, R. & Wagner, E. F. JunB can substitute for Jun in mouse development and cell proliferation. *Nat Genet* **30**, 158–166 (2002). https://doi.org/10.1038/ng790
461 Xia, Y. in *Gene Expression and Regulation* (ed Jun Ma) 219–237 (Springer New York, 2006).
462 Jain, J., Valge-Archer, V. E. & Rao, A. Analysis of the AP-1 sites in the IL-2 promoter. *J Immunol* **148**, 1240–1250 (1992).
463 Jain, J., Valge-Archer, V. E., Sinskey, A. J. & Rao, A. The AP-1 site at -150 bp, but not the NF-kappa B site, is likely to represent the major target of protein kinase C in the interleukin 2 promoter. *J Exp Med* **175**, 853–862 (1992). https://doi.org/10.1084/jem.175.3.853

464 Lee, J. U., Kim, L. K. & Choi, J. M. Revisiting the Concept of Targeting NFAT to Control T Cell Immunity and Autoimmune Diseases. *Front Immunol* **9**, 2747 (2018). https://doi.org/10.3389/fimmu.2018.02747
465 Ishihara, S. & Schwartz, R. H. Two-step binding of transcription factors causes sequential chromatin structural changes at the activated IL-2 promoter. *J Immunol* **187**, 3292–3299 (2011). https://doi.org/10.4049/jimmunol.1003173
466 Scharer, C. D., Barwick, B. G., Youngblood, B. A., Ahmed, R. & Boss, J. M. Global DNA methylation remodeling accompanies CD8 T cell effector function. *J Immunol* **191**, 3419–3429 (2013). https://doi.org/10.4049/jimmunol.1301395
467 Smith, N. P. *et al.* Resident memory T cell development is gradual and shows AP-1 gene expression in mature cells. *JCI Insight* **10** (2025). https://doi.org/10.1172/jci.insight.187381
468 Meixner, A., Karreth, F., Kenner, L. & Wagner, E. F. JunD regulates lymphocyte proliferation and T helper cell cytokine expression. *EMBO J* **23**, 1325–1335 (2004). https://doi.org/10.1038/sj.emboj.7600133
469 Ruppert, S. M. *et al.* JunD/AP-1-mediated gene expression promotes lymphocyte growth dependent on interleukin-7 signal transduction. *PLoS One* **7**, e32262 (2012). https://doi.org/10.1371/journal.pone.0032262
470 Chinenov, Y. & Kerppola, T. K. Close encounters of many kinds: Fos-Jun interactions that mediate transcription regulatory specificity. *Oncogene* **20**, 2438–2452 (2001). https://doi.org/10.1038/sj.onc.1204385
471 Koizumi, S. I. *et al.* JunB regulates homeostasis and suppressive functions of effector regulatory T cells. *Nat Commun* **9**, 5344 (2018). https://doi.org/10.1038/s41467-018-07735-4
472 Li, P. *et al.* BATF-JUN is critical for IRF4-mediated transcription in T cells. *Nature* **490**, 543–546 (2012). https://doi.org/10.1038/nature11530
473 Chandrakar, P. *et al.* Progressively differentiated T(FH)13 cells are stabilized by JunB to mediate allergen germinal center responses. *Nat Immunol* (2025). https://doi.org/10.1038/s41590-025-02077-y
474 Godec, J. *et al.* Inducible RNAi in vivo reveals that the transcription factor BATF is required to initiate but not maintain CD8+ T-cell effector differentiation. *Proc Natl Acad Sci U S A* **112**, 512–517 (2015). https://doi.org/10.1073/pnas.1413291112
475 Chang, Y. K., Zuo, Z. & Stormo, G. D. Quantitative profiling of BATF family proteins/JUNB/IRF hetero-trimers using Spec-seq. *BMC Mol Biol* **19**, 5 (2018). https://doi.org/10.1186/s12867-018-0106-7
476 Roychoudhuri, R. *et al.* BACH2 regulates CD8(+) T cell differentiation by controlling access of AP-1 factors to enhancers. *Nat Immunol* **17**, 851–860 (2016). https://doi.org/10.1038/ni.3441
477 Delpoux, A. *et al.* FOXO1 constrains activation and regulates senescence in CD8 T cells. *Cell Rep* **34**, 108674 (2021). https://doi.org/10.1016/j.celrep.2020.108674
478 Hussein, M. S., Li, Q., Mao, R., Peng, Y. & He, Y. TCR T cells overexpressing c-Jun have better functionality with improved tumor infiltration and persistence in hepatocellular carcinoma. *Front Immunol* **14**, 1114770 (2023). https://doi.org/10.3389/fimmu.2023.1114770
479 Seo, H. *et al.* BATF and IRF4 cooperate to counter exhaustion in tumor-infiltrating CAR T cells. *Nat Immunol* **22**, 983–995 (2021). https://doi.org/10.1038/s41590-021-00964-8
480 Wang, X. *et al.* MEK inhibition prevents CAR-T cell exhaustion and differentiation via downregulation of c-Fos and JunB. *Signal Transduct Target Ther* **9**, 293 (2024). https://doi.org/10.1038/s41392-024-01986-y
481 Zhang, X. *et al.* Depletion of BATF in CAR-T cells enhances antitumor activity by inducing resistance against exhaustion and formation of central memory cells. *Cancer Cell* **40**, 1407–1422 e1407 (2022). https://doi.org/10.1016/j.ccell.2022.09.013
482 Lui, Y. *et al.* Cell state and transcription factor modulation during extended ex vivo CD8⁺ T-cell expansion. *bioRxiv*, 2024.2007.2017.603780 (2024). https://doi.org/10.1101/2024.07.17.603780

483 Snyder, A. J. *et al.* Modulating AP-1 enables CAR-T cells to establish an intratumoral PD-1⁺Tcf1⁺ stem-like reservoir and overcomes resistance to PD-1 axis blockade. *bioRxiv*, 2025.2004.2010.648245 (2025). https://doi.org/10.1101/2025.04.10.648245
484 Zuo, S. *et al.* C-JUN overexpressing CAR-T cells in acute myeloid leukemia: preclinical characterization and phase I trial. *Nat Commun* **15**, 6155 (2024). https://doi.org/10.1038/s41467-024-50485-9
485 Xu, T. *et al.* Coexpression of c-Jun in multiple-chain DAP-CAR-engineered T-cells for solid tumor therapy. *Immunotherapy* **14**, 1457–1466 (2022). https://doi.org/10.2217/imt-2022-0171
486 Spigel, D. R. *et al.* 754 Phase 1 trial of LYL797, a ROR1-targeted CAR T-cell therapy enhanced with genetic and epigenetic reprogramming, in advanced triple-negative breast cancer (TNBC) and non-small cell lung cancer (NSCLC). *Journal for ImmunoTherapy of Cancer* **11**, A850–A850 (2023). https://doi.org/10.1136/jitc-2023-SITC2023.0754
487 Ahmed, R., Salmi, A., Butler, L. D., Chiller, J. M. & Oldstone, M. B. Selection of genetic variants of lymphocytic choriomeningitis virus in spleens of persistently infected mice. Role in suppression of cytotoxic T lymphocyte response and viral persistence. *J Exp Med* **160**, 521–540 (1984). https://doi.org/10.1084/jem.160.2.521
488 Pope, C. *et al.* Organ-specific regulation of the CD8 T cell response to Listeria monocytogenes infection. *J Immunol* **166**, 3402–3409 (2001). https://doi.org/10.4049/jimmunol.166.5.3402
489 Manjunath, N. *et al.* Effector differentiation is not prerequisite for generation of memory cytotoxic T lymphocytes. *J Clin Invest* **108**, 871–878 (2001). https://doi.org/10.1172/JCI13296
490 Pircher, H., Burki, K., Lang, R., Hengartner, H. & Zinkernagel, R. M. Tolerance induction in double specific T-cell receptor transgenic mice varies with antigen. *Nature* **342**, 559–561 (1989). https://doi.org/10.1038/342559a0
491 Hogquist, K. A. *et al.* T cell receptor antagonist peptides induce positive selection. *Cell* **76**, 17–27 (1994). https://doi.org/10.1016/0092-8674(94)90169-4
492 Montague, T. G., Cruz, J. M., Gagnon, J. A., Church, G. M. & Valen, E. CHOPCHOP: a CRISPR/Cas9 and TALEN web tool for genome editing. *Nucleic Acids Res* **42**, W401–407 (2014). https://doi.org/10.1093/nar/gku410
493 Perez, G. *et al.* The UCSC Genome Browser database: 2025 update. *Nucleic Acids Res* **53**, D1243–D1249 (2025). https://doi.org/10.1093/nar/gkae974
494 UniProt, C. UniProt: the Universal Protein Knowledgebase in 2025. *Nucleic Acids Res* **53**, D609–D617 (2025). https://doi.org/10.1093/nar/gkae1010
495 Borges da Silva, H. *et al.* Sensing of ATP via the Purinergic Receptor P2RX7 Promotes CD8(+) Trm Cell Generation by Enhancing Their Sensitivity to the Cytokine TGF-beta. *Immunity* **53**, 158–171 e156 (2020). https://doi.org/10.1016/j.immuni.2020.06.010
496 Nussing, S. *et al.* Efficient CRISPR/Cas9 Gene Editing in Uncultured Naive Mouse T Cells for In Vivo Studies. *J Immunol* **204**, 2308–2315 (2020). https://doi.org/10.4049/jimmunol.1901396
497 Clement, K. *et al.* CRISPResso2 provides accurate and rapid genome editing sequence analysis. *Nat Biotechnol* **37**, 224–226 (2019). https://doi.org/10.1038/s41587-019-0032-3
498 Gregersen, L. H. *et al.* SCAF4 and SCAF8, mRNA Anti-Terminator Proteins. *Cell* **177**, 1797–1813 e1718 (2019). https://doi.org/10.1016/j.cell.2019.04.038
499 Hogg, S. J. *et al.* Targeting histone acetylation dynamics and oncogenic transcription by catalytic P300/CBP inhibition. *Mol Cell* **81**, 2183–2200 e2113 (2021). https://doi.org/10.1016/j.molcel.2021.04.015
500 Kuhn, L., Vincent, T., Hammann, P. & Zuber, H. Exploring Protein Interactome Data with IPinquiry: Statistical Analysis and Data Visualization by Spectral Counts. *Methods Mol Biol* **2426**, 243–265 (2023). https://doi.org/10.1007/978-1-0716-1967-4_11

501 Szklarczyk, D. *et al.* The STRING database in 2023: protein-protein association networks and functional enrichment analyses for any sequenced genome of interest. *Nucleic Acids Res* **51**, D638–D646 (2023). https://doi.org/10.1093/nar/gkac1000
502 Wickham, H. *ggplot2: Elegant Graphics for Data Analysis*. (Springer-Verlag New York, 2016).
503 Robinson, J. T. *et al.* Integrative genomics viewer. *Nat Biotechnol* **29**, 24–26 (2011). https://doi.org/10.1038/nbt.1754
504 Yu, G., Wang, L. G. & He, Q. Y. ChIPseeker: an R/Bioconductor package for ChIP peak annotation, comparison and visualization. *Bioinformatics* **31**, 2382–2383 (2015). https://doi.org/10.1093/bioinformatics/btv145
505 McLeay, R. C. & Bailey, T. L. Motif Enrichment Analysis: a unified framework and an evaluation on ChIP data. *BMC Bioinformatics* **11**, 165 (2010). https://doi.org/10.1186/1471-2105-11-165
506 Xie, Z. *et al.* Gene Set Knowledge Discovery with Enrichr. *Current Protocols* **1**, e90 (2021). https://doi.org/https://doi.org/10.1002/cpz1.90
507 Huber, W. *et al.* Orchestrating high-throughput genomic analysis with Bioconductor. *Nat Methods* **12**, 115–121 (2015). https://doi.org/10.1038/nmeth.3252
508 Lawrence, M., Gentleman, R. & Carey, V. rtracklayer: an R package for interfacing with genome browsers. *Bioinformatics* **25**, 1841–1842 (2009). https://doi.org/10.1093/bioinformatics/btp328
509 Lawrence, M. *et al.* Software for computing and annotating genomic ranges. *PLoS Comput Biol* **9**, e1003118 (2013). https://doi.org/10.1371/journal.pcbi.1003118
510 org.Mm.eg.db: Genome wide annotation for Mouse (2026).
511 TxDb.Mmusculus.UCSC.mm10.knownGene: Annotation package for TxDb object(s) (2019).
512 Chen, H. & Boutros, P. C. VennDiagram: a package for the generation of highly-customizable Venn and Euler diagrams in R. *BMC Bioinformatics* **12**, 35 (2011). https://doi.org/10.1186/1471-2105-12-35
513 Li, X. M. *et al.* MAC-Seq: Coupling Low-Cost, High-Throughput RNA-Seq with Image-Based Phenotypic Screening in 2D and 3D Cell Models. *Methods Mol Biol* **2691**, 279–325 (2023). https://doi.org/10.1007/978-1-0716-3331-1_22
514 Jimenez-Gracia, L. *et al.* FixNCut: single-cell genomics through reversible tissue fixation and dissociation. *Genome Biol* **25**, 81 (2024). https://doi.org/10.1186/s13059-024-03219-5
515 Butler, A., Hoffman, P., Smibert, P., Papalexi, E. & Satija, R. Integrating single-cell transcriptomic data across different conditions, technologies, and species. *Nat Biotechnol* **36**, 411–420 (2018). https://doi.org/10.1038/nbt.4096
516 Chen, Y., Chen, L., Lun, A. T. L., Baldoni, P. L. & Smyth, G. K. edgeR v4: powerful differential analysis of sequencing data with expanded functionality and improved support for small counts and larger datasets. *Nucleic Acids Res* **53** (2025). https://doi.org/10.1093/nar/gkaf018
517 Castanza, A. S. *et al.* Extending support for mouse data in the Molecular Signatures Database (MSigDB). *Nat Methods* **20**, 1619–1620 (2023). https://doi.org/10.1038/s41592-023-02014-7
518 Subramanian, A. *et al.* Gene set enrichment analysis: a knowledge-based approach for interpreting genome-wide expression profiles. *Proc Natl Acad Sci U S A* **102**, 15545–15550 (2005). https://doi.org/10.1073/pnas.0506580102
519 Gu, Z., Eils, R. & Schlesner, M. Complex heatmaps reveal patterns and correlations in multidimensional genomic data. *Bioinformatics* **32**, 2847–2849 (2016). https://doi.org/10.1093/bioinformatics/btw313
520 Clough, E. *et al.* NCBI GEO: archive for gene expression and epigenomics data sets: 23-year update. *Nucleic Acids Res* **52**, D138–D144 (2024). https://doi.org/10.1093/nar/gkad965
521 Perez-Riverol, Y. *et al.* The PRIDE database at 20 years: 2025 update. *Nucleic Acids Res* **53**, D543–D553 (2025). https://doi.org/10.1093/nar/gkae1011

522 Crespo, J., Sun, H., Welling, T. H., Tian, Z. & Zou, W. T cell anergy, exhaustion, senescence, and stemness in the tumor microenvironment. *Curr Opin Immunol* **25**, 214–221 (2013). https://doi.org/10.1016/j.coi.2012.12.003
523 Mognol, G. P. *et al.* Exhaustion-associated regulatory regions in CD8(+) tumor-infiltrating T cells. *Proc Natl Acad Sci U S A* **114**, E2776–E2785 (2017). https://doi.org/10.1073/pnas.1620498114
524 Huang, Y. J. *et al.* Continuous expression of TOX safeguards exhausted CD8 T cell epigenetic fate. *Sci Immunol* **10**, eado3032 (2025). https://doi.org/10.1126/sciimmunol.ado3032
525 Kurts, C., Heath, W. R., Kosaka, H., Miller, J. F. & Carbone, F. R. The peripheral deletion of autoreactive CD8+ T cells induced by cross-presentation of self-antigens involves signaling through CD95 (Fas, Apo-1). *J Exp Med* **188**, 415–420 (1998). https://doi.org/10.1084/jem.188.2.415
526 Macian, F., Garcia-Rodriguez, C. & Rao, A. Gene expression elicited by NFAT in the presence or absence of cooperative recruitment of Fos and Jun. *EMBO J* **19**, 4783–4795 (2000). https://doi.org/10.1093/emboj/19.17.4783
527 Miyagawa, F., Gutermuth, J., Zhang, H. & Katz, S. I. The use of mouse models to better understand mechanisms of autoimmunity and tolerance. *J Autoimmun* **35**, 192–198 (2010). https://doi.org/10.1016/j.jaut.2010.06.007
528 Klein-Hessling, S. *et al.* NFATc1 controls the cytotoxicity of CD8(+) T cells. *Nat Commun* **8**, 511 (2017). https://doi.org/10.1038/s41467-017-00612-6
529 Walters, R. D., Drullinger, L. F., Kugel, J. F. & Goodrich, J. A. NFATc2 recruits cJun homodimers to an NFAT site to synergistically activate interleukin-2 transcription. *Mol Immunol* **56**, 48–56 (2013). https://doi.org/10.1016/j.molimm.2013.03.022
530 Hwang, J. S. *et al.* NFAT1 and JunB cooperatively regulate IL-31 gene expression in CD4+ T cells in health and disease. *J Immunol* **194**, 1963–1974 (2015). https://doi.org/10.4049/jimmunol.1401862
531 Boise, L. H. *et al.* The NFAT-1 DNA binding complex in activated T cells contains Fra-1 and JunB. *Mol Cell Biol* **13**, 1911–1919 (1993). https://doi.org/10.1128/mcb.13.3.1911-1919.1993
532 Gabriel, C. H. *et al.* Identification of Novel Nuclear Factor of Activated T Cell (NFAT)-associated Proteins in T Cells. *J Biol Chem* **291**, 24172–24187 (2016). https://doi.org/10.1074/jbc.M116.739326
533 Mouzaki, A. & Rungger, D. Properties of transcription factors regulating interleukin-2 gene transcription through the NFAT binding site in untreated or drug-treated naive and memory T-helper cells. *Blood* **84**, 2612–2621 (1994).
534 Kroger, A. IRFs as competing pioneers in T-cell differentiation. *Cell Mol Immunol* **14**, 649–651 (2017). https://doi.org/10.1038/cmi.2017.37
535 Lotem, J. *et al.* Runx3-mediated transcriptional program in cytotoxic lymphocytes. *PLoS One* **8**, e80467 (2013). https://doi.org/10.1371/journal.pone.0080467
536 Kalogeropoulou, M. *et al.* TAF4b and Jun/activating protein-1 collaborate to regulate the expression of integrin alpha6 and cancer cell migration properties. *Mol Cancer Res* **8**, 554–568 (2010). https://doi.org/10.1158/1541-7786.MCR-09-0159
537 Lieberman, P. M. & Berk, A. J. A mechanism for TAFs in transcriptional activation: activation domain enhancement of TFIID-TFIIA--promoter DNA complex formation. *Genes Dev* **8**, 995–1006 (1994). https://doi.org/10.1101/gad.8.9.995
538 Pham, D. *et al.* Batf Pioneers the Reorganization of Chromatin in Developing Effector T Cells via Ets1-Dependent Recruitment of Ctcf. *Cell Rep* **29**, 1203–1220 e1207 (2019). https://doi.org/10.1016/j.celrep.2019.09.064
539 So, L. *et al.* Regulatory T cells suppress CD4+ effector T cell activation by controlling protein synthesis. *J Exp Med* **220** (2023). https://doi.org/10.1084/jem.20221676
540 Puiffe, M. L. *et al.* IL4I1 Accelerates the Expansion of Effector CD8(+) T Cells at the Expense of Memory Precursors by Increasing the Threshold of T-Cell Activation. *Front Immunol* **11**, 600012 (2020). https://doi.org/10.3389/fimmu.2020.600012

541 Clain, J. A. *et al.* Lipid metabolic reprogramming of hepatic CD4(+) T cells during SIV infection. *Microbiol Spectr* **11**, e0168723 (2023). https://doi.org/10.1128/spectrum.01687-23
542 Katagiri, T., Kameda, H., Nakano, H. & Yamazaki, S. Regulation of T cell differentiation by the AP-1 transcription factor JunB. *Immunol Med* **44**, 197–203 (2021). https://doi.org/10.1080/25785826.2021.1872838
543 Gao, M. *et al.* Jun turnover is controlled through JNK-dependent phosphorylation of the E3 ligase Itch. *Science* **306**, 271–275 (2004). https://doi.org/10.1126/science.1099414
544 Chauhan, D. *et al.* Regulation of c-jun gene expression in human T lymphocytes. *Blood* **81**, 1540–1548 (1993).
545 Farina, A. R., Davis-Smyth, T., Gardner, K. & Levens, D. An early response of an AP1-junD complex during T-cell activation. *J Biol Chem* **268**, 26466–26475 (1993).
546 Jain, J., Loh, C. & Rao, A. Transcriptional regulation of the IL-2 gene. *Curr Opin Immunol* **7**, 333–342 (1995). https://doi.org/10.1016/0952-7915(95)80107-3
547 Bevington, S. L., Cauchy, P., Withers, D. R., Lane, P. J. & Cockerill, P. N. T Cell Receptor and Cytokine Signaling Can Function at Different Stages to Establish and Maintain Transcriptional Memory and Enable T Helper Cell Differentiation. *Front Immunol* **8**, 204 (2017). https://doi.org/10.3389/fimmu.2017.00204
548 Biddie, S. C. *et al.* Transcription factor AP1 potentiates chromatin accessibility and glucocorticoid receptor binding. *Mol Cell* **43**, 145–155 (2011). https://doi.org/10.1016/j.molcel.2011.06.016
549 Tatarakis, A. *et al.* Requirements for establishment and epigenetic stability of mammalian heterochromatin. *Mol Cell* **85**, 3388–3406 e3312 (2025). https://doi.org/10.1016/j.molcel.2025.08.025
550 Chen, L., Glover, J. N., Hogan, P. G., Rao, A. & Harrison, S. C. Structure of the DNA-binding domains from NFAT, Fos and Jun bound specifically to DNA. *Nature* **392**, 42–48 (1998). https://doi.org/10.1038/32100
551 Chen, L. *et al.* Only one of the two DNA-bound orientations of AP-1 found in solution cooperates with NFATp. *Curr Biol* **5**, 882–889 (1995). https://doi.org/10.1016/s0960-9822(95)00178-3
552 Preiss, N. K. *et al.* Characterizing control of memory CD8 T cell differentiation by BTB-ZF transcription factor Zbtb20. *Life Sci Alliance* **6** (2023). https://doi.org/10.26508/lsa.202201683
553 Chen, A. X. Y. *et al.* Rewiring endogenous genes in CAR T cells for tumour-restricted payload delivery. *Nature* **644**, 241–251 (2025). https://doi.org/10.1038/s41586-025-09212-7
554 Newell, C. L., Deisseroth, A. B. & Lopez-Berestein, G. Interaction of nuclear proteins with an AP-1/CRE-like promoter sequence in the human TNF-alpha gene. *J Leukoc Biol* **56**, 27–35 (1994). https://doi.org/10.1002/jlb.56.1.27
555 Samten, B. *et al.* CREB, ATF, and AP-1 transcription factors regulate IFN-gamma secretion by human T cells in response to mycobacterial antigen. *J Immunol* **181**, 2056–2064 (2008). https://doi.org/10.4049/jimmunol.181.3.2056
556 Kalari Kandy, R. R., Fan, X. & Cao, X. CD45.1/CD45.2 Congenic Markers Induce a Selective Bias for CD8+ T Cells during Adoptive Lymphocyte Reconstitution in Lymphocytopenia Mice. *Immunohorizons* **7**, 755–759 (2023). https://doi.org/10.4049/immunohorizons.2300014
557 Shin, H. Y. *et al.* CRISPR/Cas9 targeting events cause complex deletions and insertions at 17 sites in the mouse genome. *Nat Commun* **8**, 15464 (2017). https://doi.org/10.1038/ncomms15464
558 Kosicki, M. *et al.* Cas9-induced large deletions and small indels are controlled in a convergent fashion. *Nat Commun* **13**, 3422 (2022). https://doi.org/10.1038/s41467-022-30480-8
559 Kosicki, M., Tomberg, K. & Bradley, A. Repair of double-strand breaks induced by CRISPR-Cas9 leads to large deletions and complex rearrangements. *Nat Biotechnol* **36**, 765–771 (2018). https://doi.org/10.1038/nbt.4192

560 Kalter, N. *et al.* Off-target effects in CRISPR-Cas genome editing for human therapeutics: Progress and challenges. *Mol Ther Nucleic Acids* **36**, 102636 (2025). https://doi.org/10.1016/j.omtn.2025.102636
561 Simpson, B. P., Yrigollen, C. M., Izda, A. & Davidson, B. L. Targeted long-read sequencing captures CRISPR editing and AAV integration outcomes in brain. *Mol Ther* **31**, 760–773 (2023). https://doi.org/10.1016/j.ymthe.2023.01.004
562 Truckenbrod, E. N. *et al.* CD8(+) T cell self-tolerance permits responsiveness but limits tissue damage. *Elife* **10** (2021). https://doi.org/10.7554/eLife.65615
563 Balomenos, D. & Martinez, A. C. Cell-cycle regulation in immunity, tolerance and autoimmunity. *Immunol Today* **21**, 551–555 (2000). https://doi.org/10.1016/s0167-5699(00)01748-5
564 Bendle, G. M., Xue, S. A., Holler, A. & Stauss, H. J. A study of T cell tolerance to the tumor-associated antigen MDM2: cytokines can restore antigen responsiveness, but not high avidity T cell function. *PLoS One* **2**, e353 (2007). https://doi.org/10.1371/journal.pone.0000353
565 Murphy, T. L., Tussiwand, R. & Murphy, K. M. Specificity through cooperation: BATF-IRF interactions control immune-regulatory networks. *Nat Rev Immunol* **13**, 499–509 (2013). https://doi.org/10.1038/nri3470
566 Bevington, S. L. *et al.* IL-2/IL-7-inducible factors pioneer the path to T cell differentiation in advance of lineage-defining factors. *EMBO J* **39**, e105220 (2020). https://doi.org/10.15252/embj.2020105220
567 Kurup, S. P., Moioffer, S. J., Pewe, L. L. & Harty, J. T. p53 Hinders CRISPR/Cas9-Mediated Targeted Gene Disruption in Memory CD8 T Cells In Vivo. *J Immunol* **205**, 2222–2230 (2020). https://doi.org/10.4049/jimmunol.2000654
568 Nabet, B. *et al.* The dTAG system for immediate and target-specific protein degradation. *Nat Chem Biol* **14**, 431–441 (2018). https://doi.org/10.1038/s41589-018-0021-8
569 Jung, I. Y. *et al.* Tissue-resident memory CAR T cells with stem-like characteristics display enhanced efficacy against solid and liquid tumors. *Cell Rep Med* **4**, 101053 (2023). https://doi.org/10.1016/j.xcrm.2023.101053
570 Reading, S. M. *et al.* Abstract LT02: Regulation of Exhausted CD8+ T cell Differentiation by IKZF Transcription Factors. *Cancer Research* **84**, LT02–LT02 (2024). https://doi.org/10.1158/1538-7445.Fcs2023-lt02
571 Doering, T. A. *et al.* Network analysis reveals centrally connected genes and pathways involved in CD8+ T cell exhaustion versus memory. *Immunity* **37**, 1130–1144 (2012). https://doi.org/10.1016/j.immuni.2012.08.021
572 Walsh, D. A. *et al.* The Functional Requirement for CD69 in Establishment of Resident Memory CD8(+) T Cells Varies with Tissue Location. *J Immunol* **203**, 946–955 (2019). https://doi.org/10.4049/jimmunol.1900052
573 Jubel, J. M., Barbati, Z. R., Burger, C., Wirtz, D. C. & Schildberg, F. A. The Role of PD-1 in Acute and Chronic Infection. *Front Immunol* **11**, 487 (2020). https://doi.org/10.3389/fimmu.2020.00487
574 Hong, J. J., Amancha, P. K., Rogers, K., Ansari, A. A. & Villinger, F. Re-evaluation of PD-1 expression by T cells as a marker for immune exhaustion during SIV infection. *PLoS One* **8**, e60186 (2013). https://doi.org/10.1371/journal.pone.0060186
575 Giordano, M. *et al.* Molecular profiling of CD8 T cells in autochthonous melanoma identifies Maf as driver of exhaustion. *EMBO J* **34**, 2042–2058 (2015). https://doi.org/10.15252/embj.201490786
576 Yang, Y. & Cvekl, A. Large Maf Transcription Factors: Cousins of AP-1 Proteins and Important Regulators of Cellular Differentiation. *Einstein J Biol Med* **23**, 2–11 (2007). https://doi.org/10.23861/ejbm20072347
577 Papavassiliou, A. G. & Musti, A. M. The Multifaceted Output of c-Jun Biological Activity: Focus at the Junction of CD8 T Cell Activation and Exhaustion. *Cells* **9** (2020). https://doi.org/10.3390/cells9112470

578 Comandante-Lou, N., Baumann, D. G. & Fallahi-Sichani, M. AP-1 transcription factor network explains diverse patterns of cellular plasticity in melanoma cells. *Cell Rep* **40**, 111147 (2022). https://doi.org/10.1016/j.celrep.2022.111147

579 Buquicchio, F. A. *et al.* Distinct epigenomic landscapes underlie tissue-specific memory T cell differentiation. *Immunity* **57**, 2202–2215 e2206 (2024). https://doi.org/10.1016/j.immuni.2024.06.014